RADIATION DRIVEN INSTABILITIES IN STELLAR WINDS

by

RAYMOND GARY CARLBERG

M.Sc., University of British Columbia, 1975

B.Sc., University of Saskatchewan, 1972

A THESIS SUBMITTED IN PARTIAL FULFILLMENT OF

THE REQUIREMENTS FOR THE DEGREE OF

DOCTOR OF PHILOSOPHY

in

THE FACULTY OF GRADUATE STUDIES

Department of Geophysics and Astronomy

We accept this thesis as conforming

to the required standard

THE UNIVERSITY OF BRITISH COLUMBIA

October, 1978

ABSTRACT

This thesis investigates the quantitative nature of the variability which is present in the stellar winds of high luminosity early type stars. A program of optical observations with high time and spectral resolution was designed to provide quantitative information on the nature of the fluctuations. These observations found no optical variability over a time period of six hours and hence restrict the variability over this period to size scales of less than 5×10^{11} cm, but do confirm the variations on time scales exceeding one day. A class of X-ray sources comprised of a neutron star orbiting a star with a strong stellar wind provides another source of information on the variability of stellar winds. A theory of accretion onto a neutron star was developed which is used with X-ray intensity data to derive estimates of the density and velocity of the stellar wind. This analysis performed on Cen X-3 suggests that the velocity in the stellar wind increases as the wind density increases.

A theoretical analysis of the stability of a stellar wind is made to determine whether the variability may originate in the wind itself. Two types of instability are found: those that amplify pre-existing disturbances, and absolute instabilities which can grow from random motions within the gas. It is found that short wavelength disturbances ($<10^{4}$ cm) are always strongly damped by conduction, and long wavelength ones ($>10^{11}$ cm) are damped by radiation if the gas is thermally stable, that is if the net radiative energy loss increases with temperature. Intermediate wavelengths of about 10^{8-9} cm are usually subject to

an amplification due to the density gradient of the wind. The radiation acceleration amplifies disturbances of scales 10^7 to 10^{11} cm. Absolute instabilities are present if the gas is thermally unstable, if the flow is deccelerating, or if the gas has a temperature of several million degrees.

On the basis of the information derived on stellar wind stability it is proposed that a complete theory should be based on the assumption that the wind is a nonstationary flow.

CONTENTS

FIGURES

TABLES

ACKNOWLEDGEMENTS

The completion of this thesis owes a great deal to the teaching, assistance, and encouragement that I have received. My supervisor, Dr. Greg Fahlman, always provided an interested ear and a careful criticism of my ideas. He was also a source of support when needed. Drs. Gordon Walker and Jason Auman made a number of suggestions which substantially improved the presentation of the thesis.

My induction into the world of observational astronomy came with three very pleasant summers spent in Victoria at the Dominion Astrophysical Observatory. The frustrations of doing spectrophotometry with photographic plates were largely eliminated by Dr. Gordon Walker's encouragement to use his Reticon detector system. The successful observations obtained with this system owe a great deal to the advice and technical support of Dr. Walker, Dr. Bruce Campbell, Dr. Chris Pritchett, Tim Lester, and Mike Creswell. The whole data reduction process has been reduced to a straightforward and enjoyable activity by the use of Chris Pritchett's data handling package, RETICENT.

A large part of this thesis relied on the computer for its completion. The UBC Computing Centre has been a great assistance and deserves much praise for its facilities, and the provision of a large number of well documented utility programs. Particular thanks go to A. C. Hearn, originally at the University of Utah, who wrote the program REDUCE.

Financial support was provided by the National Research Council of Canada and by a MacMillan Family Fellowship.

CHAPTER 1. INTRODUCTION

The optical spectra of many hot stars were noted to have emission components on the Harvard objective prism plates (see the Henry Draper Catalogue, Cannon and Pickering 1918). Many of these stars were studied in detail, leading to Beal's (1929) proposal that the line profiles could be explained by emission from gas being ejected from the star. A great deal of information was accumulated on the optical spectra of emission line O and B stars in the following years, which is summarized in Beals (1951) and Underhill (1960). A new observational window the UV was opened by Morton (1967) using a rocket borne spectrograph. He found that 4 of the Orion stars, δ, ϵ, ζ, and ι, had absorption lines blue shifted to velocities of order 2000 Km s^{-1}. These velocities exceeded the typical escape speed of 300 Km s^{-1} by such a large factor that there was no question that the stars were losing mass at a large rate.

The Snow and Morton ultraviolet survey (1976) showed that all stars with an effective temperature greater than about $3x10^4$ K, and luminosities greater than a bolometric magnitude of -6, have a detectable supersonic wind which carries away a significant amount of the star's mass during its lifetime. Reliable mass loss rates have been obtained from optical observations (see Hutchings 1976) and UV observations (Snow and Morton 1976) which now have been extended to infrared (Barlow and Cohen 1977) and radio wavelengths (Wright and Barlow 1975), all of which provide confirming and complementary data on the magnitude of the mass loss. The derived mass loss rates for OB stars lie in the range of 10^{-9} to 10^{-5} $M_{\odot}$/year, with terminal velocities ranging from 1000 to 3000 km s^{-1}.

The stellar wind phenomenon poses several questions: what is the physical mechanism driving the mass loss? how does the mass loss effect the star's evolution? and how do these hot, luminous stars affect the interstellar medium and the evolution of a galaxy? The answers to all of these questions hinge on a thorough understanding of the physics of the stellar wind. This thesis is a contribution to the understanding of the basic nature of the stellar wind. The physical problem is to describe the dynamics of a gas moving in an intense radiation field; a situation which occurs in a number of astrophysical situations, including quasars and active galactic nuclei, (Mushotzky, et al. 1972 and Kippenhahn et al. 1975).

The line profiles of stellar wind stars, especially ones with high mass loss rates have long been known to show some variability over one day (see for instance Beals 1951, Underhill 1960, Conti and Frost 1974, Leep and Conti 1978, Brucato 1971, Snow 1977, and Rosendahl 1973). For ground based observation this time period makes it difficult to resolve the time evolution of the variation. An observational program was initiated to more closely define the nature of these reported variations, using a modern detector capable of measuring very small changes. This will be discussed in Chapter 2.

Besides optical evidence of variability, there are a number of X-ray binary stars where the X-ray source is a neutron star accreting mass from the stellar wind (Conti 1978). These sources show a number of scales of variation of their intensity which can be ascribed to variations of the stellar wind. A theoretical analysis of the accretion process and how it effects the observed intensity was made in order that the X-ray data could be used to derive the prevailing density and velocity of the stellar wind at the location of the neutron star. This analysis performed on X-ray data for the source Cen X-3 indicates a correlation between the wind velocity and density. This will be described in Chapter 3.

The basic formulation of the theory of a stellar wind from a hot, luminous star was initially put forth by Lucy and Solomon (1970), who proposed that the acceleration was produced by the scattering of photons with wavelengths that fell within a few resonance lines. This was a generalization of Milne's (1926) idea that momentum transfer from photons could selectively accelerate certain ions. This was later extended by Castor, Abbott, and Klein (1975, referred to as CAK) to include the force on many lines of many ions. The theory provided an encouraging agreement with the limited data available on the velocity as a function of radius and mass loss rates.

Recently the ultraviolet satellite observations have revealed that some highly ionized species, in particular O VI and N V, are present in the wind. These ions would not be expected to be ionized in any observable quantity by the radiation field appropriate to these stars. York, et al. (1977) have observed variations in the O VI line in three stars over a time periods as short as six hours. This observation suggests a "slab" moving outwards at an increasing velocity. The presence of O VI in the stellar wind presents a puzzle as to the source of its excitation. At the present time there are three proposals.

First, Castor (1978) has modified his radiation driven wind to an arbitrarily specified temperature higher than radiative equilibrium, which provides a suitable abundance of O VI. Second, Lamers and Snow (1978) have an empirical "warm radiation pressure" model, in which they show that the ions can be provided if the stellar wind is at a temperature of about 2×10^5 K. Neither of these models specify the source of the additional heating. Third, Hearn (1975) has proposed that stellar winds are initially accelerated in a hot corona with a temperature of several million degrees. Pursuing this idea Olson and Cassinelli (1978) have shown that a small corona, about 10% of a stellar radius, generates enough thermal X-rays to produce the required ionization ratios. To provide a heating mechanism for a corona, Hearn (1972) showed that radiation driven sound waves could be amplified while propogating outward in the atmosphere. The waves grow to a saturated amplitude sufficient to provide enough shock heating to maintain a corona (Hearn 1973). There are two difficulties with this analysis. Berthomieu et al. (1975) have pointed out that Hearn's simplifying assumptions result in a scale length for the wave amplification which is the same as the atmospheric scale length. Therefore significant amplification only occurs over lengths which invalidate the assumption of small variations of the zero order quantities over the length for amplification. In addition, the unstable waves that he finds are amplifying instabilities (Castor 1977), and require some oscillator to initiate the wave motion.

Motivated by theoretical arguments and the observations of fluctuations I have performed a stability analysis on the equations governing the moving gas in the stellar radiation field. The complete set of equations governing the motion with no *a priori* simplifications were used. An accurate description of the gas physics was developed using an approximate treatment of radiation transfer dependent only on local quantities. As a result the state of the gas can be completely specified by the local radiation field, the gas velocity and its gradient, and the density and temperature, as described in Chapter 4. The stability of the gas against vertical disturbances was investigated with the aid of a computer to provide the numerical solutions to the dispersion relation. Chapter 5 is comprised of this discussion.

The purpose of this thesis is to investigate the quantitative nature of instabilities in stellar winds and relate it to the observational and theoretical problems which have been outlined. This is not an attempt to create a unified theory of a stellar wind. Rather it is a detailed investigation of certain areas of the question in order to illuminate some of the physical mechanisms which are important in a stellar wind. This is required because not much is known about the basic physical processes which dominate the observed variability of the stellar wind.

The investigation is confined to the stellar wind itself, which is loosely defined as the region where the optical depth in the continuum is less than one and the gas is moving with greater than sonic velocities. As has been emphasized by Cannon and Thomas (1978), it is possible that some of the driving force for the the wind and hence some of the wind instabilities may originate within deeper layers of the star.

It is assumed that there is no magnetic field. This is done mostly because of the tremendous simplification of the problem which results. But there is no observational evidence for a magnetic field, although if the wind is as chaotic as this thesis suggests, a magnetic field would be difficult to detect.

In summary this thesis is motivated by observations of stellar wind variability, and suggestions by other authors that instabilities do exist which may be responsible for the creation of a high temperature corona. The investigations described are carried out in two parts. Observational evidence of the variability is acquired which suggests length and times scales of the fluctuations which are present, and a correlation between the wind velocity and density. The theoretical analysis provides physical sources of several instabilities which can exist in the stellar wind. From this information I suggest that the stellar wind is an extremely chaotic medium in which the instabilities not only provide the source for the observed variability, but also can be used to provide an ionization source for the O VI ion and the corona as postulated by Hearn. The presence of these instabilities means that a model for a stellar wind should be in the form of mean flow quantities and associated fluctuating quantities.

CHAPTER 2. OPTICAL OBSERVATIONS

For many years several of the lines in the optical spectrum of several early type stars have been reported as varying (see references cited in the Introduction). Particular attention has been paid to the star Lambda Cephei, because it is a bright O6f star in the northern sky. The Hα line has been reported to vary on time scales of one day (Leep and Conti 1978) and longer, with no apparent systematic variation. The amplitude of the variation is typically 10% of the intensity. This behaviour is fairly typical of the more luminous mass loss stars. The shortest period variations with a high confidence level are the UV observations made by the satellite Copernicus of δ Ori A, η Ori, and ζ Pup (York *et al.* 1977), where a small feature of width about 150 Km s^{-1} was seen to "move" in the O VI line between two observations spaced about 6 hours apart.

Most of the observations at optical wavelengths have been made with photographic plates, which have a photometric accuracy barely able to reveal the presence of the variation, let alone reveal much information as to its character. In fact Lacy (1977) made scanner observations of some of the lines in stars that were reported as varying and concluded on the basis of a statistical analysis of the errors present in the equivalent width that any variability present was less than the expected random error. However the equivalent width of a line averages together all material emitting at that line frequency. Observations which resolve the line can provide much more information, but at the cost of longer exposure times.

The classical description of line formation in a stellar wind was given by Beals (1951). The observed line can be considered to be made up of three almost independent parts; an underlying absorption line formed in the photosphere of the star, a superposed emission line with its centroid at zero velocity produced by emission of photons in the stellar wind, and a blue shifted absorption line which is formed in the portion of the stellar wind which is silhouetted against the star.

The analysis of line formation within the wind is simplified by the Sobolev approximation (Sobolev 1960), which says that the emission and absorption of photons in a given narrow wavelength interval, outside of the doppler core, is determined by the amount of gas moving at a velocity such that the line of sight velocity of the gas falls within the wavelength interval. This approximation is valid if the gas speed is supersonic. The assumption is supported by the observations of Hutchings (1976 and references therein) who has shown that the wind has a velocity exceeding the sound speed for distances greater than 10% of the stellar radius.

The observations were undertaken to confirm the reported variability and were to be made with sufficiently high signal to noise, spectral resolution and time resolution to clearly resolve the variations, as they developed. In particular it was thought that there might be evidence for the nature of the mechanism of the variation, for instance, a spot rotating with the star or a "blob" moving out through the wind.

All observations were carried out with the 1.2 meter telescope of the Dominion Astrophysical Observatory, Victoria, B.C. The 2.4 meter camera in the coude spectrograph was used with a red coated image slicer giving a projected slit width of 60 microns. The spectrum was detected with a 1024 element array of 25.4 micron diodes (a Reticon RL1024/C17) cooled to a temperature of -80° C (Walker <u>et al</u>. 1976). The image slicer and detector pixel size combination were chosen to give a properly oversampled spectrum. All observations were centred on the $H\alpha$ line in the first order resulting in a dispersion of .125Å/diode. Observations were made in September and October of 1977, and are tabulated below and shown in the accompanying figures.

TABLE 1: CATALOGUE OF OBSERVATIONS

#	Star	Date 1977	Time PST	Exposure seconds
1	Lambda Cep	Sept 11/12	22:13	2250
2	"	"	22:55	"
3	"	"	23:41	"
4	"	"	00:23	"
5	"	"	01:05	"
6	"	"	01:48	"
7	"	"	03:10	"
8	"	"	03:54	"
9	"	"	04:36	"
10	"	Oct 11/12	23:00	3000
11	"	"	01:08	3000
12	"	Oct 12/13	22:15	3000
13	"	Oct 16/17	21:05	3000
14	"	"	23:38	3000
15	"	"	04:28	3000
16	Alpha Cam	Oct 11/12	00:27	1500
17	"	Oct 12/13	01:35	2002
18	"	Oct 16/17	22:58	1800
19	Delta Ori	Oct 12/13	02:31	600
20	"	"	03:01	600
21	"	Oct 16/17	23:00	2641
22	"	"	03:41	2830

The lines present in the 100 Å region examined are identified in Figure 1. They include the stellar $H\alpha$ and He II 6527, the interstellar 6614 Å feature, and a multitude of narrow,

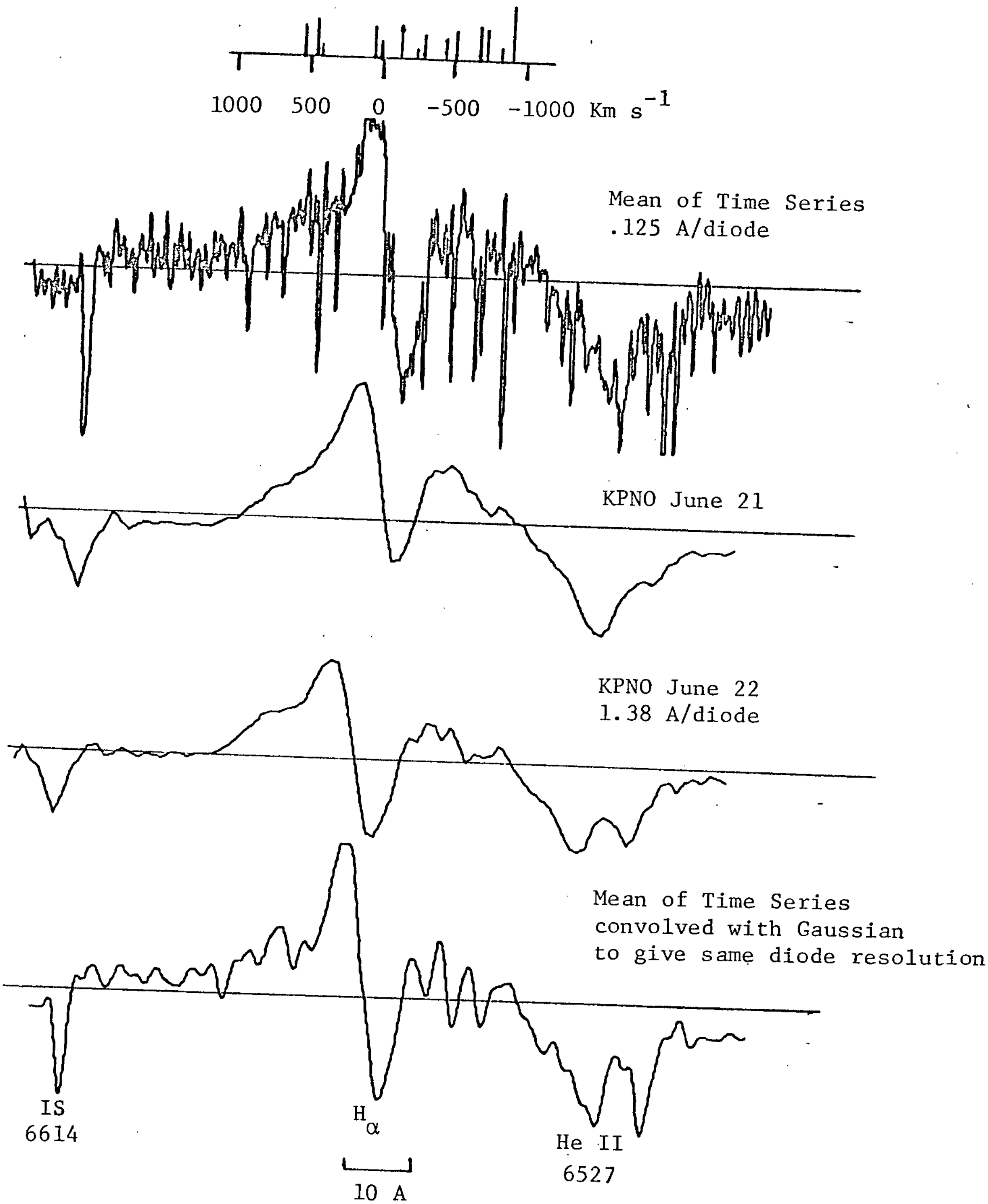

Fig. 1: Lambda Cephei: The Effect of Resolution

weak, telluric water vapour lines. The telluric water lines and their relative equivalent widths are indicated above the spectra. This data was taken from Moore et al. (1966), and may not give the exact relative intensities for these observations. All of the spectra have been filtered by a Fourier transform technique to 40% of the Nyquist frequency, which is roughly the true resolution of the spectra. All spectra had considerable (10%) response changes along the array, due mostly to a light frost on the window of the detector. This was removed by dividing by the spectrum of a lamp which was taken immediately before or after the observation. For the time series spectra the underlying shape of the spectrum did not vary within the error (0.1%) of the lamp calibration. All spectra were rectified to a linear continuum.

Figure 1 shows the absolute necessity to resolve the telluric water lines. As the Figure 2 time series of Lamda Cep over 6 hours shows, the water lines vary significantly over one hour. In Figure 1 the top spectrum shows the mean of the time series of high resolution spectra. Below it are two spectra recorded at KPNO in June, 1978 (courtesy of G. G. Fahlman and G. A. H. Walker) using a lower resolution spectrograph. The bottom spectrum in Figure 1, is the top spectrum but convolved with a Gaussian to give approximately the same instrumental resolution as the KPNO spectra. It is evident that the variation in an Hα profile can be entirely due to telluric water line variations, if the instrumental resolution is inadequate to clearly separate these variations out.

The time series of Lambda Cephei (spectral type O6f) shown in Figure 2 covers 6.5 hours. The average of this time series of observations is shown at the top of Figure 1. The lines below are the individual spectra divided by the mean, then normalized. Although there are suggestions of underlying broad (say about 10 Å) changes, these are less than the noise level. In the day to day observations shown in Figure 3, there is clear evidence of a variation at the Hα line of the emission feature at velocities near 200 Km s^{-1}, and on the absorption side at velocities near -300 Km s^{-1}.

The time series difference spectra, number 1 to 9 of Figure 2, can be analyzed to determine the statistical significance of any variations. The report by York et al. (1977) of a feature of FWHM 150 Km s^{-1} changing over a period of 6 hours is only slightly wider than some of the telluric water features, and leads to some difficultly in interpreting changes. The standard deviation of the spectra is in the range of 0.6 to 0.8% of the mean, other than for spectrum 9. Assuming the noise to have a normal distribution with this variance, the fluctuations must have an amplitude exceeding 2.57 standard deviations to have a less than 1% probability of chance occurence. This amplitude is indicated in Figure 2. The smoothed series of plots in Figure 2 are the same spectra as those on the left but averaged over 11 diodes. This reduces the variance by a factor of the square root of 11. The lines for a statistical significance of 99% are again drawn on the plot. It can be seen that there are many features which do vary significantly. But the features that are varying all correspond to the wavelengths of telluric lines, except for the feature at a velocity with respect to the Hα line of +200 Km s^{-1} (left dotted line). This exceeds the 99% significance level in records 1,2,3,6,7, and 8, going from an excess to a deficiency with respect to the mean. The variation occurs in the line (see Figure 1) near the top of the emission feature. The subtraction would be very sensitive to very small shifts of the line in this region. There are two reasons to think that this feature may not be stellar in origin. First, its variation correlates very well with the water lines at a velocity with respect to H of -700 Km s^{-1} (dotted line on right). And second, the feature shows no velocity shift over this time period, which might be expected in a wind. I conclude that real variations are present in the time series, but they are most likely due to telluric features.

Alpha Cam (spectral type O9.5Ia) was chosen because of spectral type, and the presence of the emission line at $H\alpha$. Of all the stars examined it seems to have the most significant variations, see Figure 4.

Delta Orionis (spectral type O9.5II) was observed because of the variation reported by York, et al. (1977). Observations made within one night, Oct 16/17, have no real indication of a change. There is only weak evidence for a profile change in five days, because of the confusion created by the different strength of the telluric lines. This star is a spectroscopic binary of period of 5 days, which produces velocity shifts, but probably not profile changes. This is shown in Figure 5.

The Sobolev approximation allows an estimate of the size of the region producing the photons in a given wavelength interval. Although the thickness of the shells of equal line of sight ve-

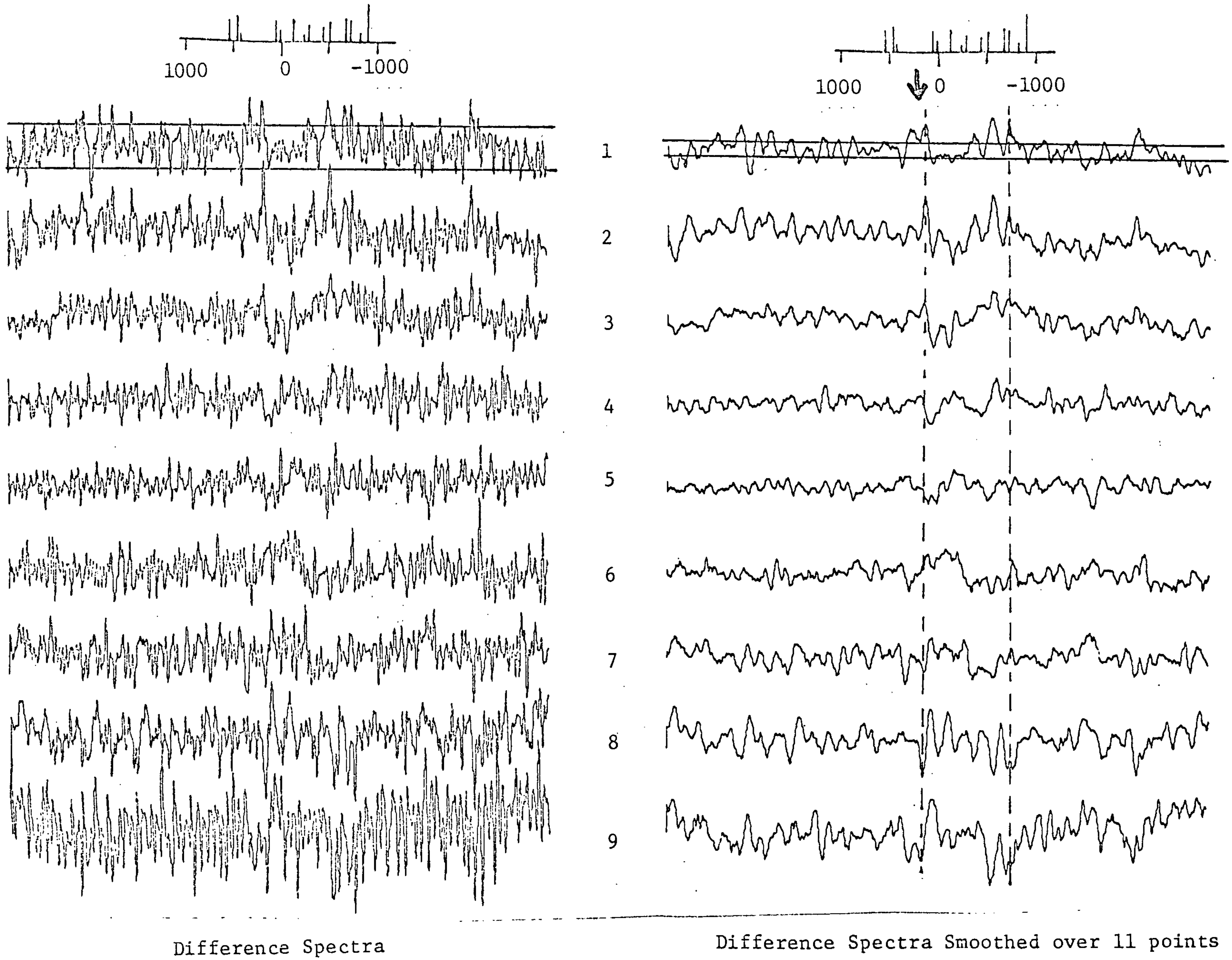

Fig. 2: Lambda Cephei time series

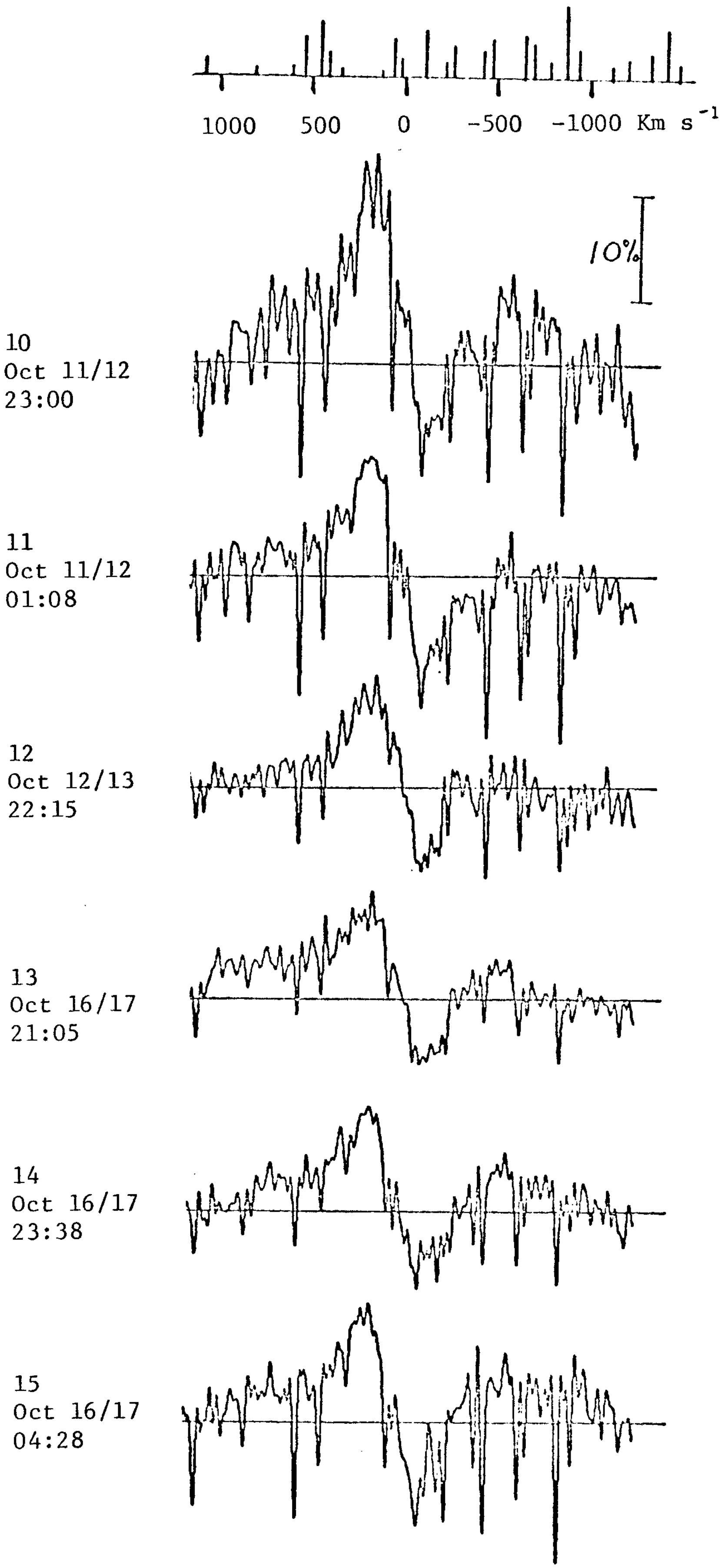

Fig. 3: Lamtda Cephei day tc day

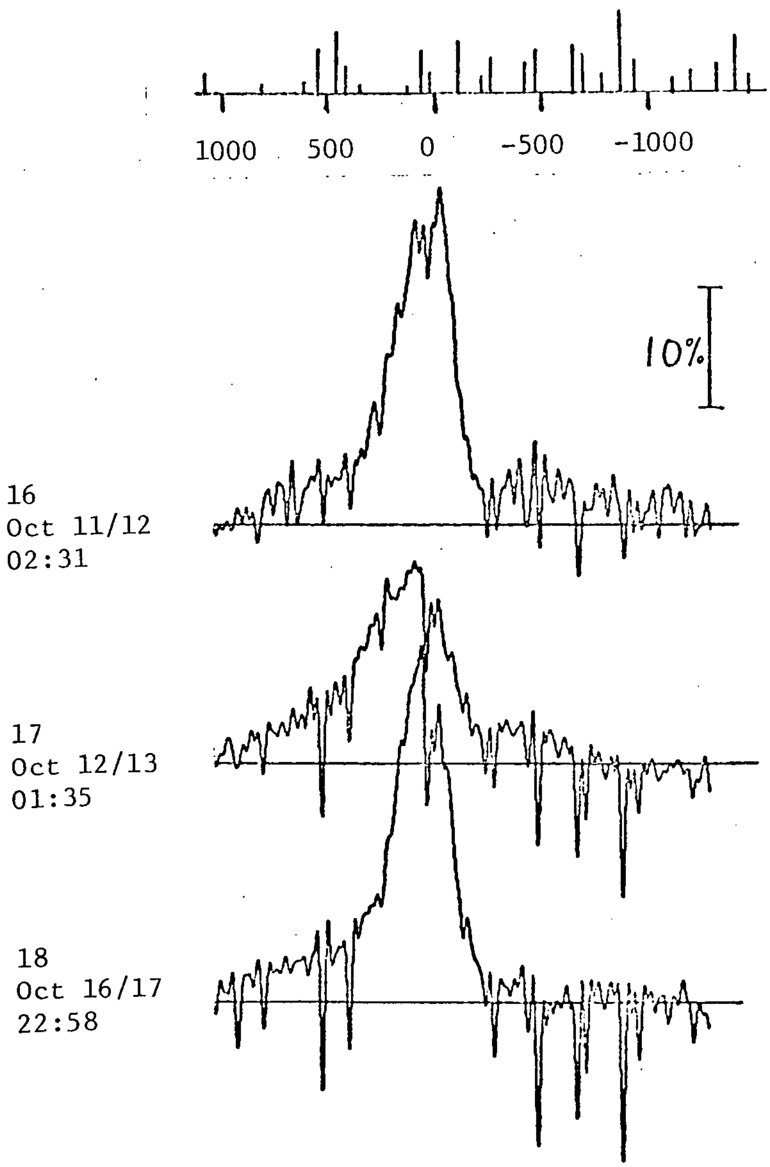

Fig. 4: Alpha Cam day to day

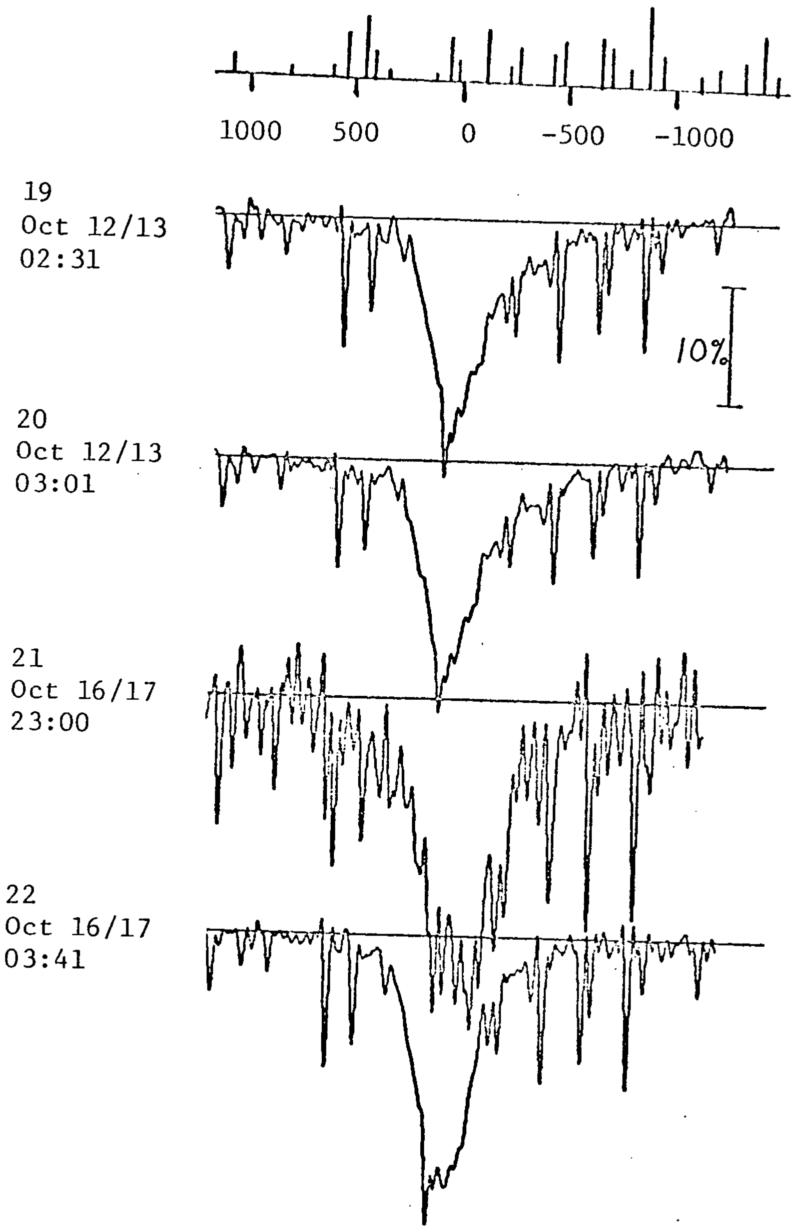

Fig. 5: Delta Ori day to day

locity will vary with the velocity and distance from the star, the contribution to the profile will be weighted towards regions of higher density. To estimate the total intensity in a wavelength interval, $\Delta\lambda$, all integrals of the emission over the shell will be replaced by average quantities. If the shell has an average line of sight thickness, Δs, then the total volume emitting in the wavelength interval is approximately $4\pi r_*^2 \Delta s f$, where f is a factor containing the difference between the true emitting area and the assumed disk of two stellar radii, $2r_*$. The constant f will be assumed to be 1. The thickness of the constant line of sight velocity shells is approximately constant over the region of dominant emission. These assumptions are justified by the actual calculations of line profiles as done by Cassinelli, et al. (1978). The error of these approximations may be as large as a factor of five, but depends on the line considered. The average shell thickness, Δs, will be estimated from the line of sight velocity gradient, dv/ds ($=\cos^2\phi\, dv/dr + \sin^2\phi\, v/r$, where ϕ is the angle between the line of sight and the star) as

$$\Delta s = \frac{\Delta\lambda}{\lambda}\frac{c}{dv/ds} = 1.4\times10^{11}\left(\frac{\Delta\lambda}{.3A}\right)\left(\frac{6562A}{\lambda}\right)\left(\frac{10^{-4}}{dv/ds}\right)\text{ cm.} \tag{1}$$

A fluctuation in the wind which changes the emission rate will be observed as some fractional change of the flux obtained by integrating over all regions emitting in that wavelength range. Assuming that the emission rate changes by 100%, in the following section an estimate will be made of the size of the fluctuation causing a given fractional intensity change. If the fluctuation is a region of size ℓ, only that part of the fluctuation which is moving at an appropriate velocity to effect the intensity in the wavelength interval contributes to the intensity change.

If the fluctuation is moving at a uniform velocity with an internal velocity dispersion less than the thermal speed, then the fractional change in intensity in one wavelength interval would be

$$\frac{\Delta I_\lambda}{I_\lambda} = \frac{\ell^3}{4\pi r_*^2 \Delta s} = 6\times10^{-3}\, \ell_{11}^3\, r_{12}^{-2} \left(\frac{\Delta\lambda}{.3A}\right)^{-1}\left(\frac{dv/ds}{10^{-4}}\right), \tag{2}$$

where ℓ_{11} is the size of the fluctuation moving with a common velocity, in units of 10^{11} cm, r_{12} is the size of the star in units of 10^{12} cm, $\Delta\lambda$ the spectral resolution in units of 0.3A, which was the spectrograph resolution used. A typical velocity gradient is found by taking a terminal velocity of 1000 Km s^{-1} reached over a distance of 10^{12} cm.

For a fluctuation which has a velocity gradient which is the same as the wind, the minimum volume emitting in a given wavelength interval would be just the velocity shell thickness cubed. In this case the intensity fluctuation is

$$\frac{\Delta I_\lambda}{I_\lambda} = \frac{(\Delta s)^3}{4\pi r_*^2 \Delta s} = 2\times10^{-5}\, r_{12}^{-2} \left(\frac{\Delta\lambda}{.3A}\right)^2 \left(\frac{10^{-4}}{dv/ds}\right)^2. \tag{3}$$

A more realistic situation might be if a fluctuation of size ℓ has only a thin slab of thickness Δs moving at the appropriate velocity to be in the desired wavelength interval. In this case

$$\frac{\Delta I_\lambda}{I_\lambda} = \frac{\ell^2 \Delta s}{4\pi r_*^2 \Delta s} = 8\times10^{-4}\, \ell_{11}^2\, r_{12}^{-2}. \tag{4}$$

The λ Cep time series restricts the magnitude of an intensity fluctuation to less than 2% over the six hour span. Equation 4 then limits the size of the largest region to change in this time to 5×10^{11} cm.

These observations have confirmed the variability of the stellar Hα line profile over times longer than one day, and conclusively show that the variation is due to the change in the profile, not changing telluric lines. The amplitude of the intensity change in any one pixel is only slightly greater than what might be due to noise, but considering that groups of more than 10 pixels show the same change gives considerable confidence to the physical reality of the change. The one time series of λ Cep has no convincing evidence for any short term variation, or evolution of the profile. The signal to noise in the time series spectra is only about 50, which was a constraint imposed on the maximum integration time by the detector cooling system.

CHAPTER 3. SUPERSONIC ACCRETION

Optical observations of variability are averages over the entire volume of emission at that particular wavelength. If the fluctuations in the wind contain components on a small scale compared to the scale of the wind, the detection of fluctuations by way of techniques in which the integrated light is observed, are limited by the signal to noise which can be acquired. The discovery of two X-ray binaries imbedded in stellar winds, namely Cen X-3 and 3U1700-37 (=HD153919) allows the possibility of using the X-ray source as a probe of the stellar wind. Since the X-ray luminosity is directly related to the rate of accretion of a small fraction of the stellar wind onto the neutron star, the intensity of the X-ray source can be used with the aid of a sufficiently detailed understanding of the accretion process to derive estimates of the density and velocity in the wind. This was the subject of the published paper which has been attached as Appendix 1. A summary of the principle results of the paper which support the conclusions of this thesis is given below.

A schematic drawing of the supersonic accretion process is shown in Figure 5 and the regions referred to are numbered in the figure. The incoming gas, region 1, is moving at a speed V with respect to the neutron star of mass M. The streamlines are bent in by the neutron star's gravitational field. The mass and the velocity define the accretion radius, $R_A=2GM/V^2$, which gives (apart from an efficiency factor which is close to one) the cross section for accretion of material. The incoming gas strikes a shock cone trailing the neutron star, called the

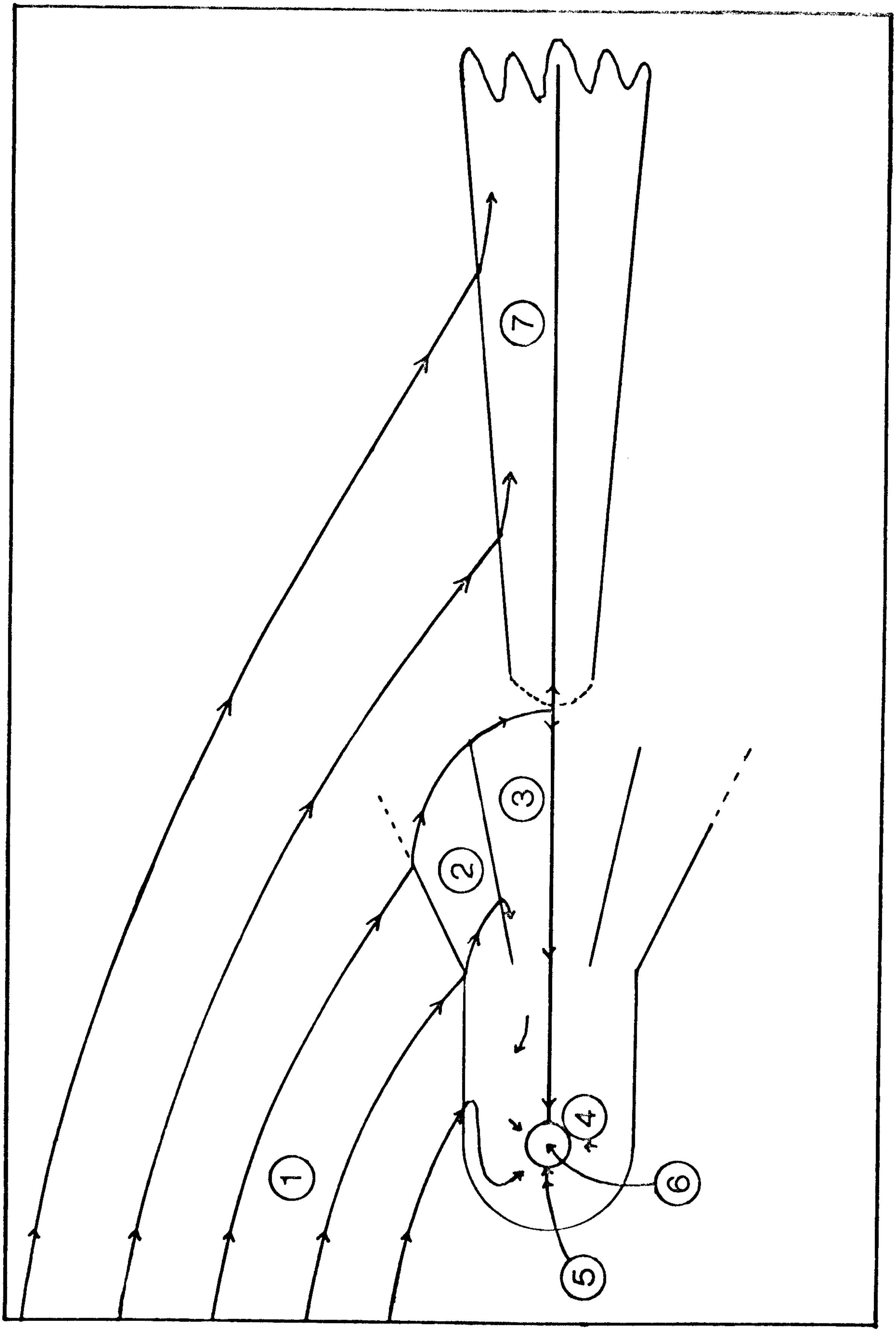

Fig. 6: Supersonic accretion schematic.

sheath, region 2. The gas is shock heated to a temperature of $3\times10^{6}(r/10^{11}cm)^{-1}$ K. If the density is sufficiently high the gas cools. In the sheath the gas loses its component of velocity away from the neutron star, joins the accretion column and starts falling down, region 3. Near the accreting neutron star the X-ray luminosity may be large enough to raise the temperature by Compton heating. The column will then expand out to an almost spherical inflow, region 4. Eventually the flow encounters the magnetosphere of the neutron star, region 5, below which the dynamics of the flow are regulated by the magnetic field. The gas strikes another shock a short distance above the surface of the neutron star, region 6, where the kinetic energy of infall is converted into thermal energy which is mostly radiated away as X-rays. The table below gives length and time scales characteristic of the different regions.

TABLE 2: SCALES IN SUPERSONIC ACCRETION

region	size scale	time scale
star	10^{12} cm	1 day
accretion column	10^{10-11} cm	500 seconds
magnetosphere	10^{8-9} cm	1 second
neutron star	10^{6} cm	1 millisecond

An analysis of this model yields several quantities which are directly related to the major parameters of interest in the stellar wind, the stellar wind density, n , and velocity. The luminosity of the unobscured source is

$$L = 4.7\times10^{36}\ n_{11}\ V_{8}^{-3}(M/M_{\odot})^{3}(R_{X}/10^{6}\ cm)^{-1}\beta\ erg\ s^{-1}, \qquad (5)$$

where β is a factor usually of order one giving the efficiency of the accretion, $n_{11}=n_0/(10^{11}\ \mathrm{cm}^{-3})$, and $V_8=V/10^8\ \mathrm{cm\ s}^{-1}$.

The angle that the shock cone makes with the axis of the accretion column is

$$\theta = 2.7^\circ\ (T_{col}/10^6\ \mathrm{K})\ V_8^{-2}\ . \qquad (6)$$

The temperature in the column, T_{col}, is not directly observable, but an upper limit can be obtained by considering the heating and cooling processes,

$$(T_{col}/10^6\ \mathrm{K}) < 1.9\ n_{11}^{4/15}\ V_8^{4/15}. \qquad (7)$$

This can be used to estimate the optical depth up the centre of the accretion column, τ_{col}, due to electron scattering

$$\tau_{col} > 2.2\ n_{11}^{-8/15}\ V_8^{52/15}. \qquad (8)$$

The electron scattering optical depth up the sheath is less than that up the column if $n_{11} V_8^{-2} < 3.5$, which is independent of the estimate of the column temperature. With these simple relations in hand and some X-ray data of an object that is clearly fueled by a stellar wind it is possible to confirm the model of the accretion process outlined above. More importantly the observations can be used to derive the density and velocity in the wind.

Two fairly good sets of published data exist for the source Cen X-3, which appears to be the clearest case of accretion from a spherical supersonic wind. The source 3U1700-37 (=HD153919) would appear to be a very strong stellar wind source from its optical spectrum (see Fahlman, Carlberg, and Walker 1977) although there are significant effects in the spectrum associated with the period of the neutron star orbiting the O6f primary. These effects may be due to a wake of disturbed gas trailing the neutron star (see Appendix 1). Or they may represent a significant distortion of the stellar wind itself. In any case, the X-ray data from 3U1700-37 has a lower count rate than Cen X-3, hence greater statistical errors. In Cen X-3 the observational situation is almost the exact reverse; the X-ray source is one of the brighter sources in the sky, but its optical companion is a 14th magnitude OB star which has been poorly studied (Conti 1978).

The X-ray data for Cen X-3 shows several scales of variability; a 4.8 second pulsation period, ascribed to the rotation of the neutron star and its magnetic field, a 2.1 day orbital period sometimes superposed with "anomalous dips", and an aperiodic change in the mean intensity level with a time scale of order one month. A particularly exciting observation was made by Pounds, et al. (1975), who observed regular dips occurring every orbit during a transition from X-ray low to high state. Jackson (1975) proposed that the two distinct dips were due to the reduction of the received flux by scattering in the two sides of the sheath of the accretion column. He deduced a velocity of the wind with respect to the neutron star of between 375 and 620 km s^{-1}, and a column semi-angle of 20°. From equation (6) and the velocities quoted by Jackson, the implied column temperature is in the range $3.5-9.6\times10^{5}$ K. Schreier et al. (1976) estimate the density in the wind as $1-5\times10^{11}$ cm^{-3}. These two estimates are consistent with the limiting temperature of 1.5×10^{6} K from Equation (7). Accepting Jackson's proposal that the double dips are due to scattering in the sheath, but using the theory developed in Appendix 1, more information can be derived from the observations. Pounds, et al. (1975) note that the relative depths of the dips decrease as the source turns on. Also, from inspection of their published data one can see that the dips appear to become single as the source turns on. A schematic tracing of the X-ray intensity is shown in Figure 7.

From these observations and the model of the long term variations proposed by Schreier, et al. A rough trajectory of the variation of the stellar wind density and velocity can be plotted, which is shown in Figure 8. At point A the source is in the X-ray low state and at B the high state. Adopting the estimate of Schreier et al. for the low state density as $5x10^{11}$ cm^{-3}, and high state density of 10^{11} cm^{-3}, fixes the densities at point A and B, but not the velocity. The data shows that as the wind density decreases allowing the source to become visible, the velocity must be such that the optical depth up the sheath exceeds the column optical depth, and be close to one in order to provide the deep dips. This puts point A near the $\tau_c=1$ line. As the wind density drops the dips have a decreasing fractional depth, which means that the velocity must be dropping fast enough that the density and velocity are moving further below the $\tau_c=1$ line. Eventually the dips become single as the density and velocity cross the $\tau_s>\tau_c$ line. The combined density and velocity variation is such that the accretion rate, and hence the intrinsic luminosity only increase slightly while going from low to high state. The source settles down at the high state, point B, with a density of 10^{11} cm^{-3} and a wind velocity with respect to the neutron star of about 500 Km s^{-1}. The optical depth up the column is so small that dips are not

Fig. 7: Cen X-3 X-ray Intensity Schematic

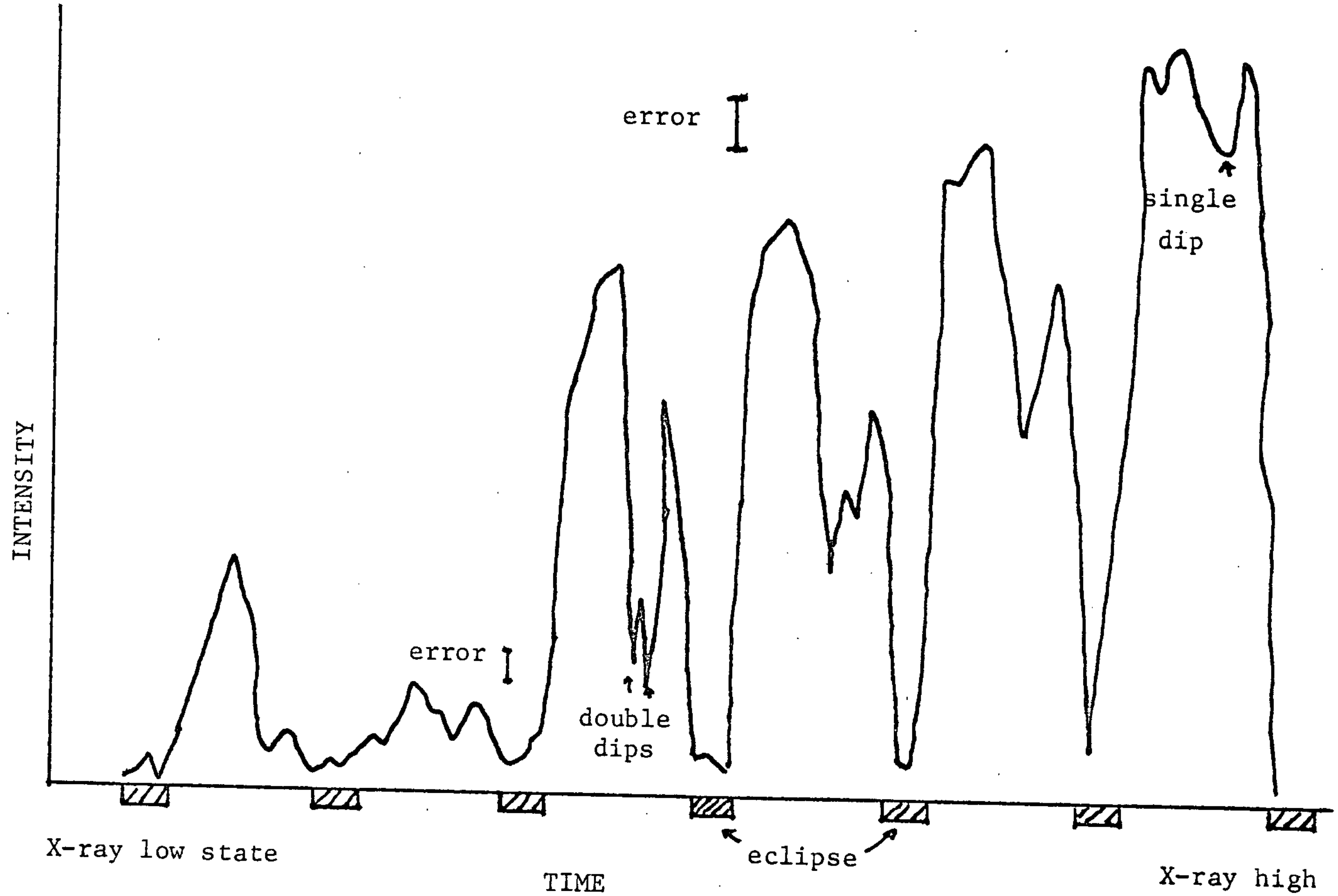

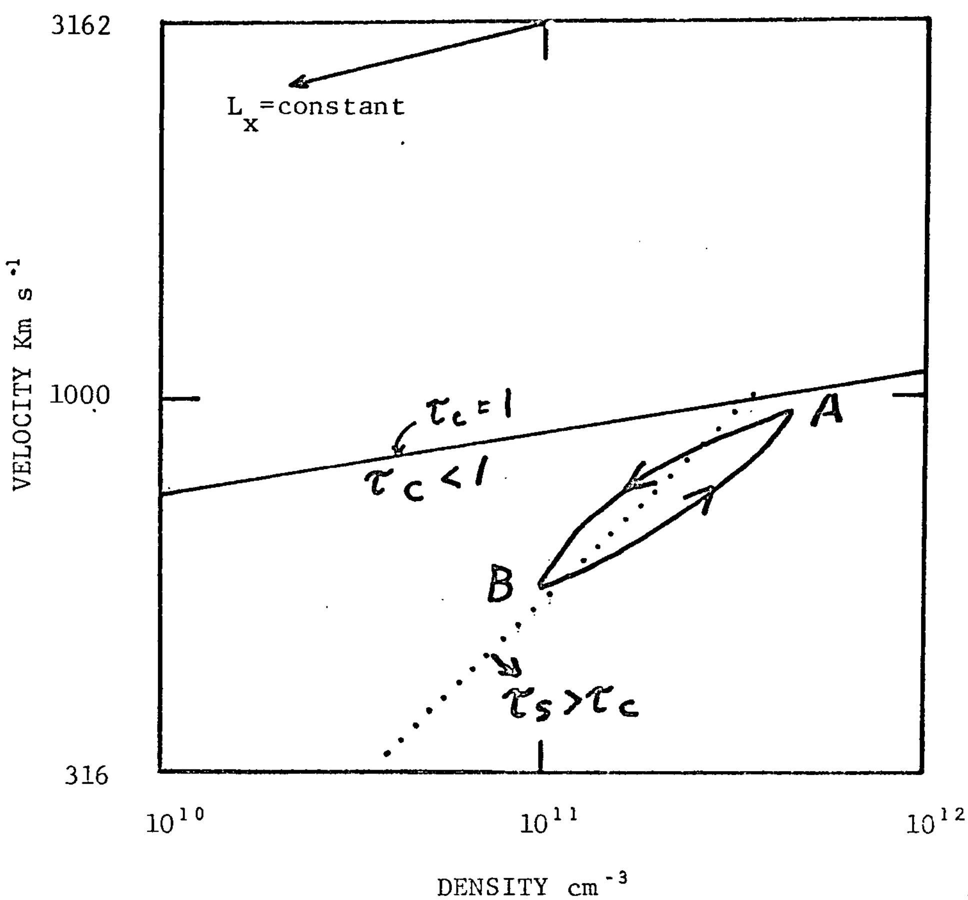

Fig. 8: Density Velocity Variation of Cen X-3

seen regularly. When the source starts to turn off the data suggests that a different density velocity trajectory is followed, such that the optical depth up the column and sheath always remains small. As the source approachs the point A again it is obscured by the increasing density of the stellar wind.

If the trajectory of the variation of the wind velocity and density is schematically correct it is possible to draw a conclusion as to the driving force for the wind. The trajectory in Figure 8 suggests a correlation between the wind velocity and the wind density which would imply the acceleration of the gas up to the location of the neutron star increases as the density in the wind increases. In the radiatively driven wind of CAK the acceleration of the wind varies as n^{-} , where is a constant slightly less than one. This implies that the radiation acceleration should drop as the density increases. On the other hand Hearn (1975) suggests that the wind is initially accelerated in a hot corona. The corona would heated by shock waves which grow from instabilities within the atmosphere. As will be discussed in Chapter 5, one of the dominant instabilities present is the thermal instability which grows on a time scale which varies as n^{-2}. This instability may provide the correlation between wind velocity and density.

The one month scale of the high low state variability is an enigma. There appears to be no natural scale in the wind to explain it, so it may be connected to the subatmosphere of the star (Cannon and Thomas 1977 and Thomas 1973).

The observations of Schreier <u>et al</u>. (1976) contain evidence that there are small scale (of order 10^{11} cm) fluctuations in the wind. The count rate clearly varies with an amplitude greater that the statistical error on time scales of about one hour. This time scale, which has been set by the spacecraft earth orbit and pointing mode, is much longer than the natural response time of the accretion process, which is about ten minutes, from Table 2. It would be extremely interesting to have data with a time resolution of a few minutes to see if the fluctuations in the wind become time resolved.

In summary the theory of supersonic accretion that was developed and applied to a limited amount of data on Cen X-3 shows that there is a positive correlation between the wind density and wind velocity during a period of transition from X-ray low to high state.

CHAPTER 4. PHYSICAL DESCRIPTION OF THE GAS

The stability of the wind will be investigated with a linearized stability analysis. The analysis requires that the prevailing physical conditions be specified. This chapter is devoted to the derivation of the required quantities. The difficult physical quantities are those describing the interaction of the gas and the stellar radiation field, which are the rate of energy gain and loss, and the radiation acceleration. Since this interaction is probably the key to the stellar wind, an accurate physical description must be used.

In order to derive the cooling rate, heating rate, and radiation force it is necessary to know the distribution of atoms over the various stages of ionization, and the rate of absorption and emission of radiation by the ions. These calculations require atomic constants to describe the radiation processes, which then become functions of the local density, temperature, and radiation field.

The radiation field is influenced by the flow of the gas, so that a good approximation to the radiation field would require knowing the details of the flow. As an approximation I have taken the unattenuated, but geometrically diluted stellar radiation field. This offers the advantage of retaining a completely local analysis at the cost of oversimplifying the radiative transfer. The approximation of the unattenuated field will have the effect of somewhat over estimating the radiation force because overlapping lines are ignored. As discussed later the effect is likely to be at most a factor of two.

The gas is assumed to be in ionization equilibrium, which is valid for time scales longer than the recombination time scale, 30 $(T/10^4\ K)^{1/2}\ n_H^{-1}$ seconds. Equilibrium implies that the rate of transitions out of an ionization state is balanced by the rate in. For element i the rate out of ionization state j is determined by the rate of ionization to the next higher ion and the recombination rate to the next lower ion. The rate into the ionization state is determined by recombinations from above and ionizations from below. Algebraically,

$$n_{ij}\ (n_e C_{ij} + \zeta_{ij} + n_e \alpha_{ij}) =$$
$$n_{i,j-1}\ (n_e C_{i,j-1} + \zeta_{i,j-1}) + n_{i,j+1}\, n_e \alpha_{i,j+1}$$

where $C_{ij}\ (n_e, T)$ is the collisional ionization rate out of j

ζ_{ij} is the photoionization rate

$\alpha_{ij}(n_e, T)$ is the recombination rate from level j to j-1.

These ionization balance equations were solved for as many atoms of significant stellar abundance for which good atomic data was available. The elements used are shown with their assumed abundances in the accompanying table. It would have been desirable to have included Nickel and Iron with their fairly high cosmic abundance and great number of spectral lines, but no reliable and consistent set of data for a wide temperature range could be found.

TABLE 3: ATOMIC ABUNDANCES

ELEMENT	Z	ABUNDANCE
Hydrogen	1	1.0
Helium	2	8.5×10^{-2}
Carbon	6	3.3×10^{-4}
Nitrogen	7	9.1×10^{-5}

Oxygen	8	6.6×10^{-4}
Neon	10	8.3×10^{-5}
Magnesium	12	2.6×10^{-5}
Silicon	14	3.3×10^{-5}
Sulfur	16	1.6×10^{-5}

These abundances were taken from Allen (1973).

Standard rates were used for all the photoionization cross sections, recombination rates, and collisional ionzation rates. But since the gas has a fairly high density (order 10^{11} cm^{-3}) and is in an intense radiation field it is necessary to make some corrections. The density effects are allowed for by adding corrections to the recombination rate for three body recombinations, and recombination to upper levels. A small correction for ionization out of upper levels is also included. The greatest difficulty is allowing for the effect of both the radiation field and the density effects on the dielectronic recombination rate. This process depends upon captures to levels of large quantum number, and it is possible that these levels may be reionized before they can stabilize by cascading down to lower levels. These effects have been crudely allowed for by calculating a multiplicative correction factor, based on a fit to the quantum mechanical calculations of Summers (1974). All these rates and corrections are discussed in Appendix 2.

The Ionization Balance

The solution to the ionization balance equations is very simple since the lowest level only interacts with the second level, and then the second level is linked to the first and third, and so on. This gives the ratio of the population in a ionization state to the population in the next lower level. A normalization completes the solution. The equations are weakly nonlinear through their dependence on the electron density, but usually two or three iterations suffices for an accuracy of about 1 part in 10^6. The results are given in terms of the ionization fraction X_{ij} for ion j of atom i, where X_{ij} summed over j is unity. To get the number of atoms of type i,j we take the product $X_{ij} A_i n$, where A_i is the abundance of atom i. In Figure 9 the ionization balance for a gas of density 10^{11} cm^{-3}, in the undiluted radiation field of the star, is shown for a range of temperatures. It is found that for the range of densities of interest the reduction of the dielectronic recombination rate by the density and radiation field effects is significant and tends to shift the ionization slightly to higher stages of ionization. At very high densities the distribution approaches to the distribution expected for LTE.

The heating and cooling rate for a gas of density 10^{11} cm^{-3} in a undiluted radiation field are shown in Figure 10. The plotted quantities are the cooling and heating rates, Λ and Γ, respectively. The plotted quantities are to be multiplied by the density squared to obtain the rates per cm^{-3}. The generalized cooling rate is taken as $\mathcal{L} = n^2 (\Lambda - \Gamma)$. The quantity $\mathcal{L}/n^2$ is plotted.

The radiative equilibrium between the photoionization heating and radiative losses holds at temperatures of about 2×10^4 K for densities around 10^{11} cm^{-3}. This is shown in Figure 10 for zero velocity of the gas with respect to the star. Of interest

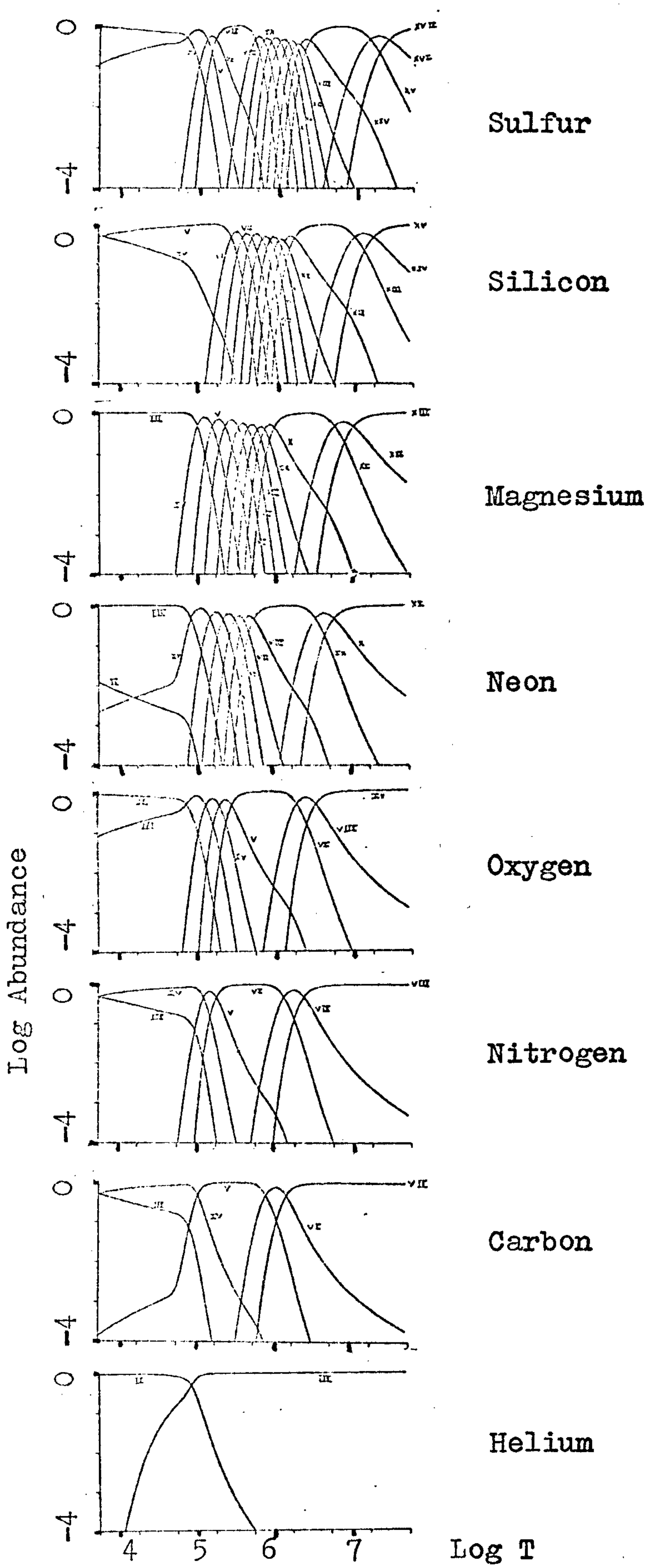

Fig. 9: Ionization Balance

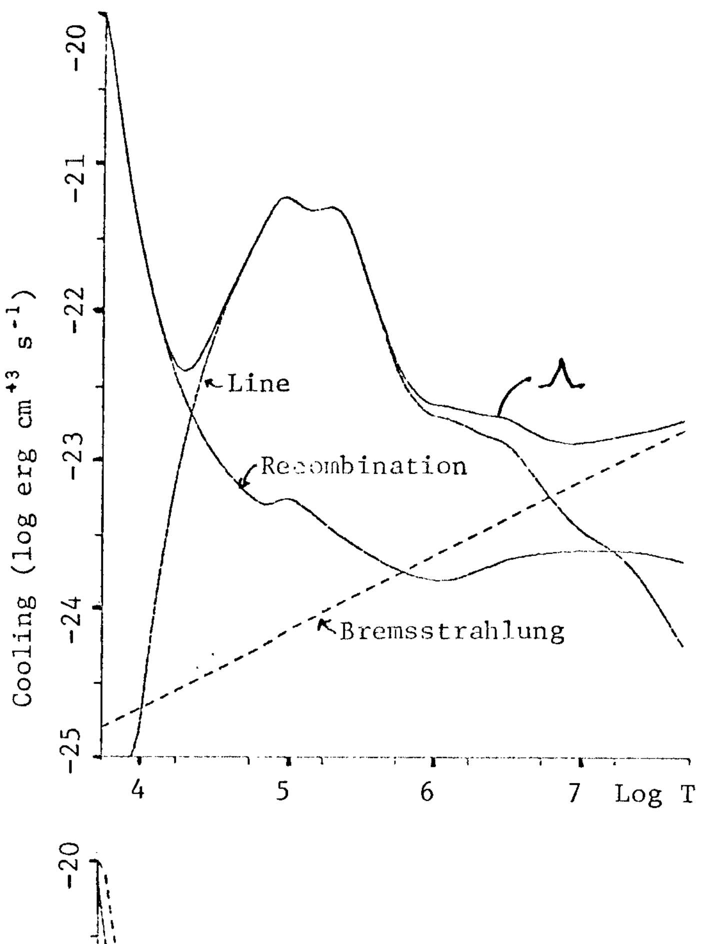

Fig. 10: Heating and Cooling Rates for Solar Abundances

to the "warm radiation acceleration" model is that near 2×10^5 K the loss rate in an optically thin medium is at a maximum. Such a temperature would be very difficult to maintain in the gas, requiring an immense input of energy from some other heat source. Between 10^6 and 10^7 K the loss rate drops to a minimum where the radiative losses would be more easily balanced. The radiation losses from such a hot gas would consist largely of X-rays, which would be suitable for producing the O VI ion, as has been suggested by Cassinelli and Olson (1978).

The gas is thermally unstable (see Field 1965) to both isochoric and isobaric disturbances when the temperature derivative of the generalized cooling rate at constant density is negative. The temperature gradient is not quite steep enough (logarithmic derivative of the cooling rate less than about -3) at any point to admit isentropic instability, wherein ordinary sound waves gain energy in the rarefactions and lose it in compressions. Even if there is a slight inaccuracy in the calculations such that this isentropic instability condition could be met, it would appear in a very narrowly defined temperature interval. Calculations by Raymond *et al.* (1978) indicate that with the inclusion of the iron group elements the slope becomes even less steep, and the gas is further away from isentropic instability.

The loss rate and its derivative turns out to be critical to the stability of an accelerating atmosphere, so it has been plotted it for the CNO elements enhanced by a factor of 10 in Figure 11. Obviously the abundance has a strong effect on the cooling rate, since the CNO elements are responsible for the cooling in the range 10^5 to 10^6 K.

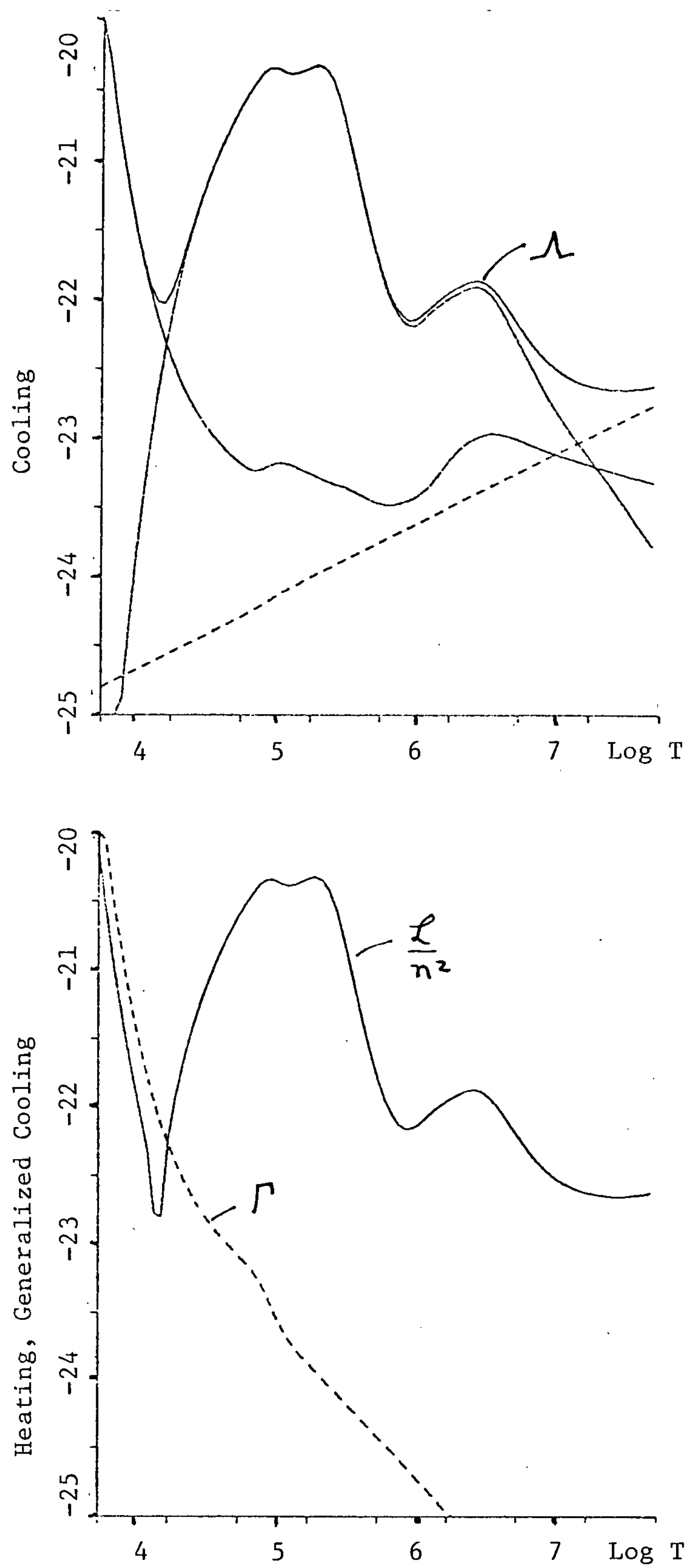

Fig. 11: Heating and Cooling with CNO=10*Solar

The stellar wind is usually optically thin at optical and longer wavelengths for continuum emission, but can become optically thick in the resonance lines, which provide the line cooling as well as most of the radiation acceleration. Using the alteration to the loss rate of Rybicki and Hummer (1978) the reduced cooling rate is shown in Figure 12 for a velocity gradient of $dv/dz=10^{-3}$. Note that the specific cooling rate (units of erg cm^{-3} s^{-1}) will still increase approximately linearly with density, since the losses vary with the cooling rate in erg cm^{+3} s^{-1} times the density squared, over the optical depth. This is a very rough calculation, since no allowance has been made for the change of the local intensity due to the optically thick lines.

Radiation Force

The radiation force is defined as

$$g_{rad} = \sum_{ij} \frac{A_i\, x_{ij}}{\bar{m}} \quad \frac{\pi F_\nu}{c}\, \sigma_{ij}(\nu)\, d\nu, \tag{9}$$

where $\bar{m} = \sum_i A_i m_i$, and m_i is the atomic weight of the various ions. If the unattenuated radiation field is used it provides an upper limit to the radiation force. A more realistic estimate is supplied by the method used by Castor, Abbott, and Klein (1975), which is based on an analysis of the radiative transfer in one spectral line originally done by Lucy (1971). With the aid of the Sobolev approximation the problem can be solved and it is found that the force due to lines is

$$g_{rad} = g^{\circ}_{rad} \quad \frac{1-e^{-\tau}}{\tau} \tag{10}$$

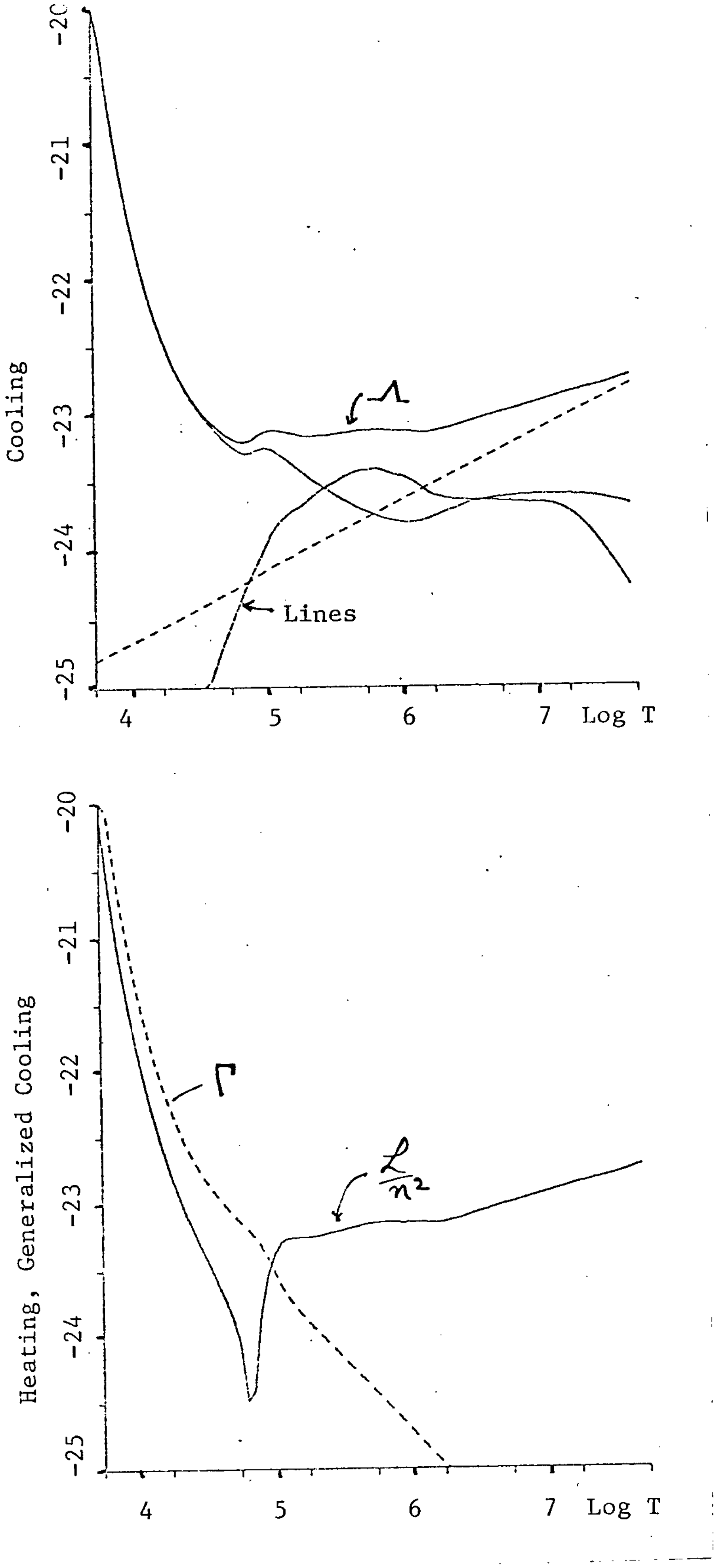

Fig. 12: Cooling with optically thick lines.

where $\tau = \pi e^2/(mc)\ f_{ij}(l) A_i X_{ij}\ nc[1/2(1+\mu^2)$
$(dv/dz - v/r) + v/r]^{-1}$ (11)

and $\pi e^2/(mc) = .02654$

g^{o}_{rad} is the acceleration in an optically thin gas

$f_{ij}(l)$ is the oscillator strength for line l of atom i ionization state j,

c is the speed of light

μ is cosine of the angle subtended by the stellar radius from the point in the gas.

In addition to the force on the lines there is the force on the electrons,

$$g_e = \frac{\pi F}{c} \sigma_e \frac{n_e}{n \bar{m}} \tag{12}$$

where F is the flux integrated over all frequencies, and is the Thomson cross section. The force on the electrons in the undiluted radiation field in a completely ionized gas is 194.7 cm s^{-2}. There also is the force on the continuum, which is usually quite small, with the undiluted radiation field at a density of 10^{11} cm^{-3} it is 63.48 cm s^{-2}.

The line acceleration is dominated by optically thick lines, and increases almost linearly with the velocity gradient. A schematic of the acceleration as a function of dv/dz is shown in Figure 11 below. In Figure 13, the acceleration is a weak function of temperature in the range $10^4 < T < 3x10^5$ K, but for temperatures larger than $2x10^5$ the force on the lines rapidly decreases. The slight hump at $2x10^5$ K is due to the CNO elements changing ionization state and the entry of some new strong lines. The rapid fall off is due to the removal of ions that

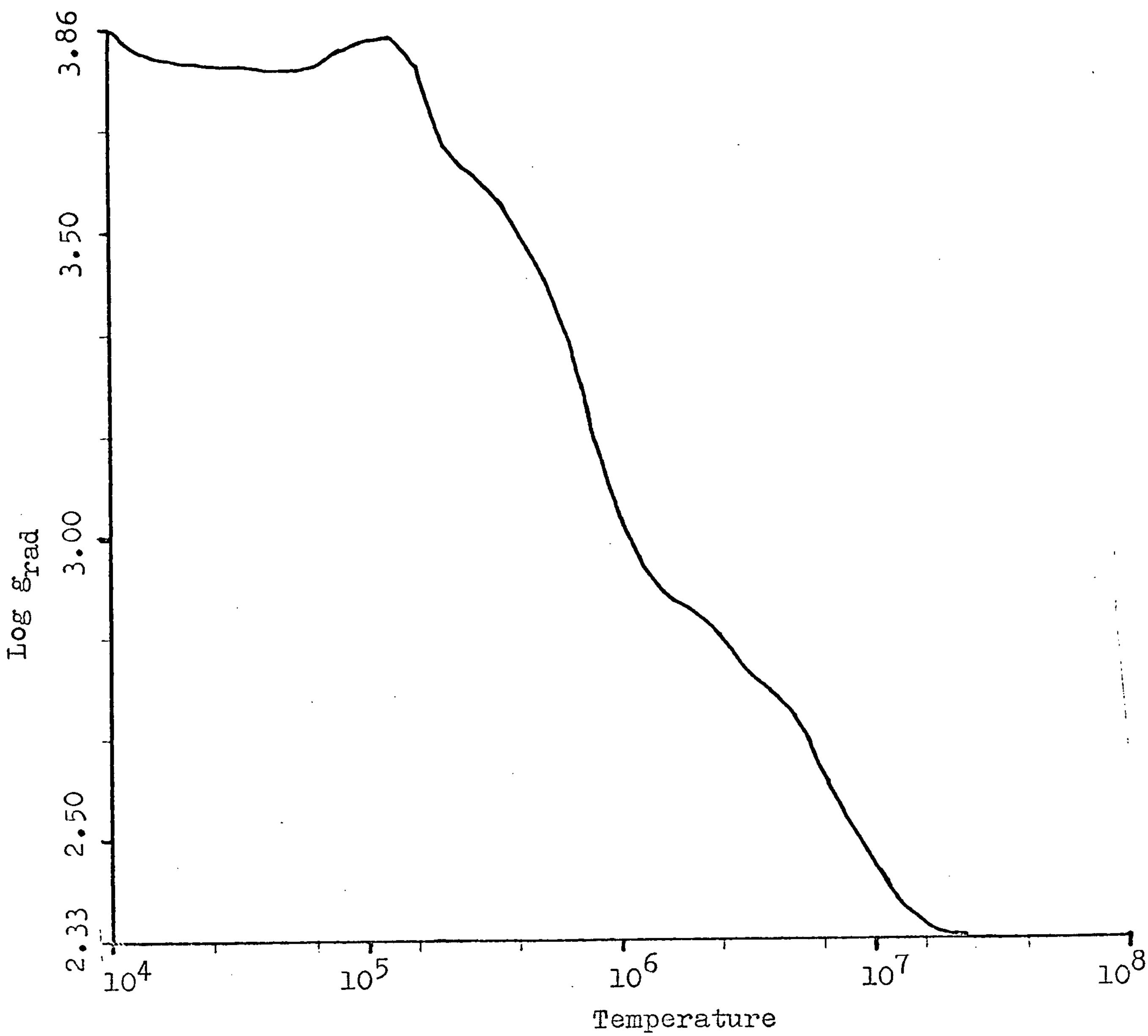

Fig. 13: Radiation Force as a Function of Temperature

have resonance lines near the maximum of the stellar radiation field. The only force left beyond 10^7 K is the force on the electrons.

The acceleration found here can be compared with the result found by CAK. The acceleration can be represented in the same form as they have,

$$g_{rad} = g_e \; M(t), \tag{13}$$

where $t=\sigma_e n_e v_{th} (dv/dz)^{-1}$, g_e is the radiation force on the electrons, and v is the thermal velocity. I find that $M(t) = .067\ t^{-0.91}$ for $n=10^{10}$, and $M(t) = .022\ t^{-0.83}$ for $n=10^{13}$ cm^{-3}, whereas CAK find $.033\ t^{-0.7}$, which is good agreement. There are two reasons for the density dependence of the acceleration. First, a few of the lines go from optically thick to thin as the density goes down, and secondly, the ionization balance is density dependent in this calculation, through the allowance for collisional ionization, and through the density dependence of the rate coefficients.

The deficiencies in this calculation of the radiation force are due to a somewhat limited line list, mostly due to the lack of any iron group elements, and more seriously a very simple treatment of radiation transfer. Within the approximation used these two deficiencies cancel each other out to a certain extent. The radiation force has been over estimated by not taking account of overlapping lines, which would involve formulating a model of the atmosphere intervening between the point in the gas and the star. The radiation force increases with the number of lines present, but the flux available decreases as the number of lines goes up. Klein and Castor (1978) have reported on new calculations made by Abbott of the radiation force. He finds that the original CAK law is bracketted by two alternative transfer schemes, and probably the CAK law represents a good approximation to the force. The calculations here are in good agreement with the CAK law.

The line acceleration varies approximately as (n_{ij}/n) $((dv/dz)/n_{ij})^{\alpha}$ where α is in the range 0.7 to 0.9. As the velocity gradient increases all lines become optically thin, and the force levels off at the maximum value. This means that the force depends on the abundances roughly to a power in the range of .1 to .3, which is a very weak function. Therefore, the radiation force is insensitive to the assumed abundances for flows in radiative equilibrium because most of the lines are optically thick.

One aspect of the radiation transfer which is important to the analysis of the stability of the flow is the shape of the lines, which can provide an immediate source of instability, as has been reported by Nelson and Hearn (1978). The instability they find only acts in subsonic flow. This has been left out because it is dependent on the details of the radiation transfer.

Momentum Balance

The number of free zero order quantities can be reduced by requiring that the equations of mass and momentum conservation be satisfied. In the case of radiative equilibrium the temperature is determined by the balance of heating and cooling, otherwise the temperature is just arbitrarily specified.

To illustrate the solutions of the mass and momentum equations the one dimensional equation of mass conservation is substituted into the momentum balance equation (see CAK and in Chapter 5, below) with zero temperature derivatives,

$$\left(v - \frac{2RT}{v}\right)\frac{dv}{dr} = \frac{2RT}{r} - g + g_{rad}. \tag{14}$$

where the form of the mass conservation equation for a spherically symmetric system has been used. Spherical geometry has been used partly because the density gradient remains negative even if the velocity gradient acquires a small negative value. The perturbations are in the form of plane waves, so all derivatives will be made with respect to the height z, instead of r.

The independent variable is chosen to be dv/dz. In Figure 14 the two sides of the momentum equation are shown as functions of dv/dz. For supersonic flow, $v^2>2RT$, there is always one decelerating solution, where the radiation force is less than the gravitational field. As can be seen from Figure 11, if the velocity isn't too large there are two solutions in which the gas is accelerated outwards. For typical stellar wind conditions the two solutions have dv/dz approximately equal to 10^{-4} and 1. The two solutions are acceptable locally, but boundary and continuity conditions may rule out the high gradient solution. By imposing continuity of velocity from subsonic to supersonic flow CAK restrict themselves to the low gradient solution. The solution with the large velocity gradient is accelerating so rapidly that the wind becomes optically thin in the resonance lines. This means that if the acceleration could be maintained over a distance of 0.1% of the stellar radius, the gas would be moving

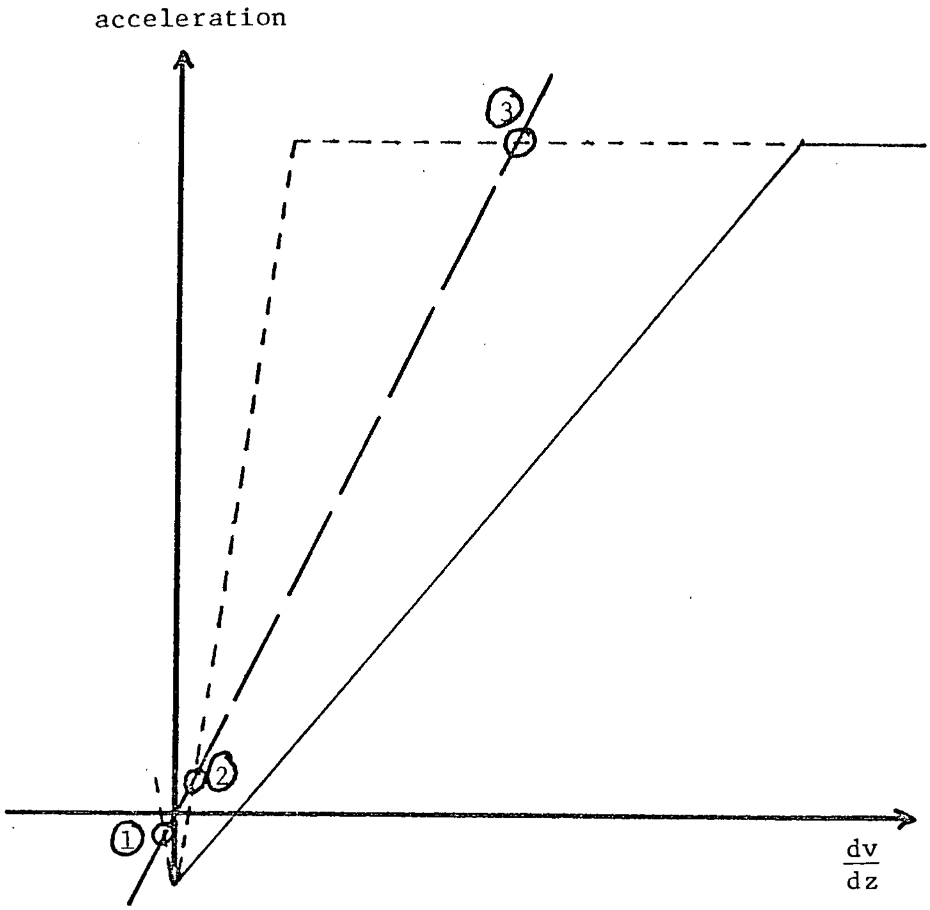

Solution to $\left(v - \frac{2RT}{v}\right)\frac{dv}{dz} = \frac{2RT}{r} - g + g_{rad}.$

$\left(v - \frac{2RT}{v}\right)\frac{dv}{dz}$

$\frac{2RT}{r} - g + g_{rad}$, low density

$\frac{2RT}{r} - g + g_{rad}$, high density

1 dv/dz < 0

2 dv/dz > 0

3 dv/dz > 0, high gradient solution

Fig. 14: The Momentum Equation Solution

at the terminal velocity. Although this solution is physically acceptable, observational evidence suggests that it may not be realized.

As can be seen from Figure 14, if the velocity becomes too large no accelerating solution can be found. The maximum velocity for which accelerating solutions exist varies with the gravity and the density of the gas. A table is given below which indicates the maximum velocity giving an outward acceleration. In Table 4 the Vmax column gives the maximum velocity at which a positive dv/dz can be found, the value of which is given in the next column. Two values for the gravity are used to show that the maximum velocity with dv/dz>0 is mostly effected by the gas density. The gas was chosen to be in radiative equilibrium, which gives a temperature of $2x10^4$ K.

TABLE 4: LIMITING VELOCITY FOR ACCELERATING SOLUTIONS

	$g=10^4$cm s^{-2}		$g=4000$cm s^{-2}	
	Vmax	dv/dz	Vmax	dv/dz
$n=10^{10}$	$4.1x10^8$	$.16x10^{-3}$	$4.45x10^8$	$.84x10^{-4}$
$n=10^{11}$	$4.7x10^7$	$.16x10^{-2}$	$5.2x10^7$	$.16x10^{-2}$
$n=10^{12}$	$5.7x10^6$	$.15x10^{-2}$	$6.0x10^6$	$.64x10^{-2}$

Table 4 shows that the maximum velocity is approximately inversely proportional to the density. The maximum velocity for acceleration decreases nearly to the sound speed at a density of 10^{12} cm^{-3}. Below this velocity the Sobolev approximation used for deriving the radiation acceleration is invalid.

If a large portion of the flow, thicker than one Sobolev shell, (the sound speed divided by the velocity gradient) acquires a velocity which is greater than the maximum for a positive velocity gradient in momentum balance, then the gas will deccelerate. This situation could arise if the flow is a chaotic medium in which elements of the fluid are propelled to velocities in excess of the maximum for acceleration, or have a density increase which makes the velocity greater than the maximum. The wind might consist of many, quite large patches, which are being accelerated and deccelerated with respect to one another. Where these regions collide their supersonic velocities would ensure shock heating which would produce temperatures appropriate to O VI and like ions. This shock heated gas would only comprise a small portion of the total gas in the flow, and after forming would be blown away from the star.

CHAPTER 5. THE STABILITY ANALYSIS

The observations suggest that a stellar wind is an extremely variable, inhomogenous flow. On scales of a day to years there are large general variations, which may originate within the star. The X-ray observations suggest small scale fluctuations of order 10^{11} cm. This observed variability could have two causes: the flow may start out in the lower atmosphere as smooth, and then enter a region of instability where it breaks up; or the existence of the flow may be depend upon some instability.

In this section the local stability of the flow will be investigated. This will be done by considering the propogation of infinitely small disturbances, i.e. a linearized analysis, with wavelengths short compared to the scale of variation within the stellar wind. This analysis is directed towards finding instabilities that are rapid amplifiers, i.e. the growth time scale is shorter than the time to move one scale length in the atmosphere; and absolute instabilities, which can actually generate oscillations or lead to "clumps" within the wind. One major limitation of this analysis is that it has only been done for one dimensional wave propogation, that is the waves can only have a velocity component which is oriented along the direction of propagation. For instance, this immediately rules out the possibility of the Rayleigh Taylor instability. (Krolik 1977, Nelson and Hearn 1978). Similar analyses, but with more approximations in the linearization, have been performed by Hearn (1972) and for quasars by Mestel _et al._ (1976).

The basic equations that apply are the conservation of mass

$$\frac{\partial \rho}{\partial t} + \nabla\cdot(\rho\vec{v}) = 0. \tag{15}$$

where ρ is the mass density and $\vec{v}$ is the gas velocity. The conservation of momentum neglecting the viscosity is given by,

$$\frac{\partial \vec{v}}{\partial t} + \vec{v}\cdot\vec{\nabla} v = \frac{-\nabla P}{\rho} - \vec{g} + \vec{g}_{rad}, \tag{16}$$

where g_{rad} (which will be sometimes abbreviated as g_r) is the acceleration due to radiation, P is the gas pressure, and g is the gravitaticnal acceleration. The conservation of energy is expressed,

$$\frac{\partial(\rho[\frac{1}{2}v^2+e])}{\partial t} = -\nabla\cdot\left(\rho\vec{v}[\tfrac{1}{2}v^2+h] - \kappa\nabla T\right) - \mathcal{L}, \tag{17}$$

where e and h are are respectively the specific internal energy and enthalpy. $\mathcal{L}$ is the generalized cooling rate in the frame of the gas, defined as $\mathcal{L}=L-(1-v/c)G$, where v is the velocity of the gas relative to the star and L and G are the local specific cocling and heating rates, respectively. The thermodynamic relaticns required are an equation cf state

$$P = kT(n+n_e), \text{ where } n_e = \sum_{ij}(j-1)n_{ij}. \tag{18}$$

The sum i,j is over the ionization states and the elements, respectively. The number density of atoms and electrons are n and n_e. The internal energy is

$$e = 3/2\ kT(n+n\ ) + \sum_{ij} n_{ij}\chi_{i,j-1}, \tag{19}$$

where χ_{ij} is the icnization energy of ion i,j with density n_{ij}. The enthalpy is defined as,

$$h = e + P/\rho. \tag{20}$$

For the conductivity κ the standard value cf Spitzer (1962) has been used.

The above equations are linearized in order to obtain a dispersion relation, which is a polynomial describing the propagation of waves of infinitesmal amplitude. The linearized equations are obtained by imposing a perturbation on the temperature, density and velocity of the form

$$Q(z,t) = Q_0(z,t) + \delta q_1(\omega k)\exp[i(kz-\omega t)], \tag{21}$$

and substituting into the conservation equations. It has been assumed that the scale of variation of $Q_0(z,t)$ and the radius of the star are much larger than the wavelength of the perturbation. Equating terms of first order in results in the system of linearized equations. This can be written as a coefficient matrix, consisting of zero order quantities, their zero order derivatives, and powers of ω and k. The determinant of the matrix gives a polynomial of third order in ω, which is the dispersion relation. Although this process could have been carried through by hand and the roots of the cubic polynomial derived analytically, it was far easier and less prone to error to do it with the aid of a computer. Besides, this analysis is eventually to be extended to more complex motions, in which case the computer would have to be used, so the experience obtained in this simpler case will be usefully applied there. The method of generating the algebraic form of the dispersion relation is outlined in Appendix 4.

To define the coefficients of the polynomial, it is necessary to know the density, velocity and temperature, their first derivatives, the second derivative of the temperature, the radiation force, cooling and heating rates, and the electron density with their temperature and density derivatives. These quantities were derived in Chapter 4.

The roots of the dispersion equation are found using a computer program which finds the roots of complex polynomials. The root found is improved in accuracy by substituting it back into the polynomial and doing a Newton's method iteration until the fractional change is less than 1 part in 10^{15}. Since the roots are computed for a sequence of k, the root for the next value of k is then estimated from the root just found by extrapolation, and the same iterative improvement performed. The limits to the accuracy of the numerical solutions means that when the roots have real and imaginary parts different by 15 orders of magnitude or the different roots themselves are widely separted, the smallest quantities may not be very accurate. The method of solution chosen was designed to suppress "numerical noise", but the resulting smoothness of the plotted roots usually overestimate the accuracy of the numbers in the cases mentioned above.

The perturbations are of the form $\exp[i(kz-\omega t)]$, consequently if the imaginary part of the frequency is positive for a given real k, then there is an instability at that wave number. This instability can act as an amplifier of a preexisting wave, in which case it is called a convective or amplifying instability, or it can grow away from the starting value, either in a monotonic growth or in ever increasing oscillations, which is called an absolute instability. A mathematical method of distinguishing between the two types of instability based on determining the behaviour of the wave as $t \to \infty$, has been developed by Dysthe (1966), Bers (1975), and Akhiezer and Polovin (1971).

They find several criteria for determining the type of stability, the easiest of which to apply is that if the simultaneous solution to D(,k)=0 and dD/dk=0, where D is the dispersion relation polynomial, exists, and has an imaginary frequency greater than zero, then the instability is absolute. This is a necessary and sufficient condition in the approximation of $t \to \infty$ in an infinite atmosphere. The criterion means that in the neighbourhood of the solution (ω_0, k_0) to the two equations the root varies as $\omega = \omega_0 + A(k-k_0)^2$, where A is a constant. This implies that an absolute instability is a saddle point of the imaginary part of the frequency as a function of k. The imaginary part of the frequency will be at a maximum with respect to real k at the solution, and this frequency will dominate the growth rate. These two nonlinear equations, D=0 and dD/dk=0, were solved simultaneously with the aid of a computer routine, using the local maximum of the imaginary part of the frequency for real wavenumbers as a starting point. An attempt was made to find common roots to the two equations by constructing the discriminant of the coefficients of the two equations. This was unsuccessful because of the impossibility of retaining sufficient numerical accuracy.

In order to understand the dispersion relation and the physical origin of the roots, analytic expressions for the roots will be derived for a number of simple limiting cases. The roots in a complex situation can be understood as superposition of these several simple cases. These limiting solutions have been derived with the aid of numerical solutions, and unless noted the calculated roots plotted came from a dispersion relation with coefficients calculated from a gas in an undiluted radiation field, with a density of 10^{11} cm^{-3}, and a velocity of 100 Km s^{-1}. The resulting equilibrium quantities are in cgs units: T = 1.97×10^{4} K; $\mathcal{L}=0$, $d\mathcal{L}/dT = .46 \times 10^{-4}$, $d\mathcal{L}/dn = 2. \times 10^{-13}$, $dv/dz = .2 \times 10^{-3}$, $dn/dz = -2.1$, $g_{rad} = 1.18 \times 10^{4}$, $dg_r/dT = -0.3 \times 10^{-1}$, and $dg_r/dn = -.15 \times 10^{-6}$. It is found that the character of the roots changes little with a variation of the physical parameters around these values for typical stellar wind conditions.

Case 1: Sound Waves In An Atmosphere

The simplest case which has a non zero growth rate is a wave propogating vertically in a static, isothermal atmosphere, with no conduction or radiation present. In this case the dispersion relation as given in the Appendix 3 reduces to

$$\omega^3\{-i\rho c_v R\} + \omega\Big\{ik^2[2R\rho(-e+h+c_v RT)] + k\Big[\frac{4R\rho}{n}\frac{dn}{dz}(-e+h)\Big] + i\,2R\rho\Big(\frac{1}{n}\frac{dn}{dz}\Big)^2(e-h+c_v RT)\Big\},$$

where $c_v = \frac{1}{R}\frac{de}{dT}$.

Defining $H=n/(dn/dz)$, this has solutions $\omega=0$ and in the limit of large and small k the nontrivial roots become

$$k\to\infty \qquad \omega \to \pm\sqrt{\frac{2(h-e+c_v RT)}{c_v}}\Big[k - \frac{i}{H}\,\frac{h-e}{h-e+c_v RT}\Big],$$

$$k\to 0 \qquad \omega \to \pm\sqrt{\frac{2(e+c_v RT-h)}{c_v H^2}}\Big[1 - i\,\frac{h-e}{e+c_v RT-h}\,kH\Big]. \tag{22}$$

This is essentially the well known solution of Lamb (1945) to the problem of wave propogation in an isothermal, exponential atmosphere. But note that the value of H, the scale height of

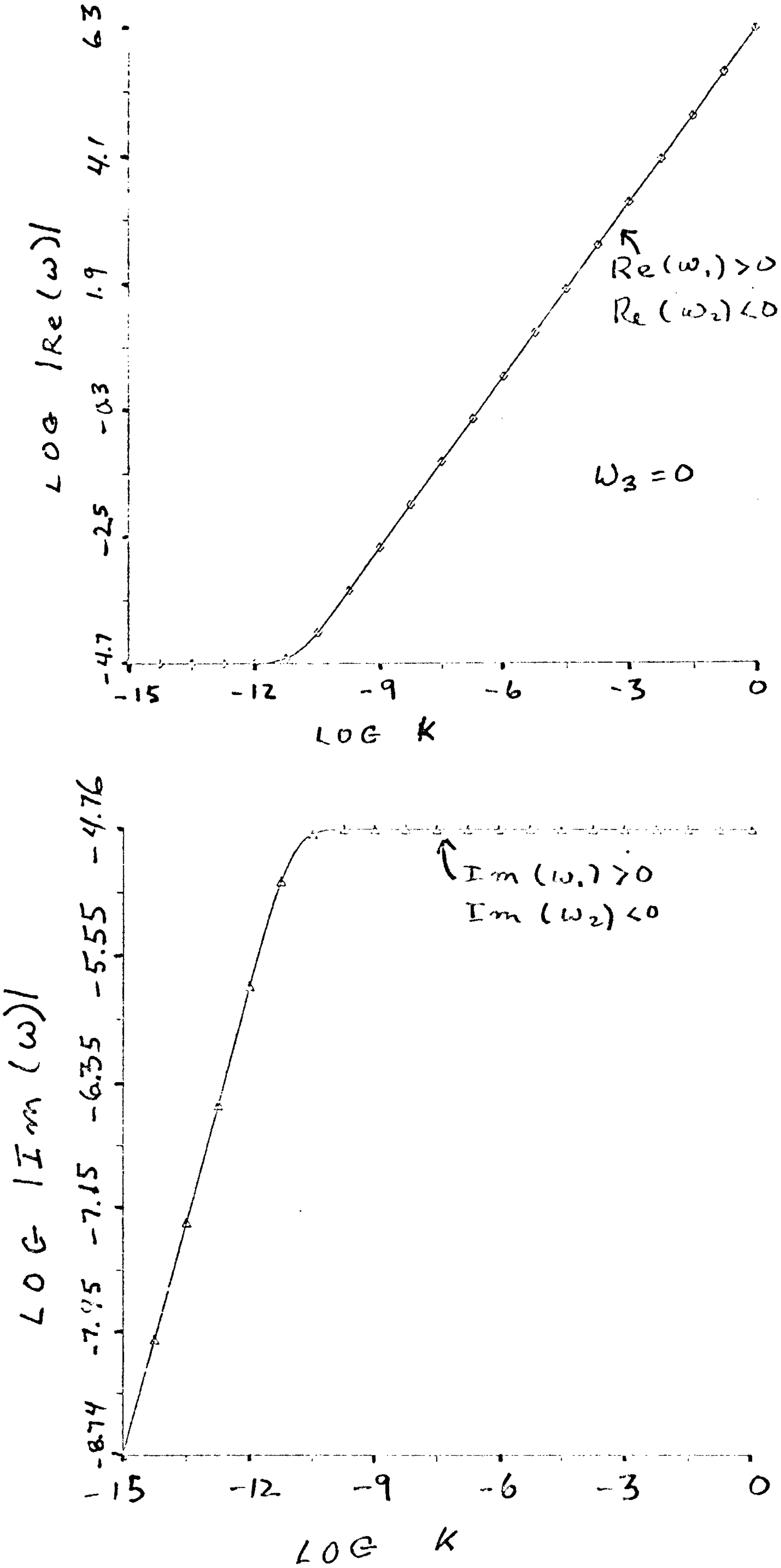

Fig. 15: Pseudo Isothermal Static Atmosphere Roots

the density gradient, used in the numerical calculations was not the isothermal scale height, but that the scale height was determined by the velocity gradient through the mass conservation equation. In the short wavelength limit ($k \rightarrow \infty$) the waves move at a phase and group velocity equal to the ordinary sound velocity. Outward moving waves are amplified and inward moving waves are damped at a rate such that the momentum carried in the wave is kept constant. These waves are not absolute instabilities. At long wavelengths ($k \rightarrow 0$) the real part of the frequency goes to a finite limit, called the acoustic cutoff frequency, and the damping goes to zero. This means that these waves have a phase velocity going to infinity, but the group velocity goes to zero and no energy is propogated. Physically this cutoff results from the atmosphere as a whole moving with the wave motion, rather than a wave propogating away from the source. The change over between the two limiting solutions occurs for k of order H^{-1}. The solution is illustrated in the accompanying Figure 15. In Figure 15, and all other graphs of the roots of the dispersion relation, the logarithm (base 10) of the real and imaginary parts of the wave frequency are separately plotted against the logarithm of the wave number. On the graph of the real part a symbol (⧖ △or ◇) on the line means that the real part is negative. On the graph of the imaginary part the same symbols indicates that the wave is unstable at that wave number, that is, the imaginary part is positive. Note that frequently the two acoustic roots have an identical magnitude, but opposite sign, so that in the plot the two lines lie on top of each other.

The plots are done for k ranging from 10^{-15} to 1 cm^{-1}, which is an unrealistically large range for the physical situation, but is done to illustrate the asymptotic limits of the roots. The physically acceptable range of wave numbers is for wave numbers less than the a wavelength of a stellar radius, 10^{-11} cm^{-1}, to a wavenumber corresponding to one mean free path, about 10^{-2} cm^{-1}.

There is a maximum frequency for which the solutions are valid, set by the longer time scale, recombination or the electron ion thermal equilibrium. The recombination frequency is

$$\omega_{rec} = .188\ n_{||}\ (T/10^4\ K)^{-1/2}\ s^{-1}, \tag{23}$$

and the electron ion equilibrium frequency is

$$\omega_{ei} = 7x10^4\ n_{||}\ (T/10^4\ K)^{-3/2}\ s^{-1}. \tag{24}$$

The maximum frequency for which the calculations are valid then is the minimum of ω_{rec} and ω_{ei}. The minimum frequency of interest would be determined by the time for the complete replacement of the star's stellar wind envelope. This frequency is about $6x10^{-5}$ s^{-1}.

Case 2: The Effect Of Conduction

Allowing conduction affects mostly the short wavelength roots. Taking the dominant terms in the dispersion relation gives,

$$\omega^3\{-i\rho c_v R\} + \omega^2 k^2 \kappa + \omega\left\{ik^2[2R\rho(-e+h+c_v RT)] + k\left[\frac{4R\rho}{H}(h-e)\right] + i\frac{2R\rho}{H^2}(e-h+c_v RT)\right\} - 2RT\kappa k^4.$$

For this case the dominant terms of the roots for $k\to\infty$ are,

$$\omega = -\frac{i\kappa}{\rho c_v R}k^2, \tag{25}$$

which is a heavily damped non propagating disturbance. The sound waves are given as

$$\omega = \pm\sqrt{2RT} - i\frac{R\rho}{\kappa}(h-e), \tag{26}$$

which are isothermal sound waves, and always damped independent of direction of propagation. The numerical solution shows that the analytic solutions only apply for $k>10^{-3}$, and that the slow root has a small real part at short wavelengths.

Case 3: Radiation Effects

In the long wavelength limit we expect radiation effects to be dominant. The dominant terms of the dispersion relation become

$$\omega^3\{-i\rho c_v R\} + \omega^2\frac{d\mathcal{L}}{dT} + \omega\left\{i2\frac{dv}{dz}\frac{d\mathcal{L}}{dT}\right\} + + \frac{dn}{dz}\left\{\frac{d\mathcal{L}}{dn}\left[\frac{2R}{n} - \frac{dq_r}{dT}\right] - \left[\frac{2}{n}\frac{RT}{H} + \frac{dq_r}{dn}\right]\frac{d\mathcal{L}}{dT}\right\} - \left(\frac{dv}{dz}\right)^2\frac{d\mathcal{L}}{dT}. \tag{27}$$

This dispersion relation has been derived under the assumption that

$$\frac{dv}{dz}\,\frac{d\mathcal{L}}{dT} \gg \frac{RT}{H^2}\,c_v R \rho . \tag{28}$$

The dominant term of one root is for $k \to 0$

$$\omega = - \frac{i}{\rho c_v R}\,\frac{d\mathcal{L}}{dT}, \tag{29}$$

which essentially is the thermal stability condition. A parcel of gas with $d\mathcal{L}/dT < 0$ would probably tend to collapse. In a general case if $d\mathcal{L}/dT$ were negative, part of the gas may cool and collapse, and other parts may rise in temperature. The existence of the hot, low density component depends on an appropriate heat source to maintain a temperature of order 10^6 to 10^7 K, where the gas is stable. If this bistable mode is possible within a stellar wind, it may lead to a two component outflow with a cool (T around 2×10^4 K) and hot (T around 10^7 K) component. The hot component may be able to supply sufficient O VI atoms that there would be no need for a coronal region.

The dominant terms of the other two roots are sound waves,

$$\omega = -i\,\frac{dv}{dz} \pm \sqrt{\frac{2RT}{|H|}} . \tag{30}$$

The roots are shown in Figure 16, for a gas with a nonzero velocity and acceleration. From Equation 30 we make the discovery that deccelerating flows are unstable, and the numerical calculation finds that it is an absolute instability. An example of this instability is discussed later and illustrated in Figure 20. Defining some basic time scales as

$t(\text{dynamic}) = 1/|dv/dz|$,

$t(\text{cool}) = \rho c_v R\,/\,|d\mathcal{L}/dT|$,

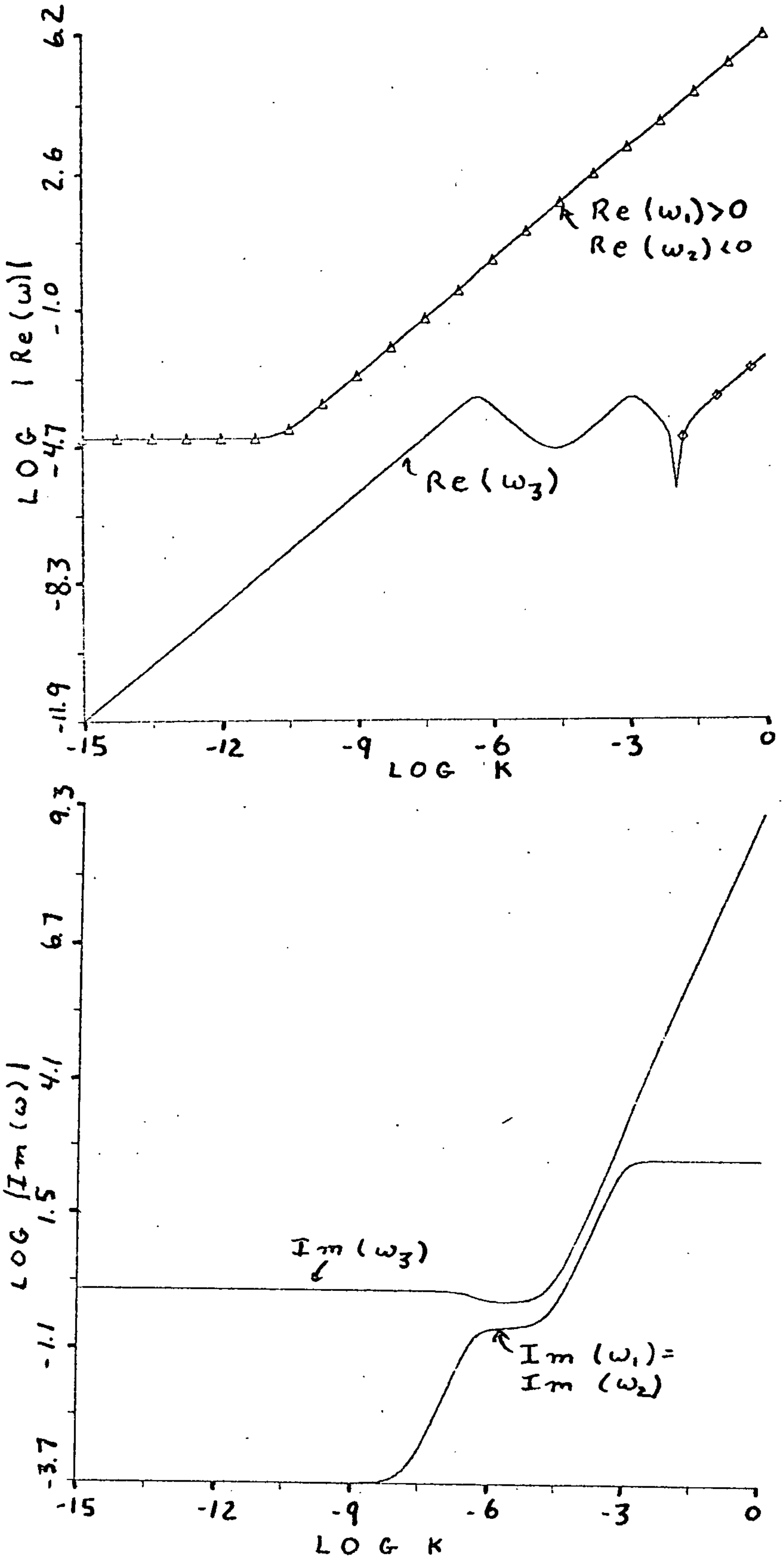

Fig. 16: Isotropic Radiation Field

t(acoustic) = H/c_{T} where $c_{T}= \sqrt{2RT}$.

The condition for the instability of deccelerating flows (Eq. 28) is,

$$t(\text{dynamic}) \times t(\text{cool}) << (t(\text{acoustic}))^2$$

Note that the conductive damping dominates the roots for $k > 10^{-4}$.

Allowing a radiation acceleration, gives the roots as plotted in Figure 17. The asymptotic limits are not changed by the radiation acceleration, but the inward propagating acoustic wave is unstable in the range of wavenumber $10^{-11} < k < 10^{-7}$. The resulting growth rate is close to 1200 seconds, but the instability is only amplifying.

The cooling due to collisionally excited lines may be diminished when the gas becomes optically thick in the resonance lines. The effect of this has been approximated by turning the loss rate off, but leaving the heating on. The roots of the dispersion relation in this case are shown in Figure 18. Besides the amplifying instability from the radiation force there is an additional range of instability for both inward and outward acoustic waves for $10^{-7} < k < 10^{-5}$. This behaviour results from the term $d\mathcal{L}/dn$ becoming signficant.

Figure 19 shows the effect of a thermal instability, $d\mathcal{L}/dt<0$. The "slow" root has a rapid growth rate, which is an absolute instability. The acoustic roots are changed only slightly, the amplification acting over a narrower range of wavenumber, and not quite as rapidly.

Figure 20 shows the pressure dominated thermal instability which is present at 10^7 K. In this case the flow speed is sub-

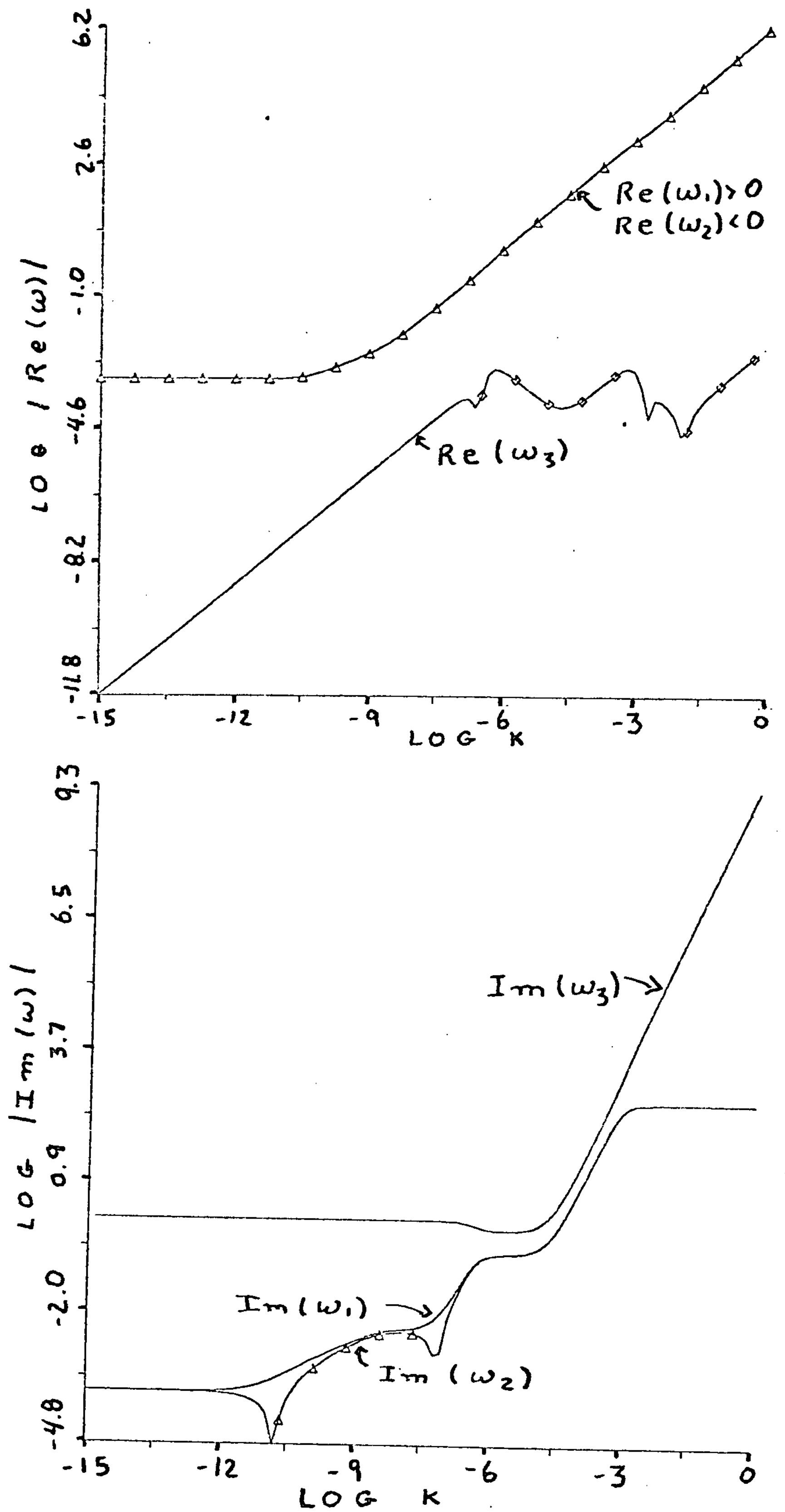

Fig. 17: Radiation Force On

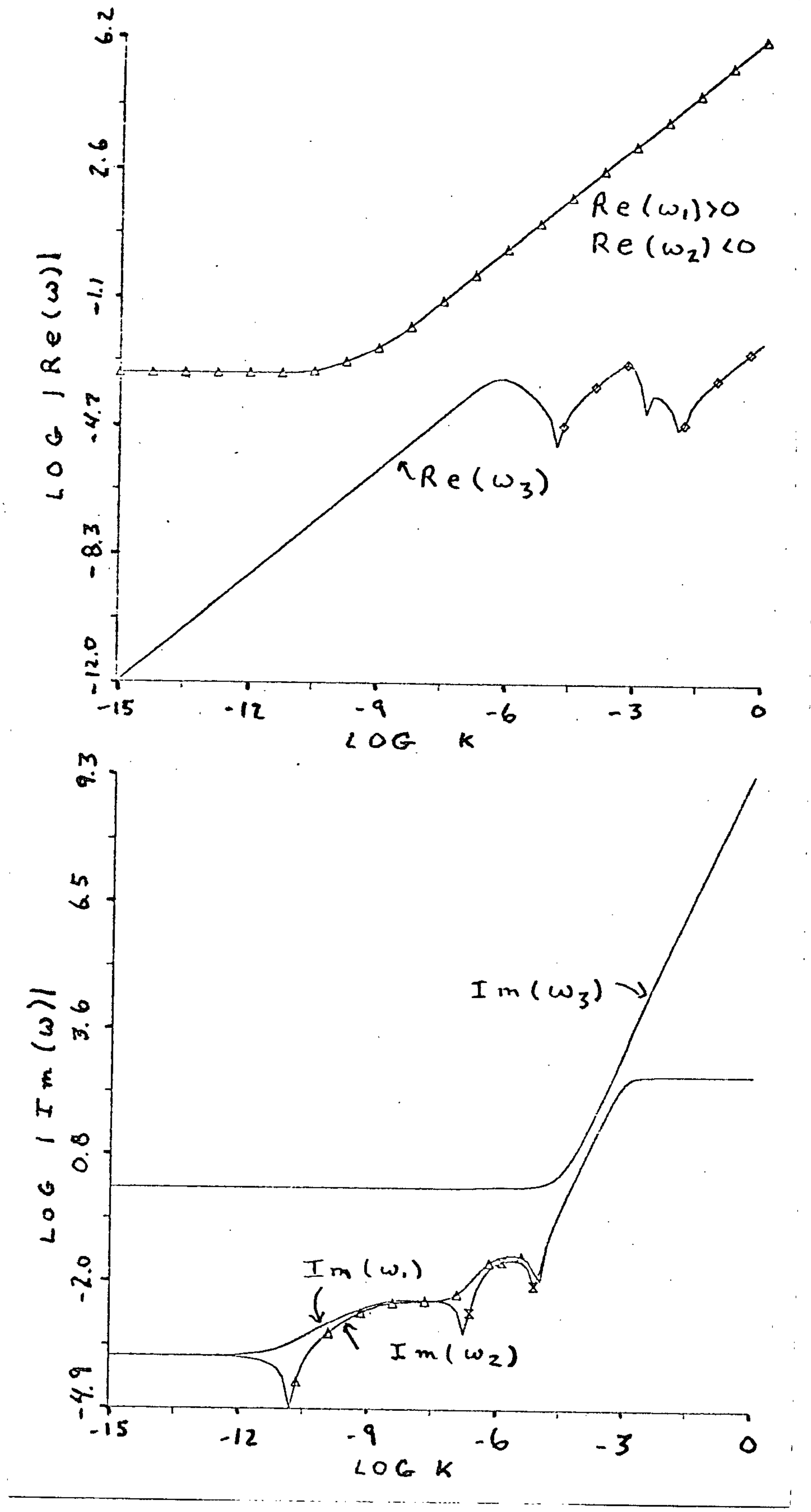

Fig. 18: No Cooling

sonic, and the radiation force is less than 5% of gravity. The instability results when Equation 28 is violated. The acoustic waves have an absolute instability at long wavelengths. The growth rate is proportional to the element abundance through the cooling rate.

An atmosphere of density 10^{12} cm^{-3} and a velocity of 100 Km s^{-1} exceeds the maximum velocity for an accelerating solution. The roots when dv/dz is negative are shown in Figure 21. This is an absolute instability at long wavelengths.

In summary the roots of the dispersion relation can be understood in terms of combinations of the roots which occur in simple physical cases. For $k > 10^{-4}$ cm^{-1}, the conduction always provides a strong damping, especially to the slow wave.

Thus it can be concluded that in the long wavelength limit, $k < 10^{-11}$, the behaviour depends on the shortest time set by the acoustic time scale, equal to the scale height divided by the sound speed; the dynamic time scale $(dv/dz)^{-1}$; and the cooling time scale, $\rho c_v R/|d\mathcal{L}/dT|$. There is always a "thermal wave", that is, a slow moving wave, compared to the sound speed, with a growth rate set by the thermal time scale. The slow wave is an absolute instability if the derivative $d\mathcal{L}/dT$ is negative. If t(acoustic) >> t(dynamic) then the acoustic waves have growth rates given by the dynamic time scale. These acoustic waves will be absolutely unstable if the velocity gradient is negative. A hot gas, with t(acoustic) < t(dynamic) will have an absolute instability arising from the acoustic waves. At $T=10^{7}$ the growth rate is about one hour, (one hour at 3×10^{6} K where $d\mathcal{L}/dt<0$) which increases as n^2, until t(acoustic) exceeds

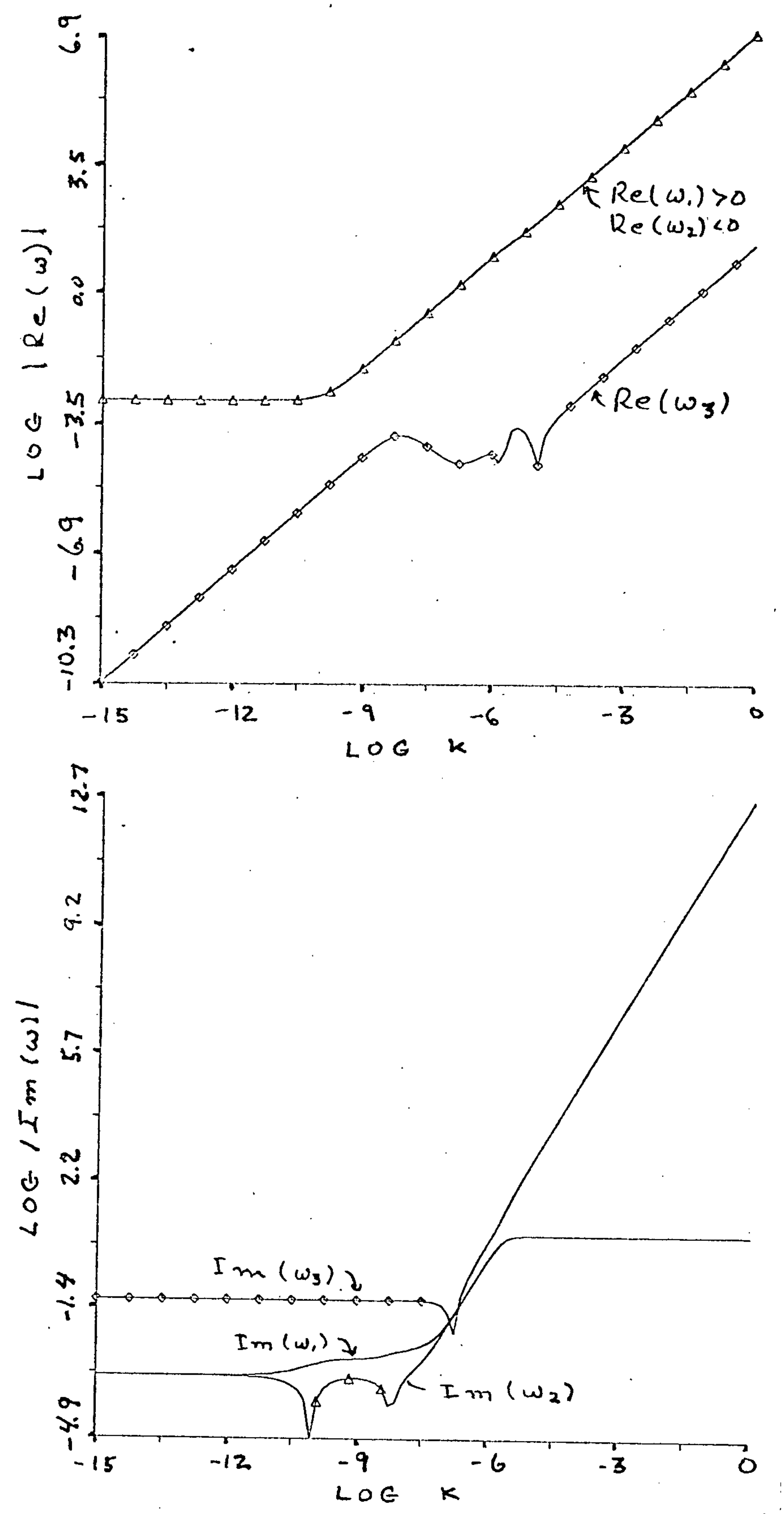

Fig. 19: Thermal Instability

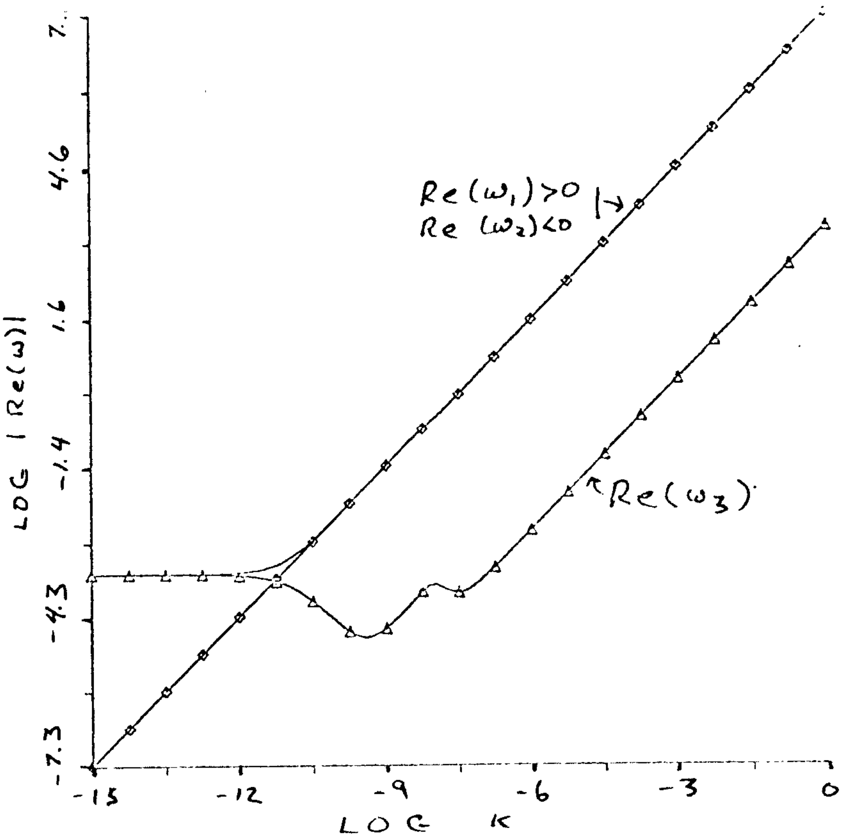

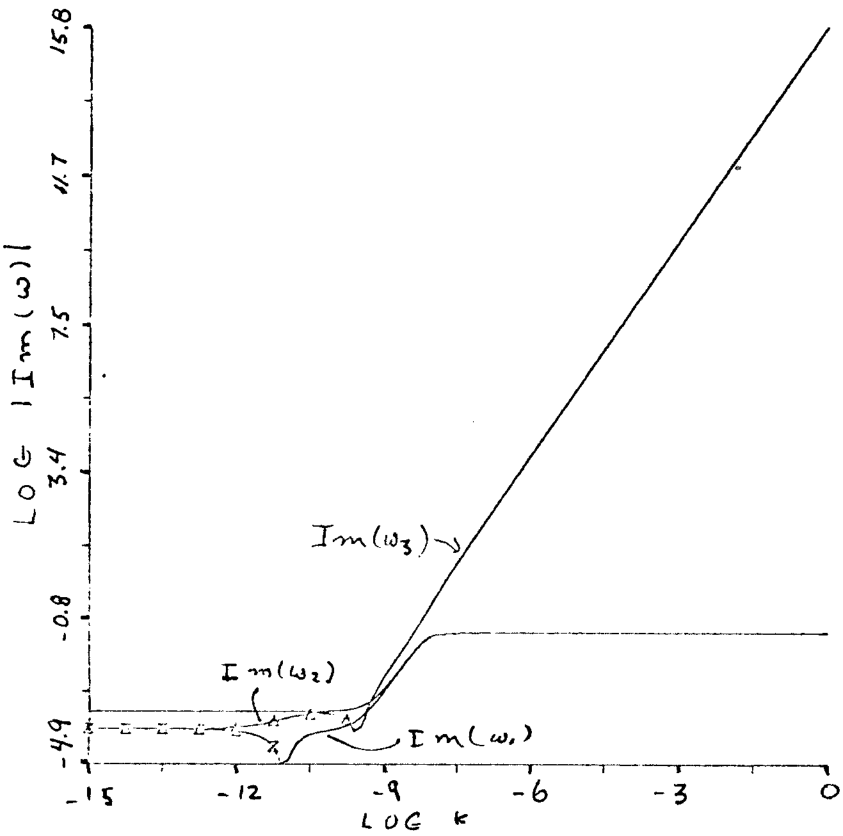

Fig. 20: High Temperature Instability

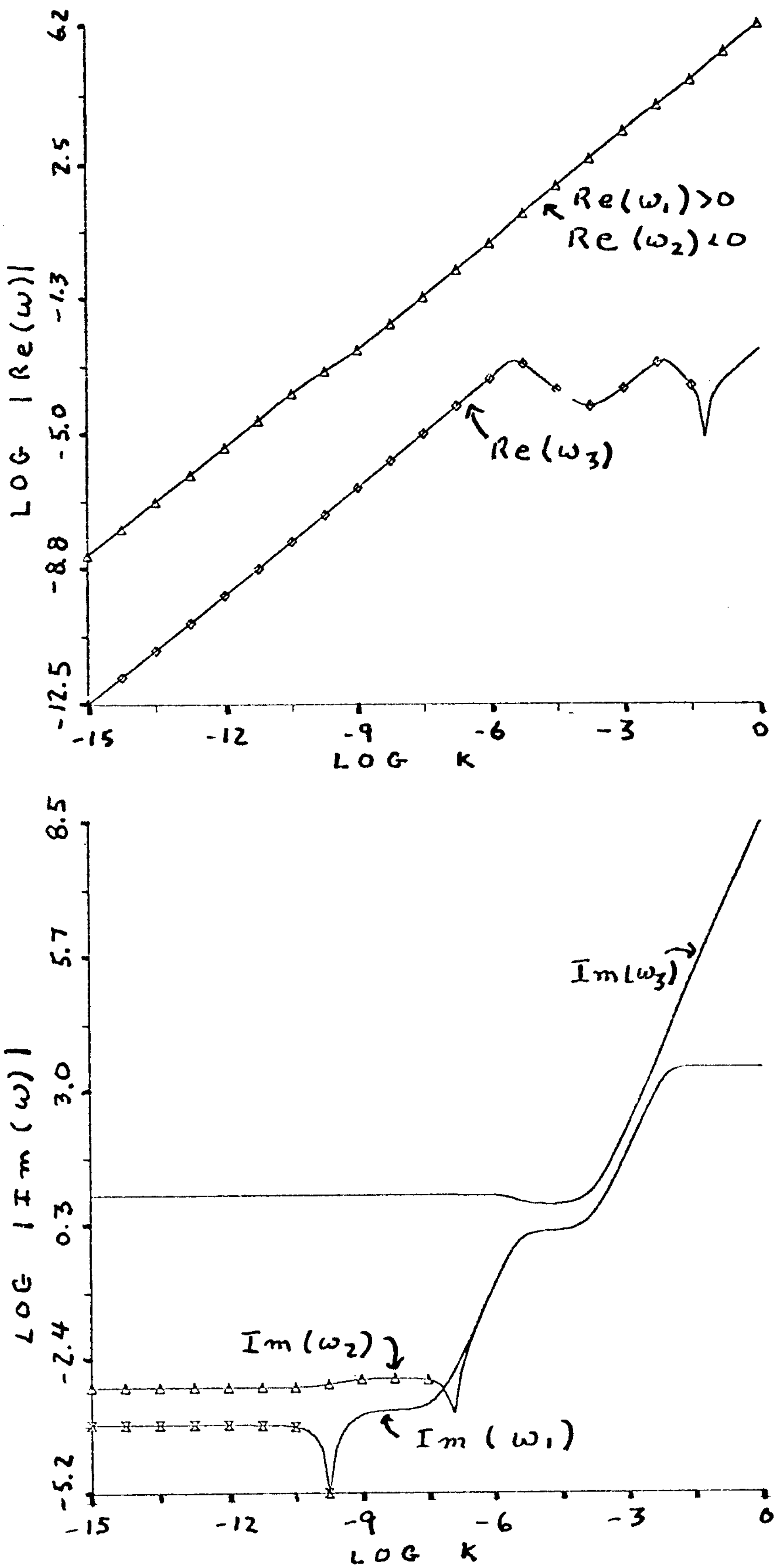

Fig. 21: Decceleration Instability at $n=10^{12}$ cm^{-3}.

TABLE 5: THE DISPERSION RELATIONS PLOTTED

Fig.	n	T	V	dv/dz	d /dT	q	Remarks
15	10^{11}	$2x10^{4}$	0	0	0	0	pseudo isothermal
16	10^{11}	$2x10^{4}$	100	$2x10^{-4}$	$5x10^{-5}$	0	isotropic
17	10^{11}	$2x10^{4}$	100	$2x10^{-4}$	$5x10^{-5}$	$1x10^{4}$	standard case
18	10^{11}	$2x10^{4}$	100	$2x10^{-4}$	$5x10^{-5}$	$1x10^{4}$	no cooling
19	10^{11}	$5x10^{5}$	100	$7x10^{-4}$	$-3x10^{-6}$	$1x10^{4}$	thermal
20	10^{11}	$1x10^{7}$	100	$5x10^{-5}$	$8x10^{-8}$	270	high temperature
21	10^{12}	$2x10^{4}$	100	$-6x10^{-4}$	$-3x10^{-3}$	$5x10^{3}$	decceleration

t(dynamic). The radiation acceleration only acts to provide an amplifying instability for inward acoustic waves. This amplification acts for an observationally interesting range of wavelengths, from $5x10^{7}$ to $5x10^{11}$ cm, with growth times of order 1200 seconds.

On the basis of this analysis the original CAK "cool" atmosphere is stable only if no waves are sent into the accelerating wind from lower layers. Otherwise the radiation force acts to provide an amplification of the inward moving (with respect to the gas, but outwards with respect to the star) acoustic wave. A corona with a temperature of several million degrees will always have an absolute instability, either the ordinary thermal instability of the radiation losses, or the "high temperature" instability outlined above, which has a growth time of order an hour.

The semi empirical model of the wind proposed by Cassinelli _et al_. (1978) has the wind heated with an initial acceleration in a hot corona, and then cooling in the outer radiatively accelerated zone. The stability analysis leaves no doubt that this situation would be expected to show fluctuations. The hot corona is subject to instabilities which may be responsible for creating the shock waves to heat it. Remnants of these fluctuations would be carried out into the wind where the length scales of 10^{7} to 10^{11} cm would be amplified.

CHAPTER 6. CONCLUSIONS

The program of optical observations conclusively shows that stellar winds do vary on time scales of one day and more. These observations were taken at sufficiently high resolution that any variations of the telluric lines could be separated from variations of the stellar lines. A star which has often been reported as varying, Lambda Cephei, was monitored with a time resolution of one hour over a period of six hours but no significant variation was seen in the H α line. This null observation puts an upper limit of about 5×10^{11} cm on the size of any "blobs" in the wind. Day to day variability was confirmed in λ Cep and α Cam, but not conclusively for δ Ori. These variations may not be due to fluctuations within the wind itself since this time scale is long enough to allow complete replacement of the material in the line formation region. Causes of the long time scale variation include rotation of the star, internal oscillations of the star, or a variation of the the emergent flux and hence the driving force for the wind.

The analysis of the X-ray observations of Cen X-3 provides confirming evidence for the suggested mechanism causing the long term X-ray intensity variation reported by Schreier et al. (1976). That is, the wind density varies sufficiently that the source is occasionally smothered by the opacity of the stellar wind. In addition I have found that as the density in the wind changes, it must be correlated with the wind velocity in order to explain the changing character of the anomalous dips in the intensity at non-eclipse phases. Besides these semi-regular dips the X-ray intensity shows intensity fluctuations on a time scales of less than one hour, which is probably due to changes in the amount of mass being accreted by the neutron star. The natural source for the variation in the accretion rate is the variation of the density and velocity in the stellar wind with size scales of 10^{10} to 10^{11} cm.

The theoretical analysis of the stability of a wind finds a number of sources of instability in the flow. In the long wavelength limit the highest growth rate, of order 10 seconds, usually holds for the thermal instability which arises whenever the cooling rate minus the heating rate has a negative derivative with respect to temperature. This situation arises in the temperature ranges of 3×10^5 to 10^7 K. The growth rate of this instability is directly related to the cooling rate, which is proportional to the abundances of the elements present. If this instability operates, one would expect significant differences between stars of different composition. That is, stars with higher CNO or metal abundances would have a greater cooling rate for temperatures exceeding 10^5 K in an optically thin gas. As a result the thermal instability would grow on a shorter time scale. This may have some bearing on Wolf-Rayet stars, which appear to have higher CNO abundances than OB stars, and definitely have higher mass loss rates. An amplifying instability for acoustic waves which is usually present is the simple growth of wave amplitude due to the density gradient in the atmosphere. In a moving atmosphere this occurs on a time scale of the gas speed divided by the scale height, about 2×10^3 seconds. The decceleration instability of acoustic waves is an absolute instability. The growth rate is $(dv/dz)^{-1}$, usually of order 1000 to 10^4 seconds. If the gas is very hot, greater than 10^6 K, there is an absolute instability which operates on the time scale of an hour. The radiation force provides an amplification for wavelengths in the range 10^8-10^{11} cm on time scales of 1200 seconds.

As a result of this work, a number of suggestions can be made for further investigation. Line variability should be pursued in order to unravel the nature of the variation. High resolution observations, with good signal to noise must be obtained. These observations should either be made in spectral regions free of telluric lines, or at a sufficiently high resolution to minimize blending with the stellar line.

A longer segment of the X-ray data should be analyzed to confirm the model given for the accretion process, and more importantly to estimate the density and velocity as a function of time.

The theoretical analysis of instabilities can be extended to allow a vertical and horizontal wave vector, and allow the wave motion to have a horizontal as well as a vertical component and then to more general waves, such as allowing vorticity. Besides dynamical generalizations, different source spectra should be allowed, particularly X-rays. This would allow the analysis to be extended to quasars and nuclei of galaxies.

The purpose of this whole study is to acquire information on the fundamental physical nature of the mass loss in the presence of a strong radiation field. My thesis is that the wind is observed to be variable, and that the variability on time scales of a day or less can be attributed to instabilities which exist in the wind. It is suggested that the presence of these instabilities changes the fundamental dynamics of the solutions to the flow of the stellar wind. The length and time scales established in the analysis will allow the nonlinear equations of the flow to be attacked with a knowledge of their local behaviour.

BIBLIOGRAPHY

2. Akhiezer, A. I. and Polovin, R. V., 1971, Sov. Phys. Uspekhi, 14, 278.

3. Aldrovandi, M. V. and Pequignot, D., 1973, Astr. Ap., 25, 137.

4. Aldrovandi, M. V. and Pequignot, D., 1976, Astr. Ap., 47, 321.

5. Barlow, M. J. and Cohen, M., 1977, Ap.J., 213, 737.

6. Beals, C. S., 1929, M.N., 90, 202.

7. Beals, C. S., 1951, Pub. DAO, IX, 1.

8. Bers, A., 1975, Plasma Physics, Ed. DeWitt, C. and Peyraud, J. (Gordon and Breach: New York), p. 121.

9. Berthomieu, G., Provost, J. and Rocca, A., 1975, Astr. Ap., 47, 413.

10. Bethe, H. A. and Salpeter, E. E. 1957. The Quantum Mechanics of One And Two Electron Atoms, (Springer-Verlag: New York).

11. Brucato, R. J., 1971, M.N., 153, 435.

12. Burgess, A. and Summers, H. P., 1976, M.N., 174, 345.

13. Burgess, A. and Summers, H. P., 1969, Ap.J., 157, 1007.

14. Cannon, A. J. and Pickering, E. C., 1918, Ann. of Obs. of Harvard Coll., Vols. 91-99.

15. Cannon, C. J. and Thomas, R. N., 1977, Ap.J., 211, 910.

16. Cassinelli, J. P. and Castor, J. I., 1973, Ap.J., 179, 189.

17. Cassinelli, J. P., Olson, G. L., and Stalio, R., 1978, Ap.J., 220, 573.

18. Castor, J. I., Abbott, D. C., and Klein, R. I., 1975, Ap.J., 195, 157.

19. Castor, J. I., 1977, in Colloquium Internationaux Du CNRS No. 250, Mouvements Dans Les Atmospheres Stellaires, ed. Cayrel, R. and Steinberg, M., (CNRS: Paris).

20. Castor, J. I., 1978, at IAU Symposium No. 83, Mass Loss And The Evolution Of O Type Stars.

21. Chapman, R. D. and Henry, R. J. W., 1971 _Ap.J._, 168, 169.

22. Chapman, R. D. and Henry, R. J. W., 1972 _Ap.J._, 173, 243.

23. Conti, P. S. and Frost, S. A., 1974, _Ap.J. Lett._, 190, L137.

24. Conti, P. S., 1978, _Astr. Ap._, 63, 225.

25. Cox, D. P. and Tucker, W. H., 1969, _Ap.J._, 157, 1157.

26. Dupree, A. K., 1968, _Astrophys. Lett._, 1, 125.

27. Dysthe, K. B., 1966, _Nuclear Fusion_, 6, 215.

28. Hearn, A. G., 1973, _Astr. Ap._, 23, 97.

29. Fahlman, G. G., Carlberg, R. G., and Walker, G. A. H., 1977, _Ap.J. Lett._, 217, L35.

30. Field, G. B. and Steigman, G., 1971, _Ap.J._, 166, 59.

31. Field, G. B., 1965, _Ap.J._, 142, 531.

32. Flower, D. R. 1968, in _IAU Symposium No. 34, Planetary Nebulae_, ed. Osterbrock, D. E. and O'Dell, C. R. (Reidel: Dordrecht), p. 205.

33. Hearn, A. G., 1972, _Astr. Ap._, 19, 417.

34. Hearn, A. G., 1975, _Astr. Ap._, 40, 355.

35. Henry, R. J. W. 1970, _Ap.J._, 161, 1153.

36. Hutchings, J. B., 1976, _Ap.J._, 203, 438.

37. Jackson, J. C., 1975, _M.N._, 172, 483.

38. Johnson, L. C., 1972, _Ap.J._, 174, 227.

39. Jordan, C., 1969, _M.N._, 142, 501.

40. Kato, T., 1976, _Ap.J. Supp._, 30, 397.

41. Kippenhahn, R., Mestel, L., And Perry, J. J., 1975, _Astr. Ap._, 44, 123.

42. Klein, R. I. and Castor, J. I., 1978, _Ap.J._, 220, 902.

43. Krolik, J. H., 1977, _Phys. Fluids_ 20, 364.

44. Lacy, C. H., 1977, _Ap.J._, 212, 132.

45. Lamb, H., 1945, _Hydrodynamics_, (Dover: New York).

46. Lamers, H. J. G. L. M. and Morton, D. C., 1976, _Ap.J. Supp._, 32, 715.

47. Lamers, H. J. G. L. M., and Snow, T. P., Jr., 1978, _Ap.J._, 219, 504.

48. Lotz, W., 1967, _Ap.J. Supp._, 14, 207.

49. Lucy, L. B. And Solomon, P. M., 1970, _Ap.J._, 159, 879.

50. Lucy, L. B., 1971, _Ap.J._, 163, 95.

51. McWhirtier, R. W. P., 1975, in _Atomic And Molecular Processes In Astrophysics_, ed. Hubbard, M. C. E. and Nussbaumer, H (Geneva Observatory: Sauverny, Switzerland), p. 205.

52. Mestel, L., Moore, D. W., and Perry, J. J., 1976 _Astr. Ap._, 52, 203.

53. Mewe, R., 1972, _Astr. Ap._, 20,215.

54. Mihalas, D., 1972, _Non-LTE Model Atmospheres for B and O Stars_, NCAR-TN/STR-76, (National Center for Atmospheric Research: Boulder).

55. Milne, E. A., 1926, _M.N._, 85, 813.

56. Moore, C. E., Minnaert, M. G. J., and Houtgast, J., 1966, _The Solar Spectrum_, NBS Monograph 61.

57. Moore, C. E., 1949, _Atomic Energy Levels_, NBS Circular No. 467.

58. Morton, D. C. and Smith, W. H., 1973, _Ap.J. Supp._, 26, 333.

59. Morton, D. C., 1967, _Ap.J._, 147, 1017.

60. Mushotzky, R. F., Solomon, P. M., And Strittmatter, P. A., 1972, _Ap.J._, 174, 7.

61. Nelson, G. D., and Hearn, A. G., 1978, _Astr. Ap._, 65, 223.

62. Pounds, K. A., Cooke, B. A., Ricketts, M. J., Turner, M. J., and Elvis, M., 1975, _M.N._, 172, 473.

63. Raymond, J. C., Cox, D. P., and Smith, B. W., 1976, _Ap.J._, 204, 290.

64. Rosendahl, J. D., 1973, _Ap.J._, 182, 523.

65. Rybicki, G. B. and Hummer, D. G., 1978, Ap.J., 219, 654.

66. Schreier, E. J., Schwartz, K., Giacconi, R., Fabbianc, G., and Morin, J., 1976, Ap.J., 204, 539.

67. Seatcn, M. J. 1958, Rev. Mod. Phys., 30, 979.

68. Seatcn, M. J., 1959, M.N., 119, 81.

69. Silk, J. And Brown, R. L., 1971, Ap.J., 163, 495.

70. Snow, T. P. Jr. and Morton, D. C., 1976, Ap.J. Supp., 32, 429.

71. Snow, T. P. Jr., 1977, Ap.J., 217, 760.

72. Sobolev, V. V., 1960, Moving Envelopes of Stars, (Harvard University Press: Cambridge).

73. Spitzer, L. Jr., 1962, Physics of Fully Ionized Gases, 2nd ed., (Interscience: New York).

74. Steigman, G., Werner, M. W., and Geldon, F. M., 1971, Ap.J., 168, 373.

75. Summers, H. P., 1974, M.N., 169, 663.

76. Sunyaev, R. A. and Vainstein, L. A., 1968, Astrophys. Lett ., 1, 193.

77. Thomas, R. N., 1973, Astr. Ap., 29, 297.

78. Underhill, A. B., 1960, in Vol. VI of Stars And Stellar Systems, Stellar Atmospheres, ed. J. Greenstein, (U. of Chicago: Chicago), p. 411.)r

79. Walker, G. A. H., Bucholz, V., Fahlman, G. G., Glaspey, J., Lane-Wright, D., Mochnacki, S., and Condal, A., 1976, Proc. IAU Colloquium 40, ed. M. Duchesne, (reidel: Dordrecht).

80. Wiese, W. L., Smith, M. W., and Glennon, B. M., 1966, NSRDS-NBS4.

81. Wiese, W. L., Smith, M. W., and Miles, B. M., 1969, NSRDS-NBS22.

82. Wilson, R., 1962, J.Q.S.R.T. 2, 477.

83. Wright, A. E., and Barlow, M. J., 1975, M.N., 170, 41.

84. Ycrk, D. G., Vidal-Madjar, A., Laurent, C., Bonnet, R., 1977, Ap.J. Lett., 213, L61.

APPENDIX 1. SUPERSONIC ACCRETION

This appendix is a reprint of the paper entitled "Radiative Effects in Supersonic Accretion", which appeared in the *Astrophysical Journal* Volume 220, p. 1041. The theory developed was used in Chapter III to deduce the correlation between the wind velocity and wind density in the observed intensity transition of Cen X-3.

THE ASTROPHYSICAL JOURNAL, 220:1041–1050, 1978 March 15

RADIATIVE EFFECTS IN SUPERSONIC ACCRETION

R. G. CARLBERG
Department of Geophysics and Astronomy, University of British Columbia
Received 1977 March 21; accepted 1977 September 22

ABSTRACT

Supersonic gas flow onto a neutron star is investigated. There are two regimes of accretion flow, differentiated by whether the gas can cool significantly before it falls to the magnetosphere. If radiative losses are negligible, the captured gas falls inward adiabatically in a wide accretion column. If the radiative energy-loss time scale is less than the fall time, the gas will cool to some equilibrium temperature which determines the width of the wake. An accreting neutron star generates sufficient luminosity that radiation heating may determine the temperature of the accretion column, provided the accretion column is optically thin. Gas crossing the shock beyond the critical radius forms an extended turbulent wake which gradually merges into the surrounding medium. As a specific example, the flow for the range of parameters suggested for the stellar wind X-ray binaries is considered.

Subject headings: shock waves — stars: accretion — X-rays: binaries

I. INTRODUCTION

Recent observations of X-ray binaries, at both optical (Conti and Cowley 1975; Dachs 1976) and X-ray (Jones *et al.* 1973; Pounds *et al.* 1975; Eadie *et al.* 1975) wavelengths, show phase-dependent absorption of radiation. It has been suggested that this is caused by a wake trailing the compact object which emits the X-rays. Models of the wake based on the X-ray observations were put forward by Jackson (1975) and Eadie *et al.* (1975). The general problem of a gravitating body moving through a gas at a velocity much greater than the sound speed was first discussed by Hoyle and Lyttleton (1939). More recently, wakes were discussed by Davidson and Ostriker (1973), Illarionov and Sunyaev (1975), and McCray and Hatchett (1975). These models are incomplete in that they lack a description of the gravitationally perturbed gas which is unbound, i.e., the far wake. Although most of these papers emphasize the importance of radiative effects, no clear analysis has been made of the variations in the flow of gas caused by radiative gains and losses.

In this paper supersonic accretion onto a neutron star is considered. There are three basic physical parameters: the mass of the accreting body and the free stream velocity and density of the gas. The dynamics of the flow are essentially determined by the free stream velocity and the mass. The angular width of the accretion column depends on its temperature, which in turn is regulated by radiative cooling and heating and is sensitive to the gas density.

The proposed description is worked out for linear motion, which is a good approximation for an accretion radius much smaller than the system dimensions. A schematic of the model is shown in Figure 1. The important regions are labeled: (1) the incoming supersonic gas; pressure forces can be neglected and streamlines are taken to be coincident with particle trajectories in a gravitational field; (2) the shock-heated sheath where the incoming gas impinges on the accretion column; the transverse component of the velocity is rapidly halted, providing pressure to contain the accretion column; (3) the accretion column, in which gas falls inward, toward the accreting body; (4) a region of spherically symmetric flow which may exist near the accreting body; (5) the base of the accretion column; beyond this the flow is regulated by the physics of the magnetosphere around the accreting object; (6) the accreting body, where the kinetic energy of the gas is liberated at a surface shock; and (7) the far wake, several hundred times the length of the accretion column. The density contrast between the far wake and the surrounding medium gradually goes to zero.

One major qualitative aspect of this model is that there is no bow shock standing off from the front of the body which is distinct from the tail shock. Undoubtedly there will be a preceding shock, but pressure waves generated there will not propagate very far in a transverse direction because the streamlines of the flow are bent in by gravitation. Consequently, the bow shock merges into the tail shock. In general, this will be the case for any body whose size is less than the "accretion radius" $R_A = 2GM/V_0^2$, where V_0 is the free stream velocity. Calculations by Hunt (Eadie *et al.* 1975) indicate that part of the infalling column may "miss" the accreting body and force the leading shock forward. This occurs because small nonradial velocities increase toward the body, by conservation of angular momentum. This effect will be ignored.

This model is to be applied to a neutron star orbiting a massive star with a strong stellar wind. For convenience, scaled variables will be used for the distance $r_v = r/R_A$: free stream density, $n_{11} = n_0/10^{11}$ cm^{-3}; free stream velocity, $V_8 = V_0/10^8$ cm s^{-1}; and

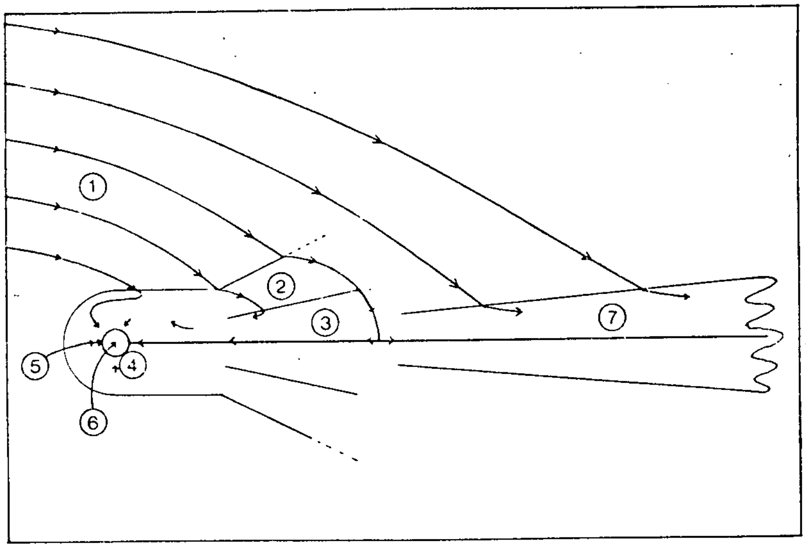

FIG. 1.—A schematic of supersonic accretion gas flow showing: (1) the incoming supersonic gas; (2) the shock-heated sheath; (3) the accretion column; (4) the possible spherically symmetric inflow at the bottom of the column; (5) the Alfvén surface at the bottom of the column; (6) the accreting body; and (7) the far wake.

mass of the accreting body, $m = M_x/M_\odot$. Similarly, in later calculations, the temperature of the column will be represented as $T_6 = T/10^6$ K. This form of notation will be used throughout.

II. DYNAMICS OF THE GAS FLOW

A gravitating body is placed in a uniform stream of gas moving at some velocity V_0. To the point where the gas crosses the tail shock, we assume that the streamlines of the flow can be found from particle dynamics, i.e., the flow is dominated by inertial forces. The velocity can be obtained from the equations of conservation of energy and angular momentum,

$$\tfrac{1}{2}(V_r^2 + V_\phi^2) - \frac{GM}{r} = \tfrac{1}{2}V_0^2$$

and

$$V_\phi = V_0 \frac{s}{r}, \tag{1}$$

where V_r and V_ϕ are, respectively, the radial and tangential components of the gas velocity relative to the accreting object. The trajectories are given by (Ruderman and Spiegel 1971),

$$\frac{1}{r} = \frac{R_A}{2s^2}(1 + \cos\phi) + \frac{1}{s}\sin\phi, \tag{2}$$

where s is the impact parameter and ϕ is the angle measured from the accretion axis. From these equations, Danby and Camm (1957) obtain the density $n = n(r, \phi)$ as

$$n = \frac{n_0}{2\sin\phi/2}\left(\frac{R_A}{r} + \sin^2\frac{\phi}{2}\right)^{-1/2} \times \left[\frac{R_A}{2r} + \sin^2\frac{\phi}{2} + \sin\frac{\phi}{2}\left(\frac{R_A}{r} + \sin^2\frac{\phi}{2}\right)^{1/2}\right]. \tag{3}$$

As a simplifying approximation, we take the case of ϕ small and $\phi^2 \ll R_A/r$, to obtain the relations,

$$s \approx (R_A r)^{1/2},$$

$$V_\phi \approx V_0(R_A/r)^{1/2},$$

and

$$n \approx \frac{n_0}{2\phi}\left(\frac{R_A}{r}\right)^{1/2}. \tag{4}$$

a) *The Sheath*

The gas crossing the shock has a discontinuity in its motion described by the equations for the conservation of the total energy and of the normal components of mass flux and momentum. Assuming that a strong shock occurs (good for Mach numbers greater than ~ 3), the postshock density and temperature are (for a ratio of specific heats $\gamma = 5/3$)

$$\rho_2 = 4\rho_1, \quad \text{and} \quad T_2 = \frac{3}{32}\frac{V_n^2}{R}, \tag{5}$$

where R is the gas constant and 1 and 2 refer to the pre- and postshock conditions, respectively. V_n ($\approx V_\phi$) is the component of velocity normal to the shock. An important point is that specific energy is conserved across a shock. If the gas is energetically unbound ahead of the shock, it will remain unbound behind the shock in the absence of cooling. On the other hand, if all the thermal energy is immediately lost, one finds that the gas is energetically bound for all radii less than R_A.

The sheath is bordered by the shock on the outside and the inward-flowing gas of the accretion column on the inside. The sheath is a dynamically defined region where the gas slows to a stop, changes direction, and joins the accretion column.

The semiangle to the shock cone will be approximated by the semiangle of the accretion column. To this end we demonstrate that the thickness of the sheath is small for the case of a narrow shock cone. The radial-velocity component is approximately parallel to the shock and is continuous across the shock. In the limit of $V_r = V_0$, one easily finds that gas entering the shock sheath at $r_0 < R_A$ will travel to a maximum distance r given by

$$\frac{1}{r} = \frac{1}{r_0} - \frac{1}{R_A}, \tag{6}$$

before the radial velocity is brought to zero. The gas would then join the accretion column.

An estimate of the sheath thickness can be obtained by equating the mass influx between r_0 and r, ($r \approx r_0$, $r \ll R_A$) $\pi n_0 V_0 r_0^2$, to the mass flux through a cross section at distance r, $n_s V_0 2\pi r \phi_s w$, where w is the thickness of the sheath, n_s the postshock density at r, and ϕ_s the angle to the shock. This gives the semiangular width of the sheath as

$$\frac{w}{r_0} = \frac{1}{4}\left(\frac{r}{R_A}\right)^{1/2}. \tag{7}$$

Thus the maximum width of the sheath is only a function of distance from the accreting object, and for $r \ll R_A$ the sheath width will be negligible.

The above calculation assumed laminar flow and no premature mixing of sheath gas into the column, whereas it is quite likely that the sheath is turbulent. The Reynolds number in the sheath is $4.1 \times 10^4 n_{11} r_v^2 \phi^{-1} V_8^{-6}$, indicating the possibility of turbulence. A turbulent sheath would come into equilibrium with the column more rapidly than laminar flow through mixing. As a consequence, a turbulent sheath would be even thinner than the limit set in equation (7).

b) The Accretion Column

The mass flux in the accretion column is simply $dM/dt = \pi \rho_0 V_0 s_c^2$, where s_c is the critical impact parameter, taken as the impact parameter of the streamline which would have a total energy of zero on the accretion axis. To allow for the thermal energy, a parameter β is introduced, such that the "true accretion radius" is equal to βR_A. In principle, β is determined once the physical parameters, the density, velocity, and accreting mass, are specified. The parameter β will be taken as the ratio of the specific kinetic energy ($\frac{1}{2}V_0^2$) to the specific enthalpy ($5RT_0$) if ($\frac{1}{2}V_0^2 < 5RT_0$), otherwise $\beta = 1$, where T_0 is the equilibrium temperature of the column at $r_v = 1$. The accretion rate is then

$$dM/dt = 3.65 \times 10^{16} n_{11} m^2 V_8^{-3}\ \mathrm{g\ s^{-1}}. \tag{8}$$

For a column in equilibrium, the transverse momentum of the incoming gas must be balanced by thermal pressure in the column,

$$2\rho_c R T_c = \rho_1 V_n^2. \tag{9}$$

From this one obtains a relation between the central temperature of the column and the opening angle,

$$\frac{T_c}{\phi_c} = \frac{V_0^2}{4(2)^{1/2} R\beta} = 2.13 \times 10^7 V_8^2 \beta^{-1}\ \mathrm{K\ rad^{-1}}. \tag{10}$$

Pressure forces are unable to support the gas, and it falls inward toward the accreting object down the accretion column at a velocity $v = (GM/r)^{1/2}$. Using equation (10) and mass conservation, we find that the equilibrium accretion column density is, for $\beta R_A \gg r$,

$$n_c = 6.40 \times 10^{13} T_6^{-2} r_v^{-3/2} n_{11} V_8^4 \beta^{-1}\ \mathrm{cm^{-3}} \tag{11}$$

The assumption that the width of the column is maintained by gas pressure is justified by the required default of any stronger forces, turbulence in particular. One can do a pressure confinement calculation similar to the one above by assuming a fully turbulent accretion column. The internal pressure in the column would be generated by the turbulent velocity, which can be taken to be a fraction f of the velocity of fall. Requiring that the opening angle of the column be less than, say, 1 radian, we find that f is restricted by

$$f^2 \leq \frac{2\sqrt{2}}{\pi}\frac{r}{\beta R_A}. \tag{12}$$

This implies that the turbulent velocity must become a smaller fraction of the fall velocity as it nears the neutron star; otherwise the turbulent pressure is impossible to contain. But the Reynolds number of the gas increases inward (except for adiabatic infall), and we would expect the turbulence, if present, to increase and disrupt the column. Therefore, if the column exists, it must be in laminar flow. There are several reasons to think that laminar flow can obtain in the column. The turbulence would probably originate in the "shear layer" between the sheath and the column, but the Reynolds number in the sheath decreases down the column. In addition, the gas is being strongly accelerated only in the radial direction, which does not provide a driving force for turbulence.

III. RADIATIVE EFFECTS

If the gas is unable to cool before joining the accretion column, the column gas will fall adiabatically and will resemble the accretion scenario found by Hunt (1971), i.e., a very wide accretion column trailing the accreting body. Note that Hunt's solutions were obtained with essentially zero pressure at the boundary of the accreting body, and that the accretion rate would probably be diminished by the nonzero base pressures of a magnetospheric shock above the neutron star. On the other hand, if the gas cools much faster than any time scale for movement, a cold, narrow, high-density column will be formed. In order to determine which regime prevails, we compare the time scales for radiative energy-loss mechanisms with the time scale for infall of the gas, which is the basic and only uniquely identifiable dynamic time scale of the problem. The fall time from the accretion radius is approximately,

$$t_f = \frac{2}{3}\frac{r^{3/2}}{\sqrt{(GM)}} = 250 r_v^{3/2} V_8^{-3} m \text{ s} . \qquad (13)$$

a) *Cooling Time Scales*

In the absence of any heating, the temperature of the gas is entirely dependent upon whether or not a significant amount of cooling can take place in the gas before it reaches the surface of the accreting body. In this section an estimate is made of the cooling time scale, which divides the density-velocity parameter space into regions of cooling and no cooling. In the following, all radiative time scales will be defined as $3kT$ divided by the appropriate heating or cooling rate, where k is Boltzmann's constant.

When the gas crosses the shock, the ions get most of the thermal energy, since they have a much shorter mean free path than the electrons. The electron-ion equilibrium time (Spitzer 1962) in the sheath is, with $n = 4n_0$, a maximum of

$$t_{eq} = 50.6 r_v^{-1} n_{11}^{-1} V_8^{3} \text{ s} . \qquad (14)$$

This time is compared with the fall time and is plotted in Figure 2. For the postshock gas, the equilibrium time decreases with density at the same rate as the cooling time and is always shorter than it. Therefore the postshock gas comes into collisional equilibrium and the electron and ion temperatures are assumed equal.

The cooling from the postshock temperature can be taken from Figure 1 of Cox and Daltabuit (1971), omitting the cooling due to forbidden and semi-forbidden lines. The postshock cooling is assumed to be unaffected by any radiation present. Two assumptions are made for the density of the postshock gas in the sheath. The rightmost line is drawn for the minimum possible postshock density, $4n_0$. This is an underestimate, since the density increases from its free stream value toward the accretion axis, by approximation (4). The angle to the shock decreases with the temperature by equation (10), and choosing the minimum temperature in the column as 10^4 K results in the cooling line on the left.

Gas flows with densities and velocities in between these two cooling lines may be subject to an instability from the cooling to noncooling state and vice versa. If hot, uncooled gas mixes into the accretion column and expands it such that the shock moves outward, it will decrease the density of the incoming gas, by approximation (4). If the density drops sufficiently, the incoming gas may no longer cool and the column will expand to its uncooled state. Consequently we take the rightmost cooling line (labeled $4n_0$) as the effective cooling line.

A point of interest is that, for gas crossing the shock at a distance of less than 3×10^{10} cm, the postshock temperature is greater than 10^7 K, for which bremsstrahlung is the dominant cooling mechanism, until the gas is close enough (see eq. [25]) to be Compton cooled. The time scale for bremsstrahlung losses varies with $n^{-1}T^{1/2}$, which remains constant with distance in the sheath, whereas the dynamic time scale is decreasing as $r^{3/2}$. Consequently, even though gas entering the column at large radii may cool, lower down the gas in the sheath may remain hot. As shown in the Appendix, the sum of the pressure force for the postshock gas

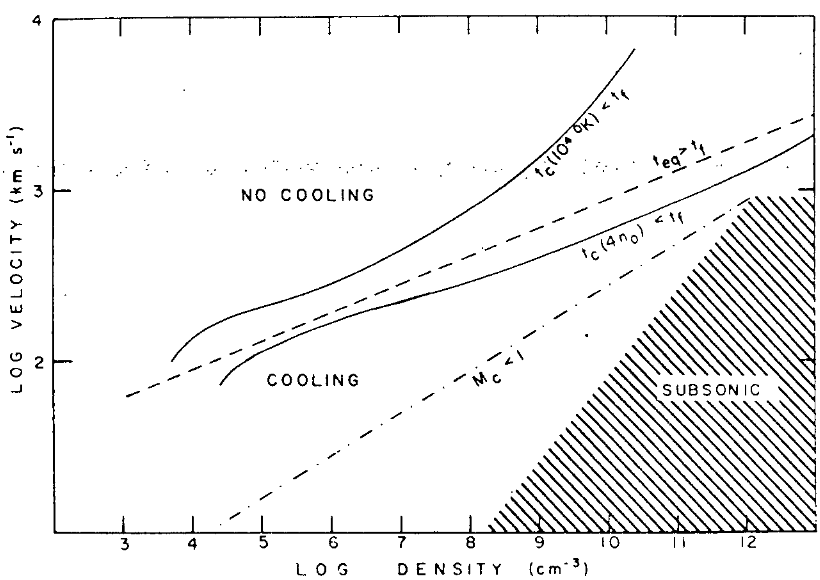

FIG. 2.—The cooling diagram constructed with the free stream density and velocity. *Solid lines*, regions of cooling for the maximum (10^4 K) and minimum ($4n_0$) densities. Cooling occurs to the right, i.e., higher densities, of these lines. Below the dashed lines ($t_{eq} < t_f$) the electron and ion temperatures are equal. The hatched region is heated to the Compton equilibrium temperature and is certainly subsonic, whereas below the dot-dashed line ($M_c < 1$) the Mach number of the incoming gas based on the Compton heating rate is less than 1.

and the gravitational force is still directed downward, but eventually the excess energy must be lost if the gas is to be gravitationally bound to the neutron star. One way to do this would be through turbulent mixing at the boundary between the upward-flowing sheath gas and the downward-flowing accretion column. This would decrease the effective cooling time for the lower sheath by diluting the hot gas with the cooler, denser gas of the column. If a mixing process is required in order to capture gas entering the column at small radii, it would imply that, if gas at the top of the column is unable to cool, then the accretion may become very inefficient.

b) *Heating*

When the accreting body is a neutron star, the accretion luminosity may be sufficient to cause significant heating of the infalling gas. (An additional problem is that the incoming gas stream may be heated to a sufficiently high temperature that the assumption of supersonic flow is invalidated. This is considered in the Appendix.) Approximate rates for photoionization and Compton heating are derived and used to construct a heating diagram similar to the previous cooling diagram. Optical depths must also be considered, because radiative heating will be impossible if the optical depth up the column becomes too large.

The accreting object is assumed to be a neutron star of radius 10^6 cm. The entire kinetic energy of the infalling gas is converted into radiation at the surface shock. The resulting luminosity is

$$L = 4.70 \times 10^{36} n_{11} V_8^{-3} m^3 (R_x/10^6\,\mathrm{cm})^{-1}\ \mathrm{ergs\ s^{-1}}\,. \quad (15)$$

An upper limit to the gas temperature in the column due to photoionization heating is required. The calculations of Hatchett, Buff, and McCray (1976) show that, for log ξ greater than 2, where $\xi = L/nr^2$, the CNO elements are completely ionized. The heating will then be limited by the total recombination rate to the ground state, so the limiting photoionization heating rate is $n_e \alpha f \chi/3$, where n_e will be taken to be the density in the column from equation (11), α is the recombination rate to all levels for completely ionized oxygen, f $(=10^{-3})$ is the fractional abundance of oxygen, increased slightly to allow for some carbon and nitrogen, and $\chi/3$ is the average energy deposited per ionization for a ν^{-1} spectrum. (The spectrum may not be ν^{-1}, but all spectra deposit an average energy of order χ.) The recombination rate used is the expression given by Allen (1973) for the total recombination rate to the ground level, $\alpha = 3 \times 10^{-10} Z^2 T^{-3/4}$. The resulting heating time is

$$t_{\mathrm{ph}} = 22.9 T_6^{15/4} r_v^{3/2} n_{11}^{-1} V_8^{-4} \beta^1 \times (f/10^{-3})^{-1} (Z/8)^{-4}\ \mathrm{s}\,. \quad (16)$$

Comparing this with the fall time, we find that the temperature is limited by

$$T_6 < 1.89 n_{11}^{4/15} V_8^{4/15} (f/10^{-3})^{4/15} \times (Z/8)^{16/15}\,. \quad (17)$$

The expression used for photoionization heating applies only if heating in a static gas would be able to attain this temperature and the absorption and scattering optical depth up the column are less than 1. The static condition, log $\xi > 2$, is equivalent to $V_8 < 1.02 T_6^{2/3} r_v^{-1/6}$, which is indicated in Figure 3, and is always satisfied in the cooling region. The photoionization absorption can be estimated from the equations of ionization balance and of optical depth,

$$n_e n_I \alpha(T) = \frac{Le^{-\tau}}{h\nu 4\pi r^2} \sigma n_G$$

and

$$\frac{d\tau}{dr} = n_G \sigma\,, \quad (18)$$

where n_e, n_I, and n_G are the number densities of electrons, ions, and ground-state absorbers, respectively. The integrals in the exact formulae have been approximated by quantities integrated over frequency, and it is assumed that one ionic species is doing the major part of the absorbing at any given temperature. In the neighborhood of 10^6 K, the major absorber is O VIII. Setting f as the fraction of atoms that are absorbing X-rays, we find a solution to the above equations similar to Mestel's (1954),

$$1 - e^{-\tau} = \frac{h\nu}{L} 4\pi f \alpha(T) \int_{r_b}^{r} n_e^2 r^2 dr\,. \quad (19)$$

The bottom of the column, r_b, has been assumed to be the magnetosphere at a distance near 10^8 cm from the center of the neutron star, and it is assumed that there is no significant opacity between the source of radiation and this lower boundary. This is consistent with the magnetospheric model of Arons and Lea (1976). Using the total recombination rate and 5 keV as an average photon energy, we find that the above integral becomes

$$1 - e^{-\tau} = 0.989 T_6^{-19/4} \ln (r/r_b) \beta^{-3} n_{11} V_8^5 \times (R_x/10^6\,\mathrm{cm})(f/10^{-3})(Z/8)^4\,. \quad (20)$$

For numerical estimates, the distance dependence of the optical depth will be ignored [$\ln (r/r_b) \sim 1$]. This optical depth is meant to be useful only as an indication of how radiative heating is attenuated. As it turns out, this estimate of the photoionization optical depth is always less than the electron scattering optical depth for the range of parameters plotted. A more precise calculation is required to estimate the transmitted spectrum as a function of frequency.

The other major source of heating in an X-ray illuminated gas is Compton scattering. The Compton heating rate is given by Buff and McCray (1974) as

$$G_c = \frac{\epsilon - \alpha^{-1} kT}{m_e c^2} \frac{L\sigma_T}{4\pi r^2}\,, \quad (21)$$

where L is the source luminosity, ϵ is a parameter which describes the effective temperature of the spectrum,

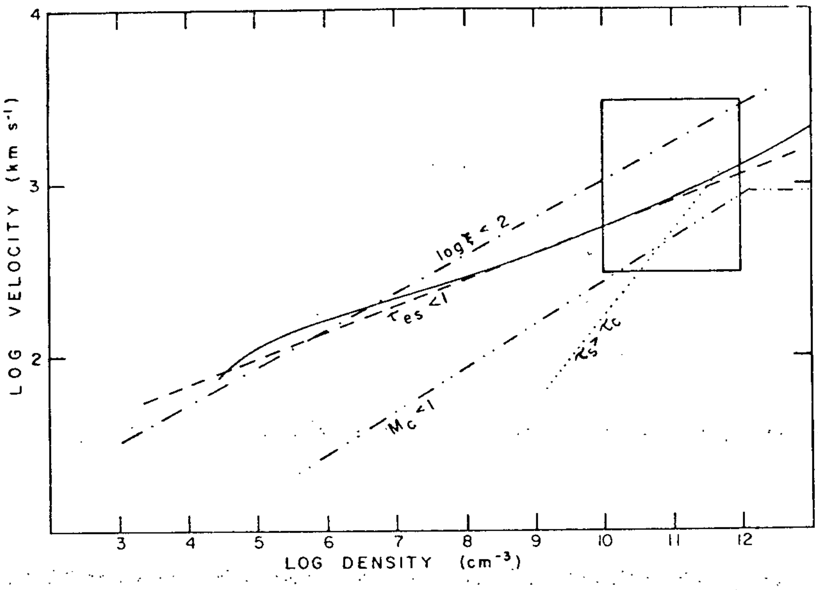

FIG. 3.—The density-velocity diagram for the photoionization heated accretion column, with a Compton heated base. The cooling line (*solid*) and the subsonic line ($M_c < 1$) are repeated from Fig. 2. For log $\xi > 2$ the approximation used for the heating rate would be valid for a static gas. As the flow parameters cross the $\tau_s > \tau_c$ (*dotted*) line, the optical depth up the sheath exceeds that of the column.

and α describes the shape of the spectrum ($\alpha = 1.04$ for a blackbody and $\frac{1}{4}$ for an exponential spectrum). In principle, α and ϵ are determined by the physical parameters n_0, V_0, M_x, and the radius of the accreting object. In view of the complexity of the calculation of the emitted spectrum, we chose to leave them as parameters. As typical values we chose $\alpha = \frac{1}{2}$ and $\epsilon = 5$ keV. This corresponds to a Compton equilibrium temperature ($kT = \alpha\epsilon$) of 2.9×10^7 K. With this choice of parameters, the Compton heating time scale is

$$t_c = 1.20 \times 10^2 T_6 n_{11}^{-1} r_v^2 V_8^{-1} m^{-1} \beta^{-1} \times (R_x/10^6 \text{ cm})^{-1} \text{ s} , \quad (22)$$

or $t_c < t_f$ for

$$n_{11} V_8^{-2} > 0.476 T_6 r_v^{1/2} \beta^{-1} m^{-2} (R_x/10^6)^{-1} . \quad (23)$$

If the base of the column becomes optically thick, the radiation will be thermalized, so that Compton heating becomes negligible as a result of the ϵ parameter's being reduced. As discussed by Felten and Rees (1972), spectrum alteration begins when the optical depth $\tau^* = (3\tau_{ff}\tau_{es})^{1/2}$ exceeds 1, where τ_{ff} and τ_{es} are the free-free and electron scattering optical depths. The calculation indicates that the optical depth at a photon energy of 5 keV is always much less than 1 as long as the flow is supersonic.

As one gets closer to the source of radiation, the time scale for Compton heating decreases faster than the fall time. The bottom of the accretion column may be heated to Compton equilibrium, even though the regions higher up may be in photoionization equilibrium, or optically thick and cold. From equation (10) we see that the column is impossible to contain for $V_8 < 0.9$, and the column will widen and may even become spherical at the bottom. For electron scattering the new effective base of the column is at a distance where the Compton heating and the fall time scales are equal,

$$r_8 = 1.39 n_{11}^2 V_8^{-6} (\alpha/0.5)^{-2} (\epsilon/5 \text{ keV})^{-2} \beta^2 . \quad (24)$$

The spherically infalling material below this has a negligible contribution to the optical depth, because the density is reduced by the much greater column angle.

The electron scattering optical depth along the column is

$$\tau_c = 9.18 n_{11} V_8 T_6^{-2} (r_b/10^8 \text{ cm})^{-1/2} . \quad (25)$$

The actual line plotted on Figure 3 for the electron scattering opacity assumes that the effective base of the column is at the Compton heated distance of equation (25) and that the column temperature is determined by the photoionization heating temperature of equation (17). The range of photoionization heating is thus extended by the reduction of column opacity. If one computes the Alfvén radius from $B^2/8\pi = 1/2\rho v^2$, one finds that in some cases the Alfvén radius exceeds the Compton heated radius and will determine the effective base of the flow. But these cases turn out to be in the region of the density-velocity diagram above the cooling line and hence of little interest to the heating calculation.

The column is effectively optically thin to the sideways loss of radiation because the sideways optical depth of the column is dominated by electron scattering and is always less than 1 for the range of parameters plotted.

The higher-energy X-rays will be attenuated by K shell absorption by elements with ionization potentials greater than the CNO elements. For a spectrum with a typical photon energy of 5 keV, the K shell cross sections of Daltabuit and Cox (1972) and the abundances of Allen (1973) suggest that the dominant K shell absorber will be silicon. The calculations of Hatchett *et al.* indicate that a typical silicon atom, for $\log \xi > 2$, will have several electrons left, and therefore will have a cross section of order 10^{-19} cm^2, which is relatively independent of temperature and radiation flux. Combining this with a fractional abundance of 3×10^{-5}, the effective cross section at the absorption edge is only 4.5 times the electron scattering cross section. Photons below the edge will be less affected, primarily interacting with only lower-abundance magnesium, and for those above, the cross section decreases approximately as E^{-3}, until another edge, due to low-abundance sulfur, is encountered. In general we expect that K absorption will be of the same magnitude as the electron scattering. Similarly, the K shell photoionization heating rate is different from Compton heating only by a multiplicative factor of order 1, and will be ignored.

c) *Accretion Scenarios*

In Figure 3 a box has been drawn which encloses the suggested range of wind densities and velocities for stellar wind X-ray sources Cen X-3 and 3U 1700−37. Only a small part of this region is subsonic and beyond the description given here. For a given density and velocity, it is possible to qualitatively describe the flow.

If the density and velocity parameters of the free stream lie above the cooling line, the accretion may be less efficient as pressure forces in the hot gas of the sheath become more important. This would be reflected in a diminished luminosity. In general, flows with parameters above the cooling line would broadly resemble the scenario found by Hunt (1971). Captured gas falls inward with its temperature rising adiabatically.

Below the cooling line, the gas temperature drops to some equilibrium value and falls down the accretion column. Although the K absorption edges will alter the spectrum somewhat, the line above which the electron scattering opacity exceeds 1 is almost coincident with the cooling line, so that heating of the most distant parts of the accretion column will be possible below the cooling line. Typical maximum temperatures for $V_8 = 1$ are $T_6 = 1$ at $n_{11} = 0.1$ and $T_6 = 3.5$ at $n_{11} = 10$. The column semiangles are 2° and 9°, respectively. The gas will remain at the equilibrium temperature specified by the local radiation field, since all radiation time scales are more rapid than the fall time. Near the source Compton heating dominates, the temperature rises to the Compton equilibrium value, and the column expands so that the infall becomes almost spherical. It is of particular interest to compare the electron scattering opacity up the column with that up the edge of the sheath in the postshock gas. The opacity up the sheath is

$$\tau_s = \sigma_T \int_{r_b}^{r_m} \frac{2n_0}{\phi} \left(\frac{R_A}{r}\right)^{1/2} dr \,. \tag{26}$$

Evaluating this integral, and choosing (somewhat arbitrarily) the maximum extent of the column to be the distance at which the density has dropped to $4/3n_0$, i.e., $r_m = R_A/(2\phi^2)$, gives

$$\tau_s = 2.26 n_{11} V_8{}^2 T_6{}^{-2} \,, \tag{27}$$

whereas the electron scattering opacity up a column with a Compton heated base is $7.79 V_8{}^4 T_6{}^{-2}$. As a result we find that the opacity up the sheath is greater than up the column if $n_{11} V_8{}^{-2} > 3.45$, a result which is independent of the column temperature. This line has been included in Figure 3.

If the stellar wind in which the neutron star is embedded has velocity and density variations, this analysis predicts potentially observable effects. The most obvious is that, if the line-of-sight optical depth is constant, the X-ray luminosity responds to variations in $n_0 V_0{}^{-3}$ (eq. [16]) on times of variation longer than about two fall times, or $500 V_8{}^{-3}$ s. This variation reflects the local structure of the wind for regions of size greater than $2R_A$ ($5 \times 10^{10} V_8{}^{-2}$ cm). Another expected effect is that, as $n_0 V_0{}^{-2}$ increases, the optical depth up the sheath will exceed that up the column. Thus, if the X-ray source is occulted by the accretion column, the X-ray absorption would change from a single dip ($\tau_c > \tau_s$) to a double dip ($\tau_c < \tau_s$). In addition, Jackson's calculations (1975) indicate that, if the gas fails to cool, the absorption up the sheath always dominates.

IV. THE FAR WAKE

The Reynolds number of the gas flow is extremely high ($V_0 R_A/\nu = 10^{12} V_8{}^{-1} m^1 T_4{}^{-5/2} n_{11}$), and the far wake is expected to be turbulent. Turbulence in supersonic flows is not well understood, but experimental studies of supersonic wakes (Demetriades 1968) indicate that a phenomenological theory as outlined by Townsend (1976) provides a reasonable description of supersonic far wakes. Unfortunately, the dynamics of laboratory wakes are not dominated by a gravitational field, and therefore the applicability of the description to this case must be carefully considered. The subsonic theory is based on the observation that the wake remains self-similar with respect to a characteristic velocity and length scale. This is combined with the momentum equation from which all small terms have been dropped. The axisymmetric far wake is found to be self-similar with respect to the half-width, l, and the turbulent velocity scale, u, defined by

$$\frac{l}{R_A} = \frac{1}{2}\left(\frac{6}{R_T}\right)^{1/3}\left(\frac{r}{R_A}\right)^{1/3},$$
$$\frac{u}{V_0} = \left(\frac{R_T}{6}\right)^{2/3}\left(\frac{R_A}{r}\right)^{2/3}, \tag{28}$$

where the so-called momentum radius R_M (the radius such that the drag force is $1/2\rho V_0{}^2\pi R_M{}^2$) has been taken to be R_A. R_T is the turbulent Reynolds number, observed by Demetriades to be 12.8.

The width scale of the wake implies that the small angle approximations for the density and transverse velocity apply for the exterior supersonic flow. Hence the effective exterior pressure will be the transverse momentum flux, which varies with distance along the wake. But the equations of momentum used to derive the length and velocity scale assumed that there was no pressure gradient in the free stream. For the gravitational wake, an order-of-magnitude estimate of the pressure gradient term in the small angle approximation finds that it is of order $u^2/l(R_A/l)$, whereas the retained terms in the momentum equation are of order u^2/l. Consequently, for $R_A \ll l$, the pressure gradient term can again be dropped. Using the half-width of equation (28), we find that R_A/l is of order $(R_A/r)^{1/3}$. Thus the equations are consistent for $r \gg R_A$, but the crucial observation that a gravitational wake is self-similar is unavailable. Experiments also indicate that the flow may not be self-similar for distances of several tens of the momentum radius, but the deviation of the turbulent velocity scale from the self-similar value is a factor of 2 or less.

For sufficiently low Reynolds numbers, part of the wake may be in laminar flow. In this case the velocity defect on the axis is $u/V_0 = 3/2R_A/r$, and the half-width varies as $(rR_A)^{1/2}$ (Lamb 1924). The Reynolds number grows with distance, and the flow will eventually become turbulent. With the extreme Reynolds numbers present here, the wake is expected to become turbulent within the sheath of the accretion column.

If the gas in the wake has no energy losses, i.e., $5RT + \frac{1}{2}v^2$ constant, the temperature on the axis is found to be

$$T - T_\infty = \frac{\gamma - 1}{2\gamma}\frac{uV_0}{R} = 3.55 \times 10^6 V_8{}^{2/3}m^{2/3}r_{12}{}^{-2/3}\ \mathrm{K}, \tag{29}$$

where T_∞ is the temperature of the gas external to the wake. This temperature implies that the turbulent velocity scale is subsonic. The temperature becomes equal to $2T_\infty$ at $R_B V_0/c_\infty$, where R_B is the Bondi radius, $10^{14}(10^4\ \mathrm{K}/T)$ cm, and c_∞ is the sound speed at T_∞.

Experimentally it is observed (McCarthy and Kubota 1964) that the pressure is approximately constant across the wake. Equating ρv^2 at the wake boundary to the gas pressure at the center gives the central density

$$n_w = 1.06 \times 10^{11} n_{11} m^{1/6} V_8{}^{-1/3} r_{12}{}^{-1/6}. \tag{30}$$

Note that this density is greater than that which would be found by using the external static pressure by a factor of

$$\frac{\rho V_n{}^2}{P} = 376.0 T_4{}^{-1} V_8{}^{1/3} r_{12}{}^{-5/6}. \tag{31}$$

The temperature estimate and density estimate of equations (30) and (31) assume that the wake is isoenergetic, but at these temperatures and densities, radiation cooling can be significant. Time scales of interest are the cooling time (where Λ is the cooling coefficient)

$$12.4 n_{11}{}^{-1} V_8{}^{5/3} r_{12}{}^{-1/2}(10^{-22}\ \mathrm{ergs\ cm^3\ s^{-1}}/\Lambda)\ \mathrm{s}, \tag{32}$$

turbulent dissipation of kinetic energy time scale,

$$3RT/(u^3/l) = 3.04 \times 10^4 V_8{}^{1/3} m^{-2/3} r_{12}{}^{5/3}\ \mathrm{s}, \tag{33}$$

and the turbulent time scale,

$$2.40 \times 10^3 V_8{}^{-1} r_{12} m^{2/3}\ \mathrm{s}. \tag{34}$$

These time scales imply that, for large distances, cooling removes most of the thermal energy from the wake. If the sound speed within the wake drops below the turbulent velocity scale, the turbulence would then become supersonic, leading to shocks which rapidly heat the gas, but the shocks would occur on the basic turbulence time scale, and would not be able to reheat the bulk of the gas. One might speculate that the temperature would decline to the minimum of 10^4 K, but with an extremely clumpy distribution. If cooling is complete, the simple model used, which does not consider the energy budget, may break down completely. Its value lies in the fact that, as the gas cools, the Reynolds number becomes even greater, and the dynamics of the gas flow in the far wake are almost certainly dominated by turbulence.

One can combine the density and width to show a column density across the wake of sufficient size to produce optical absorption of radiation from the primary. That is $n_e{}^2 2l = 2 \times 10^{33}\ \mathrm{cm^{-5}}$ for an optical depth in the wake of one at Hα, assuming the lower level is populated by recombinations at 10^4 K and depopulated by radiative transitions. This would be possible whenever the wake was silhouetted against the primary star. But these simple considerations fall well short of the ability to reproduce line profiles as seen by Conti and Cowley (1975). The wake will remain cold in the presence of an X-ray source for $L/nr^2 < 10$, or distances from the X-ray source of $r_{12} > 3L_{37}{}^{1/2} n_{11}{}^{-1/2}$. The absorption cross section for X-rays by a cold gas of cosmic abundances is about $10^{-22}(E/\mathrm{keV})^{-3}\ \mathrm{cm}^2$. Again the column densities are adequate for X-ray absorption, but the absorption would be very sensitive to the inclination of the wake with respect to the X-ray star, since the far wake is very narrow.

V. CONCLUSIONS

The supersonic accretion of gas onto a neutron star has been described, working from the basic model as shown in Figure 1; the main features are the sheath and the accretion column. The angular width of the column, a measurable quantity in the X-ray light curve, is found to depend on the ratio of V_0^2 to the column temperature, and therefore yields information about the local wind velocity provided the column temperature can be specified. An accurate estimate of the temperature would require a hydrodynamic calculation including radiation transfer, but upper limits to the temperature can be obtained by estimating the relevant heating and cooling rates.

The most important consideration in determining the thermal state of the gas is whether or not the gas can cool before it falls all the way down the accretion column. The cooling line of Figure 2 separates the flow into two main regimes. If the postshock gas in the sheath is unable to cool, it will fall inward adiabatically in a wide accretion column, with the accretion efficiency (the β factor) reduced by the thermal pressure. Below the cooling line of Figure 2, the gas will cool to an equilibrium value determined by the radiation field. In the region of the density and velocity parameters which apply to the stellar wind X-ray binaries, this means that the upper part of the accretion column will be photoionization heated to temperatures of order 10^6 K. The base of the column will be heated to the Compton equilibrium temperature, causing the pressure to rise sufficiently that the base of the column will spread to a broad inflow. It is predicted that the electron scattering will cause the X-ray light curve absorptions to change from single dips to double dips as $n_0 V_0^{-2}$ increases, if the parameters are in the cooling region.

The gas that is gravitationally perturbed but does not become bound to the neutron star forms the far wake. The high velocity and low viscosity indicate that the far wake is almost certainly turbulent. An extension of the similarity description of supersonic wakes experimentally studied provides the temperature and density in the wake. But the cooling time of the gas in the wake is then found to be less than the basic turbulence time scale, which may mean that whole description is invalid. In spite of this, we suggest that the far wake is composed of a hot gas entering the wake and denser clumps of cold gas, a description which is marginally consistent with the "wake" observations of Conti and Cowley (1975).

The model outlined here is intended to be useful for providing qualitative insight into the physics of supersonic accretion. The numerical quantities employed are expected to be accurate to a factor of 3 or so, and should provide basic regimes which can be further explored with a numerical model.

G. G. Fahlman provided invaluable advice and criticism, and read several rough drafts of this paper during the course of this research. General encouragement and useful discussions were provided by members of the UBC Institute of Astronomy and Space Science and the Dominion Astrophysical Observatory.

APPENDIX

In the case of a heated gas, the thermal pressure forces may become large enough to destroy the assumption that the flow is dominated by inertial forces. In this Appendix the region of validity of the supersonic description of accretion is examined.

The incoming free stream may be heated such that the Mach number, $M = V_0/(2\gamma RT)^{1/2}$, becomes less than 1. The maximum temperature which can be produced by Compton heating is $2.9 \times 10^7(\alpha/0.5) \times (\epsilon/5\text{ keV})$. This temperature can be attained for $n_{11}V_8^{-2} > 13.8$, which is shown as the crosshatched area in Figure 2. This gives only the area for which subsonic flow is guaranteed in the presence of Compton heating, but what is really wanted is a line on which the Mach number is equal to 1. If only Compton heating is considered, we find that (nonequilibrium) temperatures are produced such that the Mach number is less than 1 for $n_{11}V_8^{-4} > 17.2$. This line ($M_c < 1$) is shown in Figure 2. If photoionization heating is included, the subsonic region is increased very slightly at low velocities. We conclude that most of the box of Figure 3 is indeed in supersonic flow.

The deviation of streamlines from particle trajectories will depend on the ratio of pressure forces to inertial forces. As a worst case we assume that the gas is fully Compton heated. The ratio of radial pressure force to gravitational force for gas outside the shock is

$$\frac{1}{\rho}\frac{\partial p}{\partial r}\bigg/\frac{GM}{r^2} = \frac{RT_0}{r^2}\bigg/\frac{GM}{r^2} = \frac{r}{5R_T}\,. \tag{A1}$$

This implies that the net force is outward for $r > 5R_T$, where the thermal radius is $R_T = GM/5RT_0 = 3.19 \times 10^{10}T_7^{-1}$ cm. Similarly, in the transverse direction, the ratio of pressure to the momentum flux is

$$\frac{P}{\rho V_\phi^2} = \frac{r}{5R_T}\,. \tag{A2}$$

In the shock-heated sheath, the ratio of radial pressure force to gravitational force is 9/16, which will act only to reduce the effective mass of the gravitating object in the sheath. In the column the ratio of pressure forces to gravitation is, for a constant temperature, $3r/5R_T$.

In general the pressure forces can be safely ignored, even in the presence of strong heating, provided that we remain in the area of validity of the supersonic flow assumption.

REFERENCES

Allen, C. W. 1973, *Astrophysical Quantities* (3d ed.; London: Athlone Press).
Arons, J., and Lea, S. M. 1976, *Ap. J.*, **210**, 792.
Bondi, H., and Hoyle, F. 1944, *M.N.R.A.S.*, **104**, 273.
Buff, J., and McCray, R. 1974, *Ap. J.*, **189**, 147.
Conti, P., and Cowley, A. P. 1975, *Ap. J.*, **200**, 133.
Cox, D. P., and Daltabuit, E. 1971, *Ap. J.*, **167**, 113.
Dachs, J. 1976, *Astr. Ap.*, **47**, 19.
Daltabuit, E., and Cox, D. P. 1972, *Ap. J.*, **177**, 855.
Danby, J. M. A., and Camm, G. L., 1957, *M.N.R.A.S.*, **117**, 50.
Davidson, K., and Ostriker, J. P. 1973, *Ap. J.*, **179**, 585.
Demetriades, A. 1968, *AIAA J.*, **6**, 432.
Eadie, G., Peacock, A., Pounds, K. A., Watson, M., Jackson, J. C., and Hunt, R. 1975, *M.N.R.A.S. Short Comm.*, **172**, 35p.
Felten, J. E., and Rees, M. J. 1972, *Astr. Ap.*, **17**, 226.
Hatchett, S., Buff, J., and McCray, R. 1976, *Ap. J.*, **206**, 847.
Hoyle, F., and Lyttleton, R. A. 1939, *Proc. Cambridge Phil. Soc.*, **35**, 405.
Hunt, R. 1971, *M.N.R.A.S.*, **154**, 141.
Illarionov, A. F., and Sunyaev, R. A. 1975, *Astr. Ap.*, **39**, 185.
Jackson, J. C. 1975, *M.N.R.A.S.*, **172**, 483.
Jones, C., Forman, W., Tananbaum, H., Schreier, E., Gursky, H., Kellogg, E., and Giacconi, R. 1973, *Ap. J.* (*Letters*), **181**, L43.
Lamb, H. 1924, *Hydrodynamics* (5th ed.; Cambridge: Cambridge University Press).
McCarthy, J. F., and Kubota, T. 1964, *AIAA J.*, **2**, 629.
McCray, R., and Hatchett, S. 1975, *Ap. J.*, **199**, 196.
Mestel, L. 1954, *M.N.R.A.S.*, **114**, 437.
Pounds, K. A., Cooke, B. A., Ricketts, M. J., Turner, M. J., and Elvis, M. 1975, *M.N.R.A.S.*, **172**, 473.
Ruderman, M. A., and Spiegel, E. A. 1971, *Ap. J.*, **165**, 1.
Spitzer, L. 1962, *Physics of Fully Ionized Gases* (New York: Interscience).
Townsend, A. A. 1976, *The Structure of Turbulent Shear Flow* (2d ed.; Cambridge: Cambridge University Press).

R. G. CARLBERG: Department of Geophysics and Astronomy, University of British Columbia, Vancouver, B.C., Canada, V6T 1W5

APPENDIX 2. GAS PHYSICS

Photoionization

The simplest process to describe is the photoionization rate which is independent of the gas temperature and density, and is simply given by

$$\zeta_{ij} = \int_{\nu_0}^{\infty} \frac{4\pi J_\nu}{h\nu} \sigma_{ij}(\nu)\, d\nu, \qquad \text{(AII.1)}$$

where σ_{ij} is the photoionization cross-section of atom i, ionization level j. For these calculations the mean radiation field J was taken simply as the flux emerging from a model atmosphere allowing for geometrical dilution. The numerical computations used a model computed by Mihalas (1972), specifically the Non-LTE 50,000 K, log g = 4 model. Mihalas gives the radiation field in terms of the emergent flux, F , whereas the mean intensity 4 J is needed for the ionization and heating calculations. To make this change, the mean intensity was assumed to vary as the dilution, $W=1/2(1-(1-(r_*/r)^2)^{1/2})$, and the flux as $(r_*/r)^2$, where r is the stellar radius. For the computations illustrated here, all done at a radiation field corresponding to the surface of the star, $4\pi J_\nu = 2\ (\pi F_\nu)$.

Since the O VI ion is of particular importance the photoionization rates of all ions up to comparable ionization potentials (IP of O V is 113.9eV) were included.

The photoionization cross sections used in the calculations are given below. The cross sections used are given in below.

The Hydrogen cross section was taken from Bethe and Salpeter (1957).

$$\sigma = \frac{2^9 \pi^2 \alpha a_0^2}{3 Z^2} \left(\frac{Z^2 \mathcal{R}}{h\nu}\right)^4 \frac{\exp(-4\eta \operatorname{arccot}\eta)}{1-\exp(-2\pi\eta)}, \tag{AII.2}$$

where α is the fine structure constant

a_0 is the Bohr radius

$\mathcal{R}$ is the Rydberg

$\eta = (h\nu/\mathcal{R} - 1)^{-1/2}$

Z is the ion charge

The Helium I cross section was obtained from Brown (1971). The formula quoted by him was multiplied by 16 to agree with his numerical values, and a factor of 2 was included in the exponential factor to reduce to the Hydrogen formula. The cross section is

$$\sigma = \frac{2^{15} \pi^2 a_0^2 \frac{h\nu}{\mathcal{R}} (\alpha\beta Z_b)^3 (k^2 + Z_f^2) \left[\frac{I_\alpha}{(\beta + Z_b)^3} + \frac{I_\beta}{(\alpha + Z_b)^3}\right]^2}{3\left[1-\exp\left(-\frac{2\pi Z_f}{k}\right)\right]\left[1 + \frac{(4\alpha\beta)^3}{(\alpha+\beta)^6}\right]}, \tag{AII.3}$$

where

$$I_\alpha = \frac{2\alpha - Z_f}{(k^2+\alpha^2)^3} \exp\left(-\frac{2Z_f}{k} \tan^{-1}\left(\frac{k}{\alpha}\right)\right),$$

and $I_\beta = I_\alpha$ with all α's replaced by β's. The constants are

$\alpha = 2.182846$

$\beta = 1.188914$

$Z_f = 2$

$Z_b = 1$

$k = ((h\nu - 24.587\text{eV})/13.598\text{eV})^{1/2}$

The Helium II cross section is the same as the photoionization cross section of Hydrogen but with Z=2 everywhere.

For the remaining ions the cross sections have been calculated by various authors using the principles of quantum mechanics, and then making a fit to a standard polynomial to represent the data as a function of incident photon energy. Two forms for the polynomial are used here, one due to Seaton (1958)

$$\sigma(\nu) = \sigma_0 \left[\alpha \left(\frac{\nu}{\nu_0}\right)^{-s} + (1-\alpha) \left(\frac{\nu}{\nu_0}\right)^{-s-1} \right], \tag{AII.4}$$

where ν_0 is the threshold frequency and the other constants are fitting parameters. The other form is a slightly more general polynomial due to Chapman and Henry (1971)

$$\sigma(\nu) = \sigma_0 \left[\alpha \left(\frac{\nu}{\nu_0}\right)^{-s} + (\beta - 2\alpha) \left(\frac{\nu}{\nu_0}\right)^{-s-1} + (1+\alpha-\beta) \left(\frac{\nu}{\nu_0}\right)^{-s-2} \right]. \tag{AII.5}$$

TABLE 6: PHOTOIONIZATION CROSS SECTION PARAMETERS

Ion	$h\nu_0$ eV	σ_0 10^{-18}cm^2	s	α	β	Reference
C I	11.26	12.19	2.0	3.17	--	H70
C II	24.383	4.6	3.0	1.95	--	H70
C III	47.887	1.84	2.6	3.0	--	SB71
C IV	64.492	0.713	2.2	2.7	--	SB71
N I	14.534	11.42	2.0	4.287	--	H70
N II	29.601	6.65	3.0	2.86	--	H70
N III	47.448	2.06	1.62	3.0	--	H70
N IV	77.472	1.08	3.0	2.6	--	F68
N V	97.89	0.48	2.0	1.0	--	F68
O I	13.618	2.94	1.0	2.661	--	H70
	16.943	3.85	1.5	4.378	--	
	18.635	2.26	1.5	4.311	--	
O II	35.117	7.32	2.5	3.837	--	H70
O III	54.943	3.65	3.0	2.014	--	H70
O IV	77.413	1.27	3.0	0.831	--	H70
O V	113.90	0.78	3.0	2.6	--	F68
O VI	138.2	0.36	2.1	1.0	--	F68
Ne I	21.564	5.35	1.0	3.769	--	H70
Ne II	40.962	4.16	1.5	2.717	--	H70

	44.166	2.71	1.5	2.148	--	
	47.874	0.52	1.5	2.126	--	
Ne III	63.45	1.89	2.0	2.277	--	H70
	68.53	2.50	2.5	2.346	--	
	71.16	1.48	2.5	2.225	--	
Ne IV	97.11	3.11	3.0	1.963	--	H70
Ne V	126.21	1.40	3.0	1.471	--	H70
Ne VI	157.93	0.49	3.0	1.145	--	H70
Mg I	7.646	9.92	1.8	2.3	--	Iso To Si III
Mg II	15.035	3.416	1.0	2.0	--	Iso To Si IV
Mg III	80.143	5.2	2.65	2.65	--	S58
Mg IV	109.31	3.83	2.0	1.0	--	S58
Mg V	141.27	2.53	2.3	1.0	--	S58
Si I	7.37	*12.32	3	6.459	5.142	CH71
	8.151	*25.17	5	4.420	8.943	
Si II	16.345	2.65	3.0	0.6	--	SB71
Si III	33.492	2.48	1.8	2.3	--	SB71
Si IV	45.141	0.854	1.0	2.0	--	SB71
S I	10.360	12.62	3.0	21.595	3.062	CH72
	12.206	19.08	2.5	0.135	5.635	
	13.408	12.70	3.0	1.159	4.734	
S II	23.33	8.2	1.5	1.695	-2.236	CH72
S III	33.46	*.35	2.0	10.056	-3.278	CH72
	34.83	*.24	2.0	18.427	0.592	
S IV	47.30	0.29	2.0	6.837	4.459	CH72
S V	72.68	0.62	1.8	2.3	--	Iso To Si III
S VI	88.05	0.214	1.0	2.0	--	Iso To Si IV

* means that the cross section weighted by the statistical weights of the fine structure transitions. The abbreviation Iso means extrapolation along an isoelectronic sequence.

The references coded above are:

H70: Henry 1970

S58: Seaton 1958

SB71: Silk and Brown 1971

CH71 Chapman and Henry 1971

CH71 Chapman and Henry 1972

F68: Flower 1968.

The Recombination Rate

The recombination rate for Hydrogen was calculated using an expression given by Johnson (1972) which has a correction factor built in allowing for finite density. The rate to level n is

$$S(c',n) = \mathcal{D}(I_n/kT)^{3/2}\exp(I_n/kT)\sum_{i=0}^{2} g_i(n)\, x^{-i}\, E_{i+1}(x_o I_n/kT) \qquad \text{(AII.6)}$$

Above the level n_o the populations can be assumed to be in equilibrium with the continuum, that is the populations are as in Saha equilibrium. The value of n is calculated from an expression given by Jordan (1969)

$$n_o = Z^{\frac{14}{17}}\, n_e^{-\frac{2}{17}} \left[\frac{kT_e}{Z^2 R}\right]^{\frac{1}{17}} \exp\left[\frac{4Z^2 R}{17 n_o^3 kT_e}\right]. \qquad \text{(AII.7)}$$

The value of x_o is defined to be $1-(n/n_o)^2$. The constant $\mathcal{D}$ is 5.197×10^{-14} cm^2. The functions E_i are the exponential integrals, and the g (n) are Gaunt factor coefficients, determined as shown in the following table.

TABLE 7: GAUNT FACTORS

	n=1	n=2	n>2
$g_0(n)$	1.1330	1.0785	$0.9935+.2328n^{-1}-.1296n^{-2}$
$g_1(n)$	-0.4059	-0.2319	$-n^{-1}(.6282-.5598n^{-1}+.5299n^{-2})$
$g_2(n)$	.07014	.02947	$n^{-2}(.3887-1.181n^{-1}+1.470n^{-2})$

The values in this table were taken from Johnson (1972).

In order to obtain the total recombination rate, recombinations to the levels n=1 to 9 summed together.

Computations of the recombination rate for all of the other ions of interest have been made by Aldrovandi and Pequignot

(1973), with errata in Aldrovandi and Pequignot (1976). The data is provided in the form of fits to simple functions. The radiative rate is given by

$$\alpha^{r} = A_{rad}\,(T/10^4\ K)^{-\eta}. \qquad \text{(AII.8)}$$

and the dielectronic recombination rate by

$$\alpha^{di} = A_{di}\,T^{-3/2}\exp(-T_0/T)[1+B_{di}\exp(-T_1/T)]. \qquad \text{(AII.9)}$$

The various constants used are given in the accompanying table. The range of validity of the fits are Tmax/1000 < T < Tmax. Tcrit gives the temperature above which dielectronic recombination is important.

TABLE 8: RECOMBINATION FIT CONSTANTS

ATOM	ARAD	ETA	TMAX	TCRIT	ADI	TO	BDI	T1
HE I	4.3E-13	.672	1E5	5.0E4	1.9E-3	4.7E5	0.3	9.4E4
C I	4.7E-13	.624	5E4	1.2E4	6.9E-4	1.1E5	3.0	4.9E4
C II	2.3E-12	.645	1E5	1.2E4	7.0E-3	1.5E5	0.5	2.3E5
C III	3.2E-12	.770	3E5	1.1E4	3.8E-3	9.1E4	2.0	3.7E5
C IV	7.5E-12	.817	1E6	4.4E5	4.8E-2	3.4E6	0.2	5.1E5
C V	1.7E-11	.721	3E6	7.0E5	4.8E-2	4.1E6	0.2	7.6E5
N I	4.1E-13	.608	1E5	1.8E4	5.2E-4	1.3E5	3.8	4.8E4
N II	2.2E-12	.639	1E5	1.8E4	1.7E-3	1.4E5	4.1	6.8E4
N III	5.0E-12	.676	3E5	2.4E4	1.2E-2	1.8E5	1.4	3.8E5
N IV	6.5E-12	.743	3E5	1.5E4	5.5E-3	1.1E5	3.0	5.9E5
N V	1.5E-11	.850	3E6	6.8E5	7.6E-2	4.7E6	0.2	7.2E5
N VI	2.9E-11	.750	1E7	1.0E6	6.6E-2	5.4E6	0.2	9.8E5
O I	3.1E-13	.678	5E4	2.7E4	1.4E-3	1.7E5	2.5	1.3E5
O II	2.0E-12	.646	2E5	2.2E4	1.4E-3	1.7E5	3.3	5.8E4
O III	5.1E-12	.666	5E5	2.4E4	2.8E-3	1.8E5	6.0	9.1E4
O IV	9.6E-12	.670	1E6	2.5E4	1.7E-2	2.2E5	2.0	5.9E5
O V	1.2E-11	.779	6E5	1.6E4	7.1E-3	1.3E5	3.2	8.0E5
O VI	2.3E-11	.802	3E6	1.0E6	1.1E-1	6.2E6	0.2	9.5E5
O VII	4.1E-11	.742	1E7	1.5E6	8.6E-2	7.0E6	0.2	1.3E6
NE I	2.2E-13	.759	1E5	3.0E4	1.3E-3	3.1E5	1.9	1.5E5
NE II	1.5E-12	.693	1E5	3.3E4	3.1E-3	2.9E5	0.6	1.7E5
NE III	4.4E-12	.675	2E5	3.3E4	7.5E-3	2.6E5	0.7	4.5E5
NE IV	9.1E-12	.668	3E5	3.5E4	5.7E-3	2.4E5	4.3	1.7E5
NE V	1.5E-11	.684	6E5	3.6E4	1.0E-2	2.4E5	4.8	3.5E5
NE VI	2.3E-11	.704	1E6	3.6E4	4.0E-2	2.9E5	1.6	1.1E6
NE VII	2.8E-11	.771	1E6	2.9E4	1.1E-2	1.7E5	5.0	1.3E6
NE VIII	5.0E-11	.832	6E6	1.5E6	1.8E-1	9.8E6	0.2	1.4E6
NE IX	8.6E-11	.769	3E7	3.8E6	1.3E-1	1.1E7	0.2	2.6E6
MG I	1.4E-13	.855	3E4	4.0E3	1.7E-3	5.1E4	0.0	0.0
MG II	8.8E-13	.838	1E5	7.4E4	3.5E-3	6.1E5	0.0	0.0
MG III	3.5E-12	.734	3E5	6.6E4	3.9E-3	4.4E5	3.0	4.1E5

MG	IV	7.7E-12	.718	5E5	5.5E4	9.3E-3	3.9E5	3.2	8.7E5
MG	V	1.4E-11	.716	1E6	4.4E4	1.5E-2	3.4E5	3.2	1.0E6
MG	VI	2.3E-11	.695	1E6	4.5E4	1.2E-2	3.1E5	6.7	5.4E5
MG	VII	3.2E-11	.691	1E6	4.5E4	1.4E-2	3.1E5	4.4	3.6E5
MG	VIII	4.6E-11	.711	2E6	5.0E4	3.8E-2	3.6E5	3.5	1.6E6
MG	IX	5.8E-11	.804	3E6	3.4E4	1.4E-2	2.1E5	10.0	2.1E6
MG	X	9.1E-11	.830	1E7	2.4E6	2.6E-1	1.4E7	0.2	2.4E6
MG	XI	1.5E-10	.779	5E7	4.0E6	1.7E-1	1.5E7	0.2	3.5E6
SI	I	5.9E-13	.601	3E4	1.1E4	6.2E-3	1.1E5	0.0	0.0
SI	II	1.0E-12	.786	1E5	1.1E4	1.4E-2	1.2E5	0.0	0.0
SI	III	3.7E-12	.693	2E5	1.1E4	1.1E-2	1.0E5	0.0	0.0
SI	IV	5.5E-12	.821	3E5	1.7E5	1.4E-2	1.2E6	0.0	0.0
SI	V	1.2E-11	.735	6E5	9.5E4	7.8E-3	5.5E5	10.0	1.0E6
SI	VI	2.1E-11	.716	1E6	8.0E4	1.6E-2	4.9E5	4.0	1.3E6
SI	VII	3.0E-11	.702	1E6	7.4E4	2.3E-2	4.2E5	8.0	1.7E6
SI	VIII	4.3E-11	.688	2E6	6.8E4	1.1E-2	3.8E5	6.3	6.0E5
SI	IX	5.8E-11	.703	2E6	6.6E4	1.1E-2	3.7E5	6.0	1.1E6
SI	X	7.7E-11	.714	3E6	6.5E4	4.8E-2	4.2E5	5.0	2.5E6
SI	XI	1.2E-10	.855	1E7	4.5E4	1.8E-2	2.5E5	10.5	2.8E6
SI	XII	1.5E-10	.831	3E7	3.7E6	3.4E-1	1.9E7	0.2	3.1E6
SI	XIII	2.1E-10	.765	5E7	6.3E6	2.1E-1	2.0E7	0.2	4.4E6
S	I	4.1E-13	.630	3E4	2.2E4	7.3E-5	1.1E5	0.0	0.0
S	II	1.8E-12	.686	1E5	1.2E4	4.9E-3	1.2E5	2.5	8.8E4
S	III	2.7E-12	.745	2E5	1.4E4	9.1E-3	1.3E5	6.0	1.5E5
S	IV	5.7E-12	.755	3E5	1.5E4	4.3E-2	1.8E5	0.0	0.0
S	V	1.2E-11	.701	5E5	1.4E4	2.5E-2	1.5E5	0.0	0.0
S	VI	1.7E-11	.849	1E6	2.9E5	3.1E-2	1.9E6	0.0	0.0
S	VII	2.7E-11	.733	1E6	1.3E5	1.3E-2	6.7E5	22.0	1.8E6
S	VIII	4.0E-11	.696	2E6	1.1E5	2.1E-2	5.9E5	6.4	2.0E6
S	IX	5.5E-11	.711	2E6	9.0E4	3.5E-2	5.5E5	13.0	2.3E6
S	X	7.4E-11	.716	3E6	9.0E4	3.0E-2	4.7E5	6.8	1.2E6
S	XI	9.2E-11	.714	5E6	9.0E4	3.1E-2	4.2E5	6.3	1.3E6
S	XII	1.4E-10	.755	6E6	8.3E4	6.3E-2	5.0E5	4.1	3.4E6
S	XIII	1.7E-10	.832	1E7	6.0E4	2.3E-2	3.0E5	12.0	3.6E6
S	XIV	2.5E-10	.852	1E8	5.0E6	4.2E-1	2.4E7	0.2	4.6E6
S	XV	3.3E-10	.783	2E8	9.0E6	2.5E-1	2.5E7	0.2	5.5E6

A number of small changes have been made in the limits of the approximations in order to smooth the turn on transition for dielectronic recombination.

The dielectronic recombination rates computed above were based on the assumption of a low density gas with no radiation field present, whereas the envelope of a stellar wind star is an environment of moderately high density and strong radiation field which will effect the rate. Dielectronic recombination occurs when a free electron excites a bound electron to a higher energy level, thereby allowing the free electron to lose enough energy to become bound into a very high quantum level. The atom then can stabilize by a series of cascades of the two electrons to the ground state. Schematically this process is

$$A(n)^{+z} + e^- \rightleftharpoons A^{+z-1}(n', n'') \longrightarrow$$
$$A^{+z-1}(n, n'') + h\nu \longrightarrow$$
$$A^{+z-1}(n, n''') + h\nu\ ,$$

where in general $n' = n+1$ and $n'' >> n, n'''$. If the gas becomes sufficiently dense or if the radiation field strong enough, the electron in the high lying quantum level n'' can be either collisionally or radiatively ionized out of the atom before it has time to stabilize by photoemission. A rough empirical correction factor was devised to allow for this decrease in the dielectronic recombination rate.

The principal quantum number of the state at which half the captured electrons are stabilized by cascades to ground and half are reionized is given by,

$$l(\text{collisions}) = (1.4 \times 10^{15} Z^6 T^{1/2}/n_e)^{1/7} \qquad \text{Dupree (1968)}$$

$$l(\text{radiative}) = Z(3\,R \ln(l)/(WkT_{rad}))^{1/2}$$

Sunyaev and Vainstein (1968)

where W is the geometrical dilution factor of the radiation field approximated by a blackbody of temperature T_{rad}. These numbers can be calibrated against the depression of the recombination rate calculated by Summers (1974). It was found that data is roughly fitted by the multiplicative factor f, such that $\alpha^{di} = f\ \alpha^{di}(n=0, W=0)$, where f is

$$f = \exp[-2.303*(.015*a^2+.092*a)]$$

where $$a = 12.55-7*\log10(l).$$

That is, the adjusted recombination rate is found by multiplying the value found from the fits given by Aldrovandi and Pequignot times the f factor given above.

In addition to this correction to the dielectronic rate, the semicoronal approximation of Wilson (1962) has been used to add to the radiative rate. This allows for some recombination to upper levels,

$$\alpha^{u}_{i,j+1} = 1.8\times 10^{-14}\,\chi_{ij}(kT)^{-3/2}\,\chi_{ij}(\ell), \qquad \text{(AII.10)}$$

where $\chi_{ij}(l) = \chi_{ij}/l^2$ (collisions). In addition three body recombination makes significant contributions at low temperatures, and is simply approximated by (Burgess and Summers 1976)

$$\alpha^{3}_{i,j+1} = 1.16\times 10^{-8} J^3 T^{9/2} n_e\,, \qquad \text{(AII.11)}$$

where J is the charge of the ion.

Collisional Ionization

The rate of collisional ionization for Hydrogen was also taken from Johnson (1972) as

$$S_e(n_e, c') = \left(\frac{8kT}{\pi m}\right)^{1/2} \frac{2n^2}{x_0}\pi a_0^2 y'_n \left\{ A'_n\left[\frac{E_1(y'_n)}{y'_n} - \frac{E_1(z'_n)}{z'_n}\right] + \left(B'_n - A'_n \ln\frac{2n^2}{x_0}\right)\left(\xi(y'_n) - \xi(z'_n)\right)\right\},$$

(AII.12)

where

$$A'_n = \frac{32}{3\sqrt{3}\pi}\, n \sum_{i=0}^{2} \frac{g_i(n)}{i+3}\, x_0^{-(i+3)}$$

$$B'_n = \frac{2}{3} n^2 x_0^{-1}\left(3 + 2x_0^{-1} + b_n x_0^{-2}\right)$$

$$y'_n = x_0 I_n/kT$$

$$z'_n = x_0 (I_n/kT + r_r)$$

$$\xi(t) = E_0(t) - 2E_1(t) + E_2(t),$$

and the Gaunt factors and x are as for the recombination rate in Hydrogen. Only ionization from the ground state n=1 will be considered, so r_1=0.45 and b_1= -0.603.

All other ions have collisional ionization rates based upon an approximation investigated in detail by Lotz (1967). A slight modification to the original formula has been made by McWhirtier (1975) to allow for the decrease of the ionization rate at high temperatures. The rate is given by

$$C_{ij} = 8.35\times10^{-8}\sum_{s=1}^{2}[T^{1/2}/(4.88+kT/\chi_{ij}(s))n(s)$$
$$\exp(-\chi_{ij}(s)/kT)/\chi_{ij}(s)^2], \qquad \text{(AII.13)}$$

where s goes from 1 to 2 in the calculations here, n(s) is the number of electrons in the subshell, and $\chi_{ij}(1)$ is the normal ionization potential as given by Allen (1973), $\chi_{ij}(2)$ is $\chi_{ij}(1)$ plus the excitation energy of the lowest excited level in the new ion with one of the inner shell electrons removed. For instance, the ionization of C II which has an electronic configuration of $1s^2 2s^2 2p$ can proceed with the addition of 196659 cm^{-1} of energy to C III $1s^2 2s^2$ by removing the one outer shell electron, or the ionization can take 196659+52315 cm^{-1} and ionize to C III $1s^2 2s2p$, by removing one of the two s shell electrons. The energy 52315 cm^{-1} is simply the energy to go from C III $2s^2$ to C III 2s2p. The attached table gives ionization potentials (in eV) and the number of subshell electrons. The values were obtained from the tables of Lotz (1967) and Moore (1949).

TABLE 9: IONIZATION POTENTIAL AND SHELL ELECTRON POPULATIONS

ATOM	IP1	N1	IP2	N2
H I	13.598	1		
HE I	24.587	2		

HE	II	54.416	1		
C	I	11.260	2	16.6	2
C	II	24.383	1	30.9	2
C	III	47.887	2	323.	2
C	IV	64.492	1	342.	2
C	V	392.08	2		
C	VI	489.98	1		
N	I	14.534	3	20.3	2
N	II	29.601	2	36.7	2
N	III	47.448	1	55.8	2
N	IV	77.472	2	469.	2
N	V	97.89	1	492.	2
N	VI	552.06	2		
N	VII	667.03	1		
O	I	13.618	4	28.5	2
O	II	35.117	3	42.6	2
O	III	54.934	2	63.8	2
O	IV	77.413	1	87.6	2
O	V	113.90	2	642.	2
O	VI	138.12	1	669.	2
O	VII	739.32	2		
O	VIII	871.39	1		
NE	I	21.564	6	48.5	2
NE	II	40.962	5	66.4	2
NE	III	63.45	4	86.2	2
NE	IV	97.11	3	108.	2
NE	V	126.21	2	139.	2
NE	VI	157.93	1	172.	2
NE	VII	207.26	2	1072.	2
NE	VIII	239.09	1	1106.	2
NE	IX	1195.8	2		
NE	X	1362.2	1		
MG	I	7.646	2	60.420	6
MG	II	15.035	1	67.809	6
MG	III	80.143	6	118.768	2
MG	IV	109.31	5	144.42	2
MG	V	141.27	4	172.01	2
MG	VI	186.51	3	201.22	2
MG	VII	224.95	2	241.14	2
MG	VIII	265.92	1	283.38	2
MG	IX	328.0	2	1680.4	2
MG	X	367.5	1	1719.8	2
MG	XI	1761.8	2		
MG	XII	1963.	1		
SI	I	8.151	2	13.616	2
SI	II	16.345	1	22.870	2
SI	III	33.492	2	137.709	6
SI	IV	45.141	1	149.358	6
SI	V	166.77	6	217.170	2
SI	VI	205.08	5	250.48	2
SI	VII	246.49	4	285.26	2
SI	VIII	303.16	3	321.76	2
SI	IX	351.1	2	371.2	2
SI	X	401.4	1	422.4	2
SI	XI	476.1	2	2340.8	2
SI	XII	523.	1	2388.	2

SI	XIII	2438.	2		
SI	XIV	2673.	1		
S	I	10.360	4	20.204	2
S	II	23.33	3	33.747	2
S	III	34.83	2	43.737	2
S	IV	47.30	1	57.60	2
S	V	72.68	2	243.31	6
S	VI	88.05	1	258.68	6
S	VII	280.01	6	342.45	2
S	VIII	328.33	5	352.24	2
S	IX	379.1	4	402.8	2
S	X	447.1	3	469.0	2
S	XI	504.7	2	551.2	2
S	XII	565.	1	621.	2
S	XIII	652.	2		
S	XIV	707.	1		
S	XV	3224.	2		
S	XVI	3494.	1		

Again, following Wilson (1962) we make a small addition to the ionization rate allowing for high density effects of ionizations out of upper levels,

$$C_{ij}^{u} = 4.8\text{x}10^{-6}\ T^{-1/2}\exp(-\chi_{ij}/kT)/(\chi_{ij}1^{2}(\text{collisions})). \quad \text{(AII.14)}$$

<u>Charge Exchange</u>

In order to increase the general usefulness of this program the charge exchange rates of

$$H^{+} + O \rightleftharpoons O^{+} + H$$

$$H^{+} + N \rightleftharpoons N^{+} + H$$

were included using expressions exactly as given by Field and Steigman (1971) and Steigman, *et al.*, (1971). Since the temperatures here are usually in excess of 10^{4} K, the charge exchange rate is at almost constant and at its maximum.

The Heating Rate

All heating is due to energy gain by photoionization, which is simply given by

$$\Gamma_{ij} = \int_{\nu_0}^{\infty} 4\pi J_\nu \sigma_{ij}(\nu)\, d\nu. \qquad \text{(AII.15)}$$

The total gain is

$$G = \sum_{ij} n_{ij} \Gamma_{ij} . \qquad \text{(AII.16)}$$

Cooling Rates

The emission of radiation is calculated under the assumption the medium is optically thin. The cooling due to bremsstrahlung is (Cox and Tucker 1969).

$$\Lambda^{B} = 2.29\times10^{-27}\, T^{1/2}\, n_e n_H / n^2 \qquad \text{(AII.17)}$$

where n_H is the number density of Hydrogen. This loss mechanism dominates for temperatures in excess of 10^7 K.

The radiative recombination energy loss rate is

$$\Lambda^{r}_{ij} = \alpha^{r}_{ij} (\chi_{i,j-1} + kT) X_{ij}\, A_i \times \left[\frac{-0.0713 + \frac{1}{2}\ln U + 0.64\, U^{-1/3}}{0.4288 + \frac{1}{2}\ln U + 0.469\, U^{-1/3}}\right] \qquad \text{(AII.18)}$$

where $U = \chi_{ij}/kT$. The correction factor in brackets was derived from the analysis of Seaton (1959) for the recombination process in Hydrogen. It represents the correction to the radiative recombination rate required to convert it to the energy rate, accounting for the preferential capture of slow electrons.

The loss rate due to dielectronic recombinations was estimated as,

$$\Lambda_{ij}^{di} = \alpha_{ij}^{di}((\chi_{i,j-1} + \Delta E_{ij}^{\ell})X_{ij}\ A_i\ . \qquad \text{(AII.19)}$$

The recombination radiation is the dominant loss mechanism for temperatures of 2×10^4 K and less. The energy difference ΔE_{ij} is taken as the lowest energy permitted transition to the ground state.

Between 2×10^4 and 10^7 K the dominant loss mechanism is collisional excitation of lines. In principle a calculation of this rate requires the collisional cross section for excitation of a particular transition as a function of incident electron energy. With the aid of the Milne relation, which relates the collision cross section to the inverse process of photoabsorption, the loss rate can be approximated as (Mewe 1972)

$$\Lambda_i^{\ell} = 1.7\times10^{-3}T^{-1/2} \sum_{ij}\sum_{\ell} g(l) f_{ij}(l) \exp(-\Delta E_{ij}(l)/kT) A_i X_{ij} \qquad \text{(AII.20)}$$

where g is a gaunt factor, $f_{ij}(l)$ is the f value for the transition, and $\Delta E_{ij}(l)$ is the energy of the emitted photon. The g factor has been calculated by Mewe (1972) for many transitions and given a simple extension by Kato (1976) to cover all transitions. They both use the same fitting function for the Gaunt factor,

$$g = A + (By - Cy^2 + D)\exp(y)E_1(y) + Cy \qquad \text{(AII.21)}$$

where $y = \Delta E_{ij}(l)/kT$, and A, B, C, D are constants given by Mewe and Kato, which are listed in the accompanying table. E_1 is the first exponential integral. The constants are identified by a transition number (G ID), which is matched to a transition number of all the lines used in the calculation. For the actual computation the complete line list given was reduced by taking a multiplet average over fine structure levels. In the Table 10 the A, B, C, and D correspond to the constants for the fitting function. When a value of 99.0 is entered the constant becomes a simple function as given by Mewe.

TABLE 10: THE CONSTANTS FOR THE LINE GAUNT FACTOR

A	B	C	D	G ID
0.13	-0.12	0.13	0.28	1
0.04	0.04	0.02	0.28	2
0.20	0.06	0.	0.28	3
0.25	0.04	0.	0.28	4
0.27	0.03	0.	0.28	5
0.28	0.02	0.	0.28	6
0.29	0.02	0.	0.28	7
0.05	-0.04	0.	0.	8
0.05	0.01	0.	0.	9
0.02	0.02	0.	0.28	10
0.2	0.05	0.	0.28	11
0.02	0.	0.	0.	12
0.3	0.05	0.	0.28	13
0.	0.	0.07	0.	14
0.	0.	0.1	0.	15
0.	0.	0.2	0.	16
0.	0.	0.2	0.	17
0.	0.	0.04	0.	18
0.	0.	0.3	0.	19
99.	99.	99.	0.28	20
99.	99.	99.	0.28	21
99.	99.	-0.2	0.28	22
99.	0.	0.	0.	23
0.13	0.	0.	0.	24
0.11	0.	0.	0.	25
0.1	0.	0.	0.	26
0.09	0.	0.	0.	27
99.	99.	0.	0.	28
0.54	-0.25	0.	0.	29
0.43	-0.19	0.	0.	30
0.35	-0.15	0.	0.	31
0.3	-0.12	0.	0.	32
0.05	0.2	0.	0.28	33
0.2	0.15	0.	0.28	34
-0.17	0.25	0.	0.28	35
-0.04	0.2	0.	0.28	36
-0.3	0.4	0.	0.28	37
-0.3	0.5	0.	0.28	38
-0.2	0.3	0.	0.28	39
-0.2	0.5	0.	0.28	40
0.15	0.	0.	0.28	41
0.6	0.	0.	0.28	42
0.59	0.21	0.04	0.28	43
				44
0.27	0.08	0.	0.28	45
0.33	0.05	0.	0.28	46

0.36	0.04	0.	0.28	47
0.37	0.03	0.	0.28	48
0.38	0.03	0.	0.28	49

The following table gives the line list used in the calculation of the radiation acceleration and the cooling rate. The lines were taken from tables compiled by Morton and Smith (1973), Morton (private communication, but mentioned in Lamers and Morton 1976), Kato (1976), Wiese, *et al.* (1966), and Wiese, *et al.* (1969). In the table the line is identified by atom and ionization species, usually with a remark about the multiplet of origin, the wavelength is given in Angstroms, the f value of the transition, a number identifying which set of constants are to be used to calculate the Gaunt factor, the atomic number and the ion species are given.

TABLE 11: LINES USED FOR THE CALCULATIONS

ATOM		LAMDA	F VALUE	G ID	Z	J
HI	9	920.960	0.1605E-02	7	1	1
HI	8	923.150	0.2216E-02	7	1	1
HI	7	926.220	0.3183E-02	7	1	1
HI	6	930.740	0.4814E-02	7	1	1
H I	5	937.803	0.7800E-02	6	1	1
H I	4	949.743	0.1394E-01	5	1	1
H I	3	972.537	0.2899E-01	4	1	1
H I	2	1025.722	0.7910E-01	3	1	1
H I	1	1215.670	0.4162E+00	1	1	1
HE I	10	507.058	0.2093E-02	13	2	1
HE I	9	507.718	0.2748E-02	13	2	1
HE I	8	508.643	0.3991E-02	13	2	1
HE I	7	509.998	0.5931E-02	13	2	1
HE I	6	512.098	0.8480E-02	13	2	1
HE I	5	515.617	0.1531E-01	13	2	1
HE I	4	522.213	0.3017E-01	13	2	1
HE I	3	537.030	0.7342E-01	11	2	1
HE I	2	584.334	0.2763E+00	10	2	1
HE II	10	229.736	0.1201E-02	7	2	2
HE II	9	230.139	0.1605E-02	7	2	2
HE II	8	230.686	0.2216E-02	7	2	2
HE II	7	231.454	0.3183E-02	7	2	2
HE II	6	232.584	0.4814E-02	7	2	2
HE II	5	234.347	0.7799E-02	6	2	2
HE II	4	237.331	0.1394E-01	5	2	2
HE II	3	243.027	0.2899E-01	4	2	2

HE	II	2	256.317	0.7912E-01	3	2	2
HE	II	1	303.786	0.4162E+00	1	2	2
C	I	31AUTO	945.191	0.2730E+00	42	6	1
C	I	31AUTO	945.338	0.2730E+00	42	6	1
C	I	31AUTO	945.579	0.2720E+00	42	6	1
C	I	9	1260.736	0.3790E-01	41	6	1
C	I	9	1260.927	0.1260E-01	41	6	1
C	I	9	1260.996	0.9480E-02	41	6	1
C	I	9	1261.122	0.1580E-01	41	6	1
C	I	9	1261.426	0.9480E-02	41	6	1
C	I	9	1261.552	0.2840E-01	41	6	1
C	I	7	1277.245	0.8970E-01	41	6	1
C	I	7	1277.282	0.6730E-01	41	6	1
C	I	7	1277.513	0.2240E-01	41	6	1
C	I		1277.550	0.7530E-01	41	6	1
C	I	7	1277.723	0.1350E-01	41	6	1
C	I	7	1277.954	0.8970E-03	41	6	1
C	I	6	1279.229	0.3810E-02	41	6	1
C	I	5	1279.890	0.8400E-02	41	6	1
C	I	5	1280.135	0.2020E-01	41	6	1
C	I	5	1280.333	0.1510E-01	41	6	1
C	I	5	1280.404	0.5040E-02	41	6	1
C	I	5	1280.597	0.6720E-02	41	6	1
C	I	5	1280.847	0.5040E-02	41	6	1
C	I	4	1328.833	0.3920E-01	42	6	1
C	I	4	1329.086	0.1310E-01	42	6	1
C	I	4	1329.100	0.1630E-01	42	6	1
C	I	4	1329.123	0.9800E-02	42	6	1
C	I	4	1329.578	0.2940E-01	42	6	1
C	I	4	1329.600	0.9800E-02	42	6	1
C	I	3	1560.310	0.8100E-01	42	6	1
C	I	3	1560.683	0.6080E-01	42	6	1
C	I	3	1560.708	0.2020E-01	42	6	1
C	I	3	1561.341	0.1210E-01	42	6	1
C	I	3	1561.367	0.8100E-03	42	6	1
C	I	3	1561.438	0.6800E-01	42	6	1
C	I	2	1656.266	0.5660E-01	41	6	1
C	I	2	1656.928	0.1360E+00	41	6	1
C	I	2	1657.008	0.1020E+00	41	6	1
C	I	2	1657.380	0.3400E-01	41	6	1
C	I	2	1657.907	0.4530E-01	41	6	1
C	I	2	1658.122	0.3390E-01	41	6	1
CII		B1	43.200	0.3800E+00	42	6	2
CII		10	687.050	0.2700E+00	41	6	2
CII		10	687.350	0.2300E+00	41	6	2
CII		9	858.090	0.4600E-01	41	6	2
CII		9	858.550	0.4600E-01	41	6	2
CII		3	903.620	0.1700E+00	42	6	2
CII		3	903.960	0.3400E+00	42	6	2
CII		3	904.140	0.4300E+00	42	6	2
CII		3	904.480	0.8400E-01	42	6	2
C	II	2	1036.337	0.1250E+00	42	6	2
C	II	2	1037.018	0.1250E+00	42	6	2
C	II	1	1334.532	0.1180E+00	42	6	2
C	II	1	1335.662	0.1180E-01	42	6	2
C	II	1	1335.708	0.1060E+00	42	6	2

CIII	BE1	42.510	0.5660E+00	42	6	3
C III	3.09	270.324	0.3287E-02	41	6	3
C III	3.08	274.051	0.3378E-02	41	6	3
C III	3.07	280.043	0.3527E-02	41	6	3
C III	3.03	291.326	0.3817E-02	41	6	3
C III	3	310.170	0.1601E-01	41	6	3
C III	2.03	322.574	0.4680E-02	41	6	3
C III	2	386.203	0.2549E+00	41	6	3
C III	1	977.026	0.6740E+00	42	6	3
CIV	4	222.790	0.2630E-01	41	6	4
C IV	3	244.907	0.1987E-01	22	6	4
C IV	3	244.907	0.3975E-01	22	6	4
C IV	2	312.422	0.1335E+00	21	6	4
C IV	2	312.453	0.6673E-01	21	6	4
C IV	1	1548.202	0.1940E+00	20	6	4
C IV	1	1550.774	0.9700E-01	20	6	4
CV	HE1	32.800	0.2800E-01	13	6	5
CV	HE2	33.430	0.5600E-01	13	6	5
CV	HE3	34.970	0.1460E+00	11	6	5
CV	HE4	40.270	0.6940E+00	9	6	5
CVI	H5	26.000	0.8000E-02	48	6	6
CVI	H4	26.400	0.1400E-01	47	6	6
CVI	H3	27.000	0.2900E-01	46	6	6
CVI	H2	28.500	0.7900E-01	45	6	6
CVI	H1	33.700	0.4160E+00	43	6	6
N I	2	1134.165	0.1340E-01	42	7	1
N I	2	1134.415	0.2680E-01	42	7	1
N I	2	1134.980	0.4020E-01	42	7	1
N I	1	1199.549	0.1330E+00	41	7	1
N I	1	1200.224	0.8850E-01	41	7	1
N I	1	1200.711	0.4420E-01	41	7	1
NII	M10	529.680	0.8200E-01	41	7	2
NII	9	533.500	0.2600E+00	41	7	2
NII	9	533.570	0.1900E+00	41	7	2
NII	9	533.640	0.6500E-01	41	7	2
NII	9	533.720	0.2200E+00	41	7	2
NII	9	533.880	0.3900E-01	41	7	2
NII	3	644.620	0.2300E+00	42	7	2
NII	3	644.820	0.2300E+00	42	7	2
NII	3	645.160	0.2300E+00	42	7	2
NII	7	671.010	0.3700E-01	41	7	2
NII	7	671.390	0.6700E-01	41	7	2
NII	7	671.390	0.8900E-01	41	7	2
NII	7	671.620	0.2200E-01	41	7	2
NII	7	671.770	0.3000E-01	41	7	2
NII	7	671.990	0.2200E-01	41	7	2
N II	2	915.612	0.1490E+00	42	7	2
N II	2	915.962	0.4950E-01	42	7	2
N II	2	916.012	0.6190E-01	42	7	2
N II	2	916.020	0.3710E-01	42	7	2
N II	2	916.701	0.1110E+00	42	7	2
N II	2	916.710	0.3710E-01	42	7	2
N II	1	1083.990	0.1010E+00	42	7	2
N II	1	1084.562	0.2520E-01	42	7	2
N II	1	1084.580	0.7550E-01	42	7	2
N II	1	1085.529	0.1010E-02	42	7	2

N	II	1	1085.546	0.1510E-01	42	7	2
N	II	1	1085.701	0.8450E-01	42	7	2
N	III	AUTO	246.206	0.1515E-02	41	7	3
N	III	AUTO	246.249	0.1363E-02	41	7	3
N	III	AUTO	246.311	0.1515E-03	41	7	3
N	III	7.25	262.184	0.1718E-02	41	7	3
N	III	7.25	262.233	0.1546E-02	41	7	3
N	III	7.25	262.289	0.1718E-03	41	7	3
N	III	7.15	268.347	0.1801E-02	41	7	3
N	III	7.15	268.473	0.1800E-03	41	7	3
N	III	7.15	268.473	0.1620E-02	41	7	3
N	III	7.12	270.073	0.1824E-02	41	7	3
N	III	7.12	270.200	0.1823E-03	41	7	3
N	III	7.12	270.201	0.1641E-02	41	7	3
N	III	7.10	272.523	0.1857E-02	41	7	3
N	III	7.10	272.653	0.1857E-03	41	7	3
N	III	7.10	272.654	0.1671E-02	41	7	3
N	III	7.08	276.193	0.1908E-02	41	7	3
N	III	7.08	276.326	0.1907E-03	41	7	3
N	III	7.08	276.326	0.1716E-02	41	7	3
N	III	7.07	278.436	0.3878E-03	41	7	3
N	III	7.07	278.572	0.3876E-03	41	7	3
N	III	7.06	282.070	0.2481E-01	41	7	3
N	III	7.06	282.209	0.2480E-02	41	7	3
N	III	7.06	282.209	0.2232E-01	41	7	3
N	III	7.05	285.855	0.4088E-03	41	7	3
N	III	7.05	286.000	0.4086E-03	41	7	3
N	III	7.04	292.447	0.4666E-01	41	7	3
N	III	7.04	292.595	0.4149E-01	41	7	3
N	III	7.04	292.596	0.4655E-02	41	7	3
N	III	7.03	299.661	0.4492E-03	41	7	3
N	III	7.03	299.818	0.4490E-03	41	7	3
N	III	7.02	305.761	0.4677E-03	41	7	3
N	III	7.02	305.920	0.4674E-03	41	7	3
N	III	7.01	311.550	0.2427E-02	41	7	3
N	III	7.01	311.636	0.2183E-02	41	7	3
N	III	7.01	311.721	0.2426E-03	41	7	3
N	III	7	314.877	0.1091E-01	41	7	3
N	III	6	323.436	0.5235E-03	41	7	3
N	III	6	323.493	0.1047E-02	41	7	3
N	III	6	323.620	0.1308E-02	41	7	3
N	III	6	323.675	0.2615E-03	41	7	3
N	III	5.01	332.140	0.7063E-02	41	7	3
N	III	5.01	332.333	0.7046E-02	41	7	3
N	III	5	374.204	0.2918E+00	41	7	3
N	III	5	374.441	0.2625E+00	41	7	3
N	III	5	374.449	0.2916E-01	41	7	3
N	III	4	451.869	0.2381E-01	41	7	3
N	III	4	452.226	0.2379E-01	41	7	3
N	III	3	684.996	0.1207E+00	42	7	3
N	III	3	685.513	0.2412E+00	42	7	3
N	III	3	685.816	0.3013E+00	42	7	3
N	III	3	686.335	0.6022E-01	42	7	3
N	III	2	763.340	0.5664E-01	42	7	3
N	III	2	764.357	0.5657E-01	42	7	3
N	III	1	989.790	0.1070E+00	41	7	3

N III 1	991.514	0.1060E-01	41	7	3
N III 1	991.579	0.9580E-01	41	7	3
N IV 2	247.205	0.5497E+00	41	7	4
N IV 1	765.148	0.5451E+00	42	7	4
NV LI1	148.000	0.3000E-01	22	7	5
NV 3	162.560	0.6690E-01	22	7	5
NV LI2	162.560	0.6700E-01	22	7	5
NV 2	209.270	0.1570E+00	21	7	5
NV LI5	209.280	0.2360E+00	21	7	5
NV 2	209.330	0.7840E-01	21	7	5
N V 1	1238.821	0.1520E+00	41	7	5
N V 1	1242.804	0.7570E-01	41	7	5
NVI HE1	23.300	0.2800E-01	13	7	6
NVI HE2	23.770	0.5600E-01	13	7	6
NVI HE3	24.900	0.1460E+00	11	7	6
NVI HE4	28.790	0.6940E+00	9	7	6
NVII H5	19.100	0.8000E-02	48	7	7
NVII H4	19.400	0.1400E-01	47	7	7
NVII H3	19.800	0.2900E-01	46	7	7
NVII H2	20.900	0.7900E-01	45	7	7
NVII H1	24.800	0.4160E+00	43	7	7
OI M9	811.370	0.7700E-02	41	8	1
OI M5	878.450	0.3700E-01	41	8	1
O I 5	988.581	0.5100E-03	42	8	1
O I 5	988.655	0.7640E-02	42	8	1
O I 5	988.773	0.4280E-01	42	8	1
O I 5	990.127	0.1270E-01	42	8	1
O I 5	990.204	0.3810E-01	42	8	1
O I 5	990.801	0.5080E-01	42	8	1
O I 4	1025.762	0.6200E-01	42	8	1
O I 4	1025.762	0.1110E-01	42	8	1
O I 4	1025.762	0.7380E-03	42	8	1
O I 4	1027.431	0.5530E-01	42	8	1
O I 4	1027.431	0.1840E-01	42	8	1
O I 4	1028.157	0.7360E-01	42	8	1
O I 2	1302.169	0.4860E-01	42	8	1
O I 2	1304.858	0.4850E-01	42	8	1
O I 2	1306.029	0.4850E-01	42	8	1
OII 10	429.910	0.5400E-01	41	8	2
OII 10	430.040	0.1100E+00	41	8	2
OII 10	430.170	0.1600E+00	41	8	2
OII 2	539.080	0.5600E-01	41	8	2
OII 2	539.540	0.3700E-01	41	8	2
OII 2	539.850	0.1900E-01	41	8	2
OII 1	832.750	0.7000E-01	42	8	2
OII 1	833.320	0.1500E+00	42	8	2
OII 1	834.460	0.2100E+00	42	8	2
O III	228.834	0.8128E-02	41	8	3
O III	228.893	0.7996E-02	41	8	3
O III	228.988	0.7962E-02	41	8	3
O III	240.979	0.2523E-01	41	8	3
O III	241.000	0.3366E-03	41	8	3
O III	241.000	0.8409E-02	41	8	3
O III	241.000	0.3364E-01	41	8	3
O III	241.037	0.2825E-01	41	8	3
O III	248.468	0.1533E-01	41	8	3

O	III		248.538	0.6129E-01	41	8	3
O	III		248.574	0.4596E-01	41	8	3
O	III		248.618	0.5147E-01	41	8	3
O	III		248.693	0.9188E-02	41	8	3
O	III		255.000	0.1546E-02	41	8	3
O	III		255.044	0.1932E-02	41	8	3
O	III		255.113	0.4636E-02	41	8	3
O	III		255.158	0.3476E-02	41	8	3
O	III		255.188	0.1159E-02	41	8	3
O	III		255.302	0.1158E-02	41	8	3
O	III		262.000	0.5868E-01	41	8	3
O	III		262.700	0.1951E-01	41	8	3
O	III		262.700	0.1463E-01	41	8	3
O	III		262.729	0.2438E-01	41	8	3
O	III		262.882	0.4386E-01	41	8	3
O	III		262.900	0.1462E-01	41	8	3
O	III		263.692	0.1549E+00	41	8	3
O	III		263.728	0.1007E+00	41	8	3
O	III		263.768	0.2254E-01	41	8	3
O	III		263.818	0.5768E-02	41	8	3
O	III		263.818	0.1002E+00	41	8	3
O	III		263.903	0.1384E-03	41	8	3
O	III		264.257	0.2291E-01	41	8	3
O	III		264.317	0.7636E-02	41	8	3
O	III		264.329	0.5793E-02	41	8	3
O	III		264.338	0.9613E-02	41	8	3
O	III		264.471	0.5768E-02	41	8	3
O	III		264.480	0.1742E-01	41	8	3
O	III		266.843	0.9355E-02	41	8	3
O	III		266.967	0.6310E-01	41	8	3
O	III		266.985	0.4708E-01	41	8	3
O	III		267.030	0.5141E-01	41	8	3
O	III		267.050	0.1559E-01	41	8	3
O	III		267.188	0.6325E-03	41	8	3
O	III		275.281	0.3020E-01	41	8	3
O	III		275.336	0.2971E-01	41	8	3
O	III		275.513	0.2958E-01	41	8	3
O	III		280.116	0.5406E-02	41	8	3
O	III		280.234	0.1318E-01	41	8	3
O	III		280.265	0.9573E-02	41	8	3
O	III		280.328	0.3257E-02	41	8	3
O	III		280.412	0.4394E-02	41	8	3
O	III		280.483	0.3244E-02	41	8	3
O	III	6	303.411	0.1383E+00	41	8	3
O	III	6	303.460	0.4611E-01	41	8	3
O	III	6	303.515	0.3457E-01	41	8	3
O	III	6	303.621	0.5761E-01	41	8	3
O	III	6	303.693	0.3455E-01	41	8	3
O	III	5	303.769	0.3521E+00	41	8	3
O	III	6	303.799	0.1036E+00	41	8	3
O	III	5	305.596	0.4167E+00	41	8	3
O	III	5	305.656	0.3125E+00	41	8	3
O	III	5	305.703	0.1041E+00	41	8	3
O	III	5	305.836	0.6245E-01	41	8	3
O	III	5	305.879	0.4166E-02	41	8	3
O	III		308.306	0.1995E-02	41	8	3

O III 4	373.805	0.2573E-01	41	8	3
O III 4	374.005	0.6171E-01	41	8	3
O III 4	374.075	0.4627E-01	41	8	3
O III 4	374.165	0.1542E-01	41	8	3
O III 4	374.331	0.2055E-01	41	8	3
O III 4	374.436	0.1541E-01	41	8	3
O III 3	507.391	0.1387E+00	42	8	3
O III 3	507.683	0.1387E+00	42	8	3
O III 3	508.182	0.1385E+00	42	8	3
O III 2	702.332	0.1404E+00	42	8	3
O III 2	702.822	0.4676E-01	42	8	3
O III 2	702.891	0.3507E-01	42	8	3
O III 2	702.899	0.5844E-01	42	8	3
O III 2	703.845	0.3502E-01	42	8	3
O III 2	703.850	0.1051E+00	42	8	3
O III 1	832.927	0.1049E+00	42	8	3
O III 1	833.701	0.2621E-01	42	8	3
O III 1	833.742	0.7863E-01	42	8	3
O III 1	835.055	0.1048E-02	42	8	3
O III 1	835.096	0.1570E-01	42	8	3
O III 1	835.292	0.8791E-01	42	8	3
OIV B2	195.860	0.9600E-01	41	8	4
OIV B3	203.000	0.1730E+00	41	8	4
O IV 5	238.360	0.4977E+01	41	8	4
O IV 5	238.571	0.4476E+01	41	8	4
O IV 5	238.580	0.4973E+00	41	8	4
O IV 4	279.631	0.3560E-01	41	8	4
O IV 4	279.933	0.3556E-01	41	8	4
O IV 3	553.330	0.9432E-01	42	8	4
O IV 3	554.075	0.1884E+00	42	8	4
O IV 3	554.514	0.2353E+00	42	8	4
O IV 3	555.261	0.4700E-01	42	8	4
O IV 2	608.398	0.7062E-01	42	8	4
O IV 2	609.829	0.7046E-01	42	8	4
O IV 1	787.711	0.9345E-01	42	8	4
O IV 1	790.109	0.9317E-02	42	8	4
O IV 1	790.199	0.8384E-01	42	8	4
OV 2	172.160	0.5900E+00	42	8	5
O V 1	629.730	0.4405E+00	42	8	5
OVI LI1	104.810	0.3200E-01	22	8	6
OVI LI2	115.800	0.7300E-01	22	8	6
OVI 2	150.080	0.1750E+00	21	8	6
OVI 2	150.120	0.8740E-01	21	8	6
O VI 1	1031.945	0.1300E+00	20	8	6
O VI 1	1037.627	0.6480E-01	20	8	6
OVII HE1	17.420	0.2800E-01	13	8	7
OVII HE2	17.770	0.5600E-01	13	8	7
OVII HE3	18.630	0.1460E+00	11	8	7
OVII HE4	21.600	0.6940E+00	9	8	7
OVIII H5	14.600	0.8000E-02	48	8	8
OVIII H4	14.820	0.1400E-01	47	8	8
OVIII H3	15.200	0.2900E-01	46	8	8
OVIII H2	16.000	0.7900E-01	45	8	8
OVIII H1	19.000	0.4160E+00	43	8	8
NEI 2	735.890	0.1620E+00	35	10	1
NEI 1	743.700	0.1180E-01	35	10	1

NE II	324.567	0.1066E-02	41	10	2
NE II	324.570	0.1091E-01	41	10	2
NE II	325.393	0.1256E-01	41	10	2
NE II	326.519	0.4988E-02	41	10	2
NE II	326.542	0.3962E-01	41	10	2
NE II	326.787	0.2443E-01	41	10	2
NE II	327.250	0.1018E-01	41	10	2
NE II	327.262	0.5104E-01	41	10	2
NE II	327.355	0.4666E-01	41	10	2
NE II	327.626	0.2393E-01	41	10	2
NE II	328.090	0.4355E-01	41	10	2
NE II	328.102	0.5000E+00	41	10	2
NE II	329.773	0.2177E-02	41	10	2
NE II	330.214	0.2177E-02	41	10	2
NE II	330.626	0.2685E-01	41	10	2
NE II	330.658	0.9726E-02	41	10	2
NE II	330.790	0.3784E-01	41	10	2
NE II	331.069	0.8491E-02	41	10	2
NE II	331.515	0.2393E-01	41	10	2
NE II	352.247	0.2805E-02	41	10	2
NE II	352.956	0.1374E-01	41	10	2
NE II	353.215	0.1094E-01	41	10	2
NE II	353.935	0.5236E-02	41	10	2
NE II	354.962	0.1066E-01	41	10	2
NE II	355.454	0.5469E-02	41	10	2
NE II	355.948	0.4775E-01	41	10	2
NE II	356.441	0.2084E-01	41	10	2
NE II	356.541	0.7726E-02	41	10	2
NE II	356.800	0.3006E-01	41	10	2
NE II	357.536	0.2685E-01	41	10	2
NE II	361.433	0.1577E-01	41	10	2
NE II	362.455	0.1694E-01	41	10	2
NE II 4	405.846	0.1251E-01	41	10	2
NE II 4	405.854	0.1126E+00	41	10	2
NE II 4	407.138	0.1247E+00	41	10	2
NE II 3	445.040	0.1723E-01	41	10	2
NE II 3	446.226	0.8590E-01	41	10	2
NE II 3	446.590	0.6867E-01	41	10	2
NE II 3	447.815	0.3424E-01	41	10	2
NE II 1	460.728	0.3300E+00	42	10	2
NE II 1	462.391	0.3288E+00	42	10	2
NEIIIM13	227.400	0.5500E-01	41	10	3
NEIIIM11	227.620	0.1200E+00	41	10	3
NEIIIM11	229.060	0.9600E-01	41	10	3
NE III 5	251.120	0.1858E+01	41	10	3
NE III 5	251.129	0.3317E+00	41	10	3
NE III 5	251.134	0.2213E-01	41	10	3
NE III 5	251.540	0.1656E+01	41	10	3
NE III 5	251.549	0.5519E+00	41	10	3
NE III 5	251.720	0.2206E+01	41	10	3
NE III 4	267.047	0.8576E-02	41	10	3
NE III 4	267.070	0.2573E-01	41	10	3
NE III 4	267.500	0.1142E-01	41	10	3
NE III 4	267.512	0.8561E-02	41	10	3
NE III 4	267.530	0.1427E-01	41	10	3
NE III 4	267.710	0.3422E-01	41	10	3

NE III 3	283.125	0.5632E-03	41	10	3
NE III 3	283.150	0.8440E-02	41	10	3
NE III 3	283.170	0.4726E-01	41	10	3
NE III 3	283.647	0.1404E-01	41	10	3
NE III 3	283.660	0.4212E-01	41	10	3
NE III 3	283.870	0.5612E-01	41	10	3
NE III 2	313.050	0.3977E-01	41	10	3
NE III 2	313.680	0.3969E-01	41	10	3
NE III 2	313.920	0.3966E-01	41	10	3
NE III 1	488.100	0.4108E-01	42	10	3
NE III 1	488.870	0.5469E-01	42	10	3
NE III 1	489.500	0.1229E+00	42	10	3
NE III 1	489.640	0.4095E-01	42	10	3
NE III 1	490.310	0.1636E+00	42	10	3
NE III 1	491.050	0.6806E-01	42	10	3
NEIV N7	148.800	0.6100E+00	41	10	4
NEIV N1	172.600	0.5400E+00	41	10	4
NEIV M7	208.630	0.9500E-01	41	10	4
NE IV 1	541.127	0.2958E-01	42	10	4
NE IV 1	542.073	0.5905E-01	42	10	4
NE IV 1	543.891	0.8829E-01	42	10	4
NEV C9	118.800	0.2500E+00	41	10	5
NEV M8	142.610	0.2000E+00	41	10	5
NEV M7	143.320	0.6100E+00	41	10	5
NEV C5	173.900	0.8600E-01	41	10	5
NE V 3	357.950	0.1795E-01	42	10	5
NE V 3	358.480	0.1792E-01	42	10	5
NE V 3	359.390	0.1788E-01	42	10	5
NE V 2	480.410	0.1522E+00	42	10	5
NE V 2	481.280	0.5063E-01	42	10	5
NE V 2	481.360	0.6327E-01	42	10	5
NE V 2	481.367	0.3796E-01	42	10	5
NE V 2	482.990	0.1135E+00	42	10	5
NE V 2	482.990	0.3784E-01	42	10	5
NE V 1	568.420	0.9259E-01	42	10	5
NE V 1	569.760	0.2309E-01	42	10	5
NE V 1	569.830	0.6927E-01	42	10	5
NE V 1	572.030	0.9994E-03	42	10	5
NE V 1	572.110	0.1380E-01	42	10	5
NE V 1	572.340	0.7724E-01	42	10	5
NEVI B1	14.100	0.4900E+00	41	10	6
NEVI B2	98.000	0.1020E+00	41	10	6
NEVI B3	111.100	0.1750E+00	41	10	6
NEVI M9	122.620	0.5400E+00	41	10	6
NEVI M8	138.550	0.2900E-01	41	10	6
NE VI	399.820	0.4909E-01	42	10	6
NE VI	403.260	0.2434E-01	42	10	6
NE VI	410.140	0.9787E-01	42	10	6
NE VI	410.930	0.1194E+00	42	10	6
NE VI	433.180	0.5273E-01	42	10	6
NE VI	435.650	0.5243E-01	42	10	6
NE VI	558.590	0.8388E-01	42	10	6
NE VI	562.710	0.8328E-02	42	10	6
NE VI	562.800	0.7493E-01	42	10	6
NEVII BE1	13.920	0.6700E+00	41	10	7
NE VII	465.221	0.3748E+00	42	10	7

NEVIII LI1	60.810	0.3300E-01	22	10	8
NEVIII 2	88.130	0.2980E+00	41	10	8
NEVIII LI2	98.000	0.8000E-01	22	10	8
NEVIII 1	770.400	0.1020E+00	42	10	8
NEVIII 1	780.320	0.5020E-01	42	10	8
NE IX HE1	10.800	0.2800E-01	13	10	9
NE IX HE2	11.000	0.5600E-01	13	10	9
NE IX HE3	11.560	0.1490E+00	11	10	9
NE IX HE4	13.440	0.7230E+00	9	10	9
NE X 6	9.370	0.8000E-02	48	10	10
NE X 5	9.490	0.1400E-01	47	10	10
NE X 4	9.720	0.2900E-01	46	10	10
NE X 3	10.250	0.7900E-01	45	10	10
NE X 2	12.150	0.4160E+00	43	10	10
MG I	1827.940	0.5260E-01	41	12	1
MG I 2	2025.824	0.1610E+00	41	12	1
MG I 1	2852.127	0.1900E+01	42	12	1
MG II	1025.968	0.1480E-02	41	12	2
MG II	1026.113	0.7400E-03	41	12	2
MG II	1239.925	0.9680E-03	41	12	2
MG II	1240.395	0.4840E-03	41	12	2
MG II 1	2795.528	0.5920E+00	42	12	2
MG II 1	2802.704	0.2950E+00	42	12	2
MGIII NE1	171.500	0.1000E+00	34	12	3
MGIII NE2	182.500	0.8000E-02	36	12	3
MGIII 5	186.510	0.2700E+00	33	12	3
MGIII 4	187.190	0.1600E+00	33	12	3
MGIII 3	188.530	0.4000E-02	33	12	3
MG III	231.730	0.2101E+00	35	12	3
MG III 1	234.258	0.1111E-01	35	12	3
MGIV F1	120.000	0.2500E+00	41	12	4
MGIV F5	130.000	0.1340E+00	41	12	4
MGIV F2	147.000	0.1500E+01	41	12	4
MGIV F3	181.000	0.3200E+00	41	12	4
MG IV	320.994	0.1348E+00	42	12	4
MG IV	323.307	0.1339E+00	42	12	4
MGV O7	103.900	0.1200E+00	41	12	5
MGV O2	114.030	0.1800E+00	41	12	5
MGV O1	121.600	0.3000E+00	41	12	5
MGV O3	132.500	0.1340E+00	41	12	5
MGV O5	137.800	0.4800E-01	41	12	5
MGV O4	146.500	0.2900E-01	41	12	5
MG V	351.089	0.5643E-01	42	12	5
MG V	352.202	0.7500E-01	42	12	5
MG V	353.094	0.1683E+00	42	12	5
MG V	353.300	0.5607E-01	42	12	5
MG V	354.223	0.2237E+00	42	12	5
MG V	355.326	0.9293E-01	42	12	5
MGVI N7	80.100	0.2700E+00	41	12	6
MGVI N1	95.500	0.5000E+00	41	12	6
MGVI N3	111.600	0.7200E-01	41	12	6
MG VI	399.289	0.4383E-01	42	12	6
MG VI	400.676	0.8735E-01	42	12	6
MG VI	403.315	0.1302E+00	42	12	6
MGVII C9	68.100	0.2400E+00	41	12	7
MGVII C1	77.100	0.1000E+00	41	12	7

MGVII C2	78.400	0.4500E-01	41	12	7
MGVII C3	83.960	0.2100E+00	41	12	7
MGVII C4	84.020	0.6100E+00	41	12	7
MGVII C5	95.300	0.5900E-01	41	12	7
MG VII	276.145	0.1201E+00	42	12	7
MG VII	277.007	0.1197E+00	42	12	7
MG VII	278.406	0.1191E+00	42	12	7
MG VII	363.770	0.1115E+00	42	12	7
MG VII	365.230	0.4628E-01	42	12	7
MG VII	365.267	0.2777E-01	42	12	7
MG VII	365.270	0.3702E-01	42	12	7
MG VII	367.679	0.8276E-01	42	12	7
MG VII	367.701	0.2758E-01	42	12	7
MG VII	429.134	0.1040E+00	42	12	7
MG VII	431.220	0.2588E-01	42	12	7
MG VII	431.318	0.7762E-01	42	12	7
MG VII	434.615	0.1028E-02	42	12	7
MG VII	434.710	0.1540E-01	42	12	7
MG VII	434.923	0.8621E-01	42	12	7
MGVIII B1	9.470	0.5100E+00	41	12	8
MGVIII B3	64.500	0.1670E+00	41	12	8
MGVIII B2	69.000	0.1070E+00	41	12	8
MGVIII11	74.850	0.6100E+00	41	12	8
MGVIII11	75.030	0.5500E+00	41	12	8
MGVIII11	75.040	0.6100E-01	41	12	8
MGVIII10	82.590	0.2420E-01	41	12	8
MGVIII10	82.820	0.2400E-01	41	12	8
MGVIII 3	311.780	0.6800E-01	42	12	8
MGVIII 3	313.730	0.1400E+00	42	12	8
MGVIII 3	315.020	0.1700E+00	42	12	8
MGVIII 3	317.010	0.3400E-01	42	12	8
MGVIII 2	335.250	0.4500E-01	42	12	8
MGVIII 2	339.010	0.4500E-01	42	12	8
MGVIII 1	430.470	0.8800E-01	42	12	8
MGVIII 1	436.680	0.8700E-02	42	12	8
MGVIII 1	436.730	0.7800E-01	42	12	8
MGIX BE1	9.380	0.7000E+00	42	12	9
MGIX 6	62.750	0.5800E+00	41	12	9
MGIX 2	368.070	0.3140E+00	42	12	9
MGX LI1	41.000	0.3500E-01	22	12	10
MGX LI2	44.050	0.8500E-01	22	12	10
MGX LI5	57.890	0.3200E+00	21	12	10
MG XI HE4	7.310	0.2770E-01	13	12	11
MG XI HE3	7.470	0.5690E-01	13	12	11
MG XI HE2	7.850	0.1520E+00	13	12	11
MG XI HE1	9.160	0.7450E+00	13	12	11
MGXII 6	6.510	0.8000E-02	48	12	12
MGXII 5	6.590	0.1400E-01	47	12	12
MGXII 4	6.750	0.2900E-01	46	12	12
MGXII 3	7.120	0.7900E-01	45	12	12
MGXII 2	8.440	0.4160E+00	43	12	12
SI I 41.12AU	1255.276	0.2200E+00	41	14	1
SI I 41.12AU	1256.490	0.2200E+00	41	14	1
SI I 41.12AU	1258.795	0.2200E+00	41	14	1
SI I 10	1845.520	0.1520E+00	41	14	1
SI I 10	1847.473	0.1140E+00	41	14	1

SI	I	10	1848.150	0.3800E-01	41	14	1
SI	I	10	1850.672	0.1280E+00	41	14	1
SI	I	10	1852.472	0.2280E-01	41	14	1
SI	I	10	1853.152	0.1520E-02	41	14	1
SI	I	7	1977.579	0.3110E-01	41	14	1
SI	I	7	1979.206	0.1040E-01	41	14	1
SI	I	7	1980.618	0.7770E-02	41	14	1
SI	I	7	1983.232	0.1290E-01	41	14	1
SI	I	7	1986.364	0.7750E-02	41	14	1
SI	I	7	1988.994	0.2320E-01	41	14	1
SI	I	3	2207.978	0.5890E-01	42	14	1
SI	I	3	2210.894	0.4420E-01	42	14	1
SI	I	3	2211.744	0.1470E-01	42	14	1
SI	I	3	2216.669	0.4930E-01	42	14	1
SI	I	3	2218.057	0.8800E-02	42	14	1
SI	I	3	2218.915	0.5870E-03	42	14	1
SI	I	1	2506.897	0.6520E-01	41	14	1
SI	I	1	2514.316	0.1560E+00	41	14	1
SI	I	1	2516.112	0.1170E+00	41	14	1
SI	I	1	2519.202	0.3890E-01	41	14	1
SI	I	1	2524.108	0.5180E-01	41	14	1
SI	I	1	2528.509	0.3880E-01	41	14	1
SI	II	6	989.867	0.2440E+00	41	14	2
SI	II	6	992.675	0.2190E+00	41	14	2
SI	II	6	992.690	0.2430E-01	41	14	2
SI	II	5.01	1020.699	0.4820E-01	41	14	2
SI	II	5.01	1023.693	0.4800E-01	41	14	2
SI	II	5	1190.418	0.6500E+00	42	14	2
SI	II	5	1193.284	0.1300E+01	42	14	2
SI	II	5	1194.496	0.1620E+01	42	14	2
SI	II	5	1197.389	0.3230E+00	42	14	2
SI	II	4	1260.418	0.9590E+00	42	14	2
SI	II	4	1264.730	0.8600E+00	42	14	2
SI	II	4	1265.023	0.9560E-01	42	14	2
SI	II	3	1304.369	0.1470E+00	42	14	2
SI	II	3	1309.274	0.1470E+00	42	14	2
SI	II	2	1526.719	0.7640E-01	41	14	2
SI	II	2	1533.445	0.7600E-01	41	14	2
SI	II	1	1808.003	0.3710E-02	42	14	2
SI	II	1	1816.921	0.3320E-02	42	14	2
SI	II	1	1817.445	0.3690E-03	42	14	2
SI	III	11	566.610	0.4600E-01	41	14	3
SI	III	2	1206.510	0.1660E+01	42	14	3
SI	IV	2.02	327.137	0.4886E-02	41	14	4
SI	IV	2.02	327.181	0.2449E-02	41	14	4
SI	IV	2.01	361.560	0.9527E-02	41	14	4
SI	IV	2.01	361.659	0.4775E-02	41	14	4
SI	IV	2	457.818	0.2201E-01	41	14	4
SI	IV	2	458.155	0.1100E-01	41	14	4
SI	IV	1	1393.755	0.5280E+00	42	14	4
SI	IV	1	1402.769	0.2620E+00	42	14	4
SI	V	NE1	85.200	0.2700E+00	34	14	5
SI	V	NE2	90.500	0.1000E-01	36	14	5
SI	V	5	96.430	0.2000E+00	35	14	5
SI	V	4	97.140	0.8400E+00	35	14	5
SI	V	3	98.200	0.3800E-02	35	14	5

SI V 2	117.860	0.1900E+00	35	14	5
SI V 1	118.970	0.2100E-01	35	14	5
SI VI F5	69.200	0.2100E+00	41	14	6
SI VI F1	70.000	0.2500E+00	41	14	6
SI VI F2	83.000	0.1500E+01	41	14	6
SI VI F3	99.400	0.9000E+00	41	14	6
SI VI	246.001	0.1133E+00	42	14	6
SI VI	249.125	0.1119E+00	42	14	6
SI VII O7	60.800	0.1400E+00	41	14	7
SI VII O1	68.000	0.4400E+00	41	14	7
SI VII O2	69.660	0.2100E+00	41	14	7
SI VII O3	79.500	0.2600E-01	41	14	7
SI VII O5	81.900	0.4300E-01	41	14	7
SI VII O4	85.600	0.2600E-01	41	14	7
SI VII	272.641	0.3448E-01	42	14	7
SI VII	274.175	0.4571E-01	42	14	7
SI VII	275.352	0.1024E+00	42	14	7
SI VII	275.665	0.3410E-01	42	14	7
SI VII	276.839	0.1358E+00	42	14	7
SI VII	278.445	0.5627E-01	42	14	7
SI VII 1	314.310	0.3900E-01	42	14	7
SI VII 1	316.200	0.7400E-01	42	14	7
SI VII 1	319.830	0.1100E+00	42	14	7
SI VIII N7	50.000	0.3100E+00	41	14	8
SI VIII N3	69.600	0.5500E-01	41	14	8
SI IX C9	44.200	0.2300E+00	41	14	9
SI IX C1	52.800	0.2000E-01	41	14	9
SI IX C3	55.100	0.2300E+00	41	14	9
SI IX C4	55.300	0.6300E+00	41	14	9
SI IX C5	61.600	0.5700E-01	41	14	9
SI IX 3	223.720	0.1000E+00	42	14	9
SI IX 3	225.030	0.9900E-01	42	14	9
SI IX 3	227.000	0.9900E-01	42	14	9
SI IX 2	290.630	0.9200E-01	42	14	9
SI IX 2	292.830	0.2300E-01	42	14	9
SI IX 2	292.830	0.3000E-01	42	14	9
SI IX 2	292.830	0.3800E-01	42	14	9
SI IX 2	296.190	0.6800E-01	42	14	9
SI IX 2	296.190	0.2300E-01	42	14	9
SI IX 1	341.950	0.8500E-01	42	14	9
SI IX 1	345.010	0.2100E-01	42	14	9
SI IX 1	345.100	0.6200E-01	42	14	9
SI IX 1	349.670	0.8300E-03	42	14	9
SI IX 1	349.770	0.1300E-01	42	14	9
SI IX 1	439.960	0.6900E-01	42	14	9
SI X B1	6.850	0.5400E+00	42	14	10
SI X B2	39.000	0.1100E+00	41	14	10
SI X B3	47.540	0.1430E+00	41	14	10
SI X B9	54.900	0.2400E-01	41	14	10
SI X 4	253.810	0.6000E-01	42	14	10
SI X 4	256.580	0.1200E+00	42	14	10
SI X 4	258.390	0.1500E+00	42	14	10
SI X 4	261.270	0.2900E-01	42	14	10
SI X 2	272.000	0.3700E-01	42	14	10
SI X 2	277.270	0.3600E-01	42	14	10
SI X 1	347.430	0.7400E-01	42	14	10

SI	X	1	356.070	0.6600E-01	42	14	10
SI	X	1	356.070	0.7300E-02	42	14	10
SI	XI	BE1	6.780	0.7200E+00	42	14	11
SI	XI	2	303.580	0.2640E+00	42	14	11
SI	XII	LI1	28.500	0.3700E-01	22	14	12
SI	XII	LI2	31.000	0.8800E-01	22	14	12
SI	XII		499.399	0.7294E-01	42	14	12
SI	XII		520.684	0.3498E-01	42	14	12
SI	XIII	HE1	5.290	0.2800E-01	13	14	13
SI	XIII	HE2	5.410	0.5700E-01	13	14	13
SI	XIII	HE3	5.680	0.1500E+00	11	14	13
SI	XIII	HE4	6.650	0.7500E+00	9	14	13
SI	XIV	6	4.780	0.8000E-02	48	14	14
SI	XIV	5	4.840	0.1400E-01	47	14	14
SI	XIV	4	4.960	0.2900E-01	46	14	14
SI	XIV	3	5.230	0.7900E-01	45	14	14
SI	XIV	2	6.200	0.4160E+00	43	14	14
S	I	9	1295.661	0.1080E+00	41	16	1
S	I	9	1296.174	0.3610E-01	41	16	1
S	I	9	1302.344	0.6000E-01	41	16	1
S	I	9	1302.865	0.3600E-01	41	16	1
S	I	9	1303.114	0.4790E-01	41	16	1
S	I		1303.420	0.1630E-01	41	16	1
S	I	9	1305.885	0.1440E+00	41	16	1
S	I		1310.210	0.1620E-01	41	16	1
S	I		1313.250	0.1610E-01	41	16	1
S	I	8	1316.570	0.3450E-01	41	16	1
S	I	8	1316.610	0.6150E-02	41	16	1
S	I	8	1316.620	0.4110E-03	41	16	1
S	I	8	1323.521	0.3060E-01	41	16	1
S	I	8	1323.530	0.1020E-01	41	16	1
S	I	8	1326.635	0.4070E-01	41	16	1
S	I	6	1401.541	0.1580E-01	41	16	1
S	I	6	1409.368	0.1570E-01	41	16	1
S	I	6	1412.899	0.1570E-01	41	16	1
S	I	5	1425.065	0.1810E+00	42	16	1
S	I	5	1425.229	0.3220E-01	42	16	1
S	I	5	1425.240	0.2150E-02	42	16	1
S	I	5	1433.328	0.1600E+00	42	16	1
S	I	5	1433.328	0.5340E-01	42	16	1
S	I	5	1437.005	0.2130E+00	42	16	1
S	I	3	1474.005	0.7820E-01	41	16	1
S	I	3	1474.390	0.1400E-01	41	16	1
S	I	3	1474.569	0.9320E-03	41	16	1
S	I	3	1483.036	0.6940E-01	41	16	1
S	I	3	1483.232	0.2310E-01	41	16	1
S	I	3	1487.149	0.9230E-01	41	16	1
S	I	2	1807.341	0.1120E+00	41	16	1
S	I	2	1820.361	0.1110E+00	41	16	1
S	I	2	1826.261	0.1110E+00	41	16	1
S	II	1	1250.586	0.5350E-02	42	16	2
S	II	1	1253.812	0.1070E-01	42	16	2
S	II	1	1259.520	0.1590E-01	42	16	2
S	III		484.194	0.4074E-01	41	16	3
S	III		484.580	0.3111E-01	41	16	3
S	III		484.892	0.8568E-02	41	16	3

S III		485.220	0.3476E-01	41	16	3
S III		485.840	0.4179E-02	41	16	3
S III		486.154	0.2296E-03	41	16	3
S III	7	677.750	0.9644E+00	41	16	3
S III	7	678.460	0.7225E+00	41	16	3
S III	7	679.110	0.2406E+00	41	16	3
S III	7	680.690	0.8066E+00	41	16	3
S III	7	680.950	0.1440E+00	41	16	3
S III	6	680.979	0.5593E-01	41	16	3
S III	6	681.500	0.1341E+00	41	16	3
S III	7	681.587	0.9597E-02	41	16	3
S III	6	682.883	0.3346E-01	41	16	3
S III	6	683.070	0.4460E-01	41	16	3
S III	6	683.470	0.1003E+00	41	16	3
S III	6	685.350	0.3334E-01	41	16	3
S III	5	698.730	0.7406E-02	41	16	3
S III	5	700.150	0.3080E-02	41	16	3
S III	5	700.184	0.1848E-02	41	16	3
S III	5	700.290	0.2463E-02	41	16	3
S III	5	702.780	0.5523E-02	41	16	3
S III	5	702.820	0.1841E-02	41	16	3
S III	4	724.290	0.4677E+00	41	16	3
S III	4	725.852	0.4708E+00	41	16	3
S III	1	1190.206	0.2240E-01	42	16	3
S III	1	1194.061	0.1670E-01	42	16	3
S III	1	1194.457	0.5570E-02	42	16	3
S III	1	1200.970	0.1860E-01	42	16	3
S III	1	1201.730	0.3320E-02	42	16	3
S III	1	1202.132	0.2220E-03	42	16	3
S IV	5	551.170	0.9507E-01	41	16	4
S IV	5	554.070	0.9457E-01	41	16	4
S IV	4	657.340	0.9106E+00	41	16	4
S IV	4	661.420	0.8145E+00	41	16	4
S IV	4	661.471	0.9049E-01	41	16	4
S IV	3	744.920	0.3155E+00	41	16	4
S IV	3	748.400	0.6295E+00	41	16	4
S IV	3	750.230	0.8278E+00	41	16	4
S IV	3	753.760	0.1730E+00	41	16	4
S IV	2	809.690	0.1514E+00	41	16	4
S IV	2	815.970	0.1502E+00	41	16	4
S IV	1	933.382	0.4260E+00	41	16	4
S IV	1	944.517	0.2100E+00	41	16	4
S IV	1	1062.672	0.3770E-01	42	16	4
S IV	1	1072.992	0.3360E-01	42	16	4
S IV	1	1073.522	0.3730E-02	42	16	4
S V	1	786.480	0.1263E+01	42	16	5
SVI	73	191.510	0.2800E-01	41	16	6
SVI	2	248.980	0.4710E-01	41	16	6
S VI	2	249.270	0.2506E-01	42	16	6
SVI	2	249.270	0.2440E-01	41	16	6
S VII	NE1	52.000	0.4200E+00	34	16	7
S VII	NE2	54.800	0.1000E-01	36	16	7
SVII	5	60.160	0.1600E+00	41	16	7
SVII	4	60.800	0.1400E+01	41	16	7
SVII	2	72.020	0.1700E+00	41	16	7
SVII	1	72.660	0.3600E-01	41	16	7

S	VIII	F5	45.300	0.2600E+00	41	16	8
S	VIII	F1	46.000	0.2500E+00	41	16	8
S	VIII	F2	53.000	0.1500E+01	41	16	8
S	VIII	F3	63.300	0.6000E-01	41	16	8
S	VIII	F4	199.900	0.9600E-01	41	16	8
S	IX	O7	41.000	0.2300E+00	41	16	9
S	IX	O2	47.400	0.2300E+00	41	16	9
S	IX	O1	49.200	0.8000E+00	41	16	9
S	IX	O5	54.100	0.4000E-01	41	16	9
S	IX	O3	54.200	0.2400E-01	41	16	9
S	IX	O4	56.100	0.2300E-01	41	16	9
S	IX	O6	224.750	0.1600E+00	41	16	9
S	X	N7	35.500	0.3200E+00	41	16	10
S	X	N1	42.500	0.1700E+00	41	16	10
S	X	N3	47.700	0.4800E-01	41	16	10
S	X	N6	257.100	0.1900E+00	41	16	10
S	XI	C9	31.000	0.2100E+00	41	16	11
S	XI	C3	39.300	0.2100E+00	41	16	11
S	XI	C4	39.300	0.6100E+00	41	16	11
S	XI	C5	41.000	0.3500E-01	41	16	11
S	XI	C6	188.600	0.8600E-01	41	16	11
S	XI	C7	247.000	0.8400E-01	41	16	11
S	XII	B1	5.180	0.5500E+00	42	16	12
S	XII	B2	27.800	0.1120E+00	41	16	12
S	XII	B3	33.300	0.1190E+00	41	16	12
S	XII	B10	221.000	0.1600E+00	41	16	12
S	XII	B11	227.200	0.2900E-01	41	16	12
S	XIII	BE1	5.130	0.7300E+00	42	16	13
S	XIII	BE13	256.680	0.2500E+00	42	16	13
S	XIV	LI1	21.000	0.3800E-01	22	16	14
S	XIV	LI2	23.050	0.9000E-01	22	16	14
S	XIV	LI5	30.430	0.3500E+00	21	16	14
S	VI	2	248.990	0.4775E-01	41	16	14
S	XIV		417.640	0.5573E-02	42	16	14
S	XIV		445.694	0.2611E-02	42	16	14
SI	XIII	HE1	4.010	0.2800E-01	13	16	15
SI	XIII	HE2	4.100	0.5700E-01	13	16	15
SI	XIII	HE3	4.300	0.1500E+00	11	16	15
SI	XIII	HE4	5.040	0.7500E+00	9	16	15
SI	XVI	6	9.370	0.8000E-02	48	16	16
SI	XVI	5	9.490	0.1400E-01	47	16	16
SI	XVI	4	9.720	0.2900E-01	46	16	16
SI	XVI	3	10.250	0.7900E-01	45	16	16
SI	XVI	2	12.150	0.4160E+00	43	16	16

APPENDIX 3. THE LINEARIZED EQUATIONS AND THE DISPERSION RELATION

The linearized equations and the dispersion relation used here were derived with the aid of a program called REDUCE available from the UBC Computing Centre. Of particular interest here was its ability to allow the <u>algebraic</u> definition of functions of the form

$$Q(x,t)=Q_0+v(dQ/dz)+\delta q_1 \exp[i(kz-\omega t)]. \qquad \text{(AIII.22)}$$

The term v(dQ/dz) appears because the analysis is done in the frame moving along at the gas speed. These definitions are made for the density, temperature, and velocity, and other quantities such as the cooling rate have perturbations expressed in terms of their density and temperature derivatives. Then the various partial derivatives with respect to z and t in the conservation equations are evaluated, and the terms of first order in δ are collected. This gives the set of linearized equations as given below. The results eventually must be expressed in the form of a matrix of coefficients times a vector of perturbation quantities. The determinant of this matrix will give the dispersion relation. In order to reduce the number of multiplications involved in the evaluation of the determinant, the coefficients of and k have been combined together as much as possible. This is the motivation for the form of the equations below. The resulting linearized equations have coefficients which are labelled by their equation of origin, m, p, and e, for mass momentum and energy; the term being multiplied labelled by the coefficient, w, k, and c; and the linearized quantity being multiplied labelled by n, T, and v. The equations have been written in the form of a series of terms which when summed together must be equal to zero. The derivatives with respect to z are abbreviated as just the "numerator" of the derivative, i.e. dv/dz goes to dv. The "*" is the multiplication sign and ** represents exponentiation. The results are presented in the form of FORTRAN statements because this is essentially how they are output from REDUCE , and it is how they are input to the program which does the numerical computations.

The linearized equations are:

mass conservation,

```
n1*(-i*w+dv)
+t1*0
+v1*(i*k*n0+dn)=0.
```

Momentum conservation,

```
n1*(i*k*pkn+pcn)
+t1*(i*k*pkt+pct)
+v1*(-i*w+dvg)=0.
```

And energy conservation,

```
n1*(-i*w*ewn+i*k*ekn+ecn
+t1*(-i*w*ewt+i*k*ekt-k**2*conkap+ect)
+v1*(-i*w*ewv+i*k*ekv+ecv)=0.
```

In the following vc1=1.-v0/c and rhocv is the mass density divided by the number density.

```
pkn=kboltz/(n0*rhocv)*(dnedn*t0+t0)
pcn=kboltz/(n0**2*rhocv)*(-dn*t0+n0*dnedn*dt
-ne0*dt-(dnedn*dn+dnedt*dt)*t0)-vc1*dgrdn
pkt=kboltz/(n0*rhocv)*(ne0+dnedt*t0+n0)
pct=kboltz/(n0*rhocv)*(dn+dnedt*dt+dnedt*dt+dnedn*dn)-vc1*dgrdt
dvg=dv+grad0/c
```

```
ewn=(dedn*n0+e0)*rhocv
ekn=-dkdn*dt
ecn=rhocv*(dv*h0+
dv*n0*dhdn+)-d2t*dkdn-vc1*dqdn+dldn
+rhocv*(v0*(dedn*dn+dedt*dt)+dedn*v0*dn)
ewt=dedt*n0*rhocv
ekt=-dkdt*dt+(-dkdt*dt-dkdn*dn)
ect=dldt-vc1*dqdt+(dhdt*dv*n0)*rhocv-dkdt*d2t
+rhocv*dedt*v0*dn
ewv=0
ekv=h0*n0*rhocv
ecv=dn*h0+n0*(dhdt*dt+dhdn*dn))
*rhocv+g0/c
+rhocv*(n0*v0*dv)
```

In order that the above set of algebraic equations have a nontrivial solution the matrix of the coefficients must have a zero determinant, which gives the dispersion relation as follows. The dispersion relation is computed from the constants by,

$$D(\omega,k) = \sum_{m=1}^{4}\sum_{n=1}^{5} \omega^{m-1}k^{n-1}(crd(n,m)+i*cid(n,m)) \quad (1)$$

where the coefficients crd and cid are:

```
crd(1,1)=
-ecn*pct*dn-dvg*ect*dv+pct*ecv*dv+pcn*dn*ect
cid(2,1)=
-ecn*pct*n0-ecn*pkt*dn-ekn*pct*dn
-dvg*ekt*dv+pct*ekv*dv+pkt*ecv*dv+pcn*dn*ekt
+pcn*n0*ect+pkn*dn*ect
crd(3,1)=
ecn*pkt*n0
```

```
+ekn*pct*n0+ekn*pkt*dn+dvg*(-conkap)*dv-pkt*ekv*dv
+pcn*dn*conkap
-pcn*n0*ekt-pkn*dn*ekt-pkn*n0*ect
cid(4,1)=
-pkt*ekv+(-conkap)*dv)+
ekn*pkt*n0-
pcn*n0*(-conkap)-pkn*dn*(-conkap)-pkn*n0*ekt
crd(5,1)=
pkn*n0*(-conkap)
cid(1,2)=
ewn*pct*dn+dvg*ect+dvg*ewt*dv-pct*ecv-pct*ewv*dv
-pcn*dn*ewt+ect*dv
crd(2,2)=
-ewn*pct*n0-ewn*pkt*dn
-dvg*ekt+pct*ekv+pkt*ecv+pkt*ewv*dv+pcn*n0*ewt
+pkn*dn*ewt-ekt*dv
cid(3,2)=
-ewn*pkt*n0-dvg*(-conkap)+pkt*ekv
+pkn*n0*ewt-(-conkap)*dv
crd(1,3)=
dvg*ewt-pct*ewv+ect+ewt*dv
cid(2,3)=
-pkt*ewv+ekt
crd(3,3)=conkap
cid(1,4)=-ewt
```

The form of these coefficients is such that if k is replaced by the negative of its complex conjugate the root found will be the negative of the complex conjugate of the original root. This behaviour is demanded in order that the same physical solution be recovered independent of the signs of ω and k.

APPENDIX 4. THE MAJOR COMPUTER PROGRAMS

This appendix describes the major computer programs for actually performing the numerical computations. They are all written in the FORTRAN language. The photoionization cross sections and the resulting ionization and heating rates are calculated by the program PHOTION using the tables given in the appendix 2 as input. The ionization balance and heating and cooling rates are calculated by, HCMAIN with subroutine SUBCHEAT. The zero order physical quantities and radiation acceleration are worked out by, COEF. The coefficients of the dispersion relation are done in COCALC, and the roots of the dispersion relation in DISPER. The flow of the programs can be followed with the aid of the comments.

PROGRAM PHOTION

```
C        PHOTOIONIZATION AND HEATING RATES
C
      DIMENSION INDEX(16,9)
      INTEGER IZED(9)
      REAL NJNU(100),DELNU(100),PHOT(76),PHEAT(76)
       INTEGER NUO(76),NUF(76)
      REAL SIGMA(100,76),ENU(100),FLUX(100),DELE(100)
      LOGICAL VERBOS
      COMMON /A/ INDEX,IZED,DEN,T,VERBOS,NFREQ,NNCT
      COMMON /HELIUM/ ALPHA,BETA,A2,B2,ZF,ZB,DEN1,ZF2
     $ ,AEZ3,BZB31,AZB31
      COMMON /PH/ PHOT,PHEAT,NJNU,DELNU,SIGMA
      EQUIVALENCE (DELNU(1),DELE(1))
      NAMELIST /PP/ VERBOS
      DO 20 IJ=1,76
      DO 20 IN=1,100
20    SIGMA(IN,IJ)=0.
C
C UNIT 1 HAS STELLAR RADIATION FLUXES AND FREQUENCIES
C UNIT TWO HAS PHOTOIONIZATION EDGES AND STELLAR
C    FLUX FREQUENCIES
C
      READ (1) NFREQ
      READ (1) ENU,FLUX,NJNU,DELE
      READ (2,9774) (NUO(IJ),NUF(IJ),IJ=1,76)
9774  FORMAT(2I4)
C
C CALCULATE TOTAL FLUX
C
      FTOT=0.
      DO 22 IN=2,NFREQ
      FTOT=FTOT+.5*(FLUX(IN-1)+FLUX(IN))*DELE(IN)
22    CONTINUE
      VERBOS=.TRUE.
      WRITE(6,9775)
9775  FORMAT('1')
      READ(5,PP)
      WRITE(6,PP)
C
C GO THROUGH ALL ATOMS (I)
C AND ALL IONS OF ATOMS (J)
C
      DO 10000 I=1,9
      II=IZED(I)
      DO 10001 J=1,II
      IJ=INDEX(J,I)
      NUNOT=NUO(IJ)
      NUINF=NUF(IJ)
      NUINF1=NUINF-1
      NUNOT1=NUNOT+1
      PHOT(IJ)=0.0
      PHEAT(IJ)=0.0
C
```

```
C BRANCH TO CORRECT ATOM
C
C ATOMS ARE IDENTIFIED BY BRANCH LABEL
C CORRESPONDS TO Z OF ATOM
C
      GO TO (1,2,6,7,8,10,12,14,16),I
1     XIP=13.598
      ZADJ=1.0
      GO TO 9910
2     IF(J.EQ.2) GO TO 202
      ALPHA=2.182846
      BETA=1.188914
      A2=4.7648166
      B2=1.4135164
      DEN1=0.567759716
      ABZ3=139.8332
      ZF=1.
      ZB=2.
      ZF2=1.
      BZB31=0.03083696
      AZB31=0.01366421
      XIP=24.587
      GO TO 9920
202   ZADJ=0.25
      XIP=54.416
      GO TO 9910
C
C ALL FOLLOWING CALCULATIONS ARE IDENTIFIED BY THE
C Z OF THE ATOM AND THE J OF THE ION
C EG 601 IS CI
C EG 1204 IS MG III
C
6     GO TO (601,602,603,604,605,606),J
601   SIGNOT=12.19
      FZERO=11.26
      A=3.317
      S=2.0
      GO TO 9930
602   SIGNOT=4.60
      FZERO=24.383
      A=1.95
      S=3.0
      GO TO 9930
603   SIGNOT=1.84
      FZERO=47.887
      A=3.0
      S=2.6
      GO TO 9930
604   SIGNOT=0.713
      FZERO=64.492
      A=2.7
      S=2.2
      GO TO 9930
605   GO TO 9980
606   GO TO 9980
7     GO TO (701,702,703,704,705,706,707),J
```

```
701   SIGNOT=11.42
      FZERO=14.534
      A=4.287
      S=2.0
      GO TO 9930
702   SIGNOT=6.65
      S=3.0
      A=2.86
      FZERO=29.601
      GO TO 9930
703   SIGNOT=2.06
      A=3.0
      S=1.626
      FZERO=47.448
      GO TO 9930
704   SIGNOT=1.08
      A=2.6
      S=3.0
      FZERO=77.472
      GO TO 9930
705   SIGNOT=0.48
      S=2.0
      A=1.0
      FZERO=97.89
      GO TO 9930
706   CONTINUE
707   GO TO 9980
8     GO TO (801,802,803,804,805,806,9980,9980),J
801   DO 811 IN=NUNOT,NUINF
      SIGMA(IN,IJ)=2.94*SEATON(ENU(IN),13.618,2.661,1.0)
      IF(ENU(IN).LT.16.943) GO TO 811
      SIGMA(IN,IJ)=SIGMA(IN,IJ)+3.85*SEATON(ENU(IN),
     $   16.943,4.378,1.5)
      IF(ENU(IN).LT.18.635) GO TO 811
      SIGMA(IN,IJ)=SIGMA(IN,IJ)+2.26*SEATON(ENU(IN),
     $   18.635,4.311,1.5)
811   CONTINUE
      GO TO 999
802   SIGNOT=7.32
      S=2.5
      A=3.837
      FZERO=35.117
      GO TO 9930
803   SIGNOT=3.65
      S=3.0
      A=2.014
      FZERO=54.943
      GO TO 9930
804   SIGNOT=1.27
      S=3.0
      A=0.831
      FZERO=77.413
      GO TO 9930
805   SIGNOT=0.78
      S=3.0
      A=2.6
```

```
      FZERO=113.90
      GO TO 9930
806   SIGNOT=0.36
      S=2.1
      A=1.0
      FZERO=138.12
      GO TO 9930
10    GO TO (1001,1002,1003,1004,1005,1006),J
      GO TO 9980
1001  SIGNOT=5.35
      S=1.0
      A=3.769
      FZERO=21.564
      GO TO 9930
1002  DO 1012 IN=NUNOT,NUINF
      SIGMA(IN,IJ)=4.16*SEATON(ENU(IN),40.962,2.717,1.5)
      IF(ENU(IN).LT.44.166) GO TO 1012
      SIGMA(IN,IJ)=SIGMA(IN,IJ)+2.71*SEATON(ENU(IN),
     $   44.166,2.148,1.5)
      IF(ENU(IN).LT.47.874) GO TO 1012
      SIGMA(IN,IJ)=SIGMA(IN,IJ)+0.52*SEATON(ENU(IN),
     $   47.874,2.126,1.5)
1012  CONTINUE
      GO TO 999
1003  DO 1013 IN=NUNOT,NUINF
      SIGMA(IN,IJ)=1.80*SEATON(ENU(IN),63.45,2.277,2.0)
      IF(ENU(IN).LT.68.53) GO TO 1013
      SIGMA(IN,IJ)=SIGMA(IN,IJ)+2.50*SEATON(ENU(IN),
     $   68.53,2.346,2.5)
      IF(ENU(IN).LT.71.16) GO TO 1013
      SIGMA(IN,IJ)=SIGMA(IN,IJ)+1.48*SEATON(ENU(IN),
     $    ,71.16,2.225,2.5)
1013  CONTINUE
      GO TO 999
1004  SIGNOT=3.11
      FZERO=97.11
      A=1.963
      S=3.0
      GO TO 9930
1005  SIGNOT=1.40
      FZERO=126.21
      A=1.471
      S=3.0
      GO TO 9930
1006  SIGNOT=0.49
      FZERO=157.93
      A=1.145
      S=3.0
      GO TO 9930
12    GO TO (1201,1202,1203,1205),J
      GO TO 9980
1201  SIGNOT=9.92
      A=2.3
      S=1.8
      FZERO=7.646
      GO TO 9930
```

```
1202   SIGNOT=3.416
       A=2.0
       S=1.0
       FZERO=15.035
       GO TO 9930
1203   SIGNOT=5.2
       A=2.65
       S=2.0
       FZERO=80.143
       GO TO 9930
1204   SIGNOT=3.83
       A=1.0
       S=2.0
       FZERO=109.31
       GO TO 9930
1205   SIGNOT=2.53
       A=1.0
       S=2.3
       FZERO=141.27
       GO TO 9930
14     GO TO (1401,1402,1403,1404),J
       GO TO 9980
1401   DO 1411 IN=NUNOT,NUINF
       SIGMA(IN,IJ)=12.32*CHAHEN(ENU(IN),7.370,6.459,
      $                 5.142,3.)
       IF(ENU(IN).LT.8.151) GO TO 1411
       SIGMA(IN,IJ)=SIGMA(IN,IJ)+25.18*CHAHEN(ENU(IN),
      $   8.151,4.420,
      $                 8.934,5.)
1411   CONTINUE
       GO TO 999
1402   SIGNOT=2.65
       A=0.6
       S=3.0
       FZERO=16.345
       GO TO 9930
1403   SIGNOT=2.48
       A=2.3
       S=1.8
       FZERO=33.492
       GO TO 9930
1404   SIGNOT=0.854
       A=2.0
       S=1.0
       FZERO=45.141
       GO TO 9930
16     GO TO(1601,1602,1603,1604,1605,1606),J
       GO TO 9980
1601   DO 1611 IN=NUNOT,NUINF
       SIGMA(IN,IJ)=12.62*CHAHEN(ENU(IN),10.360,
      $   21.595,3.062,3.0)
       IF(ENU(IN).LT.12.206) GO TO 1611
       SIGMA(IN,IJ)=SIGMA(IN,IJ)+19.08*CHAHEN(ENU(IN),
      $   12.206,0.135,5.635,
      $ 2.5)
       IF(ENU(IN).LT.13.408) GO TO 1611
```

```
      SIGMA(IN,IJ)=SIGMA(IN,IJ)+12.70*CHAHEN(ENU(IN),
     $    13.408,1.159,4.743,
     $ 3.0)
1611  CONTINUE
      GO TO 999
1602  SIGNOT=8.20
      FZERO=23.33
      A=1.695
      B=-2.236
      S=1.5
      GO TO 9940
1603  DO 1631 IN=NUNOT,NUINF
      SIGMA(IN,IJ)=.350*CHAHEN(ENU(IN),33.46,10.056,
     $  -3.278,2.0)
      IF (ENU(IN).LT.34.83) GO TO 1631
      SIGMA(IN,IJ)=SIGMA(IN,IJ)+.244*CHAHEN(ENU(IN),
     $    34.83,18.427,
     $        0.592,2.0)
1631  CONTINUE
      GO TO 999
1604  SIGNOT=0.29
      FZERO=47.30
      A=6.837
      B=4.459
      S=2.0
      GO TO 9940
1605  SIGNOT=0.62
      A=2.3
      S=1.8
      FZERO=72.68
      GO TO 9930
1606  SIGNOT=0.214
      A=2.0
      S=1.0
      FZERO=88.05
      GO TO 9930
C
C NOW THAT CONSTANTS ARE SET UP
C IN THE RELEVANT FORMULA
C CALCULATE THE CROSS SECTION AT THE
C INTEGFREQ FREQUENCIES (UNIT 2)
C
9910  DO 9911 IN=NUNOT,NUINF
      SIGMA(IN,IJ)=ZADJ*HSIG(ENU(IN),XIP)
9911  CONTINUE
      GO TO 999
9920  DO 9921 IN=NUNOT,NUINF
9921  SIGMA(IN,IJ)=HEISIG(ENU(IN),XIP)
      GO TO 999
9930  IF(NUNOT.GE.NUINF) GO TO 9960
      DO 9931 IN=NUNOT,NUINF
9931  SIGMA(IN,IJ)=SIGNOT*SEATON(ENU(IN),FZERO,A,S)
      GO TO 999
9940  DO 9941 IN=NUNOT,NUINF
9941  SIGMA(IN,IJ)=SIGNOT*CHAHEN(ENU(IN),FZERO,SIGNOT,A,B,S)
      GO TO 999
```

```
9980   SIGMA(NFREQ,IJ)=-1.0
       GO TO 9981
999    DO 998 INU=NUNOT1,NUINF
       PHINT=.5*(NJNU(INU-1)*SIGMA(INU-1,IJ)+NJNU(INU)
      $    *SIGMA(INU,IJ))
       PHOT(IJ)=PHINT*DELE(INU)+PHOT(IJ)
       PHINT=.5*(FLUX(INU-1)*SIGMA(INU-1,IJ)+
      $ FLUX(INU)*SIGMA(INU,IJ))
       PHEAT(IJ)=PHINT*DELE(INU)+PHEAT(IJ)
998    CONTINUE
C   FLUX HAS UNITS ERG CM-2 S-1 (EV)-1
C   NJNU HAS UNITS # CM-2 S-1 (EV)-1
C   PHOT HAS UNITS # S-1
C   PHEAT HAS UNITS ERG S-1
       PHEAT(IJ)=PHEAT(IJ)
9981   WRITE(6,9771) II,J,ENU(NUNOT),ENU(NUINF)
      $    ,PHOT(IJ),PHEAT(IJ)
9771   FORMAT('0ION',2I3,' FREQUENCIES',2F12.3,
      $  ' IONIZATION, HEATING RATES',2E15.4)
       IF(VERBOS) WRITE(6,9773) II,J
9773   FORMAT('0CROSSECTIONS FOR ION (Z,N)=',2I3)
       IF(VERBOS) WRITE(6,9772)  (SIGMA(IN,IJ),
      $    IN=1,NFREQ)
9772   FORMAT(1X,10E12.3)
10001 CONTINUE
10000 CONTINUE
       WRITE(7) PHOT,PHEAT,SIGMA,FTOT
C
C FLUX HAS UNITS ERG CM-2 S-2 (EV)-1
C NJNU HAS UNITS # CM-2 S-1 (EV)-1
C PHOT HAS UNITS # S-1
C PHEET HAS UNITS  ERG S-1
C
       STOP
       END
       BLOCK DATA
       COMMON /A/ INDEX,IZED,DEN,T,VERBOS,LAST,NNOT
       INTEGER IZED(9)
       DATA IZED /1,2,6,7,8,10,12,14,16/
       DIMENSION INDEX(16,9)
       DATA INDEX /1,15*0,2,3,14*0,4,5,6,7,8,9,10*0,
      $ 10,11,12,13,14,15,16,9*0,
      $ 17,18,19,20,21,22,23,24,8*0,
      $ 25,26,27,28,29,30,31,32,33,34,6*0,
      $ 35,36,37,38,39,40,41,42,43,44,45,46,4*0,
      $ 47,48,49,50,51,52,53,54,55,56,57,58,59,60,2*0,
      $ 61,62,63,64,65,66,67,68,69,
      $    70,71,72,73,74,75,76/
       END
       REAL FUNCTION HSIG(E,XIP)
C
C FOR CALCULATING THE HYDROGEN
C CROSS SECTION
C
       IF (ABS(E-XIP).LT.0.0001) GO TO 1
       ETA1=SQRT(E/XIP-1.0)
```

```
      ETA=1./ETA1
      HSIG=3.44204E-16*(XIP/E)**4.
     $     *EXP(-4.*ETA*ATAN(ETA1))/
     $ (1.-EXP(-6.238185*ETA))
      RETURN
1     HSIG=6.30432E-18
      RETURN
      END
      REAL FUNCTION HEISIG(E,XIP)
C
C HELIUM I CROSS SECTION
C
      COMMON /HELIUM/ ALPHA,BETA,A2,B2,ZF,ZB,DEN1,ZF2
     $ ,AEZ3,BZB31,AZB31
      RK2=(E-XIP)/13.598
      IF(RK2.LE.0.0) GO TO 1
      RK=SQRT(RK2)
      FEXP=-6.283185*ZF/RK
      ALPHAI=(2.*ALPHA-ZF)*EXP(FEXP*ATAN(RK/ALPHA))
     $    *(RK2+A2)**(-3.)
      BETAI=(2.*BETA-ZF)*EXP(FEXP*ATAN(RK/BETA))
     $    *(RK2+B2)**(-3.)
      DFE=2730.667*E*ZF*AEZ3*(RK2+ZF2)*
     $    (ALPHAI*BZB31+BETAI*AZB31)**2
     $  (1.-EXP(FEXP))*DEN1
      HEISIG=8.067291E-18*DFE
      RETURN
1     IF (XIP.GT.24.587) GO TO 2
      HEISIG=8.334E-18
      RETURN
2     IF (XIP.GT.392.08) GO TO 3
      HEISIG=4.7113E-19
      RETURN
3     IF (XIP.GT.552.06) GO TO 4
      HEISIG=3.316E-19
      RETURN
4     IF(XIP.GT.739.32) GO TO 5
      HEISIG=2.46E-19
      RETURN
5     WRITE(6,1000) E,XIP
1000  FORMAT(' HEISIG PROBLEMS',2F15.4)
      RETURN
      END
      REAL FUNCTION SEATON(F,FZERO,A,S)
C
C SEATON CROSS SECTION FORMULA
C
      FN=FZERO/F
      SEATON=1.0E-18*FN**(+S)*(A+(1.-A)*FN)
      RETURN
      END
      REAL FUNCTION CHAHEN(F,FZERO,A,B,S)
C
C CHAPMAN AND HENRY CROSS SECTION FORMULA
C
      FN=FZERO/F
```

```
CHAHEN=A+(B-2.*A)*FN+(1.+A-B)*FN*FN
CHAHEN=1.E-18*FN**S*CHAHEN
RETURN
END
```

PROGRAM HCMAIN

```
C
C PARAMETERS
C  DEN:TOTAL DENSITY
C   T:   TEMPERATURE
C   FJ:  COVERSION FROM FIRST TO ZEROTH  MOMENT
C                RADIATION FIELD
C                          =1 FOR UNIDIRECTIONAL  =2 FOR A
C         HEMISPHERE
C   NIT: NUMBER OF ITERATIONS IN ION FRACTIO
C        N LOOP
C   VERBOS: OUTPUT ALL CALCULATED QUATITIES
C        AT END OF NIT LOOP
C   ULTRA:  OUTPUT DITTO EVERY CYCLE
C       TERSE=.TRUE.
C   FABUND: MULTIPLY ALL ABUNDANCES Z>2 BY T
C        HIS NUMBER
C   FE: GUESS AT ELECTRON DENSITY
C   WF: DILUTION FACTOR FOR RADIATION FIELD
C   NLINE: NUMBER OF LINES IN COOLING CALCUL
C        ATION
C  WLINE: WRITE INDIVIDUAL LINE COOLING AND HEATING
C  TOL:   TOLERANCE FOR CONVERGENCE OF RNOT,DENE,EQUILIBRIUM
C         TEMPERATURE
C  EQUIM:  TRUE FOR FORCING BALANCE OF HEATING AND COOLING
C         RATES
C  CHARGX  TRUE FOR CHARGE EXCHANGE H-N, H-O CALCULATIONS
C  NELMNT: # OF ELEMENTS STARTING WITH H IN IONIZATION CA
C        LCULATION
C         USEFUL  SOMETIMES IN EQUIM FOR PRELIMINARY
C        ESTIMATE
C  DMAX:  MAX FRACTIONAL CHANGE ALLOWED IN DELTA T,
C        PREVENTS WILD OSCILLATIONS
C  DIELEC: FALSE TURNS ALL DIELECTRONIC RECOMBINATION OFF
C  NLOOP:  NUMBER OF ITERATIONS ALLOWED IN CONVERGENCE TO
C         T IF EQUIM IS ON
C  TRAD:  RADIATION TEMPERATURE OF PHOTON SOURCE
C        WFTRAD IS APPROXIMATELY A BRIGHTNESS  TEMPERATURE
C  FUDGE: TRUE FOR REDUCTION OF DIELECTRONIC RECOMBINATION
C         WITH DENSITY
C         FUDGE FACTOR CALCULATION IS DESIRED
C  THREEB:   THREE BODY RECOMBINATION
C  DXDNDT TRUE FOR COMPUTING DERIVATIVES IN N AND T
C   SERIES IS (T,N),(T*(1+-DERDEL),N)),(T,N*(1+-DERDEL))
C OUTPUT FALSE IF NO OUTPUT OF QUANTITIES TO UNIT 7
C CNOAB CHANGE OF CNO ELEMENTS FROM SOLAR VALUES
C TSERIE TRUE IF SERIES OF TEMPERATURES TO BE CALCULATED
C DSERIE TRUE FOR A DENSITY SERIES
C SERINC SERIES STARTS FROM INPUT DENSITY AND TEMPERATURE
C    AND INCREASE LOGARITHMICALLY BY 10 TO SERINC
C SERENC MAX VALUE OF N OR T
C WTNE WEIGHT GIVEN TO OLD VALUE OF ELECTRON DENSITY
C    IN CONVERGENCE OF IONIZATION EQUATIONS.
C DV FOR ESTIMATE OF EFFECTS OF OPACITY ON LINE COOLING
```

```
C TAUMAX GREATER THAN ZERO TO TURN ON CALCULATION
C
      LOGICAL VERBOS,SEMICO,ULTRA,WLINE,EQUIM,CNVG,FIRST,
     $    CHARGX
      LOGICAL VERBO,WLIN,DIELEC,FUDGE,THREEB,TERSE,NOWAST
     $    ,QUIT,DXDNDT
      LOGICAL OUTPUT,TSERIE,DSERIE,BOTHDE,FSER
      REAL SIGMA(100,76),PHOT(76),PHEAT(76)
      REAL PPHOT(76), PPHEAT(76), CPHEAT(76)
      REAL RATIO(16),REL(16),X(17,9)
      REAL TOPIN(16),TOPOUT(16)
      REAL HLCOOL(9)
      REAL LOWLIN(76)
      INTEGER INDEX(16,9)
      INTEGER IZED(9)
      REAL ABUND(9)
      REAL CHIT(76)
      REAL IP1(76),IP2(76),CS(76)
      INTEGER NUM1(76),NUM2(76)
      REAL ARAD(76),ETA(76),TMAX(76),TCRIT(76),ADI(76),
     $    TO(76),BDI(76),
     $   T1(76),RREC(76),DREC(76),UREC(76)
      REAL AREC(76),SLTE(76)
      REAL LINLOS,LRRAD,LBREMS,PHEET
      REAL AG(49),BG(49),CG(49),DG(49)
      REAL LCOOL(76),ELINE(407),FL(407)
      REAL LCLX(76)
      INTEGER IIND(407),JIND(407),IDENT(407)
      COMMON /A/ INDEX,IZED,DEN,DENE,T,TK,TKI,T4,TSQRT,
     $    VERBO,LAST
      COMMON /RECO/ RREC,DREC,UREC,ARAD,ETA,TMAX,TCRIT,
     $    ADI,TO,BDI,T1
      COMMON /CION/ IP2,NUM1,NUM2,CS,SLTE
      COMMON /COLREC/ IP1,CHIT,RNNOT
      COMMON /LINE/ LCOOL,ELINE,FL,IDENT,IIND,JIND,NLINE
      COMMON /GFACT/ AG,BG,CG,DG
      COMMON /CONTRO/ SEMICO,ULTRA
      COMMON /CFUDJ/ FUDJ,RNOT,FUDGE
      COMMON /THICK/ X,ABUND,DV,TAUMAX
      NAMELIST /PARAM/ DEN,T,FJ,NITP,VERBOS,FABUND,FE,WF,
     $    NLINE,SEMICO
     $   ,ULTRA,WLINE,TOL,EQUIM,CHARGX,NELMNT,DMAX,DIELEC
     $    ,NLOOP,TRAD
     $   ,FUDGE,THREEB,TERSE,DXDNDT,DERDEL,OUTPUT,CNOAB
     $   ,TSERIE,DSERIE,SERINC,BOTHDE,SEREND,WTNE
     $   ,DV,TAUMAX
C
C SET UP DEFAULTS
C
      REWIND 1
      REWIND 2
      ABUND(1)=1.0
      ABUND(2)=8.5E-2
      ABUND(3)=3.3E-4
      ABUND(4)=9.1E-5
      ABUND(5)=6.6E-4
```

```
      ABUND(6)=8.3E-5
      ABUND(7)=2.6E-5
      ABUND(8)=3.3E-5
      ABUND(9)=1.6E-5
      NLOOP=15
      SEMICO=.TRUE.
      ULTRA=.FALSE.
      FUDGE=.TRUE.
      THREEB=.TRUE.
      TERSE=.FALSE.
      NOWAST=.FALSE.
      TRAD=50000.
      FJ=1.
      NITP=10
      VERBOS=.TRUE.
      WLINE=.TRUE.
      FABUND=1.
      CNOAB=1.
      FE=1.002
      WTNE=1.
      WF=1.0
      WFJOLD=-1.
      NLINE=407
      EQUIM=.FALSE.
      DMAX=.25
      DIELEC=.TRUE.
      NELMNT=9
      CHARGX=.TRUE.
      TOL=1.E-03
      DXDNDT=.FALSE.
      DERDEL=.01
      OUTPUT=.TRUE.
      FSEE=.TRUE.
      X(1,1)=0.
      TAUMAX=0.
      DV=0.
C
      TSERIE=.FALSE.
      DSERIE=.FALSE.
      BOTHDE=.FALSE.
      SERINC=.1
      SEREND=0.
C READ IN DATA
C  UNIT 1 HAS PHOTOIONIZATION DATA CALCULATED BY PHOTION
C  ASSUMED TO BE OF THE FORM: FIRST MOMENT OF RADIATION
C         FIELD*QUANTITIES
C  UNIT 2 HAS THE CONSTANTS REQUIRED FOR RECOMBINATION, I
C         ONIZATION
C    AND LINECOOLING (LINES AND EXCITATION G FACTOR)
C    LOWLIN HAS LOWEST DELTA ENERGY LINES FOR IONS WITH D
C         IELECTRONIC RECOM
C
      READ (1) PHOT,PHEAT,SIGMA,FTOT
      READ (2) ARAD,ETA,TMAX,TCRIT,ADI,TO,BDI,T1
      READ (2) IP1,NUM1,IP2,NUM2
      READ (2) ELINE,FL,IDENT,IIND,JIND
```

```
      READ (2) AG,BG,CG,DG
      READ(2) LOWLIN
C
C SET UP OF INITIAL CONDITIONS FOR MULTIPLE LOOPS
C
      ITDER=0
10000 CONTINUE
      QUIT=.FALSE.
      DIFOLD=0.
      DIFF=0.
      CNVG=.FALSE.
      ICLOOP=0
      IF(ITDER.EQ.5) DEN=DEN/(1.-DERDEL)
      IF(DXDNDT.AND.ITDER.LE.4) GO TO 10100
      ITDER=0
      IF(TSERIE.OR.DSERIE) GO TO 3001
      READ (5,PARAM,END=10001)
      LAST=INDEX(IZED(NELMNT),NELMNT)
      IF(EQUIM) DXDNDT=.FALSE.
      IF(DXDNDT) EQUIM=.FALSE.
      IF(.NOT.EQUIM) CNVG=.TRUE.
      IF (ULTRA) VERBOS=.TRUE.
      IF(TERSE)VERBOS=.FALSE.
      IF(VERBOS) WLINE=.TRUE.
      IF(TERSE) WLINE=.FALSE.
      IF(NITP.LT.2) NITP=2
      IF(X(1,1).NE.0.) GO TO 2004
      X(1,1)=0.
      X(2,1)=0.
      X(1,4)=0.
      X(2,4)=0.
      X(1,5)=0.
      X(2,5)=0.
      BUO=0.
      BDO=0.
      BUN=0.
      BDN=0.
C
C TEMPERATURE OR DENSITY SERIES LOGIC
C
2004  IF(TSERIE.OR.DSERIE) SERINC=10.**SERINC
      IF(.NOT.(TSERIE.OR.DSERIE)) GO TO 3004
      IF(.NOT.BOTHDE) GO TO 3002
      EQUIM=.FALSE.
      DXDNDT=.TRUE.
      OUTPUT=.TRUE.
3001  IF(.NOT.BOTHDE) GO TO 3002
      EQUIM=.NOT.EQUIM
      DXDNDT=.NOT.DXDNDT
      OUTPUT=.NOT.OUTPUT
3002  IF(DXDNDT.AND.ITDER.NE.0) GO TO 3004
      IF(DSERIE) GO TO 3003
      IF(.NOT.TSERIE) GO TO 3004
      IF(.NOT.FSER.AND.(.NOT.BOTHDE.OR.EQUIM)) T=T*SERINC
      IF(T.GT.SEREND) GO TO 10001
      GO TO 3004
```

```
3003  CONTINUE
      IF(.NOT.FSER.AND.(.NOT.BOTHDE.OR.EQUIM)) DEN=DEN*
     $     SERINC
      IF(DEN.GT.SEREND) GO TO 10001
3004  CONTINUE
      IF(EQUIM) GO TO 10101
10100 CONTINUE
      IF(.NOT.DXDNDT) GO TO 10101
C
C DERIVATIVE CALCULATION LOGIC
C
      ITDER=ITDER+1
      IF(ITDER.EQ.1) GO TO 10101
      IF(ITDER.EQ.2) T=T*(1.+DERDEL)
      IF(ITDER.EQ.3) T=T*(1.-DERDEL)/(1.+DERDEL)
      IF(ITDER.EQ.4) GO TO 10111
      IF(ITDER.EQ.5) DEN=DEN*(1.-DERDEL)/(1.+DERDEL)
      GO TO 10101
10111 T=T/(1.-DERDEL)
      DEN=DEN*(1.+DERDEL)
10101 CONTINUE
      IF(EQUIM) NIT=MIN0(5,NITP)
      IF(.NOT.EQUIM) NIT=NITP
      FIRST=.TRUE.
      TOLD=0.
      IF (.NOT.TERSE.OR..NOT.NOWAST) WRITE(6,1008)
1008  FORMAT('1')
      IF (.NOT.TERSE.OR..NOT.NOWAST) WRITE (6,PARAM)
C
C  SET UP TEMPERATURE, DENSITY, ABUNDANCES, FLUX FACTOR
C
      DENE=DEN*FE
      DEOLD=DENE
      IF(.NOT.FSER) GO TO 2005
      SUM=0.
C
C CALCULATION OF ABUNDANCES
C
      DO 101 IEL=1,NELMNT
      IF (IEL.GT.2) ABUND(IEL)=FABUND*ABUND(IEL)
      IF((IEL.GE.3).AND.(IEL.LE.5)) ABUND(IEL)=CNOAB*
     $     ABUND(IEL)
      SUM=SUM+ABUND(IEL)
101   CONTINUE
      DO 102 IEL=1,NELMNT
      ABUND(IEL)=ABUND(IEL)/SUM
102   CONTINUE
      FABUND=1.
      CNOAB=1.
      IF(.NOT.TERSE.OR..NOT.NOWAST) WRITE(6,1002)FABUND,
     $     NELMNT,ABUND
1002  FORMAT(' RELATIVE ABUNDANCES WITH FABUND=',F6.3,
     $    5X,'NELMNT=',I3,/1X,9E13.3)
C
C RADIATION DILUTION APPLIED
C
```

```
      WFJ=WF*FJ
      WFTRAD=WFJ*TRAD
      IF (WFJ.EQ.WFJOLD) GO TO 20001
      WFJOLD=WFJ
      WMJ=WFJ*12.56637
C
C  ADJUSTMENT TO FLUX MADE INCLUDING A 4*PI MULTIPLICATION
C
      PFTOT=FTOT*WF
      DO 103 IJ=1,76
      PPHOT (IJ)=PHOT(IJ)*WMJ
      PPHEAT(IJ)=PHEAT(IJ)*WMJ
103   CONTINUE
      FSER=.FALSE.
20001 ICLOOP=ICLOOP+1
      IF(ICLOOP.GT.NLOOP) GO TO 30000
2005  VERBO=VERBOS.AND.(CNVG.OR..NOT.EQUIM)
      WLIN=WLINE.AND.(CNVG.OR..NOT.EQUIM)
      TK=T/11604.8
      TKI=1./TK
      T4=T*1.E-4
      ETHREE=0.0
      TM45=T**(-4.5)
      TSQRT=SQRT(T)
      IF(.NOT.FIRST.AND.EQUIM) NIT=MINO(3,NITP)
122   IF(.NOT.CHARGX) GO TO 10004
      CALL CHGEX(BUO,BDO,BUN,BDN,T)
C
C  CHARGE EXCHANGE CALCULATION FOR NITROGEN AND OXYGEN
C  U IS UPRATE FOR I TO II OF N AND O
C  D IS DOWNRATE
C
      IF((X(1,1).NE.1.E-07).OR.(X(1,1).NE.0.)) GO TO 10004
      X(1,1)=1.E-07
      X(2,1)=1.
      X(1,5)=0.5
      X(2,5)=X(1,5)
      X(1,4)=0.5
      X(2,4)=X(1,4)
10004 DO 1 IT=1,NIT
      DO 2 I=1,NELMNT
      II=IZED(I)
      ZED=II
      RNUCLD=1.E4
      IF (WFTRAD.LE.0.) GO TO 45
C
C THIS IS A CALCULATION OF LOWEST LEVEL IN EQUILIBRIUM WITH
C CONTINUUM DUE TO RADIATION FIELD
C
      RNUOLD=2.72
      NNIT=0
44    RNOTNU=ZED*SQRT(3.*ALOG(RNUOLD)*157802./WFTRAD)
      NNIT=NNIT+1
      DIFN=RNOTNU-RNUOLD
      RNUOLD=RNOTNU-DIFN/(1.-.5/ALOG(RNOTNU))
      IF (RNUOLD.LE.1.) RNUOLD=2.
```

```
      IF(NNIT.GT.4) GO TO 45
      IF(ABS(DIFN/RNOTNU).GT.TOL) GO TO 44
45    II1=II+1
      IZ=II
      DO 3 J=1,II
      IJ=INDEX(J,I)
      CALL LEVEL(J,I)
      RNOT=AMIN1(RNNOT,RNUOLD,2.)+.5
      IF(I.EQ.1) RNNOTH=RNOT
      CALL CCLION(J,I)
      CALL REC(J,I)
      IF(ULTRA.OR.((IT.EQ.NIT.OR.QUIT).AND.VERBO))WRITE (
     $     6,1029)RNOT,
     $  RNNOT,RNUOLD,FUDJ
1029  FORMAT (' RNOT,RNNOT,RNUOLD,FUDGE FACTOR',2F20.1,
     $     2E15.3)
      RNNOT=RNOT
      DREC(IJ)=DREC(IJ)*FUDJ
      IF(.NOT.DIELEC) DREC(IJ)=0.0
C
C THREE BODY RECOMBINATION FROM SUMMERS AND BURGESS
C  WITH A DIFFERENT Z DEPENDENCE
C
      IF(.NOT.THREEB) GO TO 46
      RTHREE=1.16E-08*(J**3)*TM45*DENE
      IF(RREC(IJ).EQ.0.0) RTHREE=0.0
46    AREC(IJ)=RREC(IJ)+DREC(IJ)+UREC(IJ)+RTHREE
C
C    REC(J,I) IS RECOMBINATION RATE INTO J FROM J+1
C    CCL(J,I) IS COLLISION RATE OUT OF J TO J+1
C
      IF(ULTRA.OR.((IT.EQ.NIT.OR.QUIT).AND.VERBO)) WRITE(
     $     6,1001)
     $    II,J,CS(IJ),SLTE(IJ),PPHOT(IJ)
1001  FORMAT(' COLLISIONS, UPPER LEVELS, PHOTO IONIZATION '
     $       ,'RATE',
     $  ' ION  (Z,N)',2I3,3E15.4)
      IF(ULTRA.OR.((IT.EQ.NIT.OR.QUIT).AND.VERBO)) WRITE(
     $     6,1000)
     $     II,J,RREC(IJ),DREC(IJ),UREC(IJ)
1000  FORMAT(' RADIATIVE, DIELECTRONIC, UPPER LEVELS, REC'
     $     'OMBINATION ',
     $    'RATE', 2I3, 3E15.4)
C
C  TOPOUT(J) IS RATE J TO J+1
C  TOPIN(J) IS RATE J+1 TO J
C
3     CONTINUE
      IJJ=INDEX(1,I)
      TOPOUT(1)=PPHOT(IJJ)+(CS(IJJ)+SLTE(IJJ))*DENE
      IF(I.EQ.1) TOPOUT(1)=TOPOUT(1)+BDO*X(2,5)*ABUND(5)
     $         +BDN*X(2,4)*ABUND(4)
      IF(I.EQ.4) TOPOUT(1)=TOPOUT(1)+BUN*X(2,1)/ABUND(4)
      IF(I.EQ.5) TOPOUT(1)=TOPOUT(1)+BUO*X(2,1)/ABUND(5)
      TOPIN(1)=AREC(IJJ)*DENE
      IF(I.EQ.1) TOPIN(1)=TOPIN(1)+BUO*X(1,5)*ABUND(5)
```

```
     $        +BDN*X(2,4)*ABUND(4)
      IF(I.EQ.4)  TOPIN(1)=TOPIN(1)+EDO*X(1,1)/ABUND(4)
      IF(I.EQ.5)  TOPIN(1)=TOPIN(1)+BDN*X(1,1)/ABUND(5)
      IF (AREC(IJJ).EQ.0.0) GO TO 24
      RATIO(1)=TOPOUT(1)/TOPIN(1)
      GO TO 25
24    RATIO(1)=1.0
25    REL(1)=RATIO(1)
      IF(I.EQ.1) GO TO 8
      DO 4 JJ=2,IZ
      IJ=INDEX(JJ,I)
      TOPOUT(JJ)=PPHOT(IJ)+(CS(IJ)+SLTE(IJ))*DENE
      TOPIN(JJ)=AREC(IJ)*DENE
      IF (TOPIN(JJ).EQ.0.0) GO TO 5
      RATIO(JJ)=TOPOUT(JJ)/TOPIN(JJ)
      GO TO 4
5     RATIO(JJ)=1.0
4     CONTINUE
C
C RATIO(J) IS POPULATION LEVEL J+1 / LEVEL J
C REL(J) IS POPULATION RELATIVE TO LEVEL 1
C REL (1) IS POP LEVEL 2 / POP LEVEL 1
C
      DO 6 JJ=2,II
      REL(JJ)=RATIO(JJ)*REL(JJ-1)
6     CONTINUE
8     SUM=1.0
      IF (AREC(INDEX(1,I)).EQ.0.0) SUM=0.0
      IF(I.EQ.1) GO TO 31
C
C IF RATE INTO LEVEL FROM TOP IS 0 SET POPULATION TO 0.
C
      DO 7 JJ=2,II
      IF (AREC(INDEX(JJ,I)).EQ.0.0) REL(JJ-1)=0.0
      SUM=SUM+REL(JJ-1)
7     CONTINUE
      IF (AREC(INDEX(II,I)).EQ.0.) REL(II)=0.
31    SUM=SUM+REL(II)
      FNORM=1./SUM
C
C X(J,I) IS RELATIVE POP OF IONIZATION LEVEL J IN ATOM I,
C    SUM WITH I CONSTANT IS 1
C
      DO 9 J=1,II
      IF(AREC(INDEX(J,I)).GT.0.0) GO TO 16
      X(J,I)=0.0
9     CONTINUE
16    NB=J
      NB1=NB+1
      X(NB,I)=FNORM
      DO 17 J=NB1,II1
      X(J,I)=REL(J-1)*FNORM
17    CONTINUE
2     CONTINUE
C
C ELECTRON DENSITY CALCULATION
```

```
C
      DENE=0.
      DO 21 I=1,NELMNT
      II1=IZED(I)+1
      DO 22 J=2,II1
      DENE=DENE+X(J,I)*(J-1)*ABUND(I)
22    CONTINUE
21    CONTINUE
      DENE=DENE*DEN*WTNE+(1.-WTNE)*DEOLD
      FE=DENE/DEN
      WRITE (6,1010) DENE
1010  FORMAT(' NEW ELECTRON DENSITY IS',E16.7)
      IF(TERSE) GO TO 113
      DO 20 I=1,NELMNT
      II=IZED(I)
      IZ1=II+1
      IF(ULTRA.OR.((IT.EQ.NIT.OR.QUIT).AND.CNVG)) WRITE (
     $    6,1005) II
1005  FORMAT(' RELATIVE ABUNDANCES FOR ELEMENT Z=',I3)
      IF(ULTRA.OR.((IT.EQ.NIT.OR.QUIT).AND.CNVG)) WRITE(6
     $    ,1004)
     $    (J,X(J,I),J=1,IZ1)
20    CONTINUE
1004  FORMAT(1X,5(I5,E15.5))
113   IF(QUIT) GO TO 111
C
C CHECKING FOR CONVERGENCE OF ELECTRON DENSITY
C   CONVERGENCE SEEMS TO BE SLOW WITH THIS METHOD
C
      IF(ABS(DEOLD-DENE)/DENE.LT.TOL) QUIT=.TRUE.
      DEOLD=DENE
1     CONTINUE
111   CONTINUE
C
C NOTE THAT THERE IS NO LINE COOLING OF BARE IONS
C
      IF (TOLD.EQ.T) GO TO 23
      CALL LINCOL
C
C LINE COOLING CALCULATED ONLY IF TEMPERATURE HAS CHANGED
C
      IF(.NOT.EQUIM) TOLD=T
23    CONTINUE
C
C  HYDROGEN LINE COOLING LOSSES
C  DONE AS ACCURATELY AS POSSIBLE SINCE COOLING IN 1E4
C         3E4 TEMPERATURE
C  RANGE IS CRUCIAL
C
      LCOOL(1)=0.
      RNNOT=RNNOTH
      CALL HLINE(HLCOOL,1)
C         THE 1 REFERS TO LOWER LEVEL FOR TRANSITIONS
      DO 30 N=1,9
      LCOOL(1)=LCOOL(1)+HLCOOL(N)
      HLCOOL(N)=HLCOOL(N)*X(1,1)*ABUND(1)*DENE/DEN
```

```
30    CONTINUE
      IF(WLIN.AND.CNVG) WRITE(6,1011) HLCOOL
1011  FORMAT(' HYDROGEN LINE LOSSES ARE:'/1X,9E14.4)
      LINLOS=0.
      LRRAD=0.
      PHEET=0.
      DO 10 I=1,NELMNT
      II=IZED(I)
      DO 10 J=1,II
      IJ=INDEX(J,I)
C
C  ADJUSTMENT OF RECOMBINATION RATE TO ENERGY RECOMBINATION
C        ON RATE
C  USING FACTORS GIVEN BY SEATON FOR HYDROGEN
C
      UL=IP1(IJ)*TKI
      ULL2=.5*ALOG(UL)
      UL3=UL**(-.3333333)
      ABFACT=(-0.0713+ULL2+0.640*UL3)/(0.4288+ULL2+.469*
     $    UL3)
      RRCOOL=RREC(IJ)*(IP1(IJ)+TK)*ABFACT
C
C  DIELECTRONIC COOLING ASSUMES LOWEST ENERGY TRANSITION
C        IS
C    DOMINANT STABILIZING TRANSITION
C
      RDCOOL=DREC(IJ)*(IP1(IJ)+LOWLIN(IJ))
      LRRAD=LRRAD+(RRCOOL+RDCOOL)*X(J+1,I)*ABUND(I)
      LCLX(IJ)=X(J,I)*LCOOL(IJ)*ABUND(I)*FE
      LINLOS=LINLOS+LCLX(IJ)
      CPHEAT(IJ)=PPHEAT(IJ)*X(J,I)*ABUND(I)
      PHEET=PHEET+CPHEAT(IJ)
10    CONTINUE
C
C ALL ENERGY RATES ARE IN ERG CM+3 S-1
C   HEATING IS IN ERG S-1
C
      LBREMS=2.29E-27*SQRT(T)*ABUND(1)*FE
      LRRAD=LRRAD*FE*1.602192E-12
      COOL=LBREMS+LRRAD+LINLOS
      PHEETD=PHEET/DEN
      IF(.NOT.EQUIM) GO TO 38
      IF(.NOT.TERSE)WRITE (6,1021) PHEETD,COOL,T
1021  FORMAT(' HEATING, COOLING RATES CM+3 S-1',2E15.5,
     $    5X,'AT TEMPERATURE',E15.5)
      DIFCLD=DIFF
      IF(PHEETD.GT.1.0E6*COOL) DIFCLD=0.
      IF(PHEETD.LT.1.0E-6*COOL) DIFOLD=0.
      DIFF=COOL-PHEETD
      IF(CNVG) GO TO 20002
C
C RADIATIVE EQUILIBRIUM TEMPERATURE CALCULATION
C
      IF(.NOT.FIRST) GO TO 20000
      TOLD=T
      T=T*1.01
```

```
      FIRST=.FALSE.
      GO TO 20001
20000 DERIV=(DIFF-DIFOLD)/(T-TOLD)
      IF(DERIV.EQ.0.) GO TO 20002
      DELT=-DIFF/DERIV
      IF(.NOT.TERSE) WRITE(6,1022) T,DELT
1022  FORMAT(' T, DELTA T (DELT)',2E15.5)
      IF (ABS(DELT/T).GT.DMAX) GO TO 20003
      IF(ABS(DELT/T).LT.TOL) CNVG=.TRUE.
      TOLD=T
      T=T+DELT
      GO TO 20001
20003 TOLD=T
      T=T+DMAX*DELT/ABS(DELT)*T
      GO TO 20001
20002 CONTINUE
38    IF (.NOT.WLIN) GO TO 11
C
C PRINTED OUTPUT OF DETAILS OF HEATING AND COOLING RATES
C
      DO 12 I=1,NELMNT
      IZ=IZED(I)
      IJB=INDEX(1,I)
      IJE=IJB+IZ-1
      WRITE (6,1009)IZ
1009  FORMAT (' LINE COOLING LOSSES FOR ATOM OF Z',I3)
      WRITE(6,1003) (LCLX(IJ),IJ=IJB,IJE)
1003  FORMAT(1X,8E15.3)
12    CONTINUE
      IF(WFJ.LE.0.0.OR..NOT.WLIN) GO TO 11
      DO 13 I=1,NELMNT
      IZ=IZED(I)
      IJB=INDEX(1,I)
      IJE=IJB+IZ-1
      WRITE (6,1019)IZ
1019  FORMAT(' PHOTOIONIZATION HEATING RATES FOR ATOM Z='
     $    ,I3)
      WRITE(6,1003) (CPHEAT(IJ),IJ=IJB,IJE)
13    CONTINUE
C
C     INTERNAL ENERGY AND ENTHALPY IN UNITS OF ERG PER
C         CUBIC CM
C
11    EINT=0.
      DO 14 I=1,NELMNT
      IZ=IZED(I)
      DO 14 J=1,IZ
      IJ=INDEX(J,I)
      EINT=EINT+IP1(IJ)*X(J+1,I)*ABUND(I)
14    CONTINUE
      EINT=(EINT*DEN+1.5*TK*(DEN+DENE))*1.602192E-12/DEN
      ENTHAL=EINT+(DEN+DENE)*TK*1.602192E-12/DEN
      CEINT=EINT/(TK*1.602192E-12)
      CENTHP=ENTHAL/(TK*1.602192E-12)
C
C OUTPUT CALCULATED QUANTITIES
```

```
C
      IF(OUTPUT)WRITE(7)  DEN,T,WF,FJ,PHEET,COOL,LBREMS,
     $    LRRAD,LINLOS,
     $      EINT,ENTHAL,DENE,ABUND,X,LCLX,CPHEAT,PFTOT
      IF(EQUIM)  WRITE  (6,1051)  ICLOOP
1051  FORMAT  ('  NUMBER OF LOOPS TO CONVERGENCE',I4)
      WRITE(6,1006)  DEN,T,WFJ,PHEETD,COOL,LBREMS,LRRAD,
     $    LINLOS,
     $      EINT,ENTHAL,CEINT,CENTHE,DENE
1006  FORMAT  ('- PARAMETERS WERE: DENSITY, TEMPERATURE, '
     $,'DILUTION FACTOR',3E15.5/
     $  ' TOTAL HEATING/DENSITY AND COOLING RATE',2E15.5/
     $  ' THE COOLING RATES FOR BREMSSTRAHLUNG,  ',
     $ 'RECOMBINATION RADIATION, AND LINE LOSSES',3E15.5/
     $  ' INTERNAL ENERGY,ENTHALPY',2E15.5,5X,'AND COEFFI'
     $    ,'CIENTS',2E15.7/
     $  ' ELECTRON DENSITY',E15.5)
      IF(.NOT.TERSE)WRITE(6,PARAM)
      NOWAST=.TRUE.
      GO TO 10000
30000 WRITE (6,1049)  NLOOP
1049  FORMAT('  SORRY BUT MAX NUMBER OF TEMPERATURE LOOPS '
     $    ,'EXCEEDED',I3)
      GO TO 10000
10001 STOP
      END
```

PROGRAM SUBCHEAT

```
      SUBROUTINE CHGEX(BUO,BDO,BUN,BDN,T)
C
C CHARGE EXCHANGE TAKEN FROM:
C  O FIELD AND STEIGMAN
C  N STEIGMAN, WERNER, AND GELDON
C
C BUO IS BETA FOR OI TO OII  THAT IS UP
      FI(X)=ERF(SQRT(X))-1.12838*EXP(-X)*SQRT(X)
      XAC=6.034/T
      XAD=732.8/T
      XC=0.812336/T
      XD=98.64/T
      BDO=1.97E-09*(.386415*FI(XAC)+0.5*(FI(XAD)-FI(XAC))
     $     +0.529412*(1.-
     $        FI(XAD)))+2.11E-09*((0.115385*EXP(-XC)*
     $     FI(XAC-XC)+
     $        0.0294118*EXP(-XD)*FI(XAD-XD)))
      BUO=EXP(-227.45/T)*(1.97E-09-BDO)
      BUN=1.97E-09*(EXP(-11031.5/T)*.333333+EXP(-11102.3/
     $     T)*.333333+
     $       EXP(-11220.7/T)*.151515)
      BDN=1.97E-09-EXP(11031.5/T)*BUN
      RETURN
      END
      BLOCK DATA
      COMMON /A/ INDEX,IZED,DEN,DENE,T,TK,TKI,T4,TSQRT,
     $    VERBOS,LAST
      INTEGER IZED(9)
      DATA IZED /1,2,6,7,8,10,12,14,16/
      DIMENSION INDEX(16,9)
      DATA INDEX /1,15*0,2,3,14*0,4,5,6,7,8,9,10*0,
     $ 10,11,12,13,14,15,16,9*0,
     $ 17,18,19,20,21,22,23,24,8*0,
     $ 25,26,27,28,29,30,31,32,33,34,6*0,
     $ 35,36,37,38,39,40,41,42,43,44,45,46,4*0,
     $ 47,48,49,50,51,52,53,54,55,56,57,58,59,60,2*0,
     $ 61,62,63,64,65,66,67,68,69,70,71,72,73,74,75,76/
      END
      SUBROUTINE COLION(J,I)
C
C ROUTINE FOR CALCULATION OF COLLISIONAL
C IONIZATION RATES FOR ALL ELEMENTS BUT
C HYDROGEN
C
      DIMENSION INDEX(16,9) ,IZED(9)
      REAL IP1(76),IP2(76)
      DIMENSION  NUM1(76),NUM2(76),CS(76),SLTE(76)
      REAL CHIT(76)
      LOGICAL VERBOS ,SEMICO,ULTRA
      COMMON /A/ INDEX,IZED,DEN,DENE,T,TK,TKI,T4,TSQRT,
     $    VERBOS,LAST
      COMMON /CION/ IP2,NUM1,NUM2,CS,SLTE
      COMMON /COLREC/ IP1,CHIT,RNNOT
```

```
      COMMON /CONTRO/ SEMICO,ULTRA
      IJ=INDEX(J,I)
      IF(J.NE.IZED(I)) GO TO 199
3     IF(.NOT.SEMICO) RNC=1.0E06
101   CS(IJ)=COLH(RNNOT,IP1(IJ),1)
      SLTE(IJ)=0.
      RETURN
C
C  CORRECTION FACTOR FROM P 205 MCWHIRTER,R.W.P., IN ATOM
C        IC AND
C  MOLECULAR PROCESSES IN ASTROPHYSICS, ED BY MCE HUBBARD
C         AND H
C  NUSSBAUMER, GENEVA OBSERVATORY, SAUVERNY, SWITZERLAND,
C         1975.
C
199   CS(IJ)=NUM1(IJ)* EXP(-IP1(IJ)*TKI)/(IP1(IJ)*IP1(IJ))
     $      /(4.88+TK/IP1(IJ))
      IF(NUM2(IJ).LE.0) GO TO 200
      CS(IJ)=CS(IJ)+NUM2(IJ)*EXP(-IP2(IJ)*TKI)/(IP2(IJ)*
     $  IP2(IJ)) /(4.88+TK/IP2(IJ))
200   CS(IJ)=8.35E-08*TSQRT*CS(IJ)
C     CHIT(IJ)=(2.8E-28*IP1(IJ)*DENE*DENE*TKI)**.142857143
      CHIT(IJ)=IP1(IJ)/(RNNOT*RNNOT)
      SLTE(IJ)=4.8E-06*CHIT(IJ)/(IP1(IJ)*IP1(IJ)*TSQRT)*
     $    EXP(-IP1(IJ)
     $          *TKI)
      IF(.NOT.SEMICO) SLTE(IJ)=0.
      RETURN
C
C CHIT IS ESTIMATE OF IONIZATION POTENTIAL OF LOWEST LEVEL
C        IN EQ'M WITH CONT'M
C SLTE FROM WILSON
C
      END
      FUNCTION COLH(RNO,XIP,N)
C
C COLLISIONAL IONIZATION RATE FOR HYDROGEN
C
      DIMENSION INDEX(16,9)
      DIMENSION IZED(9)
      LOGICAL VERBOS
      COMMON /A/ INDEX,IZED,DEN,DENE,T,TK,TKI,T4,TSQRT,
     $   VERBOS,LAST
      X0=1.-1./(RNO*RNO)
      X02=1./(X0*X0)
      X03=X02/X0
      RN=FLOAT(N)
      RN2=RN*RN
      EPKT=XIP*TKI/RN2
      Y=X0*EPKT
C  FOR OPTICALLY  THICK CALCULATIONS CAN USE N OTHER THAN 1
      IF (N.EQ.1) GO TO 2
      A=1.9602805*RN*X03*(.3595-0.05798/X0+5.894E-03*X02)
      B=.6666667*RN2/X0*(3.+2./X0+.1169*X02)
      Z=X0*(0.653+EPKT)
      GO TO 4
```

```
2       A=1.9602805*X03*(.37767-0.1015/X0+0.014028*X02)
        B=.6666667/X0*(3.+2./X0-0.603*X02)
        Z=X0*(0.45+EPKT)
4       IF(Z.GE.170.) GO TO 3
        COLH=1.093055E-10*RN2/X0*TSQRT*Y*Y*
       $  (A*(EONE(Y,IY)/Y-EONE(Z,INZ)/Z) +
       $  (B-A*ALOG(2.*RN2/X0))*(ZETA(Y)-ZETA(Z)))
        COLH=COLH*(13.598/XIP)**2
        IF(IY.EQ.0.OR.INZ.EQ.0) GO TO 1
        RETURN
1       WRITE(6,1000) Y,Z,IY,INZ
1000    FORMAT(' ****** ERROR IN EONE',4E15.4)
        RETURN
3       COLH=0.
        RETURN
C
C JOHNSON'S COLLISIONAL IONIZATION FORMULA
C CURRENTLY ONLY FOR IONIZATION FROM LEVELS 1 AND 2
C
        END
        FUNCTION ZETA(T)
C
C LITTLE FUNCTION REQUIRED BY COLE
C
        EF=EXP(-T)
        E0=EF/T
        E1=EONE(T,IND)
        IF(IND.EQ.0) WRITE (6,100) T
100     FORMAT(' ***** ZETA EONE ERROR',E15.4)
        E2=EF-T*E1
        ZETA=E0-2.*E1+E2
        RETURN
        END
        SUBROUTINE REC(J,I)
C
C CALCULATION OF RECOMBINATION RATES FOR
C ALL ELEMENTS BUT HYDROGEN
C USES ALDROVANDI AND PEQUIGNOT TABLE
C
        DIMENSION INDEX(16,9)
        DIMENSION IZED(9)
        REAL ARAD(76),ETA(76),TMAX(76),TCRIT(76),ADI(76),
       $    T0(76),BDI(76),
       $  T1(76),RREC(76),DREC(76)
        REAL CHIT(76),UREC(76),IP1(76)
        LOGICAL VERBOS ,ULTRA,SEMICO,FUDGE
        COMMON /A/ INDEX,IZED,DEN,DENE,T,TK,TKI,T4,TSQRT,
       $   VERBOS,LAST
        COMMON /RECO/ RREC,DREC,UREC,ARAD,ETA,TMAX,TCRIT,AD
       $    I,T0,BDI,T1
        COMMON /COLREC/ IP1,CHIT,RNNOT
        COMMON /CONTRO/ SEMICO,ULTRA
        COMMON /CFUDJ/ FUDJ,RNOT,FUDGE
        IJ=INDEX(J,I)
        FUDJ=1.
        IF(J.NE.IZED(I)) GO TO 199
```

```
      IF(IP1(IJ)*TKI.GT.170.) GO TO 200
101   DREC(IJ)=0.
      RREC(IJ)=0.0
      Z=FLOAT(J)
      NNOT=RNOT
      NTOP=MINO(9,NNOT)
      DO 111 N=1,NTOP
C  CAN CHANGE DO LOOP RANGE TO 2,9 FOR OPTICALLY THICK TO
C          LYMAN ALPHA
      RREC(IJ)=RREC(IJ)+Z*RHII(IP1(IJ),N)
111   CONTINUE
      IF (NTOP.EQ.9)  GO TO 112
      RREC(IJ)=RREC(IJ)+(RNOT-FLOAT(NTOP))*Z*RHII(IP1(IJ)
     $    ,NTOP+1)
112   CONTINUE
      UREC(IJ)=0.0
      RETURN
C
C FACTOR OF 3 IS TO MAKE UP FOR TENDENCY OF TMAX QUOTED TO
C BE MUCH TO LOW
C
199   IF(T.GT.3.*TMAX(IJ)) GO TO 200
      IF(T.LT.TMAX(IJ)/2000.) GO TO 200
      RREC(IJ)=ARAD(IJ)*T4**(-ETA(IJ))
      UREC(IJ)=1.8E-14*IP1(IJ)*TK**(-1.5)*CHIT(IJ)
      IF(.NOT.SEMICO) UREC(IJ)=0.
      GO TO 299
200   RREC(IJ)=0.0
      DREC(IJ)=0.0
      UREC(IJ)=0.0
      RETURN
299   IF(T.LT.TCRIT(IJ)/10.) GO TO 300
C
C FACTOR OF 10 AN ATTEMPT TO MAKE TRANSITION SMOOTHER
C
      DREC(IJ)=ADI(IJ)*T**(-1.5)*EXP(-T0(IJ)/T)*(1.+BDI(IJ)
     $    *EXP(-T1(IJ)/
     $   T))
      IF(.NOT.FUDGE) RETURN
      ARG=12.55-7.*ALOG10(RNOT)
      IF(ARG.LE.0.) ARG=0.
      DELA=.01458333*ARG*ARG+0.09166667*ARG
      FUDJ=10.**(-DELA)
      RETURN
300   DREC(IJ)=0.0
C
C ALL BUT HYDROGEN FROM FORMULAE OF ALDROVANI AND PEQUINO
C         T IN AA
C H LIKE FROM JOHNSON
C
      RETURN
      END
      REAL FUNCTION RHII(XIP,N)
C
C RECOMBINATION TO HYDROGEN
C
```

```
      DIMENSION INDEX(16,9)
      DIMENSION IZED(9)
      LOGICAL VERBOS
      REAL IP1(76),CHIT(76)
      COMMON /A/ INDEX,IZED,DEN,DENE,T,TK,TKI,T4,TSQRT,
     $   VERBOS,LAST
      COMMON /COLREC/ IP1,CHIT,RNNOT
      COMMON /CFUDJ/ FUDJ,RNOT,FUDGE
      NNOT=RNNOT
      X0=1.-1./(RNOT*RNOT)
      X02=1./(X0*X0)
      FIN=1./N
      FIN2=FIN*FIN
      XIN=XIP*FIN2*TKI
      XTIN=X0*XIN
      X2=XTIN*XTIN
C
C ABRAMOWITZ AND STEGUN EXPRESSION FOR EXP(X) EONE(X)
C  NOTE THAT X=X0*IPN/KT, AND NEED TO MAKE CORRECTION TO
C    EXTERIOR EXP(IPN/KT)
C
      IF(XTIN.LE.10.0) GO TO 4
      EXE1=(X2+4.03640*XTIN+1.15198)/(X2+5.03637*XTIN+
     $    4.19160)/XTIN
      GO TO 5
4     EXE1=EXP(XTIN)*EONE(XTIN,INX)
      IF(INX.EQ.0) WRITE (6,1000) XTIN
1000  FORMAT('  *******EONE ERROR IN RHII*****',E15.6)
5     EXE2=1.-XTIN*EXE1
      EXE3=0.5*(1.-XTIN*EXE2)
      IF(N.GT.2) GO TO 3
      IF(N.EQ.2) GO TO 2
      G0=1.133
      G1=-0.4059
      G2=.07014
      GO TO 1
2     G0=1.0785
      G1=-0.2319
      G2=0.02947
      GO TO 1
3     G0=0.9935+0.2328*FIN-0.2196*FIN2
      G1=-FIN*(0.6282-0.5598*FIN+0.5299*FIN2)
      G2=FIN2*(0.3887-1.181*FIN+1.470*FIN2)
1     RHII=5.197E-14*XIN**1.5*EXP(XIN/(RNOT*RNOT))*
     $  (G0*EXE1+G1*EXE2/X0+G2*EXE3*X02)
C  MULTIPLY ANSWER BY Z OF ION
      RETURN
      END
      REAL FUNCTION GFN(II,IJ,IZ,Y)
C
C GAUNT FACTOR CALCULATION
C USES MEWE AND KATO DATA
C AND MEWE APPROX FOR EXP(Y)EONE(Y)
C
      DIMENSION A(49),B(49),C(49),D(49)
      DIMENSION INDEX(16,9)
```

```
      DIMENSION IZED(9)
      LOGICAL VERBOS
      REAL IP1(76),CHIT(76)
      COMMON /A/ INDEX,IZED,DEN,DENE,T,TK,TKI,T4,TSQRT,
     $   VERBOS,LAST
      COMMON /GFACT/ A,B,C,D
      COMMON /COLREC/ IP1,CHIT,RNNOT
      X=1./(IZ-3.0001)
      IF (ID.GT.28) GO TO 1
      IF (ID.EQ.20) GO TO 100
      IF (ID.EQ.22) GO TO 103
      IF (ID.EQ.21) GO TO 104
      IF (ID.EQ.23) GO TO 101
      IF (ID.EQ.28) GO TO 102
1     GFN=A(ID)+(B(ID)*Y-C(ID)*Y*Y+D(ID))*(ALOG((Y+1.)/Y)
     $        -0.4/((Y+1.)*(Y+1.)))+C(ID)*Y
      RETURN
C
C ALL A LA MEWE
C WITH ADDITIONS DUE TO KATO
C
100   A(ID)=0.7*(1.-.5*X)
      B(ID)=1.-0.8*X
      C(ID)=-0.5*(1.-X)
      GO TO 1
101   A(ID)=0.11*(1.+3.*X)
      GO TO 1
102   A(ID)=0.35*(1.+2.7*X)
      B(ID)=-0.11*(1.+5.4*X)
      GO TO 1
103   A(ID)=-0.16*(1.+2.*X)
      B(ID)=0.8*(1.0-0.7*X)
      GO TO 1
104   A(ID)=-0.32*(1.-0.9*X)
      B(ID)=0.88*(1.-1.7*X)
      C(ID)=0.27*(1.-2.1*X)
      GO TO 1
      END
      SUBROUTINE LINCOL
C
C LINE COOLING
C WITH MODIFICATIONS FOR FINITE OPACITY
C USES LINE LIST FROM MORTON
C AND MORTON AND HAYDEN SMITH
C
      REAL LCOOL(76),ELINE(407),F(407)
      INTEGER IIND(407),JIND(407),IDENT(407)
      DIMENSION INDEX(16,9)
      DIMENSION IZED(9)
      INTEGER IR(16) /1,2,3*0,3,4,5,0,6,0,7,0,8,0,9/
      REAL X(17,9),ABUND(9)
      COMMON /THICK/ X,ABUND,DV,TAUMAX
      COMMON /LINE/LCOOL,ELINE,F,IDENT,IIND,JIND,NLINE
      COMMON /A/ INDEX,IZED,DEN,DENE,T,TK,TKI,T4,TSQRT,
     $   VERBOS,LAST
      TAU=1.
```

```
      IF(DV) 11,11,12
12    COLUMN=DEN/DV
11    CONTINUE
      DO 10 IJ=1,LAST
10    LCOOL(IJ)=0.
      DO 1 L=1,NLINE
      IL=IIND(L)
      IF(IR(IL).GT.LAST) GO TO 1
      IF (IL.EQ.1) GO TO 1
C  NOTE THAT THIS IS THE Z OF THE ION
      JL=JIND(L)
      IV=IR(IL)
      IJ=INDEX(JL,IV)
      Y=ELINE(L)*TKI
      IF(TAUMAX) 5,5,4
4     TAU=3.2905E-6*F(L)*ABUND(IV)*X(JL,IV)*COLUMN/ELINE(L)
      IF(TAU-.01) 6,7,7
6     TAU=1.
      GO TO 5
7     TAU=(1.-EXP(-TAU))/TAU
5     G=GFN(IDENT(L),IJ,IL,Y)
3     LCOOL(IJ)=LCOOL(IJ)+F(L)*G*EXP(-Y)*TAU
1     CONTINUE
      DO 2 IJ=1,LAST
      LCOOL(IJ)=2.71E-15/TSQRT*LCOOL(IJ)
2     CONTINUE
      RETURN
      END
      SUBROUTINE HLINE(HLCOOL,NBOT)
C
C LINE COOLING FOR HYDROGEN
C
      REAL IP1(76),CHIT(76),HLCOOL(9)
      INTEGER INDEX(16,9),IZED(9)
      LOGICAL VERBOS
      COMMON /COLREC/ IP1,CHIT,RNNOT
      COMMON /A/ INDEX,IZED,DEN,DENE,T,TK,TKI,T4,TSQRT,
     $   VERBOS,LAST
      NNOT=RNNOT
      FB=FLOAT(NBOT)
      FB2=FB*FB
      FB4=FB2*FB2
      FIN=1./FB
      FIN2=FIN*FIN
      IF(NBOT.GT.2) GO TO 3
      IF(NBOT.EQ.2) GO TO 2
      G0=1.133
      G1=-0.4059
      G2=.07014
      GO TO 11
2     G0=1.0785
      G1=-0.2319
      G2=0.02947
      GO TO 11
3     G0=0.9935+0.2328*FIN-0.2196*FIN2
      G1=-FIN*(0.6282-0.5598*FIN+0.5299*FIN2)
```

```
      G2=FIN2*(0.3887-1.181*FIN+1.470*FIN2)
11    SB=-0.603
      IF (NBOT.EQ.2) SB=.1169
      RN=0.45
      IF (NBOT.GE.2) RN=1.94*FB**(-1.57)
      DO 9 N=1,9
      HLCOOL(N)=0.0
9     CONTINUE
      NTOP=MIN0(9,NNOT)
      NB1=NBOT+1
      DO 1 N=NB1,NTOP
      FN=FLOAT(N)
      FN2=FN*FN
      FN3=FN*FN2
      X=1.-(FB/FN)**2
      ANN=3.9205661*(FB/FN)**3/X**4*(G0+G1/X+G2/(X*X))
      BNN=4.*FB4/(FN3*X*X)*(1.+1.333333/X+SB/(X*X))
      Y=13.598*TKI/FB2*X
      RNN=RN*X
      Z=RNN+Y
      E1Y=EONE(Y,INY)
      E1Z=EONE(Z,INZ)
      IF (INY.EQ.0.OR.INZ.EQ.0) WRITE (6,1000) Y,Z
1000  FORMAT ('    *******EONE ERROR IN HLINE',2E15.5)
      HLCOOL(N)=2.3814724E-21*TSQRT*FB2*Y*Y*(ANN*((1./Y+.
     $     5)*E1Y
     $       -(1./Z+.5)*E1Z)+(BNN-ANN*ALOG(2.*FB2/X))*
     $        ((EXP(-Y)-Y*E1Y)/Y-(EXP(-Z)-Z*E1Z)/Z))*X
C
C  THE FINAL MOST X IS FOR THE ENERGY OF THE TRANSITION
C  THE CONSTANT HAS A BUILT IN 13.598EV AND AN EV TO ERG
C          CONVERSION
C
1     CONTINUE
      RETURN
      END
      SUBROUTINE LEVEL(J,I)
C
C LOWEST LEVEL IN EQUILIBRIUM WITH CONTINUUM
C
      DIMENSION IP1(76),CHIT(76)
      DIMENSION INDEX(16,9) ,IZED(9)
      LOGICAL VERBOS,SEMICO,ULTRA
      COMMON /CONTRO/ SEMICO,ULTRA
      COMMON /A/ INDEX,IZED,DEN,DENE,T,TK,TKI,T4,TSQRT,
     $   VERBOS,LAST
      COMMON /COLREC/ IP1,CHIT,RNNOT
C
C SEATON'S ESTIMATE OF LOWEST LEVEL IN EQUILIBRIUM WITH C
C         CNTINUUM
C   FOLLOWS WILSON, BUT WILSON'S NUMBERS USED.
C
      RJ=J
      RNCE=(1.4E15*RJ**6.*TSQRT/DENE)**.1428571
      RNNOT=RNCE
      IF (J.NE.IZED(I)) RETURN
```

```
      Y=6.337053E-06*T/J**2
      CONS=(Y/(DENE*DENE))**.05882353*RJ**.823594
      DO 2 IT=1,5
      CONS2=.235294/(RNCE**3*Y)
      RNC=126.*CONS*EXP(CONS2)
      DIF=RNCE-RNC
      IF(ABS(DIF).LT.0.5) GO TO 3
      RNCE=RNCE-DIF/(1.+RNC*3.*CONS2/RNCE)
2     CONTINUE
3     IF(.NOT.SEMICO) RNC=1.0E06
      IF (VERBOS) WRITE(6,1000)RNC,IT
1000  FORMAT(' CONTINUUM LEVEL',F10.1,' ITERATION #',I3)
      RNNCT=RNC
      RETURN
      END
```

PROGRAM COEF

```
C  A
C  A PROGRAM TO GENERATE PHYSICAL PARAMETERS WHICH GO
C        INTO
C  THE COEFFICIENTS CALCULATED FOR THE DISPERSION RELATION
C        N
C
C  INPUT IS FROM UNIT 1 AND CONSISTS OF THE DERIVATIVE
C        OUTPUT FROM
C    THE HEATING AND COOLING PROGRAM IN THE FORM (N,T),(N
C        ,T+/-DELT),
C    (N+/-DELN,T).
C  OUTPUT IS TO UNIT 7 AND CONSISTS OF THE ZERO ORDER
C        QUANTITIES AND
C    THEIR DENSITY AND TEMPERATURE DERIVATIVES.
C
C  NAMELIST PARAMETERS
C  WFUDGE  A FUDGE FACTOR FOR ALTERING FLUX
C  GRAV    THE GRAVITATION IN CM S-2
C  VO      THE GAS VELOCITY
C  DV      VELOCITY DERIVATIVE WHICH MAY BE CALCULATED
C        INTERNALLY,
C           BUT A STARTING VALUE IS NEEDED.
C  NONEQ   CALCULATION OF ENERGY EQUILIBRIUM BY MAKING UP
C          DIFFERENCE
C           WITH CONDUCTION.
C  DNON    AN DENSITY DIFFERENT THAN USED IN HEATING AND
C        COOLING
C  TNON    A TEMPERATURE DIFFERENT THAN USED FOR HEATING
C        AND COOLING
C  DRHO    DNON CONVERTED TO DENSITY (GM CM-3)
C  DT      TEMPERATURE DERIVATIVE
C  D2T     SECOND DERIVATIVE OF TEMPERATURE WITH RESPECT
C        TO DISTANCE.
C  CONKAP  CONDUCTION CONSTANT.
C  NLINE   NUMBER OF LINES IN FORCE CALCULATION
C  CHF THE INVERSE OF THE FACTOR TO CONVERT FROM ZERO TO
C        FIRST MOMENT
C    OF THE RADIATION FIELD
C  VERBOS  CONTROLS PRINTING IF ON SEE DETAILS OF X DERIV
C        ATIVES,ETC.
C  SKIP    IF ON NO NEW HEATING COOLING DATA READ, JUST C
C        ALCULATES FORCE
C  SLAB    FOR A STATIC ATMOSPHERE THIS IS THE EFFECTIVE
C        COLUMN DEPTH
C  CONDUC  IF OFF THE CONDUCTION QUANTITIES ARE SET TO ZE
C        RO
C  TRAD    IS THE BRIGHTNESS TEMPERATURE OF THE RADIATION
C          FIELD/WF
C                USED IN THE CALCULATION OF THE WAVE DAMPI
C        NG DUE TO RADIATION
C  DTOL    IS THE LEVEL OF THE LOGARITHMIC DERIVATIVE BEL
C        OW WHICH IT IS
C           TO ZERO.
```

```
C  DYNEQ    IF ON THE MOMENTUM EQUATION IS BALANCED BY ADJ
C          USTING DV
C  DYNIT    NUMBER OF ITERATIONS IN DYNEQ
C  DYNTOL   ACCURACY REQUIRED OF DV IN MOMENTUM BALANCE
C  WLINE    IF ON THE FORCE CALCULATION FOR EACH LINE IS O
C          UTPUT
C  SLIM     A CONVERGENCE AID IN DYNEQ, WHICH SHOULD BE SE
C          T TO ABOUT 1.5
C  SPHERE   IF ON THE DERIVATIVE OF THE DENSITY IS CALCULA
C          TED FOR A SPHERICAL
C              COORDINATE SYSTEM, ASSUMING SYMMETRY.
C  STARMU   IS THE COSINE OF THE ANGLE TO THE STAR.
C  RSTAR    IS THE DISTANCE FROM THE CENTRE OF THE STAR. O
C          NLY USED BY THE
C              DENSITY AND VELOCITY DERIVATIVE.  THE GRAVI
C          TY MUST BE ADJUSTED.
C
C
C  THE OUTPUT QUANTITIES ARE MOSTLY SELF EXPLANATORY
C    DN ENDINGS ARE DENSITY DERIVATIVES, DT ARE TEMPERATU
C          RE
C
C
      REAL LBREMS,LRRAD,LINLOS,X(17,9),LCLX(76),CPHEAT(76)
     $    ,FTOT
      INTEGER INDEX(16,9) /1, 15*0,2,3,14*0,4,5,6,7,8,9,1
     $    0*0,
     $    10,11,12,13,14,15,16,9*0,
     $    17,18,19,20,21,22,23,24,8*0,
     $    25,26,27,28,29,30,31,32,33,34,6*0,
     $    35,36,37,38,39,40,41,42,43,44,45,46,4*0,
     $    47,48,49,50,51,52,53,54,55,56,57,58,59,60,2*0,
     $    61,62,63,64,65,66,67,68,69,70,71,72,73,74,75,76/
      REAL AD(5),AT(5),AWPJ(5),AGAIN(5),ACOOL(5),AE(5),AH
     $     (5),
     $     ADE(5),AX(17,9,5)
      REAL KBOLTZ /1.38062E-16/
      REAL RGAS /8.314E7/
      REAL ABUND(9)
      REAL AMASS(9) /1.008,4.0026,12.0111,14.0067,15.9994
     $    ,20.179,
     $              24.305,28.086,32.06/
      DIMENSION ELINE(1000),F(1000),II(1000),JJ(1000),FLU
     $    X(100),
     $           FPT(100)
      INTEGER IZED(9)/1,2,6,7,8,10,12,14,16/
      LOGICAL FREEZE,NONEQ,VEREOS,SKIP,CONDUC,DYNEQ,WLINE
      LOGICAL SPHERE
      REAL*8 SLIM
      REAL VTHERM(9)
      REAL*8 DLOG10,DVOLD,DGRDDV,DSQRT,DSIGN,DABS
      REAL*8  NO,TO,VO,DN,DT,DV,RHOCV,SOUND,
     $          NEO,HO,EO,DNEDT,DNEDN,DHDT,DHDN,DEDT,DEDN,
     $          D2T,CONKAP,DKDT,DKDN,GRAV,GRAD,GRADE,DGRDT,
     $    DGRDN,
     $          GO,LO,DGDT,DGDN,DLDT,DLDN
```

```
      REAL PHOT(76),PHEAT(76),SIGMA(100,76),DELE(100)
      REAL*8 GRIJ(16,9),DXDT(16,9),DXDN(16,9)
      REAL*8 DIFF,DELV,DIFOLD,DFDDV,DP
      REAL*8 V,T,DEN
      REAL*8 CK,FKAP,DGL,GL,TAU,DEXP
      INTEGER NUO(76),NUF(76)
      INTEGER DYNIT
      COMMON /F/ ELINE,F,II,JJ,FLUX,FPT,NLINE,NFLUX
      COMMON /A/ ABUND,X,VTHERM,SLAB
      COMMON /PHORCE/ GRAD,DT,DGRDN,DXDT,DXDN,GRIJ,DGR
     $    DGRDDV
      COMMON /CONTRO/ WLINE,SPHERE,STARMU,RSTAR
      COMMON/DER/ DNU,DNL,DTU,DTL,DEN,T
      NAMELIST /PARAM/ FREEZE,WFUDGE,GRAV,V0,DV,NONEQ,DNO
     $    N,TNON,DRHO,
     $           DT,D2T,NLINE,CHF,VERBOS,SKIP,SLAB,CONDUC,T
     $    RAD
     $   ,DTOL,DYNEQ,DYNIT,DYNTOL,WLINE,SLIM,SPHERE,STARM
     $    U,RSTAR
      NAMELIST /PHYSIC/ N0,T0,V0,DN,DT,DV,RHOCV,SOUND,
     $          NE0,H0,E0,DNEDT,DNEDN,DHDT,DHDN,DEDT,DEDN,
     $          D2T,CONKAP,DKDT,DKDN,GRAV,GRAD,GRADE,DGRDT,
     $    DGRDN,
     $          G0,L0,DGDT,DGDN,DLDT,DLDN
      NFLUX=97
      FREEZE=.FALSE.
      WFUDGE=1.
      GRAV=1.E4
C
C V>0 AWAY FROM STAR, SIMILARLY Z INCREASES UPWARDS
C
      V0=0.
      DV=0.
      NONEQ=.TRUE.
      DTOL=.05
      DYNEQ=.FALSE.
      DYNIT=10
      DYNTOL=1.E-3
      SLIM=.5D0
      TRAD=50000.
      CONDUC=.TRUE.
      DNON=1.E11
      TNON=0.
      T=1.E5
      DRHO=0.
      DT=0.
      D2T=0.
      NLINE=874
      CHF=1.
      SLAB=0.
      VERBOS=.TRUE.
      WLINE=.FALSE.
      SKIP=.FALSE.
      SPHERE=.FALSE.
      STARMU=1.
      RSTAR=1.E12
```

```
      REWIND 1
      REWIND 2
C
C  READ IN LINE AND FLUX DATA (USUALLY FILE LFORCEDAT)
C
      READ (2) ELINE,F,II,JJ,FLUX,FPT
C
C INCOMING FLUX HAS BEEN MULTIPLIED BY 4*PI/C
C
      DO 49 IN=1,96
      DELE(IN)=FPT(IN+1)-FPT(IN)
49    CONTINUE
      REWIND 3
      READ(3) PHOT,PHEAT,SIGMA,FTOT1
      REWIND 4
      READ (4,9774) (NUO(IJ),NUF(IJ),IJ=1,76)
9774  FORMAT(2I4)
C
C READS FILE CONTAINING INTEGRATION FREQUENCIES WHICH WAS
C          USED BY PHOTION
C
998   READ(5,PARAM,END=999)
      IF(.NOT.VERBOS) WLINE=.FALSE.
      IF(.NOT.NONEQ.AND.V0.EQ.0.) V0=1.D7
      WRITE(6,1014)
C
C READ IN SET OF 5 OUTPUT QUANTITIES FROM HEAT COOL PROGRAM
C
1014  FORMAT('1')
      WRITE(6,PARAM)
      IF(SKIP) GO TO 111
      DO 14 I=1,5
      READ(1) D,TA,WFJ,FJ,GAIN,COOL,LBREMS,LRRAD,LINLOS,
     $        EINT,ENTH,DE,ABUND,X,LCLX,CPHEAT,FTOT
      AD(I)=D
      AT(I)=TA
      AWFJ(I)=WFJ
      AGAIN(I)=GAIN
      ACOOL(I)=COOL
      AE(I)=EINT
      AH(I)=ENTH
      ADE(I)=DE
      DO 15 IZ=1,9
      IQ1=IZED(IZ)+1
      DO 15 J=1,IQ1
      AX(J,IZ,I)=X(J,IZ)
15    CONTINUE
14    CONTINUE
      FA=ABUND(3)/3.035918E-04
      WRITE (6,1000) FJ,FA,FTOT
1000  FORMAT('0FJ,FA,FTOT',2F11.6,E15.7,/' DEN,TEMP,WFJ,H'
     $    ,'EAT,COOL,',
     $      'EINT,ENTHALPY,DENE')
      DO 1 I=1,5
      AGAIN(I)=AGAIN(I)/AD(I)
1     CONTINUE
```

```
      WRITE (6,1001) (AD(ID),AT(ID),AWFJ(ID),AGAIN(ID),
     $     ACOOL(ID),AE(ID),
     $       AH(ID),ADE(ID),ID=1,5)
1001  FORMAT(1X,8E15.7)
C
C SET UP CENTRAL VALUES
C
      DEN=AD(1)
      DENE=ADE(1)
      T=AT(1)
      N0=DEN
      NE0=DENE
      T0=T
      DEINT=AE(1)
      DENTH=AH(1)
      ENTH=AH(1)
      ST4=SQRT(SNGL(T)*1.E-04)
C
C THERMAL VELOCITY ALREADY DIVIDED BY C
C
      DO 11 I=1,9
      VTHERM(I)=4.2833E-5/SQRT(AMASS(I))*ST4
11    CONTINUE
      DENE=ADE(1)
C
C  CALCULATE UPPER AND LOWER DERIVATIVES DIFFERENCES
C
      DNU=AD(4)-AD(1)
      DNL=AD(1)-AD(5)
      DTU=AT(2)-AT(1)
      DTL=AT(1)-AT(3)
C
C  DERIVATIVES OF THE IONIZATION FRACTIONS
C
      DO 16 IZ=1,9
      IQ=IZED(IZ)
      DO 17 J=1,IQ
      GRIJ(J,IZ)=0.
      DXDT(J,IZ)=0.
      DXDN(J,IZ)=0.
      IF(AX(J,IZ,1).LE.1.E-10) GO TO 17
      DXDT(J,IZ)=.5*((AX(J,IZ,2)-AX(J,IZ,1))/DTU+
     $             (AX(J,IZ,1)-AX(J,IZ,3))/DTL)
      IF(DABS(DXDT(J,IZ)*T/AX(J,IZ,1)).LE.DTOL) DXDT(J,IZ)
     $     =0.D0
      DXDN(J,IZ)=.5*((AX(J,IZ,4)-AX(J,IZ,1))/DNU+
     $             (AX(J,IZ,1)-AX(J,IZ,5))/DNL)
      IF(DABS(DXDN(J,IZ)*DEN/AX(J,IZ,1)).LE.DTOL) DXDN(J,
     $     IZ)=0.D0
17    CONTINUE
16    CONTINUE
      IF(.NOT.VERBOS) GO TO 20
      DO 19 IZ=1,9
      IQ=IZED(IZ)
      WRITE(6,1029) IQ
1029  FORMAT(' DXDT,DXDN FOR ATOM Z=',I2)
```

```
      WRITE(6,1030)  (DXDT(J,IZ),J=1,IQ)
1030  FORMAT(1X,10E13.5)
      WRITE(6,1030)  (DXDN(J,IZ),J=1,IQ)
19    CONTINUE
20    DO 18 IZ=1,9
      IQ=IZED(IZ)
      DO 18 J=1,IQ
      X(J,IZ)=AX(J,IZ,1)
18    CONTINUE
C
C  PHYSICAL DERIVATIVES
C
      DU=0.
      DL=0.
      CALL DERIV(ADE,DNEDN,DNEDT,DTOL)
      WRITE (6,1003) DNEDN,DNEDT
1003  FORMAT(' DNEDN,DNEDT',2E15.7)
      DN2=AD(1)*AD(1)
      CALL DERIV(ACOOL,DLDN,DLDT,DTOL)
      DLDN=AD(1)*2.*ACOOL(1)+DLDN*DN2
      DLDT=DLDT*DN2
      RL=ACOOL(1)*DN2
      WRITE(6,1005) DLDN,DLDT,RL
1005  FORMAT(' DLDN,DLDT,LOSSES',3E15.7)
      CALL DERIV(AGAIN,DGDN,DGDT,DTOL)
      GAIN=AGAIN(1)*DN2
      DGAINC=GAIN/2.9979E10
      DGDN=AD(1)*2.*AGAIN(1)+DGDN*DN2
      DGDT=DGDT*DN2
      WRITE (6,1007) DGDN,DGDT,GAIN
1007  FORMAT(' DGDN,DGDT,GAINS',4E15.7)
      CALL DERIV(AE,DEDN,DEDT,DTOL)
      C=DEDT/KBOLTZ
      WRITE (6,1009) DEDN,DEDT,C
1009  FORMAT (' DEDN,DEDT,CV',4E15.7)
      CALL DERIV(AH,DHDN,DHDT,DTOL)
      C=DHDT/KBOLTZ
C
C  CONDUCTION CALCULATION FROM SPITZER
C
      WRITE(6,1011) DHDN,DHDT,C
1011  FORMAT(' DHDN,DHDT,CP',4E15.7)
      IF (CONDUC) GO TO 110
      DKDT=0.
      DKDN=0.
      CONKAP=0.
      GO TO 113
110   CONTINUE
      COULOG=9.00+3.45*ALOG10(SNGL(T))-1.15*ALOG10(DENE)
      CONKAP=1.8E-5*T**2.5/COULOG
      DKDT=2.5*CONKAP/T+CONKAP/(COULOG*T)*3.45
      DKDN=CONKAP/(COULOG*DENE)*(-1.15)
C
C  THE MEAN MASS OF AN ATOM COEFFICIENT
C
113   WRITE(6,1013) CONKAP,DKDT,DKDN
```

```
1013  FORMAT(' CONKAP,DKDT,DKDN',3E15.7)
      RHOCON=0.
      DO 10 I=1,9
      RHOCON=RHOCON+AMASS(I)*ABUND(I)
10    CONTINUE
C
C  THE FORCE DUE TO CONTINUUM RADIATION
C
      RHOCV=RHOCON*1.660531E-24
111   CONTINUE
      GRADC=0.
      DGCDN=0.
      DGCDT=0.
      DO 51 I=1,9
      IZ=IZED(I)
      DO 52 J=1,IZ
      IJ=INDEX(J,I)
      XAC=ABUND(I)*X(J,I)
      IF(XAC.LT.1.E-10) GO TO 52
      NUB=NUO(IJ)
      NUE=NUF(IJ)
      IF(NUE.EQ.NUB) GO TO 52
      GCL=0.
      DO 50 IN=NUB,NUE
      GCL=GCL+.5*(FLUX(IN+1)*SIGMA(IN+1,IJ)+FLUX(IN)*
     $    SIGMA(IN,IJ))*
     $        DELE(IN)
50    CONTINUE
      GRADC=GRADC+GCL*XAC
      DGCDN=DGCDN+GCL*DXDN(J,I)*ABUND(I)
      DGCDT=DGCDT+GCL*DXDT(J,I)*ABUND(I)
52    CONTINUE
51    CONTINUE
      DGCDN=DGCDN*CHF/RHOCV
      DGCDT=DGCDT*CHF/RHOCV
      GRADC=GRADC/RHOCV*CHF
      TRKAPC=0.
      RHO=DEN*RHOCV
      DDEN=0.
      IFIT=0
      DIFF=0.
C
C IF DYNEQ BALANCE MOMENTUM EQUATION
C
      IF(DYNEQ) WRITE(6,1062)
1062  FORMAT(6X,'DIFF',11X,,'DDEN',11X,'DV',13X,'DELV',11X
     $       'DGRDDV',9X,'GRAD',11X,'DP',13X,'IFIT')
201   CONTINUE
      GRAD=0.
      GRADE=0.
      DGRDT=0.
      DGRDN=0.
      IF(FTOT.EQ.0.) GO TO 112
      DGRDDV=0.
C
C CALCULATION OF LINE FORCE
```

```
C
      CALL FORCE(V0,DV,T,DEN)
      DGRDDV=DGRDDV/RHOCV*CHF
      GRADL=GRAD/RHOCV*CHF
      GRADE=FTOT*2.219E-35*DENE/(DEN*RHOCV)*CHF
      DGEDT=GRADE*DNEDT/DENE
      DGRDT=DGRDT*CHF/RHOCV+DGEDT+DGCDT
      DGRDN=DGRDN*CHF/RHOCV+DGCDN
C  NOTE THAN GRIJ IS NOT MULTIPLIED BY CHF
C NUMBER IS THOMSON CROSS SECTIONOVER THE SPEED OF LIGHT
      GRAD=GRADL+GRADE+GRADC
      IF(.NOT.DYNEQ) GO TO 200
      DN=-DV*N0/V0
      IF(SPHERE) DN=DN-2.D0*N0/RSTAR
      DDEN=DN
      DIFOLD=DIFF
      DP=KBOLTZ/RHO*(DT*(N0+NE0+DNEDT*T0/N0)+DN*(1.D0+
     $     DNEDN)*T0)
      DIFF=DP
     $        +GRAV-GRAD+V0*DV
      IF(IFIT.EQ.0) GO TO 202
C
C ADJUSTMENT OF DV/DZ FOR MOMENTUM BALANCE
C
      DFDDV=(DIFF-DIFOLD)/(DV-DVOLD)
      DELV=-DIFF/DFDDV
      IF(DABS(DELV).GT.DABS(DV).AND.SLIM.NE.0.D0) DELV=
     $                          DSIGN(1.D0,DELV)*DABS(DV)*SLIM
      DVOLD=DV
      DV=DV+DELV
      WRITE(6,1061) DIFF,DDEN,DV,DELV,DGRDDV,GRAD,DP,IFIT
 1061 FORMAT(1X,7E15.5,I5)

      IFIT=IFIT+1
      IF(DABS(DELV/DV).LT.DYNTOL) GO TO 200
      IF(IFIT.LE.DYNIT) GO TO 201
      GO TO 200
202   DVOLD=DV
      DV=DV*1.1D0
      IFIT=1
      GO TO 201
200   CONTINUE
      TRKAPC=GRAD/FTOT
      GRATIO=GRAD/GRADE
      GAMMA=(GRAV-GRAD)/GRAV
      WRITE(6,1012) GRAD,GRADE,GRADL,GRADC,GRATIO,GAMMA,
     $     DGRDT,DGRDN
 1012 FORMAT(' GRAD,GRADE,GRADL,GRADC,GRATIO,GAMMA,DGRDT,
     $     DGRDN'/1X,
     $        8E16.6)
 112  CONTINUE
      P0=(DEN+DENE)*T*KBOLTZ
      DP=RHO*(-V0*DV-GRAV+GRAD)
      IF(NONEQ) GO TO 46
      IF(V0.EQ.0.) GO TO 44
      DRHO=-RHO*DV/V0
```

```
      DDEN=DRHO/RHOCV
44    IF(NONEQ.AND.(V0.EQ.0.)) GO TO 45
C
C ENERGY EQUILIBRIUM FORCED
C BY USING CONDUCTIVE ENERGY TRANSPORT
C RARELY USED
C
      VC1=1.
C  IN FRAME OF STAR VC1=1
      DT=(-KBOLTZ/RHOCV*(DDEN*(1.+DNEDN))*T/DEN
     $     -V0*DV+VC1*GRAD-GRAV)/
     $     (KBOLTZ/RHOCV*(T/DEN*DNEDT+1.+DENE/DEN))
      GO TO 46
45    DDEN=((-GRAV+GRAD)*RHO-(DEN+DENE)*KBOLTZ*DT)/
     $      (KBOLTZ*T*(1.+DNEDN))
      DRHO=DDEN*RHOCV
46    DH=DHDT*DT+DHDN*DRHO/RHOCV
      DKAP=DKDT*DT+DKDN*DDEN
      TN=(DEN+DENE)*T
      SOUND=SQRT(.5*(((AD(4)+ADE(4))*AT(4)-TN)/DNU+
     $      (TN-(AD(5)+ADE(5))*AT(5))/DNL)*RGAS/RHOCON)
      IF (NONEQ) GO TO 33
      D2T=(-VC1*GAIN+RL+DDEN*V0*(1.5*V0**2+ENTH)*RHOCV
     $     +DEN*RHOCV*DV*(1.5*V0**2+ENTH)
     $     +RHOCV*DEN*(DHDT*DT+DHDN*DEN))/(-CONKAP)
33    IF(NONEQ.AND.(TNON.GT.0.)) T=TNON
      WRITE (6,1022) P0,RHO,DRHO,DP,SOUND,NONEQ,DT,
     $      DKAP,D2T
1022  FORMAT(' PHYSICAL PARAMETERS CALCULATED,P0,RHO,DRHO,',
     $     'DP,SOUND',5E15.7,/' NONEQ,DT,DKAP,',
     $     'D2T',/1X,L8,3E15.7)
      CFLUX=CONKAP*D2T+DKAP*DT
      WRITE (6,1024) CFLUX
1024  FORMAT(' CONDUCTION FLUX=', E15.7)
      IF(SKIP) GO TO 122
      DN=DDEN
      H0=ENTH/RHOCV
      E0=EINT/RHOCV
      DHDT=DHDT/RHOCV
      DHDN=DHDN/RHOCV
      DEDT=DEDT/RHOCV
      DEDN=DEDN/RHOCV
      G0=GAIN
      L0=RL
122   CONTINUE
C
C OUTPUT OF PHYSICAL QUANTITIES
C
      WRITE(7) N0,T0,V0,DN,DT,DV,RHOCV,SOUND,
     $        NE0,H0,E0,DNEDT,DNEDN,DHDT,DHDN,DEDT,DEDN,
     $        D2T,CONKAP,DKDT,DKDN,GRAV,GRAD,GRADE,DGRDT,
     $   DGRDN,
     $        G0,L0,DGDT,DGDN,DLDT,DLDN
      WRITE(6,PHYSIC)
C
C CALCULATION OF PHYSICAL LIMITING FREQUENCIES
```

```
C
      WRAD=5.6997E-03*TRAD**3*TRKAPC
      WCOOL=6.28319*L0/(E0*RHO)
      WREC=1.88E-10/DSQRT(T)*DEN
      EQC=COULOG*DENE*T**(-1.5)
      WEQPE=2.5E-02*EQC
      WEQEE=4.57E01*EQC
      WCOND=6.28*ABS(SNGL(DKDT*DT+CONKAP*D2T))/(DEDT*RHO)
      WRITE(6,1025) WRAD,WCOOL,WREC,WEQPE,WEQEE,WCOND
1025  FORMAT(' WRAD,WCOOL,WREC,WEQPE,WEQEE,WCOND',6E15.3)
      IF(DDEN.EQ.0.) GO TO 519
      HSCALE=DABS(DEN/DDEN)
      GAM=DHDT/DEDT
      WACS=GAM*GRAV/(2.*SOUND)
      WACH=SQRT(SNGL(GAM*GRAV/(4.*HSCALE)))
      WBVS=SQRT(GAM-1.)*GRAV/SOUND
      WBVH=SQRT(SNGL((GAM-1.)*GRAV/(GAM*HSCALE)))
      WRITE(6,1033) HSCALE,GAM,WACS,WACH,WBVS,WBVH
1033  FORMAT(' HSCALE,GAM,WACS,WACH,WBVS,WBVH,',6E14.3)
519   CONTINUE
      GO TO 998
999   STOP
      END
      SUBROUTINE FORCE(V,DV,T,DEN)
C
C ROUTINE TO CALCULATE LINE FORCE
C WITH SIMPLE LUCY RADIATIVE TRANSFER
C FOR ONE SCATTERING LINE
C ALWAYS MUST BE SUPERSONIC FLOW
C NO OVERLAPPING LINES ALLOWED FOR
C
      LOGICAL VERBOS
      INTEGER INV(16) /1,2,0,0,0,3,4,5,0,6,0,7,0,8,0,9/
      DIMENSION ELINE(1000),F(1000),II(1000),JJ(1000)
      DIMENSION ABUND(9),X(17,9),VTHERM(9),FLUX(100),
     $    FPT(100)
      REAL*8 DXDT(16,9),DXDN(16,9),GRAD,DGRDT,DGRDN,
     $     GRIJ(16,9)
      REAL*8 V,DV,T,DEN,DVI
      REAL*8 CK,GL,DGL,TAU,TAUC,DGRDDV,FKAP,DGLDN
      REAL*8 DABS
      LOGICAL SPHERE
      COMMON /PHORCE/ GRAD,DGRDT,DGRDN,DXDT,DXDN,GRIJ,
     $     DGRDDV
      COMMON /A/ ABUND,X,VTHERM,SLAB
      COMMON /F/ ELINE,F,II,JJ,FLUX,FPT,NLINE,NFLUX
      COMMON /CONTRO/ VERBOS,SPHERE,STARMU,RSTAR
      DVI=DABS(DV)
      IF(SPHERE) DVI=DABS(.5*(1.+STARMU*STARMU)*
     $     (DV-V/RSTAR)+V/RSTAR)
      IF=1
      FDF=1.-V/3.E10
      COLUMN=DEN*SLAB
      IF(DVI.NE.0.) COLUMN=2.9979E10/DVI*DEN
      IF(COLUMN.EQ.0.) GO TO 100
      DO 10 L=1,NLINE
```

```
      J=JJ(L)
      I=II(L)
      IV=INV(I)
3     IF(ELINE(L).GT.FDF*FPT(IF))  GO TO 2
      FNU=(FLUX(IF-1)+S*(ELINE(L)-FDF*FPT(IF)))*FDF
      CK=1.0976E-16*F(L)*ABUND(IV)
C CONSTANT IS PI*E**2/(ME*C) / (EV TO HZ CONVERSION)
      TAU=CK/ELINE(L)*COLUMN*X(J,IV)
      IF(X(J,IV).LE.1.E-10) GO TO 10
      DGL=CK*FNU
      GL=DGL*X(J,IV)
C
C  ELINE IS IN EV BUT NOTE THAN FNU IS ERG CM-2 S-1 EV-1
C
      TAUC=TAU*DVI
      IF(TAU.LE.1.E-3) GO TO 4
      IF(TAU.GT.170.) GO TO 6
      DGRDDV=DGRDDV+GL/TAUC*(1.-DEXP(-TAU)*(1.D0+TAU))
      GL=GL*(1.-DEXP(-TAU))/TAU
      DGLDN=-GL/DEN+DGL*DEXP(-TAU)*(DXDN(J,IV)+X(J,IV)/
     $     DEN)
4     CONTINUE
      DGRDDV=DGRDDV+GL/TAUC*TAU*TAU
      DGL=DGL*DEXP(-TAU)
      GO TO 5
2     IF=IF+1
      IF(IF.GT.NFLUX) RETURN
      S=(FLUX(IF)-FLUX(IF-1))/(FPT(IF)-FPT(IF-1)+1.E-50)
      GO TO 3
6     CONTINUE
      DGRDDV=DGRDDV+GL/TAUC
      GL=GL/TAU
      DGLDN=-GL/DEN
      DGL=0.
5     GRAD=GRAD+GL
      GRIJ(J,IV)=GRIJ(J,IV)+GL
      DGRDT=DGRDT+DGL*DXDT(J,IV)
      DGRDN=DGRDN+DGLDN
1     IF(VERBOS)WRITE(6,1000) L,ELINE(L),J,I,IV,FNU,TAU,
     $     GL,CK,FKAP,DGL
1000  FORMAT(1X,I3,F10.5,3I5,6E15.5)
10    CONTINUE
C
C  ALSO, WHAT ABOUT THE CONTINUUM OPACITY
C
      RETURN
C
C OPTICALLY THIN CALC
C
100   DO 101 L=1,NLINE
      J=JJ(L)
      I=II(L)
      IV=INV(I)
103   IF(ELINE(L).GT.FDF*FPT(IF)) GO TO 102
      FNU=(FLUX(IF-1)+S*(ELINE(L)-FDF*FPT(IF)))*FDF
      DGL=1.0976E-16*F(L)*ABUND(IV)*FNU
```

```
      GL=DGL*X(J,IV)
      GRAD=GRAD+GL
      GRIJ(J,IV)=GRIJ(J,IV)+GL
      DGRDT=DGRDT+DGL*DXDT(J,IV)
      DGRDN=DGRDN+DGL*DXDN(J,IV)
      IF(VERBOS)WRITE(6,1000) L,ELINE(L),J,I,IV,FNU,GL,DGL
      GO TO 101
102   IF=IF+1
      IF(IF.GT.NFLUX) RETURN
      S=(FLUX(IF)-FLUX(IF-1))/(FPT(IF)-FPT(IF-1)+1.E-50)
      GO TO 103
101   CONTINUE
      RETURN
      END
      SUBROUTINE DERIV(Q,DQDN,DQDT,DTOL)
C
C A ROUTINE TO CALCULATE DERIVATIVES
C OF PHYSICAL QUANTITIES AND CHECK
C THAT THEIR LOG DERIVATIVES EXCEED
C SOME MINIMUM, IF NOT THE ARE SET TO ZERO.
      REAL*4 Q(5)
      REAL*8 DQDN,DQDT
      REAL*8 DEN,T
      COMMON /DER/ DNU,DNL,DTU,DTL,DEN,T
      IF(Q(1).EQ.0.) GO TO 1
      DU=(Q(4)-Q(1))/DNU
      DL=(Q(1)-Q(5))/DNL
      DQDN=.5*(DU+DL)
      DLQ=DQDN*DEN/Q(1)
      IF(ABS(DLQ).LT.DTOL) GO TO 2
4     DU=(Q(2)-Q(1))/DTU
      DL=(Q(1)-Q(3))/DTL
      DQDT=.5*(DU+DL)
      DLQ=DQDT*T/Q(1)
      IF(ABS(DLQ).LT.DTOL) GO TO 3
      RETURN
1     DQDN=0.D0
      DQDT=0.D0
      RETURN
2     WRITE(6,1001) DU,DL,DQDN,DLQ,DTOL
1001  FORMAT('DU,DL,DQDN,DLQ,DTOL',5E15.7)
      DQDN=0.D0
      GO TO 4
3     WRITE(6,1002) DU,DL,DQDT,DLQ,DTOL
1002  FORMAT('DU,DL,DQDT,DLQ,DTOL',5E15.7)
      DQDT=0.D0
      RETURN
      END
```

PROGRAM CCCALC

```
C
C
C THIS PROGRAM CALCULATES THE COEFFICIENTS OF W AND K
C FOR THE DISPERSION RELATION POLYNOMIAL
C THE PHYSICAL QUANTITIES PRODUCED BY THE PROGRAM COEF
C ARE USED AS INPUT
C THE OUTPUT IS USED BY THE PROGRAM DISPER
C THIS IS A SUBROUTINE CALLED IN THE DISPER.
C
C
      SUBROUTINE COCALC(*)
      REAL*8 KBOLTZ,RMU,VC1,C,VG
      LOGICAL FREEZE
      LOGICAL MANY,RESTOR
      REAL*8 CMASS,CMTM,CENE
      REAL*8 C,VC1,MTMKN,MTMCN,MTMKT,MTMCT,DVG,
     $         EWN,EKN,ECN,EWT,EKT,ECT,EWV,EKV,ECV
      REAL*8  NO,TO,VO,DN,DT,DV,RHOCV,SOUND,
     $           NEO,HO,EO,DNEDT,DNEDN,DHDT,DHDN,DEDT,DEDN,
     $           D2T,CONKAP,DKDT,DKDN,GRAV,GRADO,GRADE,DGRDT
     $     ,DGRDN,
     $           GO,LO,DGDT,DGDN,DLDT,DLDN
      REAL*8 CRD(5,4),CID(5,4)
      COMMON /COEFS/ CRD,CID
      COMMON /CNTRO2/ MANY,RESTOR
      NAMELIST /PHYSIC/ NO,TO,VO,DN,DT,DV,RHOCV,SOUND,
     $           NEO,HO,EO,DNEDT,DNEDN,DHDT,DHDN,DEDT,DEDN,
     $           D2T,CONKAP,DKDT,DKDN,GRAV,GRADO,GRADE,DGRDT
     $     ,DGRDN,
     $           GO,LO,DGDT,DGDN,DLDT,DLDN,FREEZE
      NAMELIST /DISCO/ RMU,VC1,MTMKN,MTMCN,MTMKT,MTMCT,DVG,
     $           EWN,EKN,ECN,EWT,EKT,ECT,EWV,EKV,ECV
      IF(.NOT.RESTOR) GO TO 4
      BACKSPACE 1
      GO TO 3
4     CONTINUE
      IF(MANY) GO TO 2
3     READ(1,END=999) NO,TO,VO,DN,DT,DV,RHOCV,SOUND,
     $           NEO,HO,EO,DNEDT,DNEDN,DHDT,DHDN,DEDT,DEDN,
     $           D2T,CONKAP,DKDT,DKDN,GRAV,GRADO,GRADE,DGRDT
     $     ,DGRDN,
     $           GO,LO,DGDT,DGDN,DLDT,DLDN
2     FREEZE=.FALSE.
      C=2.9979D10
      KBOLTZ=1.380626D-16
      READ(5,PHYSIC,END=999)
      RMU=KBOLTZ/RHOCV
      VC1=1.D0
C
C THE NAMES OF THESE VARIABLES COMES FROM
C
C THE LINEARIZATION OF THE EQUATIONS OF MOTION
C
```

```
C EXCEPT NOTE THAT P THERE IS REPLACED BY MTM.
C
      CMASS=DN*V0+DV*N0
      CMTM=RMU*T0/N0*(DN+(DNEDN*DN+DNEDT*DT))+DV*V0
     $     +RMU*DT*(1.D0+NE0/N0)-VC1*GRAD0+GRAV
      CENE=-VC1*G0+L0+CONKAP*D2T+(DKDN*DN+DKDT*DT)*DT+DN*
     $     V0*RHOCV*(1.5D0*
     $      V0**2+H0)+N0*RHOCV*DV*(1.5D0*V0**2+H0)+
     $      RHOCV*N0*(DHDT*DT+DHDN*DN)
      WRITE(6,1001) CMASS,CMTM,CENE
1001  FORMAT(' CONSERVATION EQUATIONS CMASS,CMTM,CENE',
     $     3D25.12)
      VC1=1.-V0/C
C  CALCULATION DONE IN FRAME MOVING WITH GAS
      VG=0.D0
      WRITE(6,PHYSIC)
      MTMKN=KBOLTZ/(N0*RHOCV)*(DNEDN*T0+T0)
      MTMCN=KBOLTZ/(N0**2*RHOCV)*(-DN*T0+N0*DNEDN*DT
     $          -NE0*DT-(DNEDN*DN+DNEDT*DT)*T0)-VC1*DGRDN
      MTMKT=KBOLTZ/(N0*RHOCV)*(NE0+DNEDT*T0+N0)
      MTMCT=KBOLTZ/(N0*RHOCV)*(DN+DNEDT*DT+DNEDT*DT+DNEDN
     $     *DN)-VC1*DGRDT
      DVG=DV+GRAD0/C
      EWN=(DEDN*N0+(VG**2/2.+E0))*RHOCV
      EKN=VG*(.5D0*VG**2+H0+DEDN*N0)*RHOCV+(-DKDN)*DT
      ECN=RHOCV*(DN*VG*DHDN+1.5*DV*VG**2+DV*H0+
     $         DV*N0*DHDN+VG*(DHDN*DN+DHDT*DT))+D2T*(-DKDN
     $     )-VC1*DGDN+DLDN
     $   +RHOCV*(V0*(DEDN*DN+DEDT*DT)+DEDN*V0*DN)
      EWT=DEDT*N0*RHOCV
      EKT=RHOCV*DHDT*VG*N0+(-DKDT)*DT+((-DKDT)*DT+(-DKDN)
     $     *DN)
      ECT=DLDT-VC1*DGDT+(DHDT*(DN*VG+DV*N0))*RHOCV+(-DKDT
     $     )*D2T
     $    +RHOCV*DEDT*V0*DN
      EWV=VG*N0*RHOCV
      EKV=(1.5*VG**2+H0)*N0*RHOCV
      ECV=(DN*(1.5*VG**2+H0)+3.*DV*VG*N0+N0*(DHDT*DT+DHDN
     $     *DN))
     $      *RHOCV+G0/C
     $    +RHOCV*(N0*V0*DV)
C
C
C OUTPUT LINEARIZED EQUATION QUANTITIES
C THIS IS USEFUL FOR EXAMINING THE MAGNITUDES
C OF THE PHYSICAL QUANTITIES WHICH
C ARE DOMINATING THE SITUATION
C
      WRITE(6,DISCO)


      CRD(1,1)=
     $  -ECN*MTMCT*DN-DVG*ECT*DV+MTMCT*ECV*DV+MTMCN*DN*EC T
      CID(1,1)=0.D0
      CRD(2,1)=0.D0
      CID(2,1)=
```

```
$  VG*(-DVG*ECT+MTMCT*ECV-ECT*DV)-ECN*MTMCT*NO-ECN*
$     MTMKT*DN-EKN*
XMTMCT*DN-DVG*EKT*DV+MTMCT*EKV*DV+MTMKT*ECV*DV+MTMCN
$     *DN*EKT+MTMCN*
XNO*ECT+MTMKN*DN*ECT
 CRD(3,1)=
$  VG**2*ECT+VG*(DVG*EKT-MTMCT*EKV-MTMKT*ECV+EKT*DV)
$     +ECN*MTMKT*
XNO+EKN*MTMCT*NO+EKN*MTMKT*DN+DVG*(-CONKAP)*DV-MTMKT
$     *EKV*DV
$    -MTMCN*DN*
X(-CONKAP)-MTMCN*NO*EKT-MTMKN*DN*EKT-MTMKN*NO*ECT
 CID(3,1)=0.D0
 CRD(4,1)=0.D0
 CID(4,1)=
$  VG**2*EKT+VG*(DVG*(-CONKAP)-MTMKT*EKV+(-CONKAP)*DV
$     )+
$    EKN*MTMKT*NO-
XMTMCN*NO*(-CONKAP)-MTMKN*DN*(-CONKAP)-MTMKN*NO*EKT
 CRD(5,1)=
$  -VG**2*(-CONKAP)+MTMKN*NO*(-CONKAP)
 CID(5,1)=0.D0
 CRD(1,2)=0.D0
 CID(1,2)=
$  EWN*MTMCT*DN+DVG*ECT+DVG*EWT*DV-MTMCT*ECV-MTMCT*
$     EWV*DV-MTMCN*
XDN*EWT+ECT*DV
 CRD(2,2)=
$  VG*(-DVG*EWT+MTMCT*EWV-2*ECT-EWT*DV)-EWN*MTMCT*NO
$     -EWN*MTMKT*
XDN-DVG*EKT+MTMCT*EKV+MTMKT*ECV+MTMKT*EWV*DV+MTMCN*
$     NO*EWT+MTMKN*DN
X*EWT-EKT*DV
 CID(2,2)=0.D0
 CRD(3,2)=0.D0
 CID(3,2)=
$  -VG**2*EWT+VG*(MTMKT*EWV-2*EKT)-EWN*MTMKT*NO-DVG*
$     (-CONKAP)+MTMKT
X*EKV+MTMKN*NO*EWT-(-CONKAP)*DV
 CRD(4,2)=
$  2*VG*(-CONKAP)
 CID(4,2)=0.D0
 CRD(5,2)=0.D0
 CID(5,2)=0.D0
 CRD(1,3)=
$  DVG*EWT-MTMCT*EWV+ECT+EWT*DV
 CID(1,3)=0.D0
 CRD(2,3)=0.D0
 CID(2,3)=
$  2*VG*EWT-MTMKT*EWV+EKT
 CRD(3,3)=
$  -(-CONKAP)
 CID(3,3)=0.D0
 CRD(4,3)=0.D0
 CID(4,3)=0.D0
 CRD(5,3)=0.D0
```

```
      CID(5,3)=0.D0
      CRD(1,4)=0.D0
      CID(1,4)=
     $  -EWT
      CRD(2,4)=0.D0
      CID(2,4)=0.D0
      CRD(3,4)=0.D0
      CID(3,4)=0.D0
      CRD(4,4)=0.D0
      CID(4,4)=0.D0
      CRD(5,4)=0.D0
      CID(5,4)=0.D0
      WRITE(6,1000) ((CRD(J,I),J=1,5),(CID(J,I),J=1,5),I=
     $     1,4)
1000  FORMAT('0',5D25.10,/,1X,5D25.10)
      RETURN
999   RETURN1
      END
```

PROGRAM DISPER

```
C
C A PROGRAM TO FIND THE ROOTS OF THE CUBIC DISPERSION
C        RELATION
C FOUND FOR THE CASE OF ONE DIMENSIONAL PLANE WAVES
C SUBROUTINE COCALC USES THE OUTPUT FROM COEF TO
C ACTUAL FIND THE POLYNOMIAL
C
C
C THE PARAMETERS CONTROLLING THE PROGRAM ARE:
C KLOG IF TRUE A LOGARITHMIC SERIES OF K ARE GENERATED
C KMIN MINIMUM K VALUE (IF KLOG THEN THIS IS A LOG)
C KMAX MAXIMUM K VALUE
C PLREAL PLOT REAL FREQUENCIES
C PLIMAG PLOT IMAGINARY FREQUENCIES
C KINC INCREMENT BETWEEN K VALUES
C TOL IF TWO ROOTS LIE CLOSER THAN THIS THEY ARE
C     ASSUMED TO BE IDENTICAL
C ERR ACCURACY OF NDINVT SOL'N TO D=0, DD=0
C MAXIT # OF ITERATIONS IN NDINVT
C EQTOL ACCURACY OF NEWTON ITERATION ROOT IMPROVER
C NFILE FILE LINENUMBER WHERE COEFFICIENTS START
C     USUAL 1+A MULTIPLE OF 5
C LABEL TRUE TO LABEL PLOTS
C SUBDIV # OF SUBDIV USED BY NEXT ROOT ESTIMATOR
C PRMIN FOR DIFFEREN REAL PLOT Y AXIS MINIMUM
C PRINC SAME BUT INCREMENT FROM MIN FOR 10" PLOT
C PIMIN SAME AS PRMIN BUT FOR IMAGINARY PART
C PIINC SAME AS PRINC BUT IMAG
C NPRINT EVERY NPRINT'TH K VALUE AND ROOT OUTPUT TO PRINTER
C        ER
C SEMIV IF TRUE OUTPUT WILL ALLOW NPRINT TO TAKE EFFECT
C
      REAL*8 DKR(210)
      REAL*8 RD(11),ID(11),ROOTR(4),ROOTI(4),PKR(5),PKI(5
     $    )
      REAL*8 RDIS(12),IDIS(12)
      REAL*8 DELTAK
      REAL*8 DIST,DISTOL,RSAVE,DERR
      INTEGER*4 KBEG(3),KEND(3)
      REAL*8 X(4),F(4),ACCEST(4),ERR
      REAL*8 RDC(4),IDC(4)
      REAL*8 DONE /1.D0/
      REAL*8 WIM(3,210),WR(3,210)
      REAL*8 KMIN,KMAX,KINC,TOL
      REAL*8 DSIGN,DREAL,DIMAG,DLOG10,DABS,DMIN1,DMAX1
      COMPLEX*16 DCMPLX,CROOT,CDLOG
      REAL*8 CDABS,DLOG
      LOGICAL FREEZE,NONEQ,KLOG,PLREAL,PLIMAG,SOLVEQ,KNEG
     $  ,MANY,RESTOR,FIRST,DUPLIC,LABEL
      LOGICAL*1 INSTAB(3,210),ALABEL(80)
      INTEGER*4 SYM(3) /12,2,5/
      REAL*8 GREL,EQTOL,COMPAR,LDEL,DPR,DPI
      REAL*4 VPHASE(3,210),VG(3,210),AX(210),AY(210)
```

```
      COMPLEX*16 CK,DC(4),DDC(4),WC,WC2,WC3,NDC(3),DDIS,
     $    DDDK
      COMPLEX*16 DWDK,PRED(3),SLOPE(3)
      LOGICAL VERBOS,ZERIMG,FANCY,SEMIV,LPRINT
      INTEGER*4 SUBDIV
      INTEGER*4 INSTBI(3,40),NMAXL(3)
      REAL*8 WMAXL(3),DAWIM
      COMMON /NEWT/ DDIS,MAXIT
      COMMON /CCCALC/ DDC,DC,NDC
      COMMON /CPOL/ RDC,IDC
      COMMON /CONTRO/ SOLVEQ
      COMMON /CNTRO2/ MANY,RESTOR
      COMMON /DIS/ RDIS,IDIS
      NAMELIST /PARAM/ KLOG,KMIN,KMAX,PLREAL,PLIMAG,KINC,
     $    TOL
     $          ,ERR,MAXIT,VERBOS,FANCY,PINC,PKMIN,MANY
     $       ,RESTOR,EQTOL,NFILE,LABEL,SUBDIV
     $      ,PRMIN,PRINC,PIMIN,PIINC,NPRINT,SEMIV
      EXTERNAL FCN
C
C SET UP DEFAULT VALUES
C
      SUBDIV=3
      NFILE=1
      TOL=1.D-6
      EQTOL=1.D-14
      PLIMAG=.TRUE.
      PLREAL=.TRUE.
      KLOG=.TRUE.
      KMIN=-12.D0
      KMAX=-2.D0
      KINC=.1D0
      VERBOS=.FALSE.
      NPRINT=5
      SEMIV=.TRUE.
      FANCY=.FALSE.
      ZERIMG=.TRUE.
      MANY=.FALSE.
      RESTOR=.FALSE.
      MAXIT=100
      ERR=1.D-15
      FIRST=.TRUE.
      LABEL=.FALSE.
9999  IF(MANY.AND..NOT.FIRST) GO TO 9990
      NFILE=1
      READ (5,PARAM,END=9998)
C
C READ IN PARAMETER LIST OF WHAT TO DO
C
      NFILE1=NFILE-1
      IF(NFILE1.LE.0) GO TO 5
      DO 6 ISKIP=1,NFILE1
      READ(1)
6     CONTINUE
5     CONTINUE
      IF(MANY.AND..NOT.FIRST) GO TO 9990
```

```
      NK=(KMAX-KMIN)/KINC+1.5
C
C CALCULATE ARRAY OF K VALUES
C
      IF (KLOG) GO TO 2
      DO 1 I=1,NK
      DKR(I)=KMIN+(I-1)*KINC
1     CONTINUE
      GO TO 3
2     NKB=1
      NKE=NK
      DO 4 I=NKB,NKE
      DKR(I)=10.D0**(KMIN+(I-NKB)*KINC)
4     CONTINUE
3     CONTINUE
9990  WRITE (6,1000)
1000  FORMAT('1')
      IF(.NOT.LABEL) GO TO 9
      READ(5,1066,END=9998) ALABEL
      WRITE(6,1067) ALABEL
1067  FORMAT(1X,80A1)
1066  FORMAT(80A1)
9     CONTINUE
C
C PLOT SCALING QUANTITIES
C
      PINC=0.
      PKMIN=0.
      PRMIN=0.
      PRINC=0.
      PIMIN=0.
      PIINC=0.
      WRITE (6,PARAM)
      FIRST=.FALSE.
      RRMN=9.E70
C
C SEE IF ROOTS ARE PROPERLY SEQUENCED
C
      RRMX=-9.E70
      RIMN=9.E70
      RIMX=-9.E70
      DO 222 IN=1,3
      VPHASE(IN,1)=0.
      WMAXL(IN)=-9.D70
      NMAXL(IN)=0
      VG(IN,NK)=0.
222   CONTINUE
      CALL COCALC(&9998)
C
C CALCULATE POLYNOMIAL COEFFICIENTS
C
      GREL=0.D0
      I=1
      SOLVEQ=.FALSE.
      DUPLIC=.FALSE.
C
```

```
C FIND FIRST ROOT OF POLYNOMIAL
C
      CALL DISPCO(DKR(I))
      CALL CPOLY1(RDC,IDC,3,ROOTR,ROOTI,&999)
185   SOLVEQ=.TRUE.
99    DO 97 IN=1,3
      CALL NEWTON(ROOTR(IN),ROOTI(IN),EQTOL)
      WR(IN,I)=ROOTR(IN)
      WIM(IN,I)=ROOTI(IN)
97    CONTINUE
181   DO 183 IN=1,2
      IR=IN+1
184   IF(IR.GT.3) GO TO 183
      WC=DCMPLX(WR(IN,I),WIM(IN,I))
      WC2=DCMPLX(WR(IR,I),WIM(IR,I))
      COMPAR=DMAX1(CDABS(WC),CDABS(WC2))
      IF(CDABS(WC-WC2)/COMPAR.LT.TOL) GO TO 170
      IR=IR+1
      GO TO 184
183   CONTINUE
      DUPLIC=.FALSE.
189   I=I+1
C
C ESTIMATE THE VALUES OF THE NEXT SET OF ROOTS
C
      IF(I.GT.NK) GO TO 98
      DELTAK=DKR(I)-DKR(I-1)
      DO 96 IN=1,3
      CALL ADVANC(ROOTR(IN),ROOTI(IN),DELTAK,DWDK,SUBDIV)
      VG(IN,I-1)=SNGL(DREAL(DWDK))
      PRED(IN)=DCMPLX(ROOTR(IN),ROOTI(IN))
96    CONTINUE
      CALL DISPCO(DKR(I))
C
C CALCULATE COEFFICIENTS FOR NEXT K
C
      GO TO 99
170   IF(DUPLIC) GO TO 188
      IF(I.EQ.1) GO TO 188
      SOLVEQ=.FALSE.
      CALL DISPCO(DKR(I))
C
C IF DUPLICATE ROOTS ARE FOUND
C GO BACK TO POLYNOMIAL ROOT FINDER
C TO SEE IF ANOTHER ROOT CAN BE FOUND
C IF SO TRY TO PROPERLY ORDER ROOTS
C
      WRITE(6,1099) I,IN,IR
1099  FORMAT(' &&&&&&&&&&&&&DUPLICATE ROOTS  I,IN,IR',3I5
     $    )
      CALL CPOLY1(RDC,IDC,3,ROOTR,ROOTI,&999)
      NFIL=1
198   DISTOL=9.D70
      DERR=1.D70
      DO 174 IN=1,3
      IF(ROOTR(IN).EQ.0.D0) GO TO 173
```

```
      DERR=DMIN1(DABS(ROOTR(IN)),DERR)
173   IF(ROOTI(IN).EQ.0.D0) GO TO 174
      DERR=DMIN1(DABS(ROOTI(IN)),DERR)
174   CONTINUE
      DERR=DERR*1.D-3
      DPR=DLOG(DABS(DREAL(PRED(NFIL)))+DERR)
      DPI=DLOG(DABS(DIMAG(PRED(NFIL)))+DERR)
194   DO 195 IN=NFIL,3
      DIST=DABS((DREAL(PRED(NFIL))-ROOTR(IN))*
     $                  (DPR-DLOG(DABS(ROOTR(IN))+DERR)))
     $     +DABS((DIMAG(PRED(NFIL))-ROOTI(IN))*
     $                  (DPI-DLOG(DABS(ROOTI(IN))+DERR)))
      IF (DIST.GT.DISTOL) GO TO 195
      DISTOL=DIST
      INFIL=IN
195   CONTINUE
196   WR(NFIL,I)=ROOTR(INFIL)
      WIM(NFIL,I)=ROOTI(INFIL)
      IF (INFIL.EQ.NFIL) GO TO 192
      ROOTR(INFIL)=ROOTR(NFIL)
      ROOTR(NFIL)=WR(NFIL,I)
      ROOTI(INFIL)=ROOTI(NFIL)
      ROOTI(NFIL)=WIM(NFIL,I)
192   NFIL=NFIL+1
      IF(NFIL.LT.3) GO TO 198
      GO TO 185
188   DUPLIC=.FALSE.
      GO TO 189
98    SOLVEQ=.FALSE.
      DO 100 I=1,NK
      LPRINT=.FALSE.
      IF (VERBOS) LPRINT=.TRUE.
      IF ((.NOT.VERBOS.AND.SEMIV).AND.
     $   (MOD(I-1,NPRINT).EQ.0)) LPRINT=.TRUE.
166   DO 100 IN=1,3
C
C CHECK FOR INSTABILITIES
C
      IF(WR(IN,I).EQ.0.D0) GO TO 102
      GREL=WIM(IN,I)/WR(IN,I)
      IF(WIM(IN,I).LT.0.D0) GO TO 102
      INSTAB(IN,I)=.TRUE.
      IF(I.EQ.1) GO TO 105
      DAWIM=WIM(IN,I)
      IF(DAWIM.LT.0.D0) WMAXL(IN)=0.D0
      IF(WMAXL(IN).GT.DAWIM) GO TO 101
      IF(INSTBI(IN,NMAXL(IN)).EQ.I-1) GO TO 104
105   NMAXL(IN)=NMAXL(IN)+1
104   INSTBI(IN,NMAXL(IN))=I
      WMAXL(IN)=DAWIM
      GO TO 101
102   INSTAB(IN,I)=.FALSE.
101   CONTINUE
      IF(DKR(I).EQ.0.D0) GO TO 288
C
C FIND PHASE AND GROUP VELOCITIES
```

```
C CHECK FOR LOCAL MAXIMA IF UNSTABLE
C
      VPHASE(IN,I)=SNGL(WR(IN,I)/DKR(I))
288   IF (LPRINT) WRITE(6,1033) I,DKR(I),WR(IN,I),WIM(IN,
     $     I)
     $      ,VPHASE(IN,I),GREL,VG(IN,I)
1033  FORMAT(1X,I3,3D26.14,3D15.5)
C
C SAVE PLOT SCALING MAX AND MIN
C
      IF(KLOG) GO TO 131
      RIMX=AMAX1(RIMX,SNGL(WIM(IN,I)))
      RIMN=AMIN1(RIMN,SNGL(WIM(IN,I)))
      RRMX=AMAX1(RRMX,SNGL(WR(IN,I)))
      RRMN=AMIN1(RRMN,SNGL(WR(IN,I)))
      GO TO 100
131   R=SNGL(DABS(WR(IN,I)))
      IF(R.EQ.0.) GO TO 132
      RRMX=AMAX1(RRMX,R)
      RRMN=AMIN1(RRMN,R)
132   R=SNGL(DABS(WIM(IN,I)))
      IF(R.EQ.0.) GO TO 100
      RIMX=AMAX1(RIMX,R)
      RIMN=AMIN1(RIMN,R)
100   CONTINUE
      SOLVEQ=.FALSE.
      IF(.NOT.PLREAL) GO TO 300
      WRITE(6,1011) RRMX,RRMN,RIMX,RIMN
1011  FORMAT(' RRMX,RRMN,RIMX,RIMN',4E15.7)
      IF(.NOT.KLOG) GO TO 201
      RIMX=ALOG10(RIMX)
      RIMN=ALOG10(RIMN)
      RRMX=ALOG10(RRMX)
      RRMN=ALOG10(RRMN)
201   IF(.NOT.FANCY) GO TO 260
      RMM=AINT(ALOG10(ABS(RRMN)))
      IM=RRMN/10.**RMM
      WMIN=IM*10.**RMM
      RMM=AINT(ALOG10(RRMX-RRMN))
      IM=(RRMX-RRMN)/10.**RMM
      WDX=IM*10.**RMM
C
C PLOTTING
C DO SCALING
C PLOT AXES
C LABEL
C PLOT ROOT LINES
C APPLY SPECIAL SYMBOLS IF
C  REAL(W)<0, OF IMAG(W)>0.
C
      GO TO 261
260   WMIN=RRMN
      WDX=(RRMX-RRMN)/10.
261   IF(PINC.EQ.0.) PINC=(KMAX-KMIN)/10.
      IF(PKMIN.EQ.0.) PKMIN=KMIN
      INC=(NK-1)/20
```

```
      IF(PRMIN.NE.0.) WMIN=PRMIN
      IF(PRINC.NE.0.) WDX=PRINC
      CALL AXIS(0.,0.,'WAVE NUMBER',-11,10.,0.,PKMIN,PINC
     $    )
      CALL AXIS(0.,0.,'REAL ANG FREQ',13,10.,90.,WMIN,WDX
     $    )
      IF(.NOT.KLOG) GO TO 262
      CALL SYMBOL(-0.3,9.0,.14,'LOG-LOG',90.,7)
262   IF(.NOT.LABEL) GO TO 263
      CALL SYMBOL(1.,9.75,.14,ALABEL,0.,80)
263   CONTINUE
      S=10./(NK-1.)
      DO 206 I=1,NK
      AX(I)=(I-1.)*S
      AY(I)=0.
206   CONTINUE
      IF(KLOG) GO TO 250
      DO 202 IN=1,3
      DO 203 I=1,NK
      AY(I)=(SNGL(WR(IN,I))-WMIN)/WDX
203   CONTINUE
      CALL LINE(AX,AY,NK,1)
202   CONTINUE
      CALL PLOT(12.,0.,-3)
      GO TO 300
250   DO 212 IN=1,3
      NIN=0
      DO 213 I=1,NK
      IF(WR(IN,I).EQ.0.D0) GO TO 214
      AY(I)=(SNGL(DLOG10(DABS(WR(IN,I))))-WMIN)/WDX
      IF(WR(IN,I).GT.0.D0) GO TO 213
      IF(I.EQ.1) GO TO 240
      IF(WR(IN,I-1).LT.0.D0) GO TO 241
      NIN=NIN+1
      KBEG(NIN)=I
      KEND(NIN)=I
      GO TO 213
241   KEND(NIN)=I
      GO TO 213
240   NIN=1
      KBEG(NIN)=I
      KEND(NIN)=I
      GO TO 213
214   AY(I)=0.
213   CONTINUE
      CALL LINE(AX,AY,NK,1)
      IF(NIN.EQ.0) GO TO 212
      DO 248 K=1,NIN
      KB=KBEG(K)
      KE=KEND(K)
      DO 249 I=KB,KE,INC
      CALL SYMBOL(AX(I),AY(I),.14,SYM(IN),0.0,-1)
249   CONTINUE
248   CONTINUE
212   CONTINUE
      CALL PLOT(12.,0.,-3)
```

```
300   IF(.NOT.PLIMAG) GO TO 399
      DO 369 I=1,NK
      AY(I)=0.
369   CONTINUE
      IF(.NOT.FANCY) GO TO 360
      RMM=AINT(ALOG10(ABS(RIMN)))
      IM=RIMN/10.**RMM
      WMIN=IM*10.**RMM
      RMM=AINT(ALOG10(RIMX-RIMN))
      IM=(RIMX-RIMN)/10.**RMM
      WDX=IM*10.**RMM
      GO TO 361
360   WMIN=RIMN
      WDX=(RIMX-RIMN)/10.
      IF(WDX.EQ.0.) GO TO 399
361   CONTINUE
      IF(PIMIN.NE.0.) WMIN=PIMIN
      IF(PIINC.NE.0.) WDX=PIINC
      CALL AXIS(0.,0.,'WAVE NUMBER',-11,10.,0.,PKMIN,PINC
     $     )
      CALL AXIS(0.,0.,'IMAG ANG FREQ',13,10.,90.,WMIN,WDX
     $     )
      IF(KLOG) GO TO 350
      DO 252 IN=1,3
      DO 251 I=1,NK
      AY(I)=(SNGL(WIM(IN,I))-WMIN)/WDX
251   CONTINUE
      CALL LINE(AX,AY,NK,1)
252   CONTINUE
      GO TO 390
350   CALL SYMBOL(-0.3,9.0,.14,'LOG-LOG',90.,7)
      DO 351 IN=1,3
      NIN=0
      DO 352 I=1,NK
      IF(WIM(IN,I).EQ.0.) GO TO 353
      AY(I)=(SNGL(DLOG10(DABS(WIM(IN,I))))-WMIN)/WDX
      IF(WIM(IN,I).LT.0.D0) GO TO 352
      IF(I.EQ.1) GO TO 340
      IF(WIM(IN,I-1).GT.0.D0) GO TO 341
      NIN=NIN+1
      KBEG(NIN)=I
      KEND(NIN)=I
      GO TO 352
341   KEND(NIN)=I
      GO TO 352
340   NIN=1
      KBEG(NIN)=I
      KEND(NIN)=I
      GO TO 352
353   AY(I)=0.
352   CONTINUE
      CALL LINE(AX,AY,NK,1)
      IF(NIN.EQ.0) GO TO 351
      DO 348 K=1,NIN
      KB=KBEG(K)
      KE=KEND(K)
```

```
      DO 349 I=KB,KE,INC
      CALL SYMBOL(AX(I),AY(I),.14,SYM(IN),0.0,-1)
349   CONTINUE
348   CONTINUE
351   CONTINUE
390   CALL PLOT(12.,0.,-3)
399   DO 501 IN=1,3
      WRITE(6,1013) (INSTAB(IN,I),I=1,NK)
1013  FORMAT(1X,10(3X,10L1))
      NM=NMAXL(IN)
      IF(NM.EQ.0) GO TO 501
      WRITE(6,1012) IN,NM,(INSTBI(IN,I),I=1,NM)
1012  FORMAT(' INSTABILITY MAXIMA FOR GROUP',I2,I10,/1X,
     $     6(2X,5I4))
501   CONTINUE
C
C USE THE LOCAL MAXIMA AS STARTING POINTS
C FOR SOLUTION TO D=0, DD/DK=0
C
      DO 401 IN=1,3
      NNX=NMAXL(IN)
      IF(NNX.LT.1) GO TO 401
      DO 400 I=1,NNX
      II=INSTBI(IN,I)
      X(1)=WR(IN,II)
      X(2)=WIM(IN,II)
      X(3)=DKR(II)
      X(4)=0.D0
      F(1)=0.D0
      F(2)=0.D0
C
C USE NEWTON PROCEDURE (FROM UBC COMPUTER CENTRE)
C TO SOLVE EQUATIONS
C
C MAXIT 200 USUALLY USED
C
C
C NOTE ABOUT COEFFICIENT STRUCTURE:::::::::::::
C      IF K GOES TO -K*, THEN W GOES TO -W*
C      WHICH MEANS THAT THE SAME PHYSICAL ROOT RETURNS
C
      CALL DISPCO(X(3))
      WC=DCMPLX(X(1),X(2))
      WC2=WC*WC
      WC3=WC*WC2
      DDDK=DDC(1)*WC3+DDC(2)*WC2+DDC(3)*WC+DDC(4)
      F(3)=DREAL(DDDK)
      F(4)=DIMAG(DDDK)
      WRITE(6,1054) I,IN,X,F
1054  FORMAT('OSTART',2I3,8D15.7)
      CALL NDINVT(4,X,F,ACCEST,MAXIT,ERR,FCN,&996)
      WRITE(6,1015) (X(IC),ACCEST(IC),IC=1,4)
1015  FORMAT(' X ACCEST',4(D18.7,D10.2))
      IF (X(2).LT.0.D0) GO TO 402
      CALL DISPCO(X(3))
      CALL CPOLY1(RDC,IDC,3,ROOTR,ROOTI,&999)
```

```
      DO 505 IIN=1,3
      CALL NEWTON(ROOTR(IIN),ROOTI(IIN),EQTOL)
      WC=DCMPLX(ROOTR(IIN),ROOTI(IIN))
      WC2=WC*WC
      WC3=WC2*WC
      DDDK=DDC(1)*WC3+DDC(2)*WC2+DDC(3)*WC+DDC(4)
      DDDK=-DDDK/(NDC(1)*WC2+NDC(2)*WC+NDC(3))
      WRITE(6,1055) DDDK,ROOTR(IIN),ROOTI(IIN)
1055  FORMAT(' ######## ABSOLUTE INSTABILITY, GROUP VELOC'
     $    ,'ITY',2D16.8,
     $   5X,'W=',2D15.5)
505   CONTINUE
      GO TO 402
996   WRITE(6,1056)ERR,X,ACCEST
1056  FORMAT(' *******NDINVT FAILED**** ERR,X,ACCEST'/,1X,
     $        9D13.5)
402   CONTINUE
400   CONTINUE
401   CONTINUE
      GO TO 9999
9998  CALL PLOTND
      STOP
997   NP=997
      GO TO 990
998   NP=998
      GO TO 990
999   NP=999
990   WRITE(6,1020) NP
1020  FORMAT(' **************CPOLY1 TROUBLES***',I4)
      GO TO 9999
      END
      SUBROUTINE DISPCO(K)
C
C CALCULATES COEFFICIENTS OF DISPERSION RELATION FOR REAL
C          K
C
      LOGICAL SOLVEQ
      REAL*8 DREAL,DIMAG,K,K2,K3,K4
      COMPLEX*16 DDC(4),DC(4),NDC(3),DCMPLX
      REAL*8 CRD(5,4),CID(5,4),RDC(4),IDC(4)
      COMMON /CCCALC/ DDC,DC,NDC
      COMMON /CPOL/ RDC,IDC
      COMMON /COEFS/ CRD,CID
      COMMON /CONTRO/ SOLVEQ
      K2=K*K
      K3=K2*K
      K4=K3*K
      IF(SOLVEQ) GO TO 1
      DO 100 I=1,4
      IB=5-I
      RDC(I)=CRD(1,IB)+CRD(2,IB)*K+CRD(3,IB)*K2
     $        +CRD(4,IB)*K3+CRD(5,IB)*K4
      IDC(I)=CID(1,IB)+CID(2,IB)*K+CID(3,IB)*K2
     $        +CID(4,IB)*K3+CID(5,IB)*K4
100   CONTINUE
1     CONTINUE
```

```
      DO 102 I=1,4
      IB=5-I
      DC(I)=DCMPLX(CRD(1,IB),CID(1,IB))
     $       +DCMPLX(CRD(2,IB),CID(2,IB))*K
     $       +DCMPLX(CRD(3,IB),CID(3,IB))*K2
     $       +DCMPLX(CRD(4,IB),CID(4,IB))*K3
     $       +DCMPLX(CRD(5,IB),CID(5,IB))*K4
      DDC(I)=DCMPLX(CRD(2,IB),CID(2,IB))
     $        +DCMPLX(CRD(3,IB),CID(3,IB))*2.D0*K
     $        +DCMPLX(CRD(4,IB),CID(4,IB))*3.D0*K2
     $        +DCMPLX(CRD(5,IB),CID(5,IB))*4.D0*K3
      IF(IB.EQ.1) GO TO 102
      NDC(I)=DC(I)*DFLOAT(IB-1)
102   CONTINUE
      RETURN
      END
      SUBROUTINE NEWTON(RR,RI,TOL)
C
C DOES NEWTON METHOD IMPROVEMENT OF ROOTS
C VALUES FROM ESTIMATE OR ROOT FINDER
C ARE SUBSTITUTED BACK INTO THE FULL EQUATION
C
      REAL*8 RR,RI,TOL,RDC(4),IDC(4),RATIO
      REAL*8 DREAL,DIMAG
      COMPLEX*16 DDC(4),DC(4),NDC(3),DIS,DDIS,DELW,WC,WC2
     $    ,WC3
      COMPLEX*16 DCMPLX
      REAL*8 CDABS,WABS
      COMMON /NEWT/ DDIS,MAXIT
      COMMON /CCCALC/ DDC,DC,NDC
      ILOOP=0
      WC=DCMPLX(RR,RI)
2     WC2=WC*WC
      WC3=WC2*WC
      DIS=DC(1)*WC3+DC(2)*WC2+DC(3)*WC+DC(4)
      DDIS=NDC(1)*WC2+NDC(2)*WC+NDC(3)
      IF(DREAL(DDIS).EQ.0.D0.AND.DIMAG(DDIS).EQ.0.D0) GO
     $    TO 3
      DELW=-DIS/DDIS
      WABS=CDABS(WC)
      IF(WABS.EQ.0.D0) GO TO 1
      RATIO=CDABS(DELW)/WABS
      WC=WC+DELW
      IF(RATIO.LE.TOL) GO TO 1
      ILOOP=ILOOP+1
      IF (ILOOP.LT.MAXIT) GO TO 2
      WRITE(6,1000) WC,RATIO
1000  FORMAT(' MAXIMUM NUMBER OF ITERATIONS EXCEEDED. W R',
     $ 'OOT IS NOW',
     $     2D25.15,'    ERROR=',D15.5)
      GO TO 1
3     WRITE(6,1001) WC,DIS,RATIO
1001  FORMAT(' DERIVATIVE GOES TO ZERO. WC,DIS,ERROR.',
     $    4D15.5)
1     CONTINUE
      RR=DREAL(WC)
```

```
      RI=DIMAG(WC)
      RETURN
      END
      SUBROUTINE ADVANC(WR,WI,DELTAK,DWDK,SUBDIV)
C
C ESTIMATES NEXT ROOT IN K SEQUENCE FROM PRESENT
C ROOT AND DERIVATIVE
C
      REAL*8 WR,WI,DREAL,DIMAG,DELTAK,DK,DFLOAT
      INTEGER*4 SUBDIV
      COMPLEX*16 DDC(4),DC(4),NDC(3),WC,DDIS,DWDK
      COMPLEX*16 DCMPLX,WC2,WC3,WC4
      COMMON /NEWT/ DDIS,MAXIT
      COMMON /CCCALC/ DDC,DC,NDC
      WC=DCMPLX(WR,WI)
      DK=DELTAK/DFLOAT(SUBDIV)
      DO 1 I=1,SUBDIV
      WC2=WC*WC
      WC3=WC2*WC
      DDIS=NDC(1)*WC2+NDC(2)*WC+NDC(3)
      DWDK=-(DDC(1)*WC3+DDC(2)*WC2+DDC(3)*WC+DDC(4))/DDIS
      WC=WC+DWDK*DK
1     CONTINUE
      WR=DREAL(WC)
      WI=DIMAG(WC)
      RETURN
      END
      SUBROUTINE FCN(X,F)
C
C SUBROUTINE CALLED BY NDINVT
C EVALUATES D AND DD/DK FOR COMPLEX W AND K
C
      REAL*8 X(4),F(4)
      COMPLEX*16 CK,CW,CW2,CW3,DD,DDDK
      COMPLEX*16 DDC(4),DC(4),NDC(3)
      COMPLEX*16 DCMPLX
      REAL*8 DREAL,DIMAG
      COMMON /CCCALC/ DDC,DC,NDC
      CK=DCMPLX(X(3),X(4))
      CALL DISCO(CK)
      CW=DCMPLX(X(1),X(2))
      CW2=CW*CW
      CW3=CW*CW2
      DD=DC(1)*CW3+DC(2)*CW2+DC(3)*CW+DC(4)
      F(1)=DREAL(DD)
      F(2)=DIMAG(DD)
      DDDK=DDC(1)*CW3+DDC(2)*CW2+DDC(3)*CW+DDC(4)
      F(3)=DREAL(DDDK)
      F(4)=DIMAG(DDDK)
      RETURN
      END
      SUBROUTINE DISCO(CK)
C
C CALCULATES DISPERSION POLYNOMIAL FOR COMPLEX K
C
      REAL*8 DREAL,DIMAG
```

```
      COMPLEX*16 DDC(4),DC(4),NDC(3)
      COMPLEX*16 CK,CK2,CK3,CK4
      COMPLEX*16 DCMPLX
      REAL*8 CRD(5,4),CID(5,4)
      COMMON /CCCALC/ DDC,DC,NDC
      COMMON /COEFS/ CRD,CID
      CK2=CK*CK
      CK3=CK2*CK
      CK4=CK3*CK
      DO 100 I=1,4
      IB=5-I
      DC(I)=DCMPLX(CRD(1,IB),CID(1,IB))
     $       +DCMPLX(CRD(2,IB),CID(2,IB))*CK
     $       +DCMPLX(CRD(3,IB),CID(3,IB))*CK2
     $       +DCMPLX(CRD(4,IB),CID(4,IB))*CK3
     $       +DCMPLX(CRD(5,IB),CID(5,IB))*CK4
      DDC(I)=DCMPLX(CRD(2,IB),CID(2,IB))
     $        +DCMPLX(CRD(3,IB),CID(3,IB))*2.D0*CK
     $        +DCMPLX(CRD(4,IB),CID(4,IB))*3.D0*CK2
     $        +DCMPLX(CRD(5,IB),CID(5,IB))*4.D0*CK3
100   CONTINUE
      RETURN
      END
```